MEMBRANE SEPARATION IN TEXTILE WASHING PROCESSES

Hul, Jacob Peter van ‘t

Membrane Separation in Textile Washing Processes
Thesis Enschede. – With Ref. – With Summary in Dutch
ISBN 90-36512964

Printed by Print Partners Ipskamp B.V., Enschede, The Netherlands

MEMBRANE SEPARATION IN TEXTILE WASHING PROCESSES

PROEFSCHRIFT

ter verkrijging van
de graad van doctor aan de Universiteit Twente,
op gezag van de rector magnificus,
prof.dr. F.A. van Vught,
volgens besluit van het College voor Promoties
in het openbaar te verdedigen
op donderdag 3 juni 1999 te 15.00 uur.

door

Jacob Peter van 't Hul

geboren op 25 december 1969
te Coevorden

Dit proefschrift is goedgekeurd door de promotor prof.dr.ir. T. Reith
en de assistent-promotor dr.ir. I.G. Rácz.

Promotiecommissie:

Prof.dr. F.A. van Vught (Rector Magnificus Universiteit Twente)

Prof.dr. W.E. van der Linden (Dekaan Faculteit Chemische Technologie, Universiteit Twente)
Dr. M.S.A. Vrijland (Referent, Faculteit Chemische Technologie, Universiteit Twente)

Prof.dr.-ing. T. Melin (Institut für Verfahrenstechnik, RWTH Aachen)
Prof.dr.-ing. H. Strathmann (Faculteit Chemische Technologie, Universiteit Twente)
Prof.dr.ir. M.M.C.G. Warmoeskerken (Faculteit Chemische Technologie, Universiteit Twente)
Dr.ir. H. Futselaar (Stork Friesland)

Voorwoord

Alhoewel het uitvoeren van een promotie-onderzoek een puur solistische onderneming lijkt, is in het algemeen een promovendus niet succesvol zonder de hulp van anderen. Het hier beschreven onderzoek vormt geen uitzondering op deze regel.

In de eerste plaats wil ik de co-promotor en mentor, Imre Rácz, bedanken voor zijn steun en interesse gedurende de afgelopen jaren en de promotor Tom Reith, voor de mogelijkheid om in zijn groep dit onderzoek te verrichten. Daarnaast wil ik alle collega's van de onderzoekgroepen Scheidingstechnologie en Technologie van Gestructureerde Materialen bedanken voor de goede sfeer aan koffie- en tafeltennistafel. In het bijzonder ook mijn kamergenoten, Sander Rekveld en Jan Ophoff, voor hun inhoudelijke interesse en discussies.

Het onderzoek zou zeker niet mogelijk zijn geweest zonder de geldschieters. Hiervoor wil ik het bureau Senter bedanken en de deelnemende textiel- en membraanbedrijven in de begeleidings- en gebruikerscommissie. Vooral de medewerkers van membraanbedrijf Stork Friesland voor hun inzet bij het ontwerpen en bouwen van de experimentele opstelling. Daarnaast wil ik TNO-textiel en TNO-MEP bedanken voor de samenwerking binnen het project 'Recycling van processtromen in de textielindustrie'.

Op het uitvoerende vlak hebben veel HTS- en MTS-studenten, hetzij als afstudeerder of stagiair, mij geholpen bij het uitvoeren van de experimenten. William Tieben, Sebastiaan Lens en Hans Ophoff hebben hierbij de inleidende filtratie-experimenten uitgevoerd. Hun werk vormde een solide basis voor het onderzoek dat uitgevoerd is door Frederik Spenkelink. Ondanks zijn jonge leeftijd heeft Frederik bewezen dat hij uitstekend zelfstandig kon werken en kon omgaan met begeleiding 'op afstand' per e-mail. Sterker nog: de uitvoering van de experimenten verliep beter als Frederik zo weinig mogelijk 'gestoord' werd door ondergetekende.

Daarnaast hebben Matthijs van Stratum en Patrick Nieland als vrijwilliger aan het project meegewerkt. De eerste zeer kort de laatste wat langer, voordat zij elders een nieuwe werkplek vonden. Vooral Patrick heeft hierbij erg veel 'kleine' projectjes uitgevoerd en zijn experimentele hand is dan ook in veel hoofdstukken van dit proefschrift terug te vinden.

Voor het soepele verloop van de experimenten op het technische en organisatorische vlak wil ik technici van de onderzoekgroep Scheidingstechnologie, Bert Vos en Alfons Rooks, bedanken. Verder ook dank aan de glasblazers en technici van de fijnmechanische werkplaats voor hun inzet en hun gedegen adviezen aangaande technische zaken. Ik heb hier ontzettend veel van geleerd. Met name wil ik Harry Olde Veldhuis hier noemen die vooral aan het eind van het traject ervoor zorgde dat de membraan filtratie installatie kon blijven draaien.

In het kader van hun studie hebben een aantal studenten kortlopende projecten uitgevoerd binnen dit promotie onderzoek. De stromingspotentiaalmetingen werden gedaan door IAESTE stagiair Barry Quirke uit Ierland. De studenten Wendy Wes, Huub Hofstede en Anja van der Brugge voerden een BK-P opdracht uit. Martin Jansen, Sandor Zuurendonk en Jeroen Oderkerk voerden in het kader van het HTS-doorstroom programma een literatuurstudie uit. Al deze personen wil ik bedanken voor hun ijver en inzet.

Speciaal woord van dank aan Prof. Thomas Melin van het Institut für Verfahrenstechnik van de RWTH te Aken voor de mogelijkheid om binnen zijn groep het nanofiltratie onderzoek uit te voeren. Ludger Eilers voor het regelen en wegwijs maken van de zaken daarom heen, Thomas Paesch die met veel inzet en nauwgezetheid de experimenten heeft uitgevoerd en Gerd Spalding voor het opzetten en uitvoeren van de HPLC analyses. Ik denk met genoegen terug aan deze Duitse periode en de gezellige leuke sfeer binnen de groep van professor Melin.

Uiteraard mag ik ook mijn paranimfen en vrienden, Matthijs van Stratum en Edward Span, niet vergeten voor hun hulp bij de promotieplechtigheid. Ik wil verder mijn vrienden, veelal bekenden van het Symfonisch Blaasorkest Enschede en de voetbalvereniging E.F.C. ‘PW’, bedanken voor de fijne tijd de afgelopen jaren.

Als laatste wil ik mijn familie bedanken voor hun getoonde belangstelling. Dit geldt in het bijzonder voor mijn ouders en broer Martijn; jullie steun en interesse hebben veel voor mij betekend.

Contents

Chapter 1

Recycling of process-streams in the textile refining industry

Summary

In this chapter an introduction into the environmental problems of the textile refining industry is given. Membrane technology is introduced as part of the solution to these environmental problems, by recovery and re-use of valuable components and energy from waste streams and concentration of waste volume which can be profitable for further waste elimination processes. The treatment of wastewater from washing processes subsequent to reactive dyeing processes by reverse osmosis and nanofiltration was chosen as topic of study. At the end of this chapter the contents of this thesis are outlined.

1.1 Waste problem in the textile refining industry

The textile refining industry is that part of the textile industry, where textile products (fabric, yarns, clothes) are given special properties like colour, flame retardancy, soil repellence ability, antistatic properties etc. [4]. In the textile refining processes a huge amount of chemicals, e.g. bleaching agents, dyeing agents and other auxiliaries, are used. After these treatments, a considerable part of the applied components has to be removed from the textile. This is usually done by rinsing with water, used as a carrier in these washing processes, at elevated temperatures. This way of processing implies a large consumption of fresh water, energy and chemicals and a large production of waste streams. Therefore it contributes to environmental problems like the lowering of the groundwaterlevel, the salting of the soil, the colourization of surface water and contamination of the environment by components, which can not be eliminated in communal wastewater treatment plants. Because of these issues, the textile refining industry is nowadays confronted with more stringent legislation and raising costs concerning fresh water intake and waste water discharge.

1.2 Methods to solve waste problems in the textile refining industry

Prevention of waste production, waste elimination and separation processes in order to minimise the unwanted contribution to environmental pollution and to control the costs of water intake and waste water discharge are the three issues which have become rising interest in the textile refining industry. In 1993 an IOP-prevention project, sponsored by the office 'Senter' of the Dutch ministry of Economic Affairs, was started with the aim to study the applicability of these issues for the textile refining industry. In this IOP program, the survey and the prevention of waste production in the textile refining industry was executed by the centre of textile research of TNO (part of TNO-industry, formerly located in Delft now located in Enschede). The waste elimination techniques were studied by the department 'Environment, Energy and Process Innovation' of TNO (i.e. TNO-MEP, located in Apeldoorn). Separation processes were studied in the Separation Technology group at the Department of Chemical Engineering of the University of Twente. This research into separation technology, focused on the applicability of membrane technology for a selected textile refining process, is presented in this thesis.

Prevention of waste production means that components causing environmental problems should be replaced by less harmfull components. Some simple mutations have already been introduced in the textile refining industry, but these changes go slow as in most cases prevention demands the design of complete other textile refining methods.

The waste water streams from all textile processes of a textile refining company are usually collected together and, after some pH adjustments, sent to communal waste water treatment plants, based on aerobic oxidation. However some applied components (e.g. reactive dyes) have been specially designed that degradation by aerobic oxidation is prevented! Other techniques like anaerobic reduction or chemical oxidation techniques, preferably applied on selected waste (side) streams, should then be used. The investigation of these techniques have already been reviewed [18, 20], but the costs per volume of waste are usually large. This is intensified by the fact that a lot of waste streams contain only a little amount of waste in a relatively large volume of water.

1.3 Membrane technology

Separation technologies can be used to fulfil the purpose of recycling of valuable components and energy in textile refining processes and to fulfil the purpose of lowering the specific costs for further treatment by reducing the waste volume. In this study membrane separation

technology on aqueous waste streams will be investigated. The reasons to choose for membrane technology are:

- membrane processes are fast processes with a short residence time, as no adsorption or reaction steps are required. This makes membranes very applicable for process-integrated solutions.
- membrane processes are modular designed and the capacity can be easily enlarged.
- membrane processes are in general less component-specific than other separation processes (e.g. adsorption) and therefore very suitable to treat waste streams with a mixture of components.

In figure 1.1 the main concept of using membrane processes is outlined.

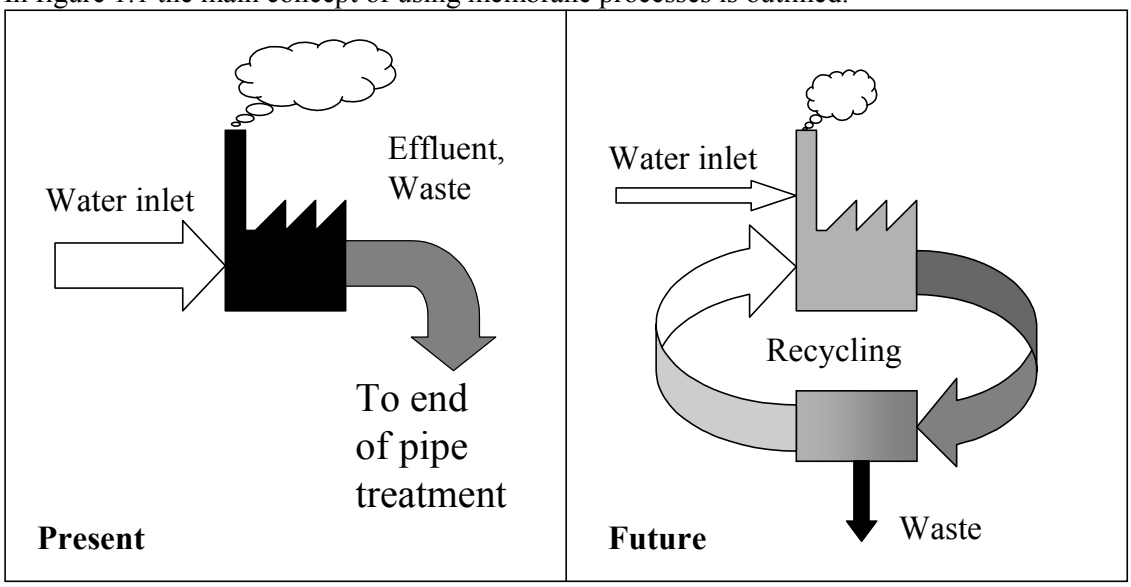

Figure 1.1 Objective of the IOP project: The application of membrane processes for recycling of 'valuable components' (e.g. water) in the textile refining industry.

There are many textile processes, each producing specific waste streams. Performing membrane research on all waste streams is too complex. Therefore one waste stream was selected as topic of study i.e. the wastewater from washing processes subsequent to reactive dyeing processes. It is expected that knowledge developed in this study will also be useful for other textile refining processes. The reasons for the selection of wastewater from reactive dyeing and subsequent washing processes are:

- The reactive dyeing processes are very popular as the quality of the textile products is high compared to products from other dyeing processes
- The fixation degree on the fabric of reactive dyes is only 70 percent and the reactive dyeing thus considerably contributes to the colour content of the total waste stream
- Reactive dyes and their derivatives are not adequately eliminated in communal waste water treatment plants

Waste streams originating from two basic forms of reactive dyeing processes, the pad-steam process and the pad-batch process, are chosen as topic of study. The difference between the pad-steam process and the pad-batch process is that, next to different applied auxiliaries, the former is a continuous as the latter is a batch process.

In the pad-steam process the dye is brought onto the fabric by transporting the fabric through a dyeing bath. Subsequent to that the fabric is transported in a second bath, where NaCl and NaOH (pH ~ 13) are added onto the fabric. The role of these inorganic salts is to enhance the dye uptake in the fibres of the fabric and to enhance the reaction rate of the dyes with the

fabric. To obtain a fast reaction in this continuous process, high temperatures are required. Therefore the fabric is brought into contact with steam in the 'steamer'. In some cases urea is added, before the fabric enters the steamer, to make the fabric more hygroscope in order to get a faster heat transmission between the steam and the fabric.

In the pad batch process the dyes are not fixated on the fabric by high temperatures but by applying long reaction times. The dyes and dyeing auxiliaries (e.g. caustic soda and sodium silicates) are brought onto the fabric and then the 'batch' (the folded fabric containing the dyeing liquor) is left aside for several hours for the reaction to take place.

During the residence in the dyeing bath and steamer or 'batch', 30 % of the applied reactive dyes react with water in stead of reacting with the functional groups on the textile fabric. This is called the hydrolysation reaction that turns the dye into the unreactive, hydrolysed form. The hydrolysed dyes cannot be re-used again as reactive dyes and need to be washed out together with other auxiliary components.

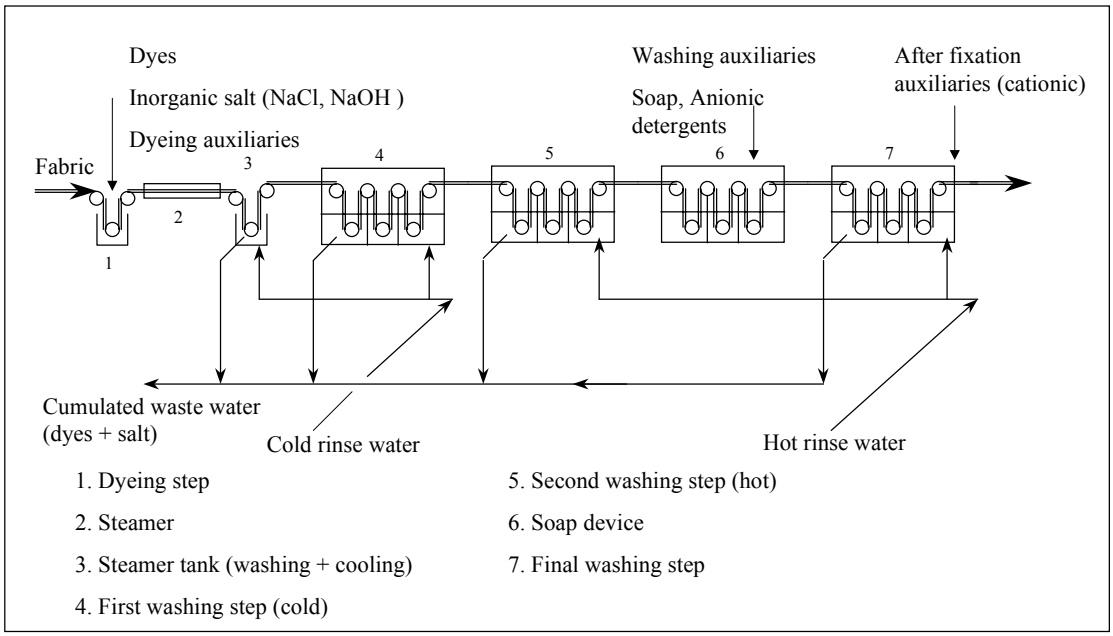

Figure 1.2 Example of a (pad-steam) washing process subsequent to a reactive dyeing process.

In the subsequent washing processes the fabric is rinsed in several washing units. Usually cold washing water (T ~ 20 °C) is used in the first washing section. In this section most part of the small inorganic salts (i.e. NaCl, Na_2SO_4 and NaOH) with high diffusion rates from the fabric to the washing water will be removed. Rinsing with hot water in the first washing section is dissuaded by most textile researchers and textile manufacturers, as the combination of high temperature and high pH will enhance the detachment reaction of covalent bonded dyes. The diffusion rate of the hydrolysed dyes from the fabric into the water is much smaller and rinsing at higher temperatures (~ 80 °C) and the addition of washing agents (e.g. soap) is necessary in the proceeding washing sections. Even then the removal of the hydrolysed dyes is about 90 percent and often an after-fixation agent is added in the last washing section or on an extra pad subsequent to the washing section. This after-fixation agent lowers the mobility of the hydrolysed dyes in the fabric, which means that the dyes are released only gradually in the domestic laundry.

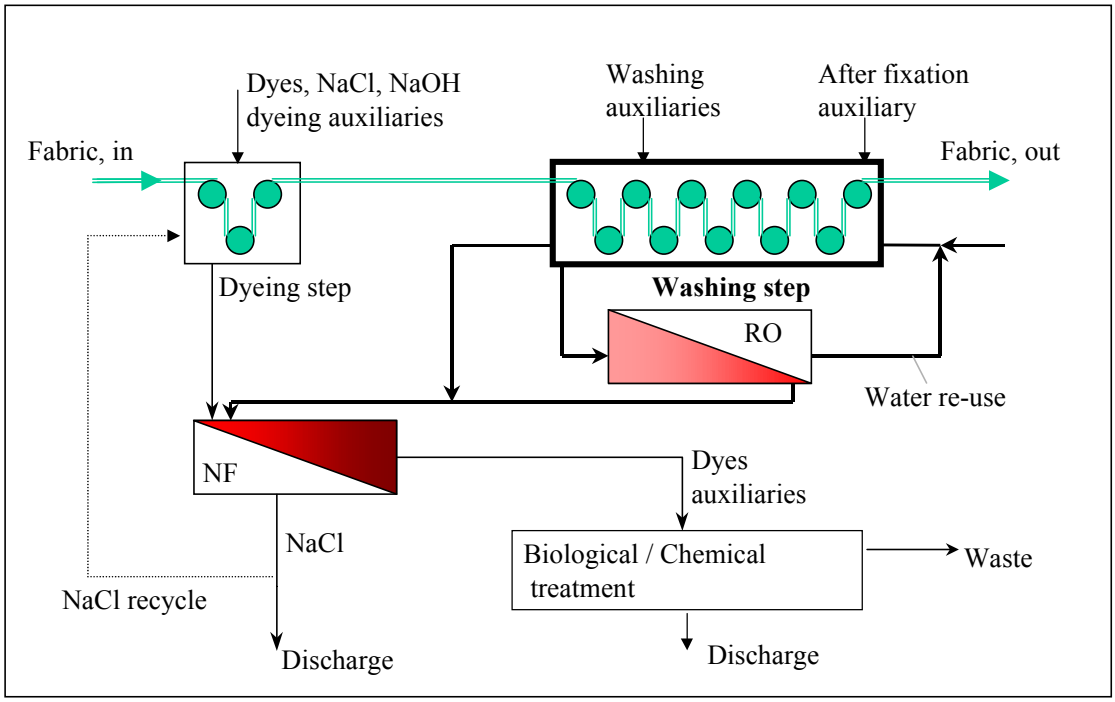

Figure 1.3 Recycling and treatment of process-streams in a textile dyeing and subsequent washing processes by the application of membrane separation processes.

In order to produce fresh process water out of the wastewater, considered here, Reverse Osmosis (RO) is the most robust membrane technology as RO rejects almost all solutes, including mono valent ions like Na^+ and Cl^-. Membranes with pore sizes larger than a few nanometer (i.e. ultrafiltration (UF) and microfiltration (MF)) are not suitable as the dyes (with molecular masses between 300 and 2000 g/mole) will be transported easily through these membranes. Nanofiltration (NF) will reject organic components with molecular masses above 300 g/mole and multivalent ions. NF can be classified as an intermediate membrane technology between RO and UF. If only dye components have to be removed or Na_2SO_4 is used in stead of NaCl, nanofiltration (NF) seems preferable, as less membrane area compared to RO has to be installed. However it was proven that NaCl diminishes the washing out of hydrolysed dyes [19] and thus RO has to be used for the recycling of purified process water in the washing process. Using RO for this purpose, the recovery of water and the concentration of the wastewater volume will be limited by the osmotic pressure difference over the membrane. Further reduction of the wastewater volume can then be achieved by NF as is shown in figure 1.3. The permeate stream of the NF should be decolourised which implies that in most cases this waste stream, containing a NaCl solution can be drained off to the surface water without further implications. However in some areas, where the salination of the soil is a main environmental problem, this is not possible and recovery of the NaCl should be considered. A further concentration (electrodialysis or reverse osmosis) step will then be necessary before the NaCl can be re-used in the dyeing process, provided that the permeate stream was adequately decolourised.

It must be emphasised again that membrane filtration is not a process to solve environmental problems on it's own but it should be integrated in the total wastewater treatment. Its functions are to recover valuable products (e.g. process water) and energy and to minimise the waste volume, which may be beneficial for further elimination processes (figure 1.2)

1.4 Membrane research

In this paragraph membrane research on wastewater from textile (reactive) dyeing and subsequent washing processes by other investigators is reviewed. The aim of these membrane investigations was the recycling of water and energy, the recovery of valuable products and the minimisation of the waste volume.

Erswell [7] and Buckley [8] describe pilot plant tests with nanofiltration membranes for the recovery of salt from used dyeing baths. The salt (NaCl) will pass through the membrane, as the dyes will be rejected. The highest NaCl transport is achieved at low permeate fluxes, however the dye retention will decrease going to lower fluxes, so an optimisation should be made here. Furthermore some alterations in the dyeing processes were proposed in order to make their concept work. This implies the usage of standard electrolyte solutions, pH alterations and the abandonment of the use of Na_2SO_4 as electrolyte, as Na_2SO_4 is rejected by the NF membrane. The concept does not seem to be attractive economically, as NaCl is not really a valuable product and the designed permeate fluxes of 10 lt/m^2hr will lead to membrane processes with a very large membrane area.

Bonomo [9] describes pilot plant tests with reverse osmosis, nanofiltration and ultrafiltration of wastewater form washing processes subsequent to reactive dyeing processes. The ultrafiltration process does not decolourise the waste stream. The nanofiltration process leads to complete decolourization with a permeate flux of 70 lt/m^2hr at 10 bar. The reverse osmosis membrane also desalinates the waste stream considerably (NaCl retention of 93 %), however the retention for the reactive dyes was somewhat lower than in the nanofiltration process. Severe membrane fouling was observed if the waste stream contained dispersed dyes, which are applied together with reactive dyes in some dyeing processes.

Treffrey Goatley et al [10] designed a pilot plant with two stages. The stages consist of different types of RO membranes. These RO membranes are generally applied in respectively brackish water desalination (first stage) and sea water desalination (second stage). 'Recycling of the retentate' is applied in the second stage in order to obtain higher water recoveries, which means that the cross-flow velocity is kept high in order to minimise membrane fouling. The total water recovery is 85 to 95 percent at a mean permeate flux of 15 lt/m^2hr.

A nanofiltration process for the treatment of mixed waste streams from reactive dyeing process has been designed by Rautenbach et al [11]. A total wastewater volume of 16 m^3/hr is filtrated at a mean permeate flux of 16.7 lt/m^2hr. The permeate (NaCl solution) can be drained off into the environment. The retentate is further treated in a wet oxidation process. The partly desalination of this retentate stream by NF is considered to be an advantage as the corrosion by NaCl in the wet oxidation is decreased.

Tegtmeyer [12] conducted research on the treatment of waste streams from a reactive dyeing process and subsequent washing processes by nanofiltration. The dye retention by NF was 99% and a permeate flux of 64 lt/m^2hr was achieved.

Fritsch [13] conducted research to the treatment of synthetic waste streams that were similar to actual waste streams. He came to the conclusion that it should be possible to relate the permeate flux decline to certain components (or combination of components) present in the actual waste stream. He proposed to set-up a 'Negativ-katalog' (~ black-list) of components which should be abandoned from the dyeing and washing process if their waste water has to be treated by membrane filtration processes.

Wenzel et al. [14] conducted research on the treatment of wastewater from reactive dyeing and subsequent washing processes. Membrane filtration processes (nanofiltration and reverse osmosis) were compared to adsorption on activated carbon.

In the late seventies and early eighties the treatment of wastewater from reactive dyeing processes and subsequent washing processes with dynamically formed membranes was investigated. These membranes were formed in situ from a colloidal suspension on a porous support. Promising membrane material was made from hydrated zirconia oxide in combination with polyacryl acid (ZR(IV)-PAA membrane). The application of these membranes for the treatment of all sorts of coloured textile wastewater was reported by Porter et al. [15], Brandon et al. [22], El-Nashar [16] and Groves et al. [21].

A complete treatment of textile wastewater from a textile refining company was proposed by Gaeta [17]. The purpose was to come to a zero-discharge system with re-use of all applied components. Nanofiltration and reverse osmosis membranes were integrated in this design.

Reverse osmosis is a membrane technology known for more than 30 years now. Main applications aim at the production of potable water by desalination of sea and brackish water on large-scale [5]. Main problem of these applications is membrane fouling. Practical experiences and sometimes research have already led to complete water treatment by RO technology including prefiltration steps, membrane module design, membrane process design and membrane cleaning procedures in order to diminish the consequences of membrane fouling. Just copying this technology for applications on industrial wastewater is not clear cut or even impossible as

- The composition of an industrial waste stream is different from sea or brackish water leading to other forms of membrane fouling.
- The RO processes producing potable water have only one product stream which is the fresh water of the permeate. The concentration of waste into a small volume is not an issue for these processes in contrary to the RO-treatment of wastewater in the (textile) industry. This means that the volume reduction factor (feed flow divided by retentate flow) in the production of potable water is lower than in the applications where the waste should be concentrated, leading to other membrane process designs.

The first RO membranes were made of cellulose acetate. The advantage of this membrane material is that it is relatively hydrophilic and adsorption of organic matter onto the membrane is thus relatively low. Its disadvantage is that this material is very sensitive to thermal, chemical and biological attack. For instance the pH of the filtration solution must be controlled between 4 and 6.5 in order to prevent hydrolysis of the membrane material. [6]

RO membranes based on polyamide (PA) show a better resistance against thermal, chemical and biological attack and can be used in alkaline (till pH = 10) conditions. These membranes are normally preferred to membranes made of CA for the treatment of industrial waste streams. Their disadvantage, compared to CA, is that they are more susceptible to membrane fouling as PA membranes are less hydrophilic. In this study an RO membrane made of PA is chosen.

The term nanofiltration appeared in literature at the end of the eighties, although similar membranes were already known under the name loose reverse osmosis membranes. As the name suggests these membranes are RO membranes with a more open or ‘loose’ structure. Furthermore some NF membranes are presented to have special electrochemical properties as they bear fixed charges leading to salt rejection properties controlled by charge (or Donnan) exclusion. It is stated that ‘multivalent ions will be rejected as monovalent ions can pass through the membrane’. In chapter three a discussion about this Donnan exclusion phenomenon and its importance for the rejection of inorganic salts by NF membranes will be given.

1.5 Aim of the membrane research presented in this thesis

The aim of this research is to determine the applicability of reverse osmosis and nanofiltration membrane separation processes for the purification of wastewater from selected washing processes subsequent to reactive dyeing processes. The research is focused on membrane fouling. Membrane filtration of actual textile waste water and synthetic textile waste water was executed in order to determine which components or combination of components, present in the selected waste water, contribute to membrane fouling. This membrane fouling is linked to the properties of the membranes and the solutes in order to come to recommendations how to prevent membrane fouling or clean fouled membranes.

1.6 Outline of this dissertation

In **chapter 2** a process model of a washing process subsequent to a pad-steam process is extended by membrane filtration processes in order to calculate the contents of the several waste streams from this washing process and to decide where the membrane filtration should be applied.

In **chapter 3** theoretical considerations concerning solvent and solute transport through membranes are outlined. The occurrence of concentration polarisation and membrane fouling as function of the composition of the wastewater and the physico-chemical properties of the membrane are discussed.

In **chapter 4** the experimental methods during filtration experiments with actual and synthetic textile wastewater are outlined. Furthermore both RO and NF membrane are characterised for their physico-chemical properties and their permeability for water and selected model solutions.

In **chapter 5** RO and NF research on actual textile wastewater is presented in order to get an overview of the important phenomena. Special attention is paid to membrane fouling and decolourisation of the waste streams. This preliminary study and other studies on actual textile wastewater determine the contents of the synthetic solutions to be researched. The synthetic solutions contain components, present or representative for present components in the real textile wastewater. Furthermore some real textile auxiliaries will be used as well.

In **chapter 6** the treatment of synthetic solutions by reverse osmosis are presented.

In **chapter 7** the treatment of synthetic solutions by nanofiltration are presented.

In **chapter 8** nanofiltration of selected synthetic solutions at varying cross-flow velocities is discussed. The results are used in an economical analysis. Also RO and NF on actual textile wastewater are discussed and economically analysed.

In **chapter 9** RO and NF on synthetic solutions containing an anionic or a cationic surfactant will be discussed. The design of these experiments is set by the electrochemical analysis of chapter 4 and the parametric studies of chapter 6 and 7. Furthermore the filtration of a cationic auxiliary and an anionic auxiliary is discussed.

Acknowledgement

The author wishes to thanks M. Jansen for performing the literature search.

Literature

[1] Pierce, J. Colour in textile effluents - the origins of the problem. JSDC 110: 131-133. (1994).

[2] Jekel, M. Wastewater treatment in the textile industry. in Treatment of wastewaters from textile processing. Colloquium TU Berlin 17-18 nov. (1997).

[3] Groff, K. A. Textile Waste. Water Environment Research 64(4): 425-429 (1992).

[4] Vigo, T.L. Textile processing and properties, preparation, dyeing, finishing and performance. 2nd ed. Elsevier Science Amsterdam, (1997).

[5] Amjad, Z., ed. Reverse osmosis: membrane technology. Van Nostrand Reinhold. Z., New York;
(1993).

[6] Mulder, M.H.V., Basic principles of membrane technology. Kluwer Academic Publishers, Dordrecht (1996).

[7] Erswell, A., C.J. Brouckaert, and C.A. Buckley, The reuse of reactive dye liquors using charged ultrafiltration membrane technology. Desalination, 1988. 70: p. 157-167.

[8] Buckley, C.A., Membrane technology for the treatment of dyehouse effluents. Water science technology, 10: 203-209 (1992).

[9] Bonomo, L., et al., Nanofiltration and reverse osmosis treatment of textile dye effluents. Récents progrès en génie des procédés, 6(20): 327-336 (1992).

[10] Treffry-Goatley, K., C.A. Buckley, and G.R. Groves, Reverse osmosis treatment and reuse of textile dyehouse effluents. Desalination, 47: 313-319 (1983).

[11] Rautenbach, R. and R. Mellis, Hybrid Processes involving membranes for the treatment of highly organic/inorganic contaminated waste water. Desalination, 101: 105-113 (1994).

[12] Tegtmeyer, D., Möglichkeiten und chancen einer membrantechnischen abwasserbehandlung in de textilfärberei. Melliand textilberichte, 74(2): 148-151 (1993).

[13] Fritsch, J. Untersuchungen der Aufbereitung von Abwässern aus Textilbleichern mittels Nanofiltration. in Aachener Membrane Kolloquium. Aachen (1993).

[14] Wenzel, H., et al., Reclamation and reuse of process water from reactive dyeing of cotton. Desalination, 106: 195-203 (1996).

[15] Porter, J.J. and G.A. Goodman, Recovery of hot water,dyes and auxiliary chemicals from textile wastestreams. Desalination, 49: 185-192 (1984).

[16] El-Nashar, A.M., Energy and water conservation through recycle of dyeing wastewater using dynamic Zr(IV)-PAA membranes. Desalination, 33: 21-47 (1980).

[17] Gaeta, S.N. and U. Fedele, Recovery of water and auxiliary chemicals from effluents of textile dye houses. Desalination, 83: 183-194 (1991).

[18] Kornmüller, A. ed., Treatment of wastewaters from textile processing, Colloquium TU Berlin 17-18 november (1997).

[19] Luiken, A.H., Uitspoelen van ongefixeerde reactieve kleurstoffen. Personal communication, (1997).

[20] Mishra, G. and M. Tripathy, A critical review of the treatments for decolourization of textile effluent. Colourage, Oct.: 23-38 (1993).

[21] Groves, G.R., et al., Dynamic membrane ultrafiltration and hyperfiltration for the treatment of industrial effluents for water reuse. Desalination, 47: 305-312 (1983).

[22] Brandon, C.A., et al., Closed cycle textile dyeing: Full scale renovation of hot wash water by hyperfiltration. Desalination, 39: 301-310 (1981).

Chapter 2

The application of membrane technology for reuse of process water and minimisation of wastewater in a textile washing range

- Benefits and limitations of the implementation of membrane processes in a textile washing range subsequent to a pad-steam reactive dyeing process – paper presented in Journal of Society of Dyers and Colourists Volume 113 October 1997 (p 287-294).

Summary

Recycling of process-streams and reduction of waste disposal using membrane technology in a continuous textile washing process after dyeing with reactive dyes have been investigated theoretically. A mathematical process model of a conventional open-width washing range has been extended by membrane processes to determine the benefits and limitations of the modified washing processes. The concentrations of hydrolysed reactive dyes, NaCl, urea and caustic soda have been calculated with this process model. Reverse osmosis for desalination and decolourising and nanofiltration for decolourising have been implemented as membrane technology. Reusing filtered wash water in a previous wash step results in more water saving than recycling to the same wash step according to the process calculations. The total fresh water demand can be reduced by 70 % and the total wastewater volume by 90 % compared to the conventional process. Greater reduction of fresh water use is limited by the osmotic pressure difference between the retentate and permeate streams.

2.1 Introduction

Several processes are carried out in the textile industry to obtain textile products with the desired properties. Excess chemicals used in these processes to meet the desired product properties need to be washed out. The amount of wash water can be more than 100 litres per kg product, resulting in huge streams of waste. At present in the Netherlands these waste streams are treated in municipal treatment plants. In the future this procedure will be confronted with rising costs or even prohibited. At the same time the availability of fresh process water will decrease and its price will increase. A research project has been started with the aim to investigate the application of membrane separation in textile washing processes with the purpose to recycle water back into the process. This way of processing can also result in energy conservation as parts of the washing processes are executed at elevated temperatures.

Wastewater containing reactive dyes is considered as a problematic waste of the textile industry as they are removed less efficiently when compared with other dye classes by activated sludge sewage treatment works [5]. Moreover, the fixation of the reactive dyes on the textile fabrics is low, 70 % on average, compared to other dye classes (over 90 % on average). The continuous washing process following a pad-steam reactive dyeing process (figure 2.1) has been studied here.

2.2 Process description

The pad-steam reactive dyeing process consists of a dyeing bath and a steamer. In the dyeing bath the substrate (woven or knitted fabric) is brought into contact with a dye liquor (see figure 2.1). The fixation (reaction of the dyes with the fabric) occurs in the steamer. The (dry) fabric stream is 1000 kg/hr. The entrapped liquid stream is 0.6 kg per kg dry fabric. The components which (greater parts) must be washed out are listed in table 2.1.

Table 2.1 Contents of the fabric after the fixation process * This is 30 % of the total dye uptake in the preceding dyeing step, which is 12 g/kg per dry fabric

Components	Component concentration [g/kg dry fabric]	Function in the dyeing process
Non-fixed hydrolysed reactive dyes	3.6 *	to dye the fabric
Common salt (NaCl)	150	to enhance the dye uptake by the fabric
Urea	80	to enhance the water uptake in the steamer
Caustic soda	9.6	to enhance the reaction between dye and fabric

Non-fixed hydrolysed reactive dyes and auxiliary chemicals need to be washed out in a washing range (figure 2.1) to meet the product specifications. The temperature and liquid throughput of the several wash sections in the washing range can be found in table 2.2.

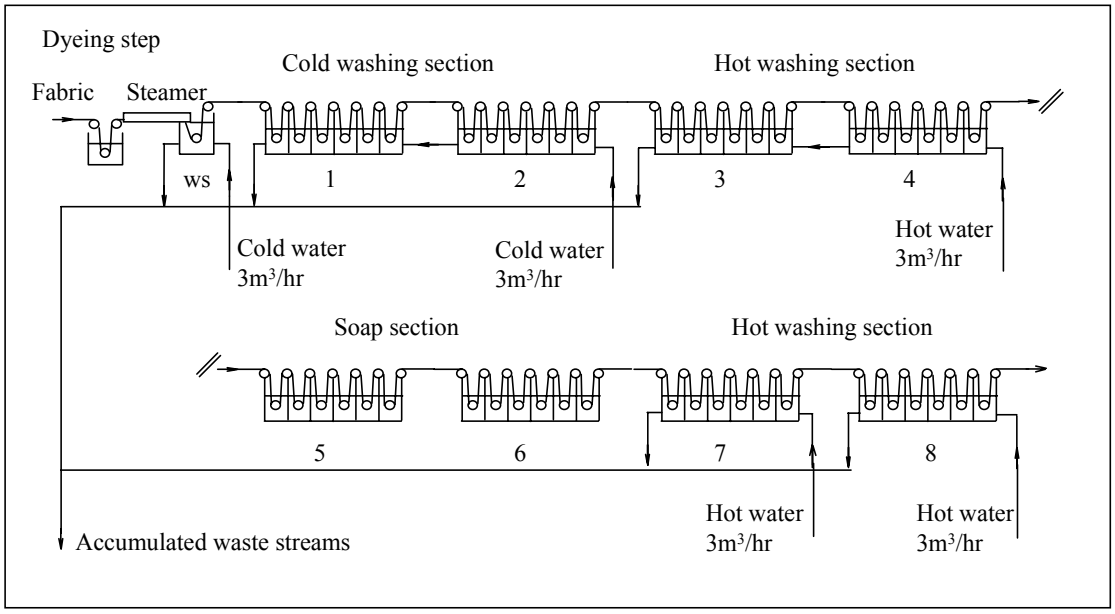

Figure 2.1 Flow diagram of dyeing step and subsequent open width washing range of a conventional reactive dyeing process (pad-steam), based on information of Ciba Geigy [4]

Table 2.2 Data of the washing process

Wash section	Liquid throughput [m^3/hr]	Temperature [°C]
Waterseal (ws)	3	± 40
Cold (units 1+2)	3	20
Hot (units 3+4)	3	80
Soap (units 5+6)	0	80
Hot (unit 7)	3	80
Hot (unit 8)	3	80

Furthermore, many auxiliary components are used such as anionic and non-ionic detergents, emulsifiers and pH-buffers. At present it is not feasible to account totally for the presence of these components, since their washing-out efficiency in the washing range has not been reported [3]. Their influence in the membrane separation processes will be dealt with in a qualitative way in this study.

The waterseal behind the steamer has several functions. It is an effective barrier to oxygen penetration into the steamer. It cools the fabric and it stops the reaction between fabric and dyes. It is also a (small) wash unit. The eight other wash units consist of several compartments each. The fabric is transported through the compartments by guide-rollers. The wash units 1 and 2 must be operated at moderate temperatures (20-30 °C), as higher temperatures in combination with high pH may cause already fixed dyes to hydrolyse [4]. In these units the greater part of salt, urea and caustic soda are washed out and the pH drops. The washing out of the non-fixed dyes has to be carried out at higher temperatures with soap. Not all the non-fixed dyes can be washed out economically. The remaining non-fixed dyes can be fixed on the fabric after the washing process by immobilising them with a cationic surfactant.

The final quality of the product is defined by the overall removal of the non-fixed dyes. In conventional processes this removal is about 90 %. The total quantity of wash water to achieve this removal is 15 litre per kg substrate. It should be mentioned that procedures for textile washing differ from company to company and even from product to product in the same company. This case is taken as a specific example that shows both the benefits and

limitations of process water reuse and minimisation of wastewater in a textile washing range by process-integrated membrane separation.

2.3 Washing efficiency

A wash unit consists of several compartments (six in this case). In figure 2.2 a simple model of one compartment is shown. Ideal mixing is assumed in the bulk, the fabric and associated fluid pass through under plug flow conditions.

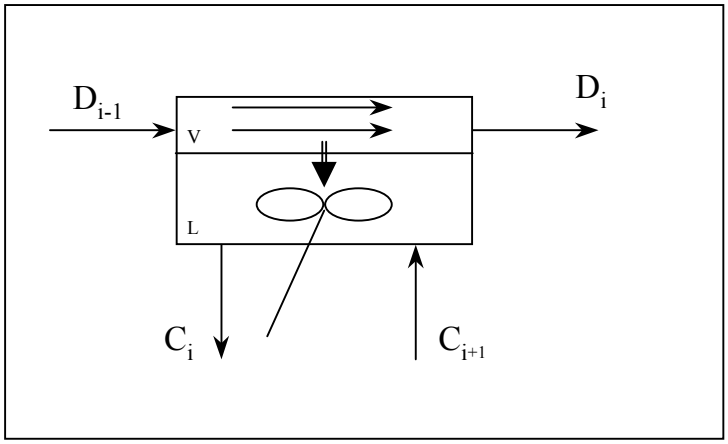

Figure 2.2 Model of a compartment in a wash unit V = textile fabric; L = wash water

A quantitative description of the mass transfer between fabric and liquid is not used in this model, as the entrainment of wash water in the fabric is a complicated factor. Therefore the washing efficiency of each compartment is defined similar to a Murphree plate efficiency for distillation [8].

$$M = \frac{D_{i-1} - D_i}{D_{i-1} - D_i^*} \qquad (2.1)$$

In which D_{i-1} and D_i are the concentrations of a component, based on dry fabric, in the fabric flows entering respectively leaving the compartment. D_i^* is the component concentration in the fabric leaving the compartment which is assumed to be in equilibrium with the wash water. The equilibrium parameter is defined as:

$$D_i^* = m \cdot C_i \qquad (2.2)$$

Experimental investigations of a wash compartment have been carried out by Luiken et al. [3]. They calculated efficiencies by assuming m=1 (table 2.3). This is not the case in the actual situation and the values of M can only be used in concentration ranges close to the experimental ones in these investigations. The efficiency becomes then:

$$M = \frac{D_{i-1} - D_i}{D_{i-1} - C_i} \qquad (2.3)$$

The concentrations C_i and D_i in the stationary state can be calculated, as the fabric streams (V in kg/hr) and wash streams (L in kg/hr) are known, using the mass balance:

$$V \cdot (D_{i-1} - D_i) + L \cdot (C_{i+1} - C_i) = 0 \qquad (2.4)$$

The overall washing process is described by wash compartments in series (figure 2.3).

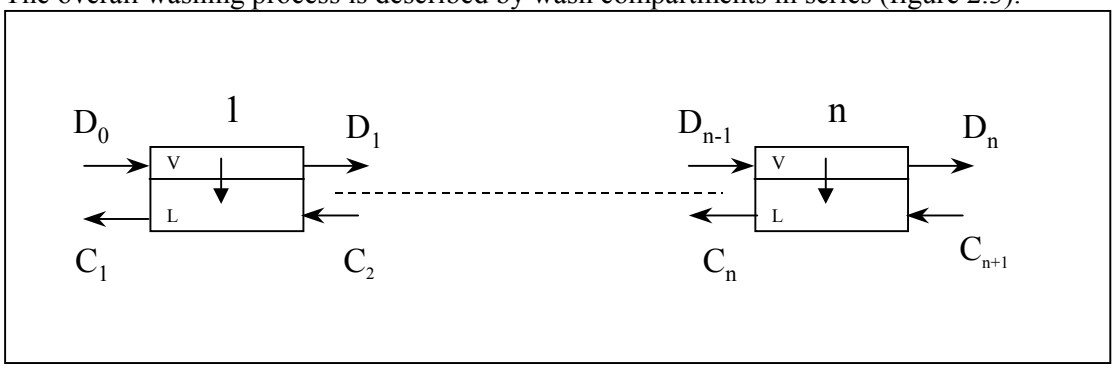

Figure 2.3 Model of a wash unit consisting of compartments in series

For compartments in series a relationship for the D_n as function of D_0 and C_{n+1} can be derived out of equations (3) and (4) if M is constant:

$$D_n = \frac{\frac{1}{F} - 1}{\frac{1}{F} - \left(\frac{1}{P}\right)^n} \cdot D_0 + \frac{1 - \left(\frac{1}{P}\right)^n}{\frac{1}{F} - \left(\frac{1}{P}\right)^n} \cdot C_{n+1} \qquad (2.5)$$

In which F is the liquor ratio defined as liquid flow divided by fabric flow.

$$F = \frac{L}{V} \qquad (2.6)$$

and:

$$P = \frac{M}{F} + 1 - M \qquad (2.7)$$

The temperature of the fabric and wash water streams are calculated by assuming that the outgoing wash streams and the outgoing fabric streams have the same temperature.

2.4 Performance of the conventional open-width washing range

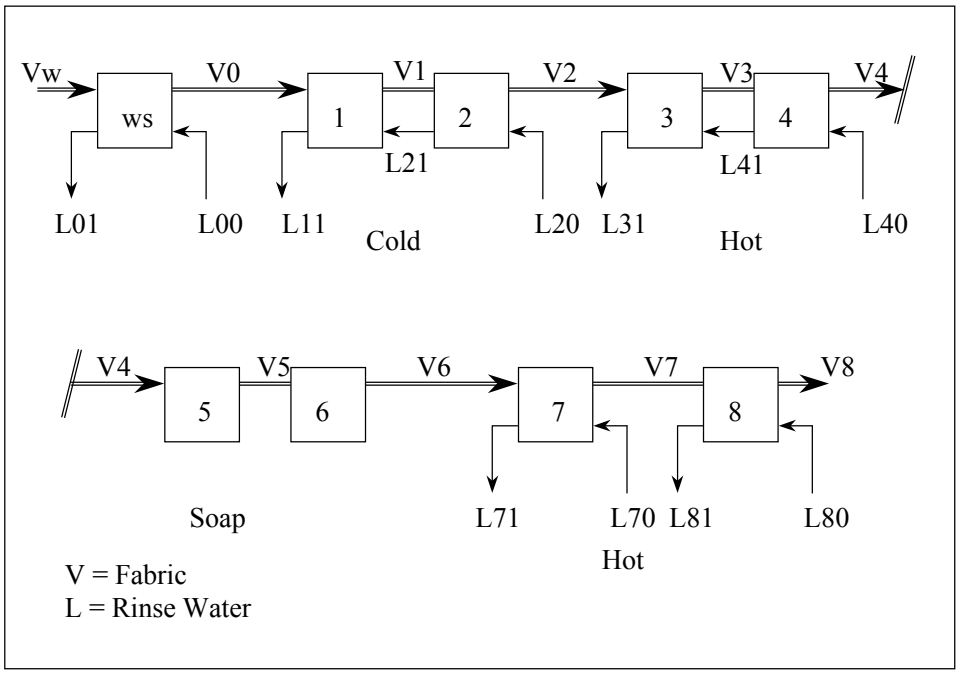

Figure 2.4 Diagram of the conventional Washing Process A1.

The efficiencies for Process A1 (figure 2.5) are given in table 2.3. From this, with equations 2.3-2.7, it can be calculated that 15 cubic metres per hour of water must be used to meet a calculated overall removal efficiency of 87.7 % of non-fixed dyes. The fabric stream Vw contains 3.6 and V8 thus 0.443 gram non-fixed dyes per kg dry fabric. The liquor ratio is constant along the washing range i.e. 3.

Even without the use of membranes water can be saved. This has been shown in Process A2 (figure 2.5). Here unit 1 is connected to the waterseal and unit 8 to unit 7. The connection between unit 3 and 2 has not been made because of the difference of the temperatures between these sections and the connection between unit 7 and 4 has not been made in order to keep the soap in the last wash sections. The wash water supply for Process A2 to meet an overall removal efficiency of 87.7 % of non-fixed dyes is 11.7 cubic metres per hour with a (constant) liquor ratio of 3.9.

Table 2.3 Reported efficiencies for a conventional Washing Process [3]

	non-fixed hydrolysed dyes	salt, urea, caustic soda
waterseal (ws)	0.2	0.5
unit 1 compartment 1	0.2	0.4
unit 1 compartment 2	0.1	0.2
rest of unit 1 and unit 2	0.05	0.2
units 3+4	0.05	0.25
units 7+8	0.05	0.2

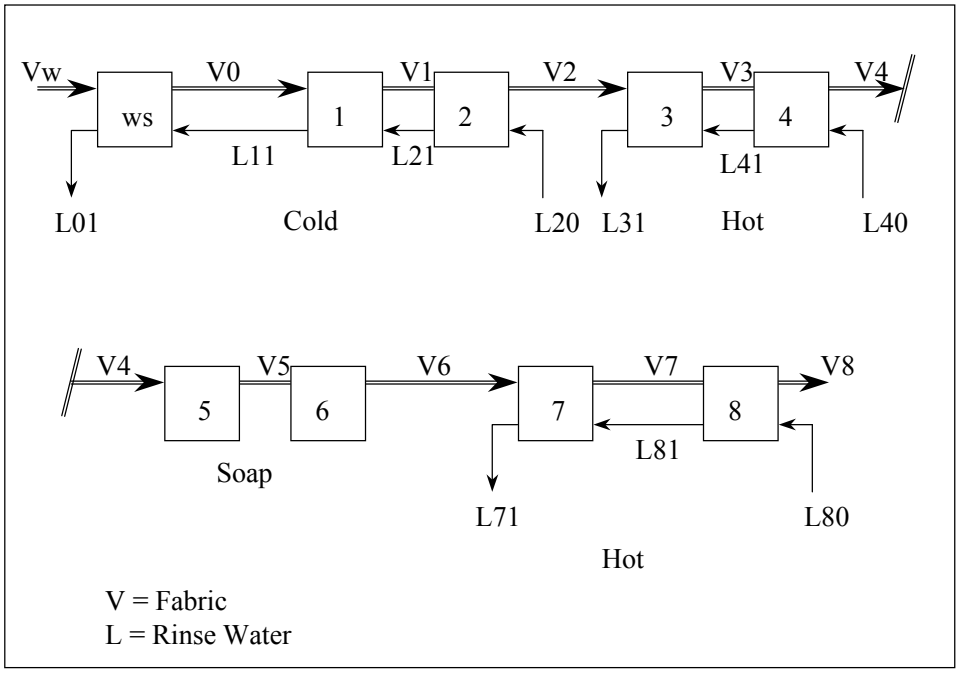

Figure 2.5 Diagram of the modified conventional Washing Process with more countercurrent washing (Process A2)

The concentrations of all components in the incoming fresh water streams are taken to be zero except for NaCl which is taken to be 0.25 g/l [9].

2.5 Introduction of membrane separation into the washing process

When introducing membranes into the continuous washing process the following questions may be considered:

- which membrane separation step to use?
- where to install the membrane separation in the process?
- where to recycle the wash water after filtration?

To fulfil the aim of recycling the wash water has to be desalinated and decolourised. This can be performed in one step by reverse osmosis (RO). However, in case of the osmotic pressure becoming too high to achieve a reasonable trans-membrane permeate flux, nanofiltration (NF) has been proposed for concentrating only high molecular weight organic wastes (dyes in this case). The permeate of the nanofiltration is a NaCl solution which may not be recycled to the washing process, but may be reused in other contiguous textile finishing processes. (e.g. dyeing processes).

The membrane separation processes have been considered following two methods:

- Process-integrated treatment with recycling of the wash water into the washing process. The aim here is to minimise the use of water and energy. Reverse osmosis is used for this purpose.
- End of pipe treatment with no recycling of wash water into the washing process Here the aim is to minimise (or concentrate) the waste streams. Nanofiltration is used for this purpose.

In principle all streams Lx1 (figure 2.1) may be treated by a membrane separation process. However, this is not economically attractive in first instance. The selected approach here is to treat the wash sections separately (cold washing; hot washing before soap addition, hot

washing after soap addition). The streams L01, L31 and L71 have been chosen for membrane separation treatment.

A process-integrated method of operation may be carried out in two ways:

1. Applying complete countercurrent flow in the process by reusing the filtered wash water to a previous wash unit (Washing Process B, schematically outlined in figure 2.7. A heat exchanger is necessary to cool down stream L31 for reuse in the cold section. This heat may be used to partly heat up incoming stream L80.

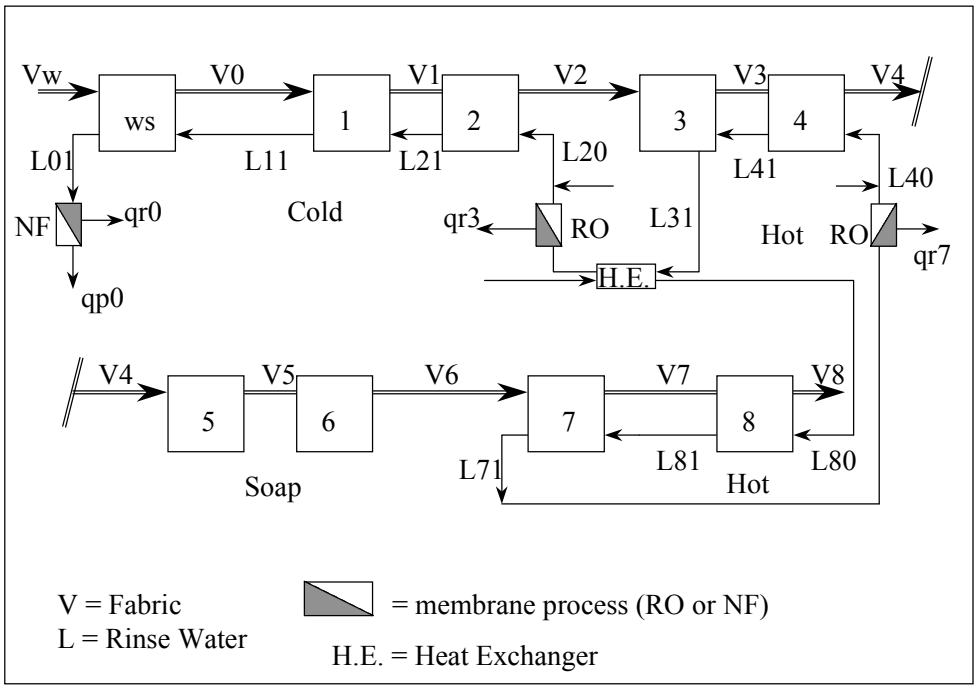

Figure 2.6 Washing Process B

2. Another way of using membrane separation is to treat each wash section separately (Washing Process C schematically outlined in figure 2.7). The wash water out of one section (e.g. units 3 and 4) is recycled after filtration to the same wash section. For the cold section this is not recommended as a large temperature rise will occur. Therefore stream L11 instead of stream L01 has been chosen for recycling. The advantages of Process C over Process B are that no extraneous components (e.g. soap) will enter specific wash sections and that the flexibility of processing is higher as process-integration is carried out on a smaller scale. Flexibility of processing may be needed in washing processes that are short in duration and batch-like.

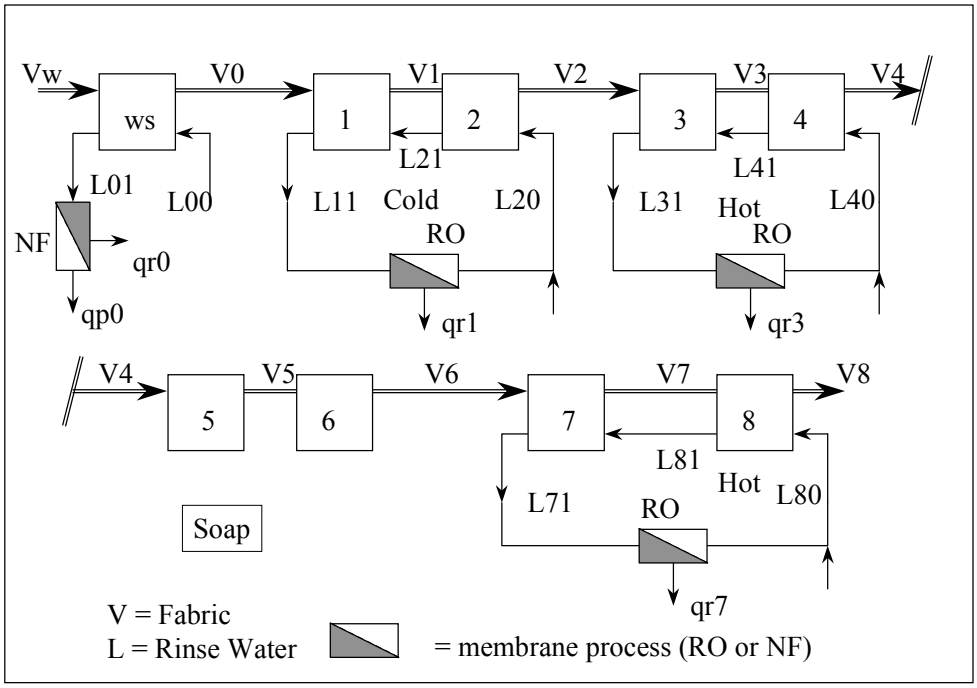

Figure 2.7 Washing Process C

In the calculations the membranes separation steps are characterised by two parameters for respectively the retention and the volume reduction factor. The module configuration and required membrane area are not taken into account. The retention is defined as:

$$\mathrm{Ret} = 1 - \left[\frac{C_p}{C_r}\right] \tag{2.8}$$

Where C_p and C_r are the concentrations of the permeate and retentate respectively. The volume reduction factor (VRF) is defined as the flow of the feed entering the separation step divided by the flow of the retentate leaving the separation step.

$$\mathrm{VRF} = \frac{\Phi_{\mathrm{Feed}}}{\Phi_{\mathrm{Retentate}}} \tag{2.9}$$

For both Processes B and C the membrane separation steps used are reverse osmosis (streams L11, L31, L71) and nanofiltration (stream L01). For purpose of a sensitivity analysis by alteration of the separation conditions, membranes with different rejection characteristics (table 2.5) have been used for both reverse osmosis and nanofiltration.

Table 2.4 Retention of the solutes by the different membrane types

Membranes		dye	NaCl	urea, caustic soda
Type 1	RO	0.95	0.9	0.5
low retention	NF	0.95	0	0
Type 2	RO	0.99	0.99	0.5
high retention	NF	0.99	0	0

The volume concentration factor is taken to be 10, except for RO of stream qr1 in Process C that is taken to be 2.

2.6 Results and discussion

The main objectives of this case study were to show the benefits and limitations in the use of membrane separation processes in an open-width textile washing range. The benefits discussed here are:

- reduction of water consumption
- minimisation of wastewater volume
- energy saving

The limitations considered in this study are:

- temperature rise in the cold wash sections
- the required trans-membrane pressures for membrane processes
- altered wash water compositions

2.6.1 Benefits of the modified processes derived from the simulations

2.6.1.1 Reduction of water consumption

The aim of the calculations on the modified processes (figure 2.6 and 2.7) was to determine the influence of the characteristics of the applied membrane processes on the water saving by keeping the final quality of the fabric constant (i.e. dye removal = 87.7 %). Complete water recovery is impossible as the retentate streams always discard water. The reduction of the water consumption in the modified processes is due to the use of membrane separation processes and more countercurrent method of processing. The latter fact can be shown by comparing Process A1 and Process A2. Results are summarised in table 2.5.

Table 2.5 Fresh water use and energy use * Calculated by the temperature rise needed for the hot section (energy for reverse osmosis process not included) ** with heat exchanger

Process	Rejection by the membranes	Cold water consumption [m^3/hr]	Hot water consumption [m^3/hr]	Energy demand * per hour [kW]	Percentage of water saving
Process A1		6	9	628	0
Process A2		3.9	7.8	543	22
Process B1	low (type 1)	0.47	5.21	363 136 **	62
Process B2	high (type 2)	0.41	4.51	314 124 **	67
Process C1	low (type 1)	7.61	1.01	415	43
Process C2	high (type 2)	5.55	0.74	338	58

2.6.1.2 Wastewater volume reduction

The reduction of wastewater volume in Processes B and C compared to Process A1 are of the same order (90 - 93 %, table 2.8) This is due to the fact that the volume concentration factor of the NF, where the main part of waste is concentrated, is set at a value of 10 for both processes. The dye concentration in the produced salt water, stream qp0 (figure 6 and figure 7), will be increased by a higher volume concentration factor or a lower retention of the dye. The separation between dye and salt thus requires membranes with a high retention of dyes and low retention of the salt under process conditions. More waste reduction can be achieved by combining the stream L01 with the retentate streams from the reverse osmosis processes. The possibilities of this use of nanofiltration technology are not identified yet and more research is required.

Table 2.6 Reduction of wastewater volume and production of salt water

Process	Wastewater dye [kg/hr]	Wastewater flow [m^3/hr]	Salt water dye [kg/hr]	Salt water flow [m^3/hr]
Process A1	3.16	15.00		
Process A2	3.16	11.70		
Process B1	2.41	1.42	0.75	4.26
Process B2	2.97	1.23	0.19	3.69
Process C1	2.94	1.52	0.22	4.56
Process C2	3.10	1.11	0.06	3.33

2.6.1.3 Energy saving

Reduction of energy consumption in the washing process occurs as a result of a lower hot water intake. However, with decreasing fresh hot water intake more additional heating in the wash units will be necessary. Corrections for these conditions were necessary in Process C. The energy saving in the modified processes without extra heat exchange is approximately 30-50 % (table 2.5).

The energy saving in the modified processes seems promising but the same saving may be reached by applying heat exchangers only instead of membranes in combination with heat exchangers. Furthermore, the membrane processes will increase the energy demand as high pressures are needed. However the energy demand for such processes is quite low, approximately 3-5 kWh per m^3 permeate and thus the increase is approximately 12-25 kW per membrane system.

2.6.2 Limitations of the modified processes

2.6.2.1 Temperature rise in the cold wash section

In Process C the temperature of the wash water in the first compartment of the first unit is comparable to the temperature in the conventional process. In Process B this temperature is approximately 5-10 °C higher than the temperature in the conventional process (table 2.7). Limitations on this rise in temperature have a negative influence on the water recovery ability of the process, i.e. more water is needed in the waterseal for cooling. However, there is no consensus about these limitations among industrialists and researchers in the textile industry. Schulz et al. [2] have claimed that it is not necessary to perform the first washing step at a moderate temperature. They proposed to wash with hot water along the washing range in order to diminish the number of wash units. From the process point of view, this method of processing will have improved opportunities for water and energy recycling as complete countercurrent processing in combination with membrane separation can be applied without an additional heat exchanger. However, the occurrence of high pH (~10) and high temperatures (~ 80°C) can not be tolerated by commercial polymeric membranes. Moreover

2.6.2.2 Required trans-membrane pressure for membrane processes

The trans-membrane pressure ΔP (bar) required to obtain a reasonable permeate flux J_v (litre/m^2hr) in reverse osmosis is determined by both membrane and fluid properties. A rough estimate of this flux can be given by [7]

$$J_V = A \cdot (\Delta P - \Delta \Pi) \qquad (2.10)$$

Here A is the (clean water) permeability of the membrane. The influence of the fluid properties is described in this study by the osmotic pressure difference ΔΠ (bar).

$$\Delta \Pi = R \cdot T \cdot (C_r - C_p) \qquad (2.11)$$

Here R is the gas constant and T the temperature. C_r and C_p are the sum of the concentrations (in mole/m^3) of all solutes for respectively retentate and permeate.

Too much flux decline due to too high osmotic pressure differences may be avoided by:
- Decreasing the volume concentration factor: the retentate concentration C_r will decrease
- Decreasing the rejection of the solutes by the membrane: the permeate concentration C_p will increase

The first measure, a lower VRF, has already been taken in the RO unit treating stream L11 of Processes C (figure 2.7). However, the osmotic pressure of the retentate is still high (over 25 bars). This RO process is therefore not recommended.

Effect of the second measure can be shown by comparing the osmotic pressure differences (ΔΠ) between retentate and permeate of Processes C1 and B1 with C2 and B2. Treating a stream with high rejection membranes results in higher osmotic pressure differences. The difference in ΔΠ between Processes B and C is mainly due to the stronger accumulation of urea in Processes C.

Table 2.7 Osmotic pressure differences (ΔΠ) between retentate and permeate in membrane systems and temperature rise in 1st compartment of 1st unit. * volume concentration factor = 2 instead of 10

Process	ΔΠ qr1 [bar]	ΔΠ qr3 [bar]	ΔΠ qr7 [bar]	Temperature [°C] 1st comp. 1st unit
Process A1				25.4
Process A2				24.2
Process B1		8.0	1.4	31.5
Process B2		16.4	2.7	32.3
Process C1	25.5 *	11.6	2.8	23.5
Process C2	39.2 *	19.6	3.0	25.9

2.6.2.3 Alteration of the wash conditions

Recycling of process water leads to (unwanted) accumulation of components, which are not rejected by the membranes. These components may have an influence on the washing out efficiency of other components. In this empirical model for the washing process influences of salt, urea and caustic soda concentrations on the washing out efficiency of the dyes are not implemented. However, it is known from practice that NaCl does have an influence on the washing performance [3].

The NaCl concentrations in the wash units 7 and 8 in Process C2 (with high rejection membranes) is lower than those in Process A1 en Process B2. The high rejection membranes produce a permeate stream with a lower salt concentration than in the original fresh water used in the conventional process. Therefore very high rejection membranes (over 99 % NaCl rejection) are not necessary here.

In Appendix A dye concentration, NaCl concentration and pH as function of the position in the washing range are shown. The differences of the concentrations between the conventional and the modified processes are small, so it can be concluded that the process model may be used here.

The pH in the hot section of Process C is calculated to be higher than the pH in the conventional process and Process B, because of the higher concentration of caustic soda. This may enhance the unwanted hydrolysation reaction of already fixed dyes. Furthermore the membrane materials can be damaged at the occurrence of high pH and high temperature simultaneously. Lowering the pH by adding acid is thus recommended here.

2.6.2.4 Fouling of membranes and concentration polarisation

The required membrane area for a given permeate capacity is determined by the permeate flux. This flux depends on the membrane properties, transmembrane pressure and the osmotic pressure difference (eq. 2.10). The osmotic pressure difference (eq. 2.11) has been determined in this study under bulk conditions of retentate and permeate. However, phenomena in the boundary layer adjacent to a membrane surface will have more influence on the flux than bulk properties. Solutes rejected by the membrane will accumulate in the boundary layer and increase the resistance against permeation. This phenomenon, called concentration polarisation, enhances the fouling of the membrane by adsorption of components on the membrane resulting in a decline of the permeate flux in time. For the wastewater considered here, little is known about the fouling-flux behaviour in membrane systems. This is complicated by the fact that this wastewater contains auxiliary chemicals like surfactants. More research on flux decline phenomena will be carried out during the present research project.

2.7 Conclusions

Recycling of water and energy by the use of process-integrated membrane technology in an open width textile washing range has been analysed. An empirical process model has been used to determine the concentrations in the process streams and to estimate the possibilities for reusing water and energy and decreasing the total waste volume. Two process modifications of the textile washing range have been suggested. The filtered wash water from a wash step can be recycled to a previous wash step (Process B) or to the same wash step (Process C). Process B is better in terms of total water and energy savings and continuous processes. Process C is more suitable in terms of process flexibility and batch processing.

The water saving in Process B is approximately 60 to 70 % and in Process C approximately 50 to 60 %. An additional benefit is energy conservation by reduction of hot water intake. Reduction of wastewater volume is the most attractive element using membrane separation, as draining this dye-containing wastewater will be restricted in the nearby future. This reduction is about 90 volume percent in both processes.

From a processing point of view it can be stated that reuse of process water and minimisation of waste volume in a textile washing range by membrane separation are promising. Important

criteria for the applicability of nanofiltration and reverse osmosis in this textile washing process are retentions (of dyes and salt) and membrane fouling. More research will be carried out within this research project towards these phenomena.

Acknowledgement

The author wishes to thank Senter (Ministry of Economic Affairs) for their financial support and A. Luiken (TNO Delft) and C.J.N. Rekers (Stork Friesland) for their contribution.

Symbols

		units
$\Delta\Pi$	Osmotic pressure difference	[bar]
ΔP	Trans-membrane pressure	[bar]
Φ_{Feed}	Feed flow membrane process	[m^3]
$\Phi_{Retentate}$	Retentate flow membrane process	[m^3]
A	Clean water permeability	[m/s bar]
C	Concentration in wash water	[kg/kg water]
C_p	Permeate concentration	[mole/m^3 water]
C_r	Retentate concentration	[mole/m^3 water]
D	Concentration in the fabric	[kg/kg dry fabric]
F	Liquor ratio	[kg water/kg dry fabric]
J_v	Permeate solvent flux	[m/s]
L	Wash water flow	[kg/s]
m	Equilibrium constant	[-]
M	Efficiency	[-]
R	Gas constant per mole	[J/mole K]
Ret	Retention	[-]
T	Temperature	[K]
V	Dry fabric flow	[kg/s]
VRF	Volume Reduction Factor	[-]

Literature

[1] H.J.L.J. van der Linden, J. Groot Wassink, H.J. Vos. Non-stationary mass transfer in open-width washing machines, Text. Res. J. 54: 77 (1984).
[2] G. Schulz, D. Fiebig, H. Herlinger. Minimierung der Umweltbelastung bei Prozessen der Textilveredlungsindustrie, Melliand Textilberichte 2: 137-143. (1993).
[3] A.H. Luiken, G.J.M. Schrijer, D.W. Ravensberger. Recycling of rinse water in rinsing processes of non-fixed reactive dyes, Confidential TNO-rapport (1993).
[4] Cibacron Farbstoffe in der Foulard Färberei, Product information Ciba Geigy.
[5] J. Pierce. Colours in textile effluents - the origins of the problem, JSDC, vol.110 (april 1994).
[6] H.J.L.J. van der Linden, J. Groot Wassink. A new approach in process analysis and design of textile finishing equipment, IFATCC-congress Barcelona. (1975).
[7] R. Rautenbach and R. Albrecht. Membrane Processes, John Wiley & Sons Chichester (1989).
[8] R.K. Sinnott. Coulson & Richardson's Chemical Engineering, vol. 6, 2nd ed., Pergamon Press, Oxford (1993).
[9] Vlisco Helmond B.V., Personal communication.

Appendix 2A Concentrations of dye and salt, and pH in the different streams of the washing processes.

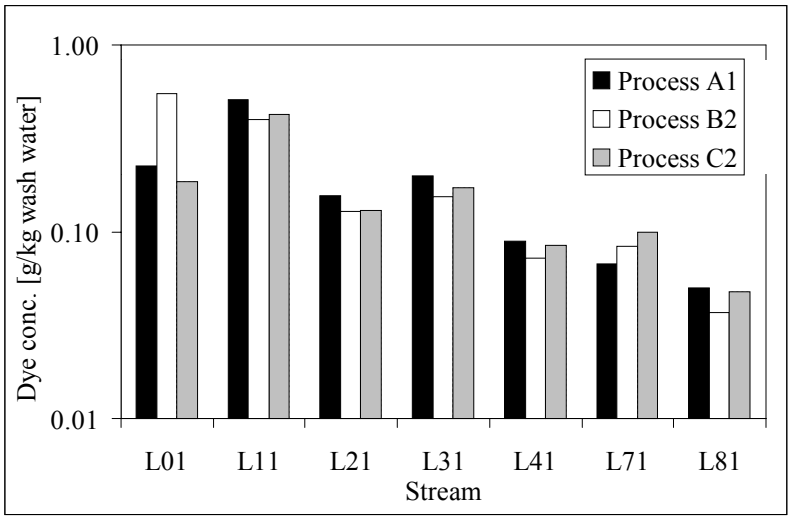

Figure 2A.1 Dye concentration in the various streams of the washing processes.

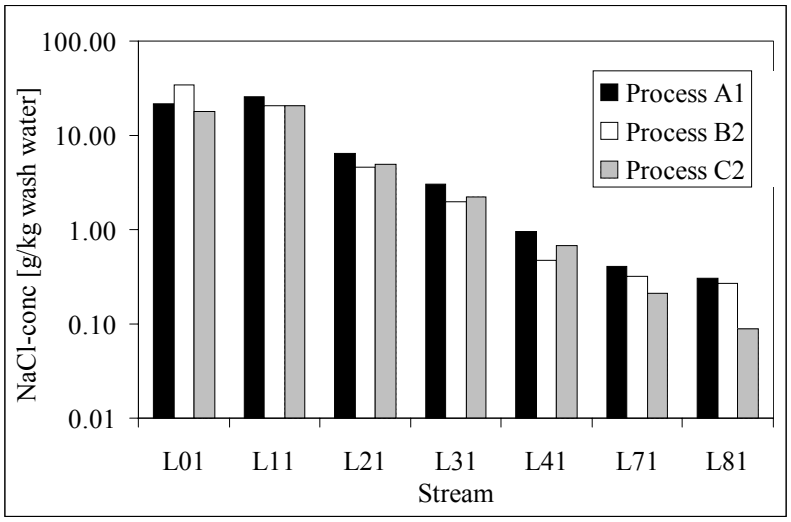

Figure 2A.2 NaCl-concentration in the various streams of the washing processes.

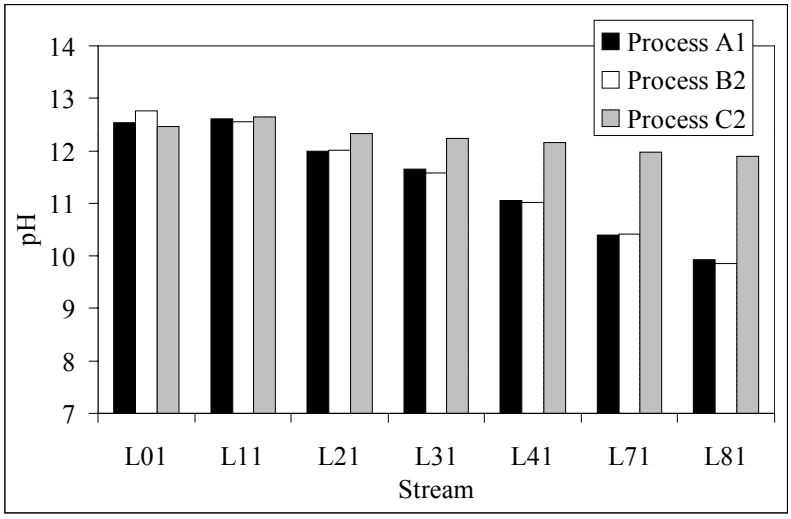

Figure 2A.3 pH of the various streams in the washing processes.

Chapter 3

Theoretical background membrane filtration

Summary

Permeate flux of the solvent and separation of the solutes are the main issues when treating wastewater by membranes. Preferential adsorption of components or deposition of insoluble components on the membrane can lead to an increase of resistance against transport of the solvent, leading to a decline in the permeate flux. This phenomenon is called membrane fouling. Membrane fouling can also influence separation characteristics as the retention of a solute is determined by the ratio of the transport rates of solute and solvent. In this chapter theoretical considerations will be given about the influence of membrane properties, hydrodynamic conditions and chemical compositions of the waste stream on membrane fouling and solute separation characteristics of RO and NF membranes.

3.1 Introduction

The use of membrane technology for the treatment of wastewater from the washing process subsequent to reactive textile dyeing processes can lead to a reduction of fresh water consumption and a decrease of total wastewater volume as was shown in the proceeding chapter. Criteria for good operation are reasonable permeate fluxes and retention of the key components dye and NaCl by RO and dye by NF membranes.

This chapter will describe the influence of process parameters on permeate flux and separation characteristics, which are (expected to be) relevant for the treatment of wastewater from a textile reactive dyeing and subsequent washing process by RO and NF membranes.

Special attention will be paid to electrostatic properties of the membrane influencing solvent flux and solute retention. The electrostatic properties of the membrane have their origin in the fixed charges of the membrane. The amount of fixed charges determine the Donnan potential, which can be used to explain ionic solute up-take in the membrane and the zeta potential, which will be used to explain membrane fouling in combination with the electrodynamic properties of the membranes.

3.2 Factors influencing solvent permeate flux

3.2.1 Transmembrane pressure and osmotic pressure

The permeate flux of the solvent is proportional to the driving force across the membrane

$$J_v = A \cdot (\Delta P - \Delta \Pi_{i,p}) = \frac{(\Delta P - \Delta \Pi_{i,p})}{\eta \cdot R_m} \qquad (3.1)$$

The parameter A is called the solvent permeability coefficient of the clean membrane, which is a combination of the solubility and the mass transport of the solvent in the membrane. The driving force for solvent permeation is the pressure difference minus the osmotic pressure difference over the membrane. The osmotic pressure difference between two process streams can be determined directly with a membrane osmometer or indirectly by measuring the freezing point depression with an osmometer.

$$\Delta \Pi_{i,p} \cong R \cdot T \cdot (C_i - C_p) \qquad (3.2)$$

In dilute solutions the osmotic pressure is linear proportional to the total molar concentration (for completely dissociated electrolytes the total molar concentration is defined as the total ion concentration) of dissolved solutes according to the Van ‘t Hoffs relation (eq.3.2). At higher concentrations non-linear relationships or tabulated data are available in the literature [1].

The osmotic pressure difference between feed and permeate has to be known to estimate the maximal permeate flux which can be obtained at a certain transmembrane pressure for a given membrane (neglecting thus concentration polarisation and membrane fouling).

3.2.2 Concentration polarisation

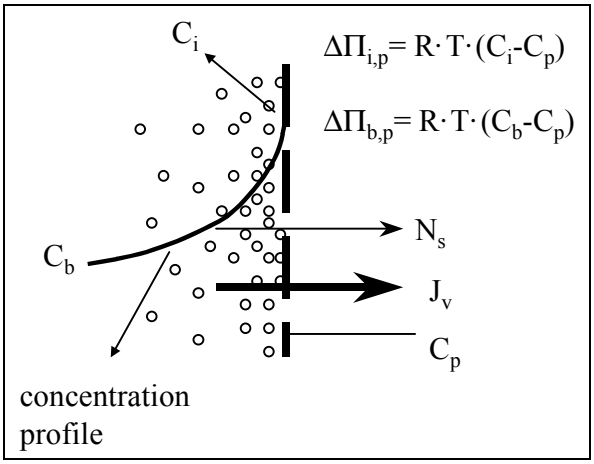

Figure 3.1 Concentration polarisation

Concentration polarisation is the phenomenon that solutes accumulate in the boundary layer as these solutes are rejected by the membrane (figure 3.1). A steady concentration profile is established when the convective solute transport towards the membrane is counterbalanced by the diffusive solute transport towards the bulk. Equation 3.3, which can be used for all pressure driven membrane processes, describes this solute accumulation [2, 3].

$$\left[\frac{C_i - C_p}{C_b - C_p}\right] = \exp\left[\frac{J_v}{k}\right] \qquad (3.3)$$

In this equation, the convective transport of solutes towards the membrane is characterised by the permeate solvent flux (J_v) and the diffusive solute transport to the bulk by the mass transfer coefficient (k). The mass transfer coefficient can be determined from well-known Sherwood correlations for different hydrodynamic circumstances [4, 5 and 6].

The increased concentration at the membrane surface leads to a higher osmotic pressure difference over the membrane. Combining eq. 3.2 with eq. 3.3 the permeate solvent flux across the boundary layer and the membrane can be calculated:

$$J_v = A \cdot \left[\Delta P - \Delta\Pi_{b,p} \cdot \exp\left[\frac{J_v}{k}\right]\right] \qquad (3.4)$$

3.2.3 Membrane fouling

In the description of concentration polarisation the limiting step for the permeate flux is thus only determined by the back diffusion of the solute. Other phenomena resulting in permeate flux decline, like adsorption or deposition on or in the membrane of components present in the wastewater, are called membrane fouling. Two models, the gellayer model and the resistance in series model, describing the influence of membrane fouling on the permeate flux, will be discussed here. In both models the concentration polarisation phenomenon is included in the description of the membrane fouling. Subsequent to that, influences of other parameters and other phenomena on membrane fouling will be discussed and two examples (silicates and anionic surfactants) of membrane fouling by components present in the textile wastewater will be presented.

The gellayer model, based on the concentration polarisation model (eq. 3.3), takes maximal membrane interface concentration to be the gel concentration. Under the assumption that the gelmaking components do not permeate through the membrane eq 3.5 can be derived from eq 3.3:

$$\left[\frac{C_g}{C_b}\right] = \exp\left[\left[\frac{J_v}{k}\right]_{max}\right] \qquad (3.5)$$

This model is often successfully applied in microfiltration and ultrafiltration processes when fouling occurs by gelating components. The permeate flux is then measured at different bulk concentrations and the C_g can be determined at the point where the permeate flux is zero by extrapolation. The gellayer model can only be applied if the permeate flux is constant and an increase of the transmembrane pressure has no influence on the permeate flux.

The second method is based on the addition of an extra resistance in series (according to Darcy's law) for the solvent permeation by membrane fouling (and concentration polarisation). The requirement for a constant permeate flux, like in the gellayer model, is not necessary for this model. This description is often applied to characterize the growth of the fouling layer (R_f) as function of time.

$$J_v = \frac{(\Delta P - \Delta \Pi_{b.p})}{\eta \cdot (R_m + R_f)} \qquad (3.6)$$

It is often observed that a membrane with a more open morphology exhibits more membrane fouling. Two (not completely) independent explanations can be given for this. Firstly, the concentration polarisation is increased if the solvent flux through the membrane is increased leading to a higher solute concentration at the membrane surface. Secondly, internal membrane fouling will occur if the membrane has a more open structure.

In the following paragraphs two examples of membrane fouling, i.e. by precipitation (scaling by silicates) and by preferential adsorption (adsorption of an anionic surfactant), are discussed. Influences of the electrochemical properties of the membrane, the NaCl concentration and pH of the waste solution will also be discussed. Membrane fouling by precipitation means that the solubility limit of this component in the solution is exceeded and that the component ‘precipitates’ on the membrane. Membrane fouling by preferential adsorption means that membrane fouling occurs at concentrations below any solubility limit. The difference between the two mechanisms is somewhat arbitrarily, but very useful in practice. Generally spoken, membrane fouling by preferential adsorption will be more severe as foulants, even present in very small concentrations, can completely block the membrane.

Prevention of membrane fouling by these foulants, by a prefiltration step, will not help and it is advised to avoid the use of these components in the textile refining processes.

3.2.3.1 Scaling by silicates

Silica and components derived from silica (e.g. silicates) are notorious for their fouling behaviour in RO filtration treating surface water [7]. Two forms of silica are distinguished: reactive and colloidal. Above a solubility concentration, agglomeration of reactive silica will occur into particles of colloidal size. It is stated [7] that silica in the colloidal form is the fouling component in reverse osmosis systems, by forming a scale layer on the membrane.

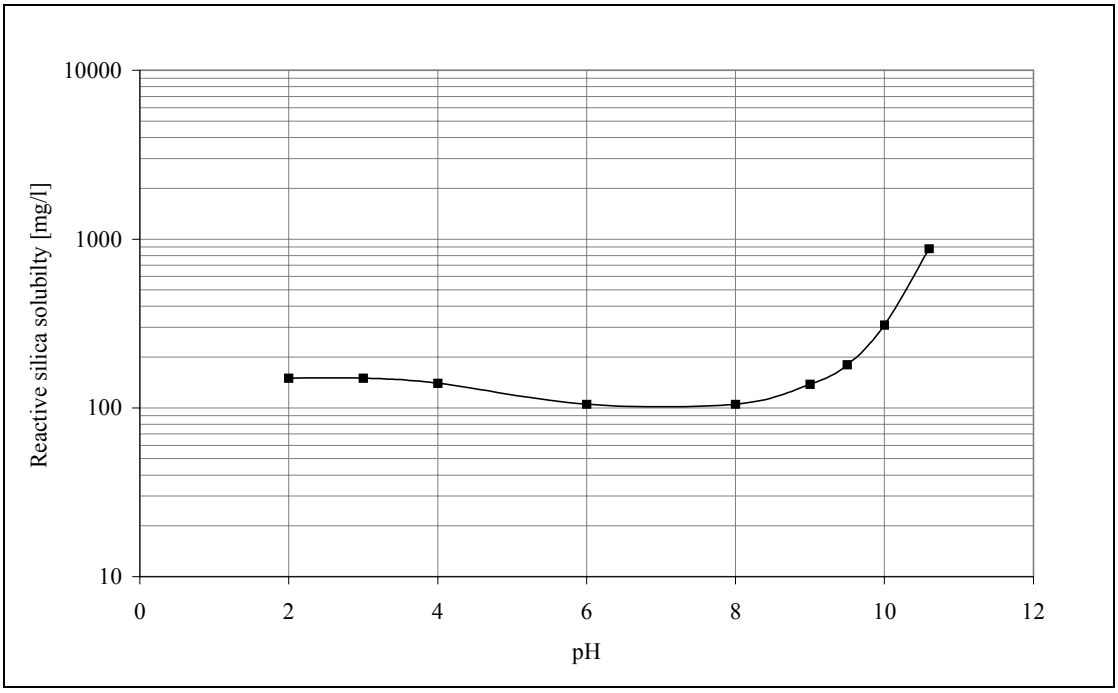

Figure 3.2 Reactive silica solubility in water as function of pH at 25 °C.

The pH and NaCl concentration can have an influence on the membrane fouling behaviour of silicates. Increasing the pH from neutral to basic conditions will decrease the membrane fouling tendency as the solubility of reactive silica increases (figure 3.2. [7]). Increasing the NaCl concentration will increase the rate of colloidal silica formation according to Iler [8], and thus the threat of membrane fouling.

3.2.3.2 Preferential adsorption of surfactants

Preferential adsorption of surfactants means the formation of a layer of surfactant monomers on a (membrane) surface in structures, called hemimicelles [10]. This can lead to membrane fouling even at low surfactant concentration, resulting in complete blocking of the membrane surface.

Considering surfactant adsorption onto membranes two membrane-surfactant interactions, i.e. electrostatic and electrodynamic, can be distinguished (figure 3.3). Electrostatic interaction occurs between an ionic component or ionic part of a component and an ‘electrically charged’ membrane surface. ‘Electrically charged’ means that the membrane contains fixed, immobile ionic groups, electrically counterbalanced by free moving ions.

The ionic part of the surfactant is called the head, which is negatively charged in case of an anionic and positively charged in case of a cationic surfactant. The tail of the surfactant is uncharged. The electrostatic interaction, repulsive if the membrane and ionic head group have the same charge and attractive in case of opposite charge, is very sensitive towards pH and 'background' salt concentration. A change of pH means ad- or desorption of protons and thus a decrease or increase of the number of electrical charged groups in the membrane. An increase of NaCl concentration leads to more shielding of the electrical charges by counter ions and thus to a lower influence of the electrostatic interaction. The electrostatic nature of a membrane surface can be determined by measuring the zeta potential, which is done in chapter 4.7.

Electrodynamic interactions occur between components as a consequence of the mutual influence of the components on their electron distributions. This is called electrical polarization and components can be classified in polar (easily polarisable) and apolar (hardly polarisable). As water is a very polar component, other components (solutes) and membrane surfaces can be classified in water like, i.e. hydrophilic (~ polar), or water repellent, i.e. hydrophobic (~ apolar). In simple chemical terminology, components with the same polarity will 'like' each other. Thus as rule of thumb membrane fouling by a specific solute on a specific membrane will occur more easily if the solute and the membrane are more hydrophobic.

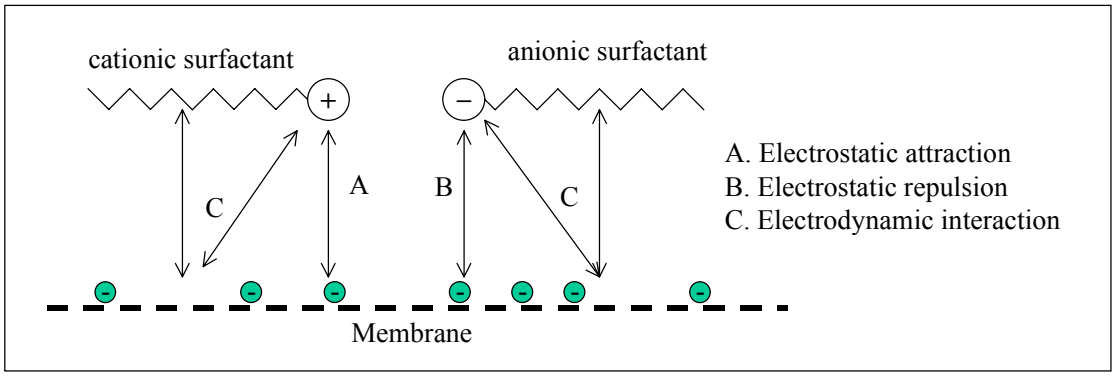

Figure 3.3 Interactions between ionic surfactants and an anionic membrane [9,10]

The hydrophilicity of the membrane can be determined by measuring the contact angle between a water droplet and the membrane surface. However the simple concept of polar/apolar often fails to explain membrane fouling. The method presented by Van Oss [24,25] is recommended to explain membrane fouling phenomena by surfactants more quantitatively (chapter 4.8).

Electrodynamic and electrostatic phenomena, although of completely different origin, can not be distinguished separately, as an ion also will exhibit electrodynamic interactions on non-charged components. Membranes often can be made more 'hydrophilic' by introducing more fixed-charges in the membrane matrix. However reduction of membrane fouling is then not always achieved, as the electrostatic attraction of dislike charges will be increased as well.

3.2.3.3 Surfactant aggregation and precipitation

Electrodynamic and electrostatic phenomena influence not only the adsorption of surfactants on a surface but also the formation of micelles, i.e. soluble aggregates of surfactants in solution. Micelles of ionic surfactants will be formed above the critical micelle concentration (cmc) and above the so-called 'Krafft temperature'. Below the cmc all the surfactants will be present in the monomer form. At the Krafft temperature the solubility concentration equals the critical micelle concentration and further cooling will lead to precipitation of the surfactant. [23]

It is supposed that the Krafft temperature and the cmc will influence membrane fouling considerably. Precipitation below the Krafft temperature (during membrane filtration) is unwanted, as it is very likely that a (precipitated) layer of surfactants will be formed on the membrane surface. The influence of the cmc is less straightforward. On one hand concentration polarisation will be increased, as the diffusivity of the micelle aggregates is larger than the diffusivity of the surfactant monomers. On the other hand if surfactant monomers contribute to membrane fouling by preferential adsorption, the introduction of micelles might prevent the forming of a hemimicelle on the membrane surface.

3.3 Factors influencing solute permeate flux and solute separation

3.3.1 Single solute – solvent system

The separation of a component by the membrane is expressed by its retention, defined as:

$$\mathrm{Ret} = 1 - \frac{C_p}{C_b} \qquad (3.7)$$

To explain the influences of the process parameters on the retention, a solution containing one solute (non-ionic component or electrolyte) and one solvent (i.e. water) is considered here.

The retention of the solute is dependent on the
- mass transport of solute and solvent in the membrane and in the boundary layer adjacent to the feed side of the membrane
- solubility or uptake of solute and solvent in the membrane matrix

It was not the aim of this thesis to investigate these phenomena quantitatively, as it is done in other studies [6,11,12,13,14,15]. Only an overview of those phenomena, which are of interest in this study, will be discussed briefly.

The concentration of the solute in the permeate can be described by eq 3.8 if the volumetric flux of the solute is much lower then the volumetric flux of the solvent.

$$C_p = \frac{N_S}{J_V} \qquad (3.8)$$

The driving force for solute transport through the membrane is a function of the concentration difference (diffusive transport) and the pressure difference (convective transport) over the membrane:

$$N_S = k1 \cdot \Delta C + k2 \cdot \Delta P \qquad (3.9)$$

In case of RO the solute transport for most solutes is diffusive and the convective term can be neglected (k2 ~ 0). In case of transport across NF membranes of small solutes or monovalent ions (e.g. NaCl) the convective contribution to the solute transport can not be neglected. Concentration polarisation has an influence on the separation conditions as the solute concentration at the interface is increased compared to the bulk concentration (figure 3.1).

Solubility phenomena in the membrane are normally not elaborated in the description of mass transport models across RO and NF membranes as those phenomena are lumped together with mass transport parameters. An exception to this is the Donnan exclusion phenomenon, which is often applied to explain the separation characteristics of 'charged' NF membranes.

Donnan exclusion of solute co-ions occurs at the interface of a membrane with fixed charges. As the fixed charges can not freely 'move out' of the membrane matrix the membrane will absorb solute counterions and repel solute co-ions. The concentration of a specific solute ion in the membrane is described by [16], in which the electrical potential difference between the solution and the membrane is expressed as the Donnan potential Φ_D.

$$\frac{a'_i}{a_i} = \frac{\varphi'_i \cdot c'_i}{\varphi_i \cdot c_i} = \exp\left[\frac{-Z_i \cdot F}{R \cdot T} \cdot \Phi_D\right] \qquad (3.10)$$

This description is valid under the following assumptions:
- the ions are taken as ideal point charges
- the fixed charges on the membrane are homogeneously distributed
- the membrane surface is smooth
- the solvent (water) has no influence
- membrane swelling phenomena are not taken into account

The Donnan potential can be calculated with the electro-neutrality condition in the membrane:

$$Z_f \cdot c'_f + \sum_i Z_i \cdot c'_i = Z_f \cdot c'_f + \sum_i Z_i \cdot c_i \cdot \frac{\varphi_i}{\varphi'_i} \cdot \exp\left[\frac{-Z_i \cdot F}{R \cdot T} \cdot \Phi_D\right] = 0 \qquad (3.11)$$

The concentrations of the ions in the membrane can be calculated if the concentration of fixed charges and the activity coefficients (φ_i and φ'_i) in the solution and membrane as function of the concentrations are known. The theory of the Donnan exclusion predicts an increasing ion uptake if $Z_i \cdot \Phi_D$ decreases. The Donnan potential has a negative value for an anionic membrane and a positive value for a cationic membrane, which means thus that co-ions will be excluded from the membrane and counter-ions will be sorbed into the membrane.

Characterisation of NF membranes is usually done with the electrolyte solutions NaCl, Na_2SO_4, $MgCl_2$ and $MgSO_4$. The uptake of the ions according to the Donnan exclusion can be calculated qualitatively by setting φ_i and φ'_i set to one. At relatively low electrolyte concentrations ($C_{el} < 0.3 \cdot c'_f$), the theory predicts for an anionic membrane that the co-ion uptake decreases going from: $Na_2SO_4 > NaCl > MgSO_4 > MgCl_2$. In case of higher electrolyte concentration ($C_{el} < 0.5 \cdot c'_f$), this sequence is: $NaCl > Na_2SO_4 > MgCl_2 \sim MgSO_4$.

For some membranes the experimental determined retentions for electrolyte solutions can be partly explained by the Donnan exclusion theory [12]. However for a lot of membranes the Donnan exclusion theory predicts the observed retention characteristics not accurately [12],

especially at higher feed concentrations. For example, most nanofiltration membranes show a higher retention for $MgSO_4$ than for NaCl.

Donnan exclusion is thus in a lot of cases not the main determining phenomenon, as real ions in solution don't behave as point charges which do not have any interference with their surroundings. Furthermore the mobility of the ions across the membrane will also play an important role. Both uptake and mobility of the ions in the membrane will depend on the size of the ions. Ions with a higher effective size will penetrate less easily into the membrane (size exclusion) and will be faced with a higher friction in the membrane.

The ions themselves have a size referred to as Pauling radius[17,22], but their effective size, referred to as the hydrated radius [22], in solution is bigger due to a shell of 'bound' water molecules around the ions. Furthermore clustering of ions in solution (without settling) will increase the effective size, which is proven to be the case for $MgSO_4$ solutions [19].

Table 3.1 Mobility and dimension of ions.

Ion	Diffusion coefficient at infinite dilution [$10^{-9}\cdot m^2/s$]	Pauling radius [17,22] [nm]	Hydrated radius [22][nm]
Na^+	1.33	0.095	0.36
Mg^{2+}	0.77	0.065	0.43
Cl^-	2.03	0.181	0.33
SO_4^{2-}	1.06	0.290	0.38

Data on the hydrated radii suggest that the size of the ions can hardly be used to explain salt retentions as the sizes of the ions considered are in the same range. Data on the diffusion coefficient suggest that the transport rate in the membrane of two-valent ions will be lower than the transport rate of monovalent ions, leading to higher retentions which is often observed for many NF membranes [11].

3.3.2 Multicomponent solutions

If membrane filtration is executed on a solution of several electrolytes, ions of the same sign can have an influence on each other's uptake by the membrane. Two cases are distinguished here:

A. The increased uptake in an anionic membrane of a monovalent ion (Cl^-) by the presence of a multivalent ion (SO_4^{2-}). (Donnan exclusion)
B. The decreased retention of NaCl by the presence of a non-permeating (due to steric hindrance) ion (for example a surfactant or a dye). [6,20,21] leading to up-hill transport of NaCl. (Donnan equilibrium)

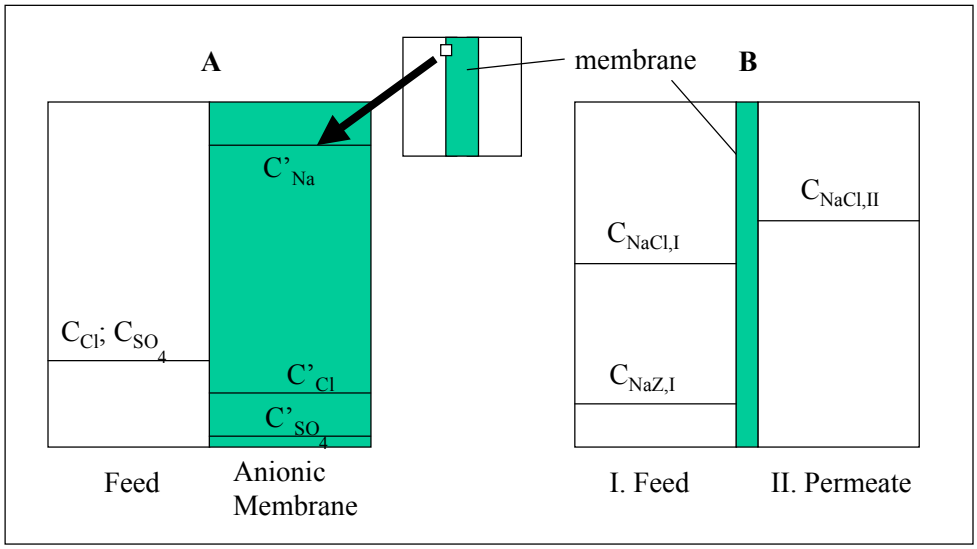

Figure 3.4 Donnan exclusion by the membrane (case A) and Donnan equilibrium between two compartments separated by a semi-permeabel membrane (case B) [21].

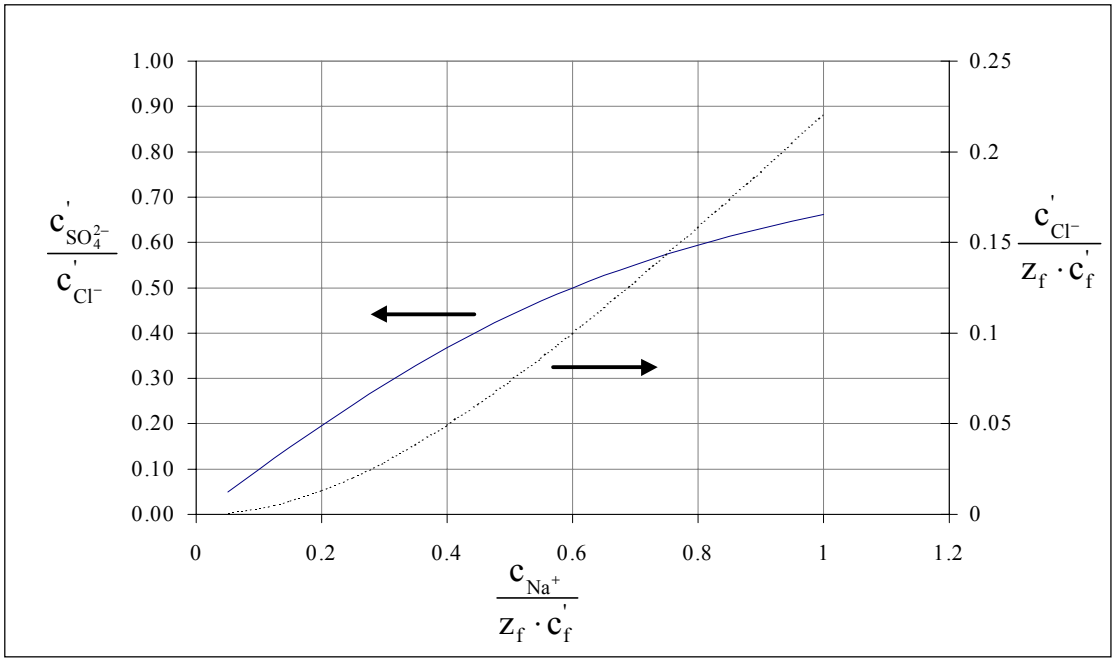

Figure 3.5 Theoretical calculations of the selective co-ion uptake (straight line) by an anionic membrane for the mono-valent ion, Cl^- and to the two-valent ion, SO_4^{2-} as function of the relative mono-valent counter-ion, Na^+, concentration (Case A). The feed is a 1:1 $NaCl/Na_2SO_4$ solution. The dotted line represents the relative membrane concentration of the counter-ion Na.

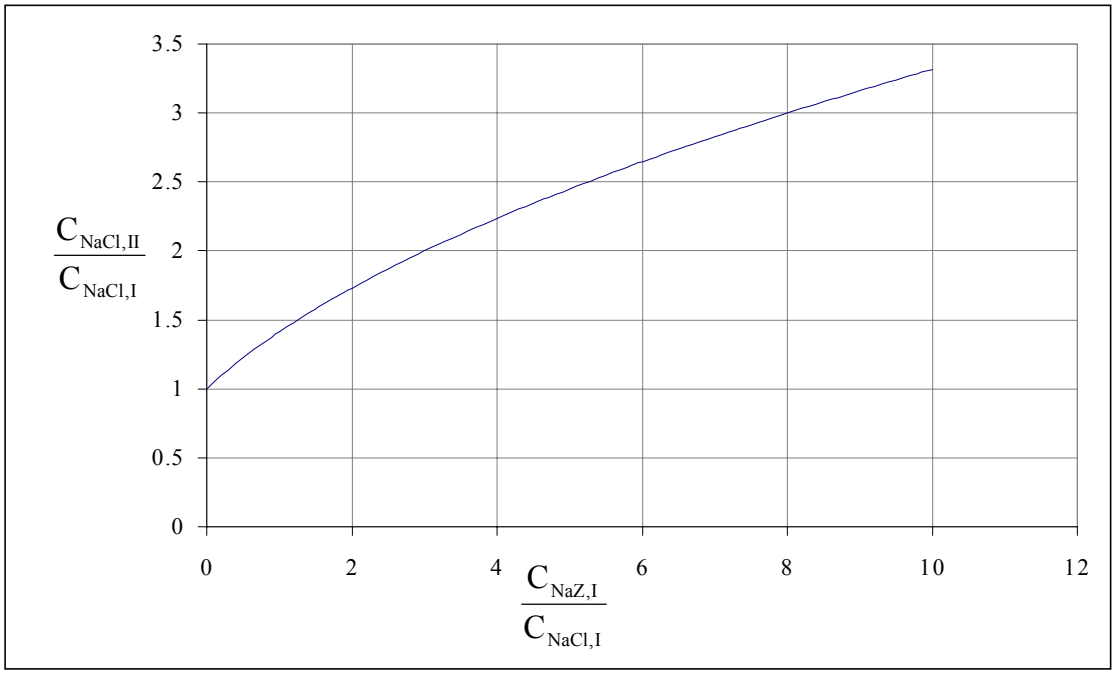

Figure 3.6 Increase of NaCl concentration in the permeate as function of the concentration of the non-permeating ion (Z) in the feed; Case B. eq (3.18).

An important difference between case A and case B is that the membrane of case A must contain fixed charges as for the membrane in case B this condition does not have to be fulfilled, as it only has to reject ion Z by steric hindrance.

Case A can be (theoretically) calculated using the Donnan description as presented in equation 3.11 and 3.12. Results are presented in figure 3.5 for an anionic membrane. At low electrolyte concentration the uptake of SO_4^{2-} is decreased in favour of the uptake of Cl^- by the membrane.

Case B is often referred to as the salting out effect leading to up-hill transport of NaCl. The membrane does not have to bear fixed charges as it is taken to be ideal permselective, which means that Na^+ and Cl^- ions can permeate through the membrane and Z^- ions can not. The description of this phenomena starts by stating the fact that the activities of NaCl at both sides of the membrane are equal. This is expressed in eq 3.12, by taking the activity coefficients to be one.

$$C_{Na,I} \cdot C_{Cl,I} = C_{Na,II} \cdot C_{Cl,II} \qquad (3.12)$$

Addition of NaZ to a NaCl solution at the left side of the membrane results in

$$C_{Na,I} = C_{NaCl,I} + C_{NaZ,I} \qquad (3.13)$$

$$C_{Cl,I} = C_{NaCl,I} \qquad (3.14)$$

$$C_{Na,II} = C_{Cl,II} = C_{NaCl,II} \qquad (3.15)$$

Substitution of the equations (3.13-15) into equation (3.12) results in

$$C_{NaCl,II} = \sqrt{(C_{NaCl,I} + C_{NaZ,I}) \cdot C_{NaCl,I}} \qquad (3.16)$$

Figure 3.6 shows the relative concentration of NaCl at the right side of the membrane (permeate) as function of the relative concentration of NaZ at the left side of the membrane (feed). Both concentrations are related to the NaCl-concentration in the feed. The concentration of the permeating electrolyte NaCl in the permeate is higher than in the feed (i.e. up-hill transport).

In the literature this effect has been paid much attention as up-hill transport is considered to be very peculiar by many researchers [6,20]. However it will only be measurable in case of a large NaZ / NaCl ratio and by an analytical method which is specific for Cl^- ions. In this study this effect will not appear as the NaZ/NaCl ratio in the textile wastewater is small.

3.4 Consequences for this research

The above analysis deals with the two major factors in membrane filtration for aqueous solutions: the permeate flux of the solvent (i.e. water) and the (selective) separation of the solutes. Theoretical considerations have been given here which can explain/describe the filtration and separation characteristics when filtrating textile wastewater by nanofiltration and reverse osmosis.

The permeate flux can be severely decreased by components present in the wastewater to be filtrated. Due to interactions with the membrane preferential adsorption can occur and due to chemical composition the conformation of components in the solvent can change (e.g. micellisation, emulsification or desolubilisation) leading to deposition on the membrane of these components.

Textile wastewater from the washing process subsequent to a reactive dyeing process can contain components that can preferentially adsorb on the membrane or be deposited, leading to flux decline. It is the aim of this thesis to pinpoint which components under which conditions do foul the membranes. The conditions to be varied are hydrodynamic conditions (like transmembrane pressure and cross-flow velocity), chemical conditions (like pH and NaCl concentration) and temperature.

From the separation point of view the retention of NaCl by the RO membrane and the retention of the hydrolysed reactive dyes by the NF membrane are key factors and will be monitored as function of the hydrodynamic conditions and chemical compositions of the waste streams.

Symbols

ΔP	transmembrane pressure	[Pa]
$\Delta\Pi_{b.p}$	osmotic pressure difference over the membrane	[Pa]
η	dynamic viscosity	[Pa·s]
ρ_{water}	density of water	[kg/m^3]
φ	activity coefficient of an ion in solution	[-]
φ'_i	activity coefficient of an ion in the membrane	[-]
Φ_D	Donnan potential	[V]
A	hydraulic permeability	[m/(s·Pa)]
a'_i	activity of an ion in the membrane	[mole/m^3]
a_i	activity of an ion in solution	[mole/m^3]

c'_f	concentration of fixed electrical charges in membrane	[mole/m^3]
c'_i	concentration of an ion in the membrane	[mole/m^3]
C_b	solute (bulk) concentration in the feed	[mole/m^3]
C_g	gel concentration	[mole/m^3]
C_i	solute concentration at membrane interface	[mole/m^3]
c_i	concentration of an ion in solution	[mole/m^3]
C_p	solute concentration in the permeate	[mole/m^3]
$C_{Y,I}$	concentration of component Y in compartment I	[mole/m^3]
$C_{Y,II}$	concentration of component Y in compartment II	[mole/m^3]
F	Faraday constant	[A·s/mole]
J_v	permeate flux	[m/s]
k	solute mass transfer rate in boundary layer	[m/s]
k1	diffusive solute transport parameter in membrane	[m/s]
k2	convective solute transport parameter in membrane	[mole/(m^2·s·Pa)]
N_s	solute flux through membrane	[mole/m^2·s]
R	gas constant	[Joule/(mole K)]
Ret	solute retention	[-]
R_f	resistance for solvent transport in fouling layer	[m^{-1}]
R_m	membrane resistance for water transport	[m^{-1}]
T	temperature	[K]
Z_f	charge number of fixed electrical charges in membrane	[-]
Z_i	charge number of an ion	[-]

Literature

[1] Weast, R.C., CRC handbook of chemistry and physics. 1st student edition ed. (1988).

[2] Mulder, M.H.V., Basic principles of membrane technology. Kluwer Academic Publishers, Dordrecht (1996).

[3] Rautenbach, R. and R. Albrecht, Membrane Processes. Wiley, Chichester, (1981).

[4] Gekas, V. and Hallstroem, B., Mass transfer in the membrane concentration polarization layer under turbulent cross flow, I. Critical literature review and adaptation of existing Sherwood correlations to membrane operations, Journal of Membrane Science, 30: 153-170 (1987).

[5] Gekas, V. and Hallstroem, B., Mass transfer in the membrane concentration polarization layer under turbulent cross flow, II. Application to the characterization of ultrafiltration membranes, Journal of Membrane Science, 37: 145-163 (1988).

[6] Schirg, P., Charakterisierung von Nanofiltrationsmembranen für die Trennung von wässrigen Farbstoff-Salzlösungen, Doctoral thesis ETH Zürich. (1992).

[7] Comb, L. F., Silica, silica chemistry and reverse osmosis. Ultrapure water 13(1): 41-43 (1996).

[8] Iler, R.K., The chemistry of silica : solubility, polymerization, colloid and surface properties, and biochemistry. John Wiley, New York (1979).

[9] Myers, D., Surfaces, interfaces, and colloids. VCH, New York (1990).

[10] Koopal, Modeling association and adsorption of surfactants in structure performance relationships in surfactants ed. Esumi, K. and Ueno, M., Surfactant science series vol. 70, Marcel Dekker, New York 396-469 (1997).

[11] Schaep, J. et all, Influence of ion size and charge in nanofiltration, Separation and Purification Technology 14 155-162. (1998).

[12] Peeters, J.M.M., Characterization of nanofiltration membranes, Doctoral thesis University of Twente, Enschede (1997).

[13] Nyström, M., L. Kaipia, et al., Fouling and retention of nanofiltration membranes,

Journal of Membrane Science 98: 249-262 (1995).
[14] Cadotte, J., R. Forester, et al., Nanofiltration membranes broaden the use of membrane separation technology, Desalination 70: 77-88. (1988).
[15] Ikeda, K., T. Nakano, et al., New composite charged reverse osmosis membrane. Desalination 68: 109-119. (1988).
[16] Helfferich, F., Ion exchange. McGraw-Hill, New York.(1962).
[17] Horvath, A.L., Handbook of aqueous electrolyte solutions, physical properties, estimation and correlation methods. Ellis Horwood, Chichester. (1985).
[18] Atkins, P.W., Physical Chemistry, 4th edition, Oxford University Press, Oxford (1990).
[19] Marcus, Y., Ion solvation. John Wiley, Chichester. (1985).
[20] Perry, M. and C. Linder. Intermediate reverse osmosis ultrafiltration (RO UF) membranes for concentrating and desalting of low molecular weight organic solutes. Desalination 71: 233-245 (1989).
[21] Donnan, F.G., Theory of membrane equilibria and membranepotentials in the presence of non-dialysing electrolytes. A contribution to physical-chemical physiology, Z. Phys. Chem. 17: 572 (1911).
[22] Nightingale, E.R., Phenomenological theory of ion solvation. Effective radii of hydrated ions. J. Phys. Chem., 63: 1381-1387 (1959).
[23] Brasser, P., Precipitation of ionic surfactant solutions near the Krafft temperature. PhD thesis University of Delft. (1998).
[24] Oss, C.J.v., Interfacial forces in aqueous media. M. Dekker, New York. (1994).
[25] Rekveld, S., Ellipsometric studies of protein adsorption onto hard surfaces in a flow cell, Doctoral Thesis, University of Twente. (1997).

Chapter 4

Experimental equipment, analysis and characterization methods

Summary

This chapter gives an overview of the membrane equipment used in the filtration experiments and the methods that were applied in order to determine the membrane performance (i.e. permeate flux and separation of components). Characterisation of both membranes with (non-fouling) inorganic salt solutions (e.g. NaCl, $MgSO_4$ and Na_2SO_4) have been executed to use as reference in the parametric studies (chapters 6 and 7). Furthermore the reverse osmosis (RO) and the nanofiltration (NF) membranes have been characterised for their electrostatic and electrodynamic properties in order to explain the origin of membrane fouling.

4.1 Introduction

Membrane filtration experiments can be performed in the dead-end mode or in the cross-flow mode. In this research the cross-flow mode has been chosen, as it is a better approximation of practical situations than the dead–end operation considering constant concentrations and hydrodynamic conditions. In order to give explanations for flux and separation characteristics when filtering wastewater, membranes have to be characterised. Possible characterisation methods for reverse osmosis and nanofiltration membranes are:

1. Determination of the clean water flux by filtration of demineralised water (clean water test).
2. Determination of the solvent permeate flux and a solute retention for a solution containing one non-fouling solute (= standard filtration test or SFT).
3. Determination of electrostatic properties of the membrane by an electrokinetic measurement (e.g. streaming potential [1]).
4. Determination of electrodynamic properties (apolar/polar properties) of the membrane by a physico-chemical measurement (contact angle measurements [2]).

The first two are characterisation methods, which are directly related to the performance of a membrane. The latter two are physico-chemical characterisation methods that will be used to explain interactions between the membrane and specific solutes in the wastewater. In this research a SFT for RO and a SFT for NF have been used in stead of the common used clean water tests, because of:

1. There is no consensus what ‘clean’ water really is. What level of impurities is still tolerable to call a liquid clean water?
2. There are strong indications that high-demineralised water can cause membrane damage, as free ions in the membrane matrix are pulled out of the membrane resulting in a weaker membrane structure.
3. The ‘clean’ water flux can be calculated from the SFT if the osmotic pressure difference over the membrane (taking concentration polarisation into account) is known.
4. The membrane manufacturer also uses an SFT.
5. Solvent permeate flux and solute retention can be determined in one experiment if the SFT is used.

The latter two characterisation methods focus on the material properties that are important for adsorption of solutes onto the membrane surface. A complete quantitative description of electrostatic and electrodynamic contributions to the material properties is too elaborate [12]. Therefore the electrodynamic and electrostatic contributions will be handled separately.

4.2 Experimental set-up

Performing membrane filtration experiments in the cross-flow mode, two basic forms of experimental set-up are distinguished. The feed/bleed set-up and the one-pass set-up. In the feed/bleed set up main part of the stream leaving the membrane module is directly recirculated (recycle stream) to the feedside of this module without leaving the high-pressure zone (figure 4.1). In the one-pass set-up the total stream leaving the module is depressurised without direct recirculation of (a part of) this retentate back to the feed side of the module. (figure 4.2).

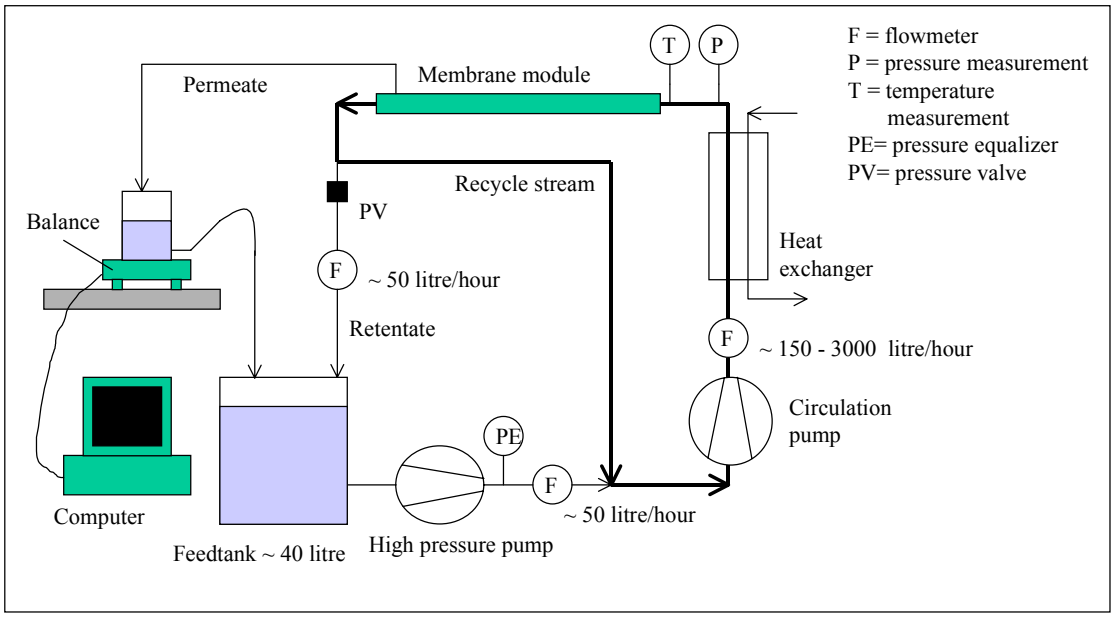

Figure 4.1 Feed-bleed set-up of a membrane filtration system

The criteria for selection of the set-up are the ability to control process parameters like:
temperature
pressure
cross-flow velocity
concentration when performing fouling experiments

The one-pass set-up looks attractive, as theoretically only one pump is necessary. However, this pump must provide both (high) pressure and cross-flow. This will lead to a large energy consumption as the feed flow is relatively large for such systems and a bad controllability of the temperature as a considerable amount of cooling is necessary.

Generally spoken the controllability of pressure and cross-flow is judged to be better in the feed/bleed system than in the one-pass system as the high pressure pump (in combination with the pressure valve) provides the pressure and the circulation pump provides the cross-flow. However experience with both systems in this research showed that controllability in both systems could be achieved satisfactorily by the use of frequency converters for controlling the speed of the motor of the pumps.

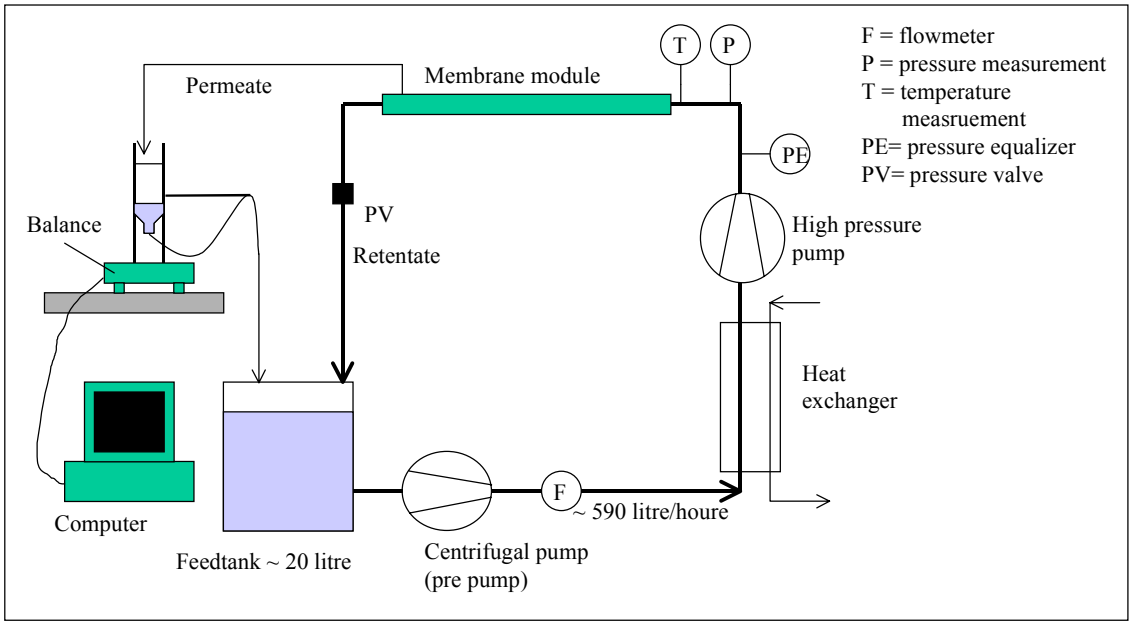

Figure 4.2 One-pass set-up membrane filtration system.

Table 4.1 Advantage/disadvantage of the different membrane filtration set-ups
* If using frequency converters

Controllability of:	One-pass set-up	Feed \bleed set-up
Power consumption	-	+
Temperature	-	+
Pressure, cross-flow	+*	+*
Concentration	+	-

The disadvantage of the recycle set-up compared to the one-pass set-up is the impracticability to get a constant concentration in the recycle loop during a filtration experiment. Due to the fact that the retentate flow can be considerably smaller than the feed flow, the concentration in the recycle loop will start to increase and become higher than the concentration in the feed tank, as the massflow of solute brought in the recycle loop by the feed stream has to be equal to the outgoing massflow of the retentate stream if the solute is completely rejected by the membrane. This problem is often not identified in membrane pilot studies in literature, leading to wrong interpretations about fouling of membrane-solute systems. In appendix 4A the concentration build-up (in time) during an experiment is calculated and measures are given to manage this concentration build-up.

The one-pass set up was used for the parametric study of the nanofiltration. All other experiments (preliminary study, RO-parametric study and the NF-optimisation study) have been done with the recycle set-up.

In the preliminary experiments only rinsing with demineralised water was done before installing a new membrane, but there are strong indications that this was not sufficient (chapter 5). Therefore in subsequent studies the installation was always cleaned thoroughly before installing a new membrane following the procedures in table 4.2.

Table 4.2 Cleaning procedures before the installation of a new membrane. * The solutions were made with demineralised water.

1.	Install the membrane housing, without a membrane, in the installation.
2.	Rinse the installation with a 250 ml chlorine solution in 30 litre water* during at least 30 min. Cast all outgoing streams back into the feed tank.
3.	Remove the chlorine solution. Rinse the installation with demineralised water during at least 30 min. Cast all outgoing streams out of the installation.
4.	Rinse the installation with a 75 ml of Ultrasil 75 (acid) solution in 30 litre water* during at least 30 min. Cast all outgoing streams back into the feed tank.
5.	Remove the acid solution. Rinse the installation with demineralised water during at least 30 min. Cast all the outgoing streams out of the installation.
6.	Rinse the installation with NaOH solution* (minimal pH of 10) during at least 30 min. Cast all outgoing streams back into the feed tank.
7.	Remove the acid solution. Rinse the installation with demineralised water during at least 60 min. Cast all the outgoing streams out of the installation.

4.3 Membranes

The membranes used in this research are the RO-WFCX and the NF-WFN membranes of membrane manufacturer Stork Friesland. The membrane modules consisted of one membrane tube with an active membrane surface area of about 800 square centimetre. General data concerning the membranes are listed in table 4.3.

Table 4.3 Characteristics of the used membranes, according to Stork except for * which are own measured values.

Both membranes	
membrane shape	tubular 14.4 mm
internal diameter *	d_i = 13.75 mm
length *	1.75 m
internal membrane area *	S = 0.07559 m^2 (of 1 tube)
Reverse osmosis	
type	WFCX
material	polyamide / polysulfone
fixed electric charges	negatively charged (will be checked in chapter 4.7)
clean water flux	> 45 lt/m^2hr at 40 bar
NaCl retention	> 98.5 %
standard filtration test	filtration with a 0.2 wt % NaCl solution at 35 bar during at least 10 hours
Nanofiltration	
type	WFN
material	polyamide / polysulfone
fixed electric charges	negatively charged (will be checked in chapter 4.7)
clean water flux	> 125 lt/m^2hr at 20 bar
$MgSO_4$ retention	> 95 %
standard filtration test	filtration with a 0.5 wt % $MgSO_4$ solution at 10 bar during at least 10 hours

Although most membranes received had been tested by the membrane manufacturer with a SFT, the membranes were always tested again before use (during at least two hours). This turned out to be very important as drying of the membranes, which had been wetted before, turned out to be disastrous. The permeate flux of a specific batch of NF-membranes decreased 50 % during storage! After this experience only untested, dry, virgin membranes were ordered from the manufacturer and the standard test was performed during at least 16 hours before use. Between the experiments the membranes were prevented for drying by keeping them in the membrane installation which was kept filled with water.

4.4 Methods of measurement

During the experiments the permeate flux was measured and recorded by a computer continuously. At certain time intervals samples of both retentate and permeate were taken in order to determine the retentions for the key components, dye and NaCl.

4.4.1 Permeate flux measurement

The permeate flows of one membrane tube are 0.05 - 5 litre/hour for the reverse osmosis membrane and 2-20 litre/hour for the nanofiltration membrane. Measuring these low flows continuously in time with an automatic flowmeter is difficult, expensive or even impossible if a great accuracy is required. Generally in most membrane research the permeate flux is measured at limited time intervals by hand. In this research a special developed system consisting of a beaker, a siphon and a balance has been used. The siphon prevents the beaker from flooding by emptying it within a few seconds. The permeate mass over a certain time (Δm) is determined on a balance (Mettler PM 1500 or Mettler PM 3000), which was read out by a computer. The permeate volumetric flux is then calculated by eq. 4.1 taking the density of the permeate water as 1000 kg/m^3.

$$J_v = \frac{\Delta m}{\rho \cdot S \cdot \Delta t} \qquad (4.1)$$

4.4.2 Measurement of retention

In order to determine observed retentions of dye and NaCl by the membranes their average concentration or a derivative of their concentration in retentate and permeate should be measured. As the permeate flow is much smaller than the cross-flow in the membrane tube, the concentration of the retentate is supposed to be the same as the average bulkconcentration in the membrane tube.

$$Ret_m = 1 - \frac{C_p}{C_b} = 1 - \frac{C_p}{C_R} \qquad (4.2)$$

The dye concentration was measured with a spectrophotometer (visible spectroscopy). The absorbance of both retentate and permeate was determined at the wavelength of maximal absorbance of the permeate. Dividing this adsorption unit by the cuvet length (1 cm) gave the spectral absorbance [m^{-1}]. Spectral absorbances of the permeates were compared with the values given in the German legislation for waste water discharge (table 4.4) in order to have a reference point for discharging permeate streams to the environment.

Table 4.4 Discharge standards for maximal allowed colour content of wastewater according to the German legislation.

wavelength [nm]	spectral absorbance [m^{-1}]
436	7
525	5
620	3

The NaCl retention was determined in the standard tests and in experiments where relative to other components a considerable amount of NaCl had been added (> 10 g/l). The NaCl-concentrations were determined by measuring the conductivity. The influence of other components can be neglected at these high NaCl concentrations. The apparatus used in the RO parametric study (HI 9032, Hanna Instruments) was calibrated with pure NaCl concentrations. (figure 4.3).

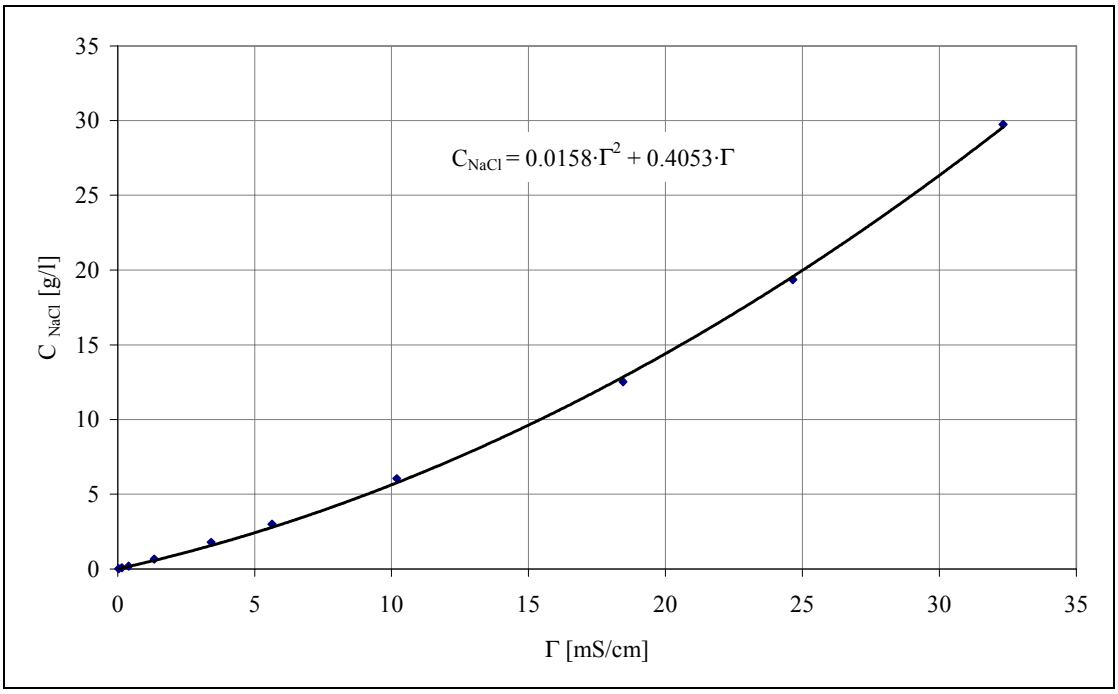

Figure 4.3 Calibration of conductivity meter (NaCl concentration vs. conductivity).

4.4.3 Osmotic pressure

A high (molar) concentration difference between permeate and retentate in pressure driven membrane processes means a high osmotic pressure difference over the membrane and thus a less driving force for permeation (chapter 3.1). In the NF parametric study osmotic pressure differences were determined by measuring the osmolality directly with an osmometer based on the freezing point method (Advanced Instruments wide-range Osmometer 3W2). For the RO experiments with high NaCl concentrations this osmotic pressure difference can be estimated by the difference in conductivity between retentate and permeate, as NaCl is the main component determining conductivity and molality. The relation between NaCl conductivity and osmotic pressure is presented in figure 4.4 [3].

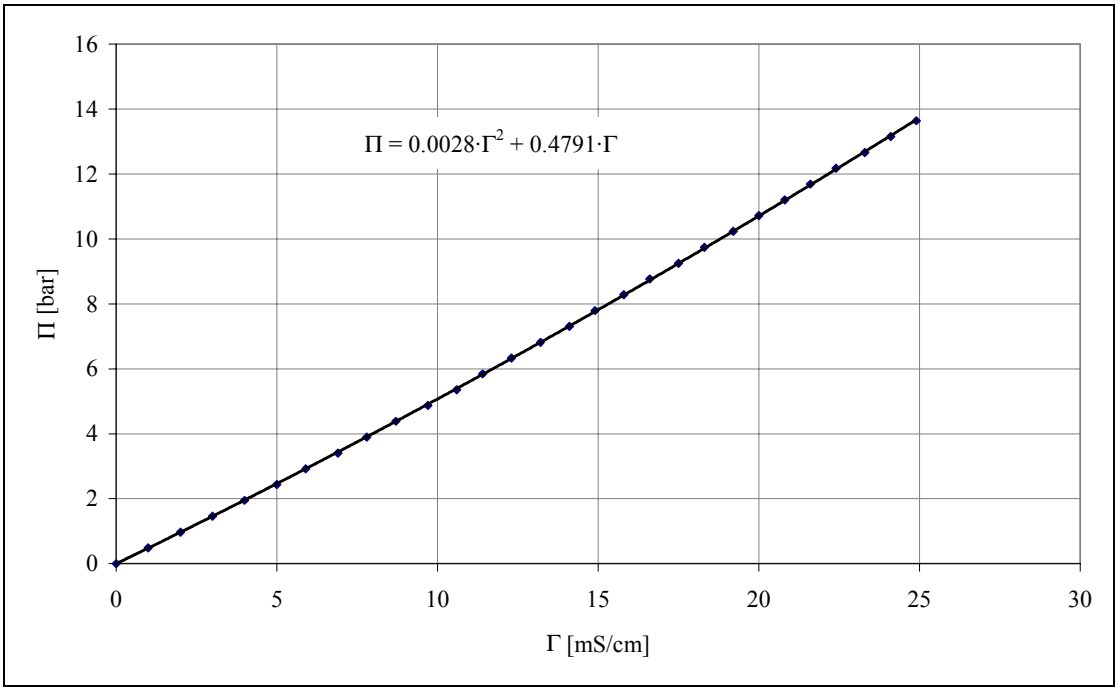

Figure 4.4 Osmotic pressure as function of conductivity for NaCl-solutions [3].

4.5 Mass transport characterization of reverse osmosis membranes with NaCl-solutions

4.5.1 Introduction

For the RO-treatment of textile wastewater from reactive dyeing and subsequent washing processes the retention of NaCl by the membrane is an important parameter. The aims of the methods, presented here, to characterise this retention are:

1. Give reference values for mass transport and retention in order to compare them with NaCl retentions of wastewater (i.e. the RO-parametric study, chapter 6).
2. Determine the mass transport parameters of NaCl in the membrane with varying NaCl concentrations at varying hydrodynamic conditions (cross-flow and transmembrane pressure) in order to predict the NaCl retention as function of the NaCl concentration and hydrodynamic conditions.

The solution diffusion model, describing the solvent flux and the solute flux, will be used here. The mass-transport parameters are determined with a graphical method independent of the concentration polarisation.

4.5.2 Theory

In membrane processes, accumulation of solutes in the boundary layer adjacent to the membrane will occur as a consequence of a higher mass transport resistance for the solute in the membrane than in this boundary layer (figure 4.5). This phenomenon is called concentration polarisation and influences the driving forces for both solvent and solute flux.

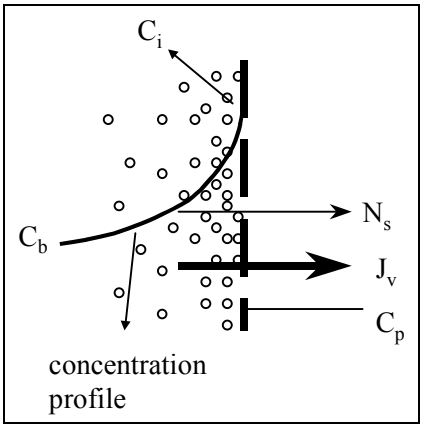

Figure 4.5. Concentration polarisation

For a dense membrane, like an RO membrane, the solution diffusion model is commonly used. In this model the solvent permeate flux is linearly dependent on the effective transmembrane pressure, which is the adjusted pressure difference minus the osmotic pressure difference over the membrane (eq. 4.3). The solute flux across the membrane is linearly dependent on the concentration difference over the membrane.

$$J_v = A \cdot (\Delta P - \Delta \Pi_{i,p}) \tag{4.3}$$

$$N_s = B_0 \cdot (C_i - C_p) \tag{4.4}$$

The concentration in the permeate is defined as the solute flux divided by the solvent flux:

$$C_p = \frac{N_S}{J_v} \tag{4.5}$$

In case of the filtration of NaCl solutions the osmotic pressure difference over the membrane can be assumed to be linear and the equation of Van ‘t Hoff can be used. It must be mentioned that in case of electrolyte solutions the total ion concentration should be taken as the solute concentration.

$$\Delta \Pi_{i,p} = R \cdot T \cdot (C_i - C_p) \tag{4.6}$$

The equations (4.3 – 4.6) can be rearranged to yield:

$$R \cdot T \cdot C_p = B_0 \cdot \frac{\Delta P}{J_v} - \frac{B_0}{A} \tag{4.7}$$

Plotting the left hand side of eq. 4.5 against $\Delta P/J_v$ will give a straight line with slope B_0 and intercept B_0/A at the y-axis. This graphical analysis is further referred to as Method I.

Method I can be applied without any assumptions about the mass transfer of the solute in the boundary layer, in contrary with the method proposed by Murthy and Gupta [2], further referred to as Method II. For Method II an observed salt transport parameter (B_m eq. 4.8) is defined as function of the observed retention (eq 4.2).

$$B_m = J_v \cdot \frac{1 - Ret_m}{Ret_m} \tag{4.8}$$

Measuring B_m as function of transmembrane pressure and cross-flow velocity at a fixed NaCl concentration will provide a method to determine the intrinsic salt transport parameter B_0 (eq 4.9) which is based on the definition of the intrinsic retention (eq. 4.10).

$$B_0 = J_v \cdot \frac{1 - Ret}{Ret} \tag{4.9}$$

$$Ret = 1 - \frac{C_p}{C_i} \tag{4.10}$$

In Method II the equations for B_m and B_0 are substituted in the general description for the concentration polarisation (eq. 4.11) to yield equation 4.12

$$\frac{J_v}{k} = \ln\left[\frac{C_i - C_p}{C_b - C_p}\right] \tag{4.11}$$

$$\ln[B_m] = \ln[B_0] + \frac{J_v}{a \cdot v^{0.8}} = \ln[B_0] + \frac{\beta}{a} \tag{4.12}$$

So plotting $\ln(B_m)$ against β will give a slope a^{-1} and an intercept $\ln(B_0)$ with the y-axis. The intrinsic salt transport parameter B_0 is used to characterise the salt transport across the membrane.

The parameter a can be compared to the value which can be derived from the well-known Sherwood relations for turbulent flow in a tube.

$$Sh = \frac{k \cdot d_i}{D} = 0.023 \cdot Re^{0.8} \cdot Sc^{0.33} = 0.023 \cdot v^{0.8} \cdot d_i^{\,0.8} \cdot \nu^{-0.47} \cdot D^{-0.33} \tag{4.13}$$

During the filtration of pure NaCl solutions by the RO-WFCX membranes the parameter a should have the value: (by substituting d = 0.01375 m, $D = 1.5 \cdot 10^{-9}$ m^2/s [3] and $\nu = 10^{-6}$ m^2/s):

$$a = 0.023 \cdot d_i^{\,-0.2} \cdot \nu^{-0.47} \cdot D^{0.67} = 4.39 \cdot 10^{-5} \cdot \left[\frac{m}{s}\right]^{0.2} \tag{4.14}$$

4.5.3 RO experiments with pure NaCl solutions

Experiments were performed with the recycle set-up described in section 4.2. The transmembrane pressure was varied at 20, 30 and 35 bar, and four NaCl concentrations were examined. Two membranes were used, the first one for RONaClexp 2 the latter one for the other three sets of experiments.

Table 4.5 NaCl concentration levels.

Exp	Conductivity Retentate [mS/cm]	NaCl concentration [g/l]	membrane	Remarks
RONaClexp1	4.097	1.9	membrane 2	Comparable to SFT
RONaClexp2	6.368	3.2	membrane 1	
RONaClexp3	13.650	8.5	membrane 2	
RONaClexp4	19.872	14.3	membrane 2	Comparable to filtration tests RO parametric study

The NaCl concentration was measured with the conductivity meter (HI 9032, Hanna Instruments) that was calibrated with known NaCl –concentrations (figure 4.3). In order to get stable measurements, experiments could only be performed after the membranes had been pressurised at 35 bar for more than 20 hours. Drying the membranes turned out to be very bad for their performance. Although the permeate flux was reasonable, the retention of the membrane was very low. It was once observed that after drying a membrane two days of filtration at 35 bar were necessary to obtain stable results again.

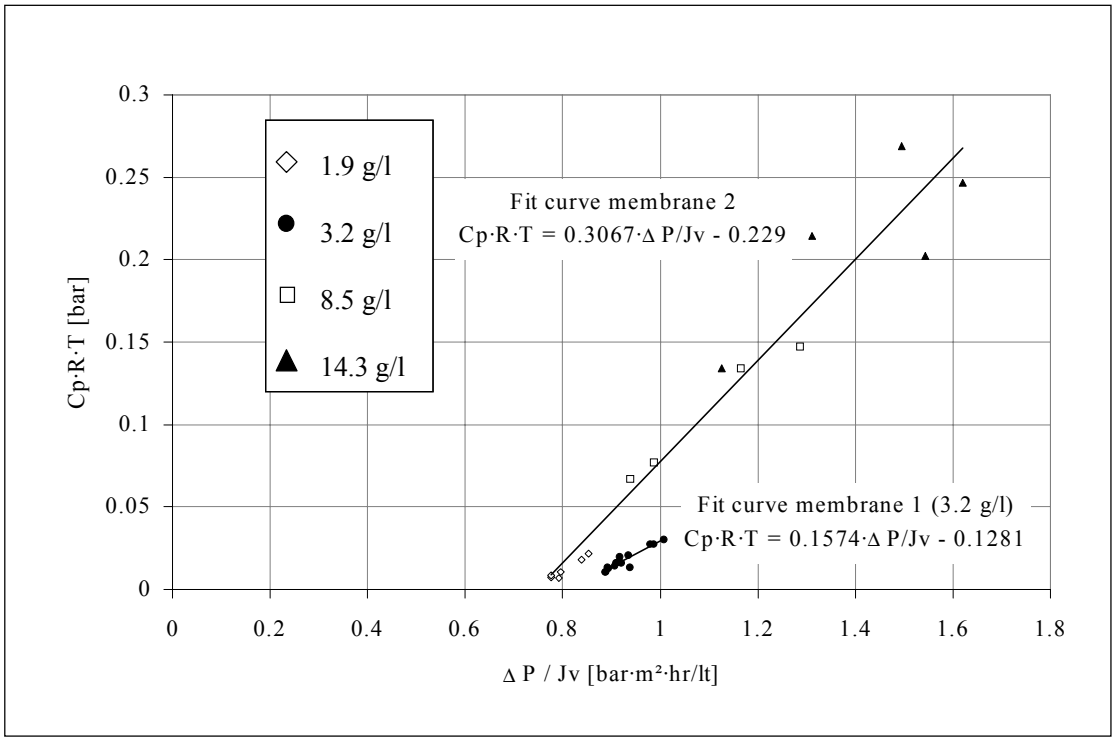

Figure 4.6 Graphical analysis derived from the solvent and solute flux descriptions presented as Method 1 (eq. 4.7).

Table 4.6 Results RONaClexp1 (1.92 g NaCl/lt; 4097 µS/cm)

TMP [bar]	Cross-flow velocity[m/s]	Jv [lt/m^{2}hr]	NaCl Retention [-]	Bm [lt/m^{2}hr]	C_p [mg /lt]
20	1.1	25.89	0.990	0.262	20.4
20	4.4	26.65	0.991	0.242	18.0
30	0.27	35.90	0.978	0.808	43.5
30	0.55	37.70	0.987	0.497	24.8
35	0.27	41.18	0.974	1.099	51.8
35	4.4	44.71	0.992	0.361	16.2

Table 4.7 Results RONaClexp2 (3.22 g NaCl/lt; 6368 µS/cm).

TMP [bar]	Cross-flow velocity [m/s]	Jv [lt/m^{2}hr]	NaCl retention [-]	B_m [lt/m^{2}hr]	C_p [mg /lt]
20	0.27	19.85	0.9760	0.488	72.8
20	0.55	21.41	0.9837	0.355	49.4
20	1.1	21.90	0.9870	0.288	39.8
20	2.2	21.99	0.9879	0.269	37.7
20	4.4	22.07	0.9886	0.254	34.6
30	0.27	30.65	0.9785	0.673	65.8
30	0.55	32.71	0.9846	0.512	47.4
30	2.2	33.62	0.9897	0.350	31.4
30	4.4	33.86	0.9916	0.286	25.9
35	0.27	35.49	0.9787	0.772	66.0
35	0.55	38.04	0.9875	0.482	38.5
35	1.1	39.16	0.9903	0.384	30.4
35	2.2	37.27	0.9898	0.384	31.2
35	4.4	39.40	0.9917	0.330	25.7

Table 4.8 Results RONaClexp3 (8.47 g NaCl/lt; 13650 µS/cm)

TMP [bar]	Cross-flow velocity [m/s]	Jv [lt/m^{2}hr]	NaCl Retention [-]	B_m [lt/m^{2}hr]	C_p [mg /lt]
20	0.27	15.54	0.945	0.904	353.4
30	1.1	30.50	0.972	0.879	185.3
35	0.27	30.15	0.951	1.553	321.6
35	4.4	37.85	0.976	0.931	160.3

Table 4.9 Results RONaClexp4 (14.27 g/l NaCl; 19872 µS)

TMP [bar]	Cross-flow velocity [m/s]	Jv [lt/m^{2}hr]	NaCl Retention [-]	B_m [lt/m^{2}hr]	C_p [mg/lt]
20	1.097	12.35	0.938	0.816	591.5
20	4.387	13.15	0.949	0.707	485.5
30	0.548	23.10	0.946	1.319	514.9
35	0.274	23.55	0.933	1.691	644.6
35	4.387	31.45	0.966	1.107	321.6

Results of the four sets of the experiments are presented in Tables 4.6 to 4.9. The graphical presentation of Method I is presented in figure 4.6 and its' results are shown in table 4.10.

Table 4.10 Results of the graphical analyses according to Method I.

Membrane	C_{NaCl} [g/l]	slope	intercept y-axis	A [lt/m²hrbar]	B_0 [lt/m²hr]
Membrane 2	1.9; 8.5; 14.3	0.3067	- 0.2290	1.34	0.31
Membrane 1	3.2	0.1574	- 0.1281	1.23	0.16

Table 4.11 Main results of the graphical analyses according to Method II.

Membrane	C_{NaCl} [g/l]	B_0 [lt/m²hr]	a [(m/s)$^{0.2}$]
Membrane 2	1.9	0.23	$2.07 \cdot 10^{-5}$
Membrane 1	3.2	0.26	$2.39 \cdot 10^{-5}$
Membrane 2	8.5	0.75	$3.43 \cdot 10^{-5}$
Membrane 2	14.3	0.78	$2.15 \cdot 10^{-5}$

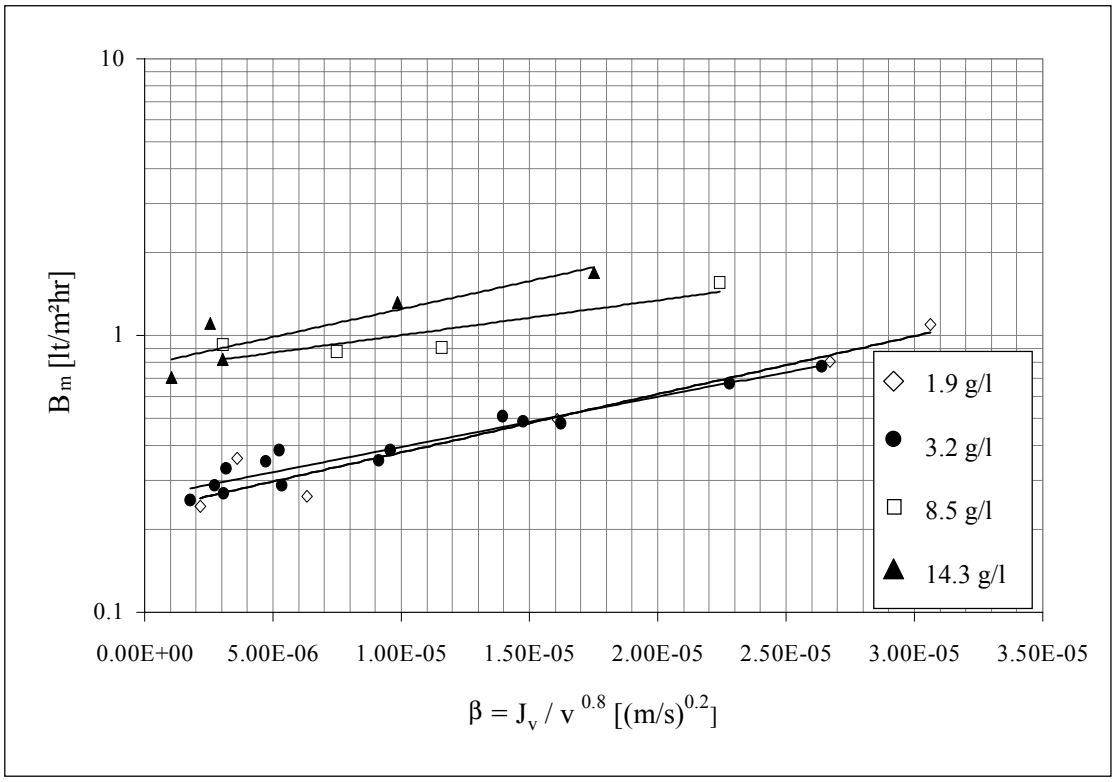

Figure 4.7 Graphical analysis according to Method II [4] (eq. 4.12) derived from solute transport and general description of concentration polarisation.

From graphical method I it can be seen that the membranes have different permeabilities. Both permeabilities are larger than the minimum value given by the membrane manufacturer. The parameter determination from this method I is however questionable:

- The data points of a specific NaCl-concentration have x-axis values that are close together and are far away from the y-axis. As a consequence of this, huge errors will occur.
- The spreading of the data points is better when these points are collected at higher varying concentrations. However the influence of the concentration on B_0 is not taken into account.

From graphical method II it seems that the salt transport parameter is dependent on the feed concentration. A higher concentration means a (non-linear) increase of the salt transport. This

is probably due to an enhanced uptake of NaCl by the membrane at higher concentrations following a Donnan-like description (chapter 3.4). The experimental value of the mass transport parameter (a) is between 50-75 % of the theoretical value (eq. 4.14). The origin for this may be due to entrance effects in the first section of the membrane tube.

$$J_v = A \cdot \Delta P - A \cdot R \cdot T \cdot c_b \cdot \frac{\exp\left[\frac{J_v}{k}\right]}{1 + \frac{B_0}{J_v} \cdot \exp\left[\frac{J_v}{k}\right]} \qquad (4.15)$$

The data of the experimental set RONaClexp2 has been fitted to the osmotic pressure model using equation 4.15, with A = 1.23 lt/(m^2·hr·bar), B_0= 0.20 lt/(m^2·hr), a = 2.39·10^{-5} (m/s)$^{0.2}$. The fitting is accurate except for the permeate flux measured at a transmembrane pressure of 35 bar and cross-flow velocity of 2.2 m/s. The origin for this is that the membrane was not conditioned as this was the first measuring point of the experimental series determined after ~ 20 hours of operation. It can be concluded that the osmotic pressure model as presented here can be well applied for predicting the solvent and solute transport when filtrating pure NaCl solutions and that concentration polarisation effects can be neglected at cross-flow velocities higher than 1 m/s.

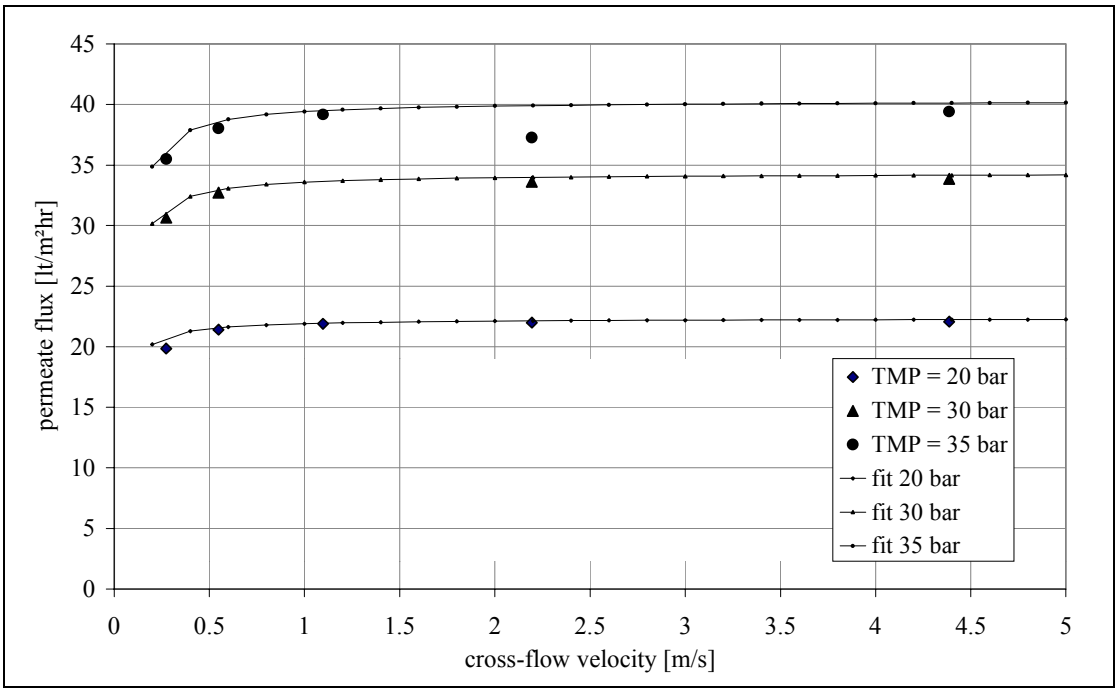

Figure 4.8 Measured and fitted permeate flux data for exp RONAClexp2.

4.5.6 Conclusion

Two methods are presented here to characterise solute (NaCl) and solvent transport in the membrane and boundary layer for the tubular RO membrane under turbulent conditions. The first method is used to estimate solute and solvent transport parameters in the membrane without calculating concentration polarisation phenomena. The second method is used to calculate the solute transport parameter in the membrane and in the boundary layer. Although both methods do not exactly yield the same results, it can be concluded that an increase of NaCl concentration increases the intrinsic salt transport parameter across the membrane (i.e. B_0). Results can be used to estimate flux and NaCl retentions for the RO membrane considered here, as function of cross-flow velocity, transmembrane pressure and NaCl concentration. Furthermore these data will also be used as a reference for RO parametric study with real wastewater (Chapter 6) containing high NaCl concentrations by using Method II.

4.6 Characterization of nanofiltration membrane with inorganic salt solutions

4.6.1 Aim

The aim of the characterisation methods presented here is to measure the flux / retention characteristic of the nanofiltration membrane with inorganic ions NaCl, Na_2SO_4 and $MgSO_4$, under real process conditions (transmembrane pressure and cross-flow velocities). NaCl is taken, as it is also present in the textile wastewater. The results with the pure NaCl solutions can be compared to the results of the NF parametric study. Na_2SO_4 is taken, as it can be present in textile waste in stead of NaCl. If the retention of Na_2SO_4 by the NF membrane is adequate then the NaCl in the dyeing process can be replaced by Na_2SO_4 and the reverse osmosis in the modified washing processes (chapter 2) by nanofiltration. $MgSO_4$ is taken as it is used by the membrane manufacturer for characterisation of the NF membranes.

4.6.2 Experiments

Five experimental sets were performed each with one composition at varying process conditions (Table 4.12). The experimental set-up used was the feed/bleed set-up. The concentrations of the electrolytes were determined by measuring the electrical conductivity.

Table 4.12 Experimental design NF characterisation.

Exp	components	Conc. [g/l]	Conc. [mole/l]	transmembrane pressure [bar]	cross-flow velocities [m/s]
NFNaClexp1	NaCl	1.7	0.029	10, 15, 20	0.25; 4
NFNaClexp2	NaCl	9.6	0.164	10, 15, 20	0.25; 4
NFNaClexp3	NaCl	30.1	0.516	10, 15, 20	0.25; 4
NFNaSOexp	Na_2SO_4	2.7	0.019	10	0.25; 1; 2; 4
NFMgSOexp	$MgSO_4$	3.7	0.031	10	0.25; 2; 4

4.6.3 Results and discussion

The permeate flux and measured retention for the NaCl characterisation experiments are listed in Tables 4.13 to 4.14. The results are graphically presented in figure 4.9.

Table 4.13 Results NFNaClexp1 (1.7 g/l NaCl)

Transmembrane pressure [bar]	Cross-flow velocity [m/s]	permeate flux [lt/m^{2}hr]	measured retention [-]
10	0.27	106.6	0.074
10	4.4	112.9	0.465
15	0.27	151.8	0.047
15	4.4	168.3	0.514
20	0.27	201.3	0.041
20	0.27	197.9	0.022
20	4.4	218.3	0.553
20	4.4	220.8	0.542

Table 4.14 Results NFNaClexp2 (9.6 g/l NaCl)

Transmembrane pressure [bar]	Cross-flow velocity [m/s]	permeate flux [lt/m^{2}hr]	measured retention [-]
10	0.27	94.87	0.034
10	4.39	98.83	0.212
10	4.39	99.93	0.213
15	0.27	138.09	0.018
15	4.39	145.72	0.261
20	0.27	176.53	-0.008
20	4.39	191.78	0.292

Table 4.15 Results NFNaClexp3 (30.1 g/l NaCl)

Transmembrane pressure [bar]	Cross-flow velocity [m/s]	permeate flux [lt/m^{2}hr]	measured retention [-]
10	0.27	81.8	0.027
10	4.39	84.0	0.106
15	0.27	116.6	0.023
15	4.39	125.1	0.138
20	0.27	146.9	0.020
20	4.38	161.8	0.152

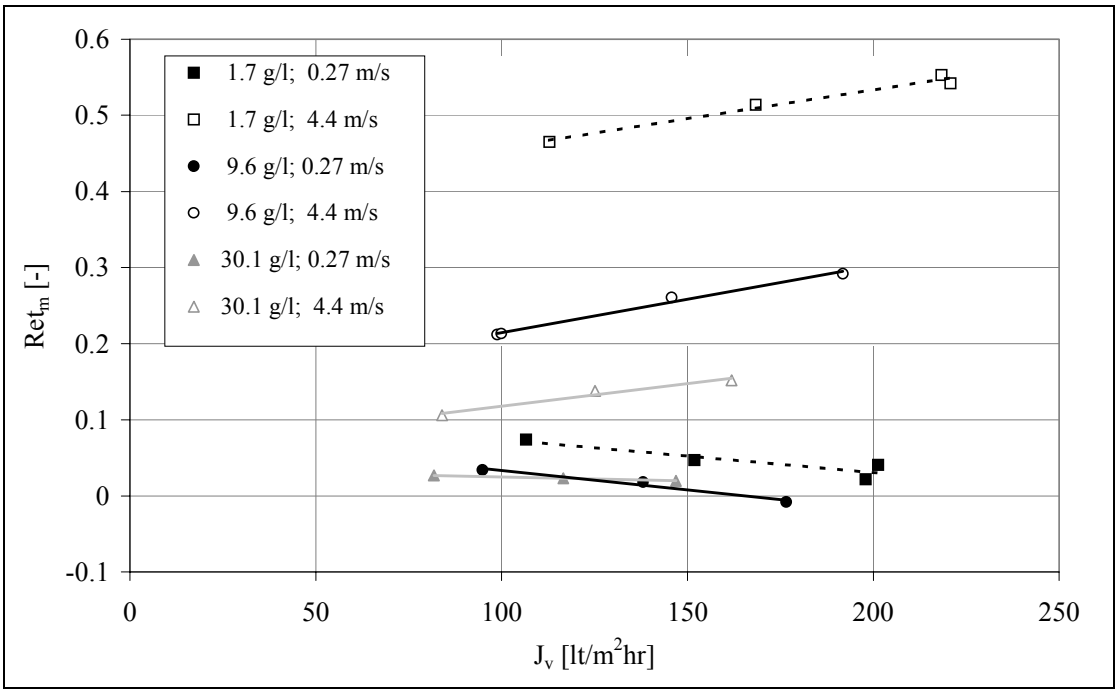

Figure 4.9 Flux and retention experiments of NF characterisation with NaCl-solutions.

At high cross-flow velocity the measured retention is remarkably higher than at low cross-flow velocity. This can be explained by the fact that the concentration at the membrane interface becomes higher if the cross-flow velocity is decreased. If the intrinsic retention will stay constant, the measured retention will than be decreased. (figure 4.10).

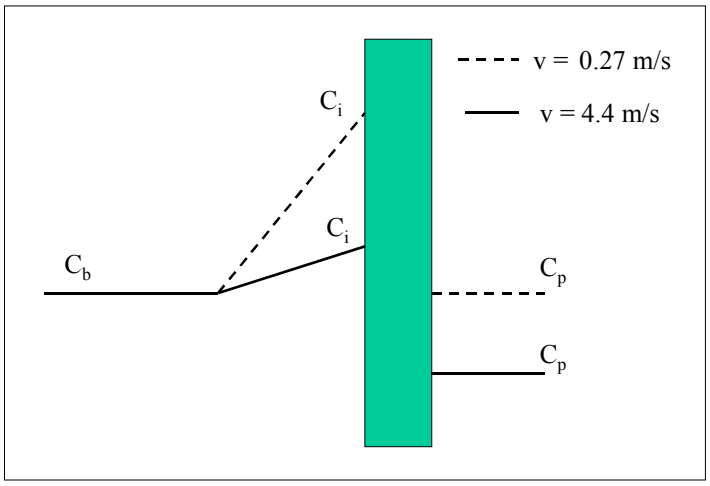

Figure 4.10 Concentration profiles at varying cross-flow velocities leading to huge variations in measured retentions.

Moreover, increasing the concentration decreases the retention at the same conditions. The huge influence of NaCl-concentration on the NaCl-retention can be explained by the Donnan mechanism. An increase in concentration increases the co-ion uptake by the membrane and thus the molar flux of this co-ion in the membrane. (chapter 3). At low cross-flow velocities the retention decreases with increasing pressure (or permeate flux) as at high cross-flow velocities this retention increases with increasing pressure (or permeate flux). This may be qualitatively explained by the facts that an increasing transmembrane pressure will increase both the solvent and the solute flux. As the solute retention is a function of both fluxes (eq. 4.5) a maximal retention will be reached at a certain transmembrane pressure and solvent flux.

This maximal value is dependent on the cross-flow velocity. At high cross-flow velocity the maximum will be reached at a higher transmembrane pressure than for a low cross-flow velocity. The origin for this may be that the solute transport across the membrane is relatively increased more than the solvent transport across the membrane as the solute interface concentration (C_i) is increased exponentially (concentration polarisation equation, eq. 3.3 and eq. 4.11) going from high to low cross-flow velocities.

Table 4.16 Results NFNaSOexp (2.7 g/l Na_2SO_4)

Transmembrane pressure [bar]	Cross-flow velocity [m/s]	Permeate flux [lt/m^{2}hr]	Measured retention [-]
10	0.548	92.721	0.562
10	1.096	104.423	0.699
10	2.194	111.799	0.769
10	4.387	108.052	0.790

Table 4.17 Results NFMgSOexp (3.7 g/l $MgSO_4$)

Transmembrane pressure [bar]	Cross-flow velocity [m/s]	Permeate flux [lt/m^{2}hr]	Measured retention [-]
10	0.274	44.57	0.846
10	2.194	98.26	0.966
10	4.387	97.56	0.973

The retention for Na_2SO_4 is lower than for $MgSO_4$. This means that the retention mechanism cannot be explained by the Donnan mechanism. According to the Donnan exclusion the negatively charged membrane should absorb more Mg^{2+} ions and thus the $MgSO_4$ flux will be larger than the Na_2SO_4 flux. The origin for this phenomenon can be the difference between Na^+ and Mg^{2+} transport due to steric hindrance (pore exclusion) in the membrane matrix enhanced by the clustering phenomena of $MgSO_4$ (chapter 3.3).

4.7 Electrostatic properties of the membranes measured by streaming potential method

4.7.1 Introduction

As stated before nanofiltration (NF) and reverse osmosis (RO) processes suffer from fouling phenomena (i.e. flux decline) due to unwanted adsorption of components rejected by the membrane. A way to understand and cope with these problems is to know the physico-chemical nature of the membrane. Electrokinetic measurements like the streaming potential measurements can be done to link fouling studies on membranes to the membranes' chemical properties.

In the streaming potential cell an applied hydrostatic pressure causes an electrolyte solution to stream along a membrane surface. When the membrane contains fixed charged groups the distribution of the ions in solution near the surface will be influenced in such a manner that an electric potential over the flow path of the cell will be established. This electric potential is linearly dependent on the hydrostatic pressure [7] under the condition that the flow is laminar. The objective of the research is to determine the membrane charge at different pH and thus the iso-electric point of the membranes.

4.7.2 Theoretical background

The membrane surface can have fixed electric charges as a consequence of specific ionic functional groups in the membrane material or specific adsorption of ionic components. When the surface is brought into contact with an ionic solution a rearrangement of the ions in solution will occur. Counter-ions will accumulate in the layer adjacent to the membrane surface or even adsorb at this surface. This layer, called the electric double layer, is a few nanometer thick and can be distinguished in a fixed and a mobile part. The zeta potential, which is defined as the potential at the plane of shear between the streaming fluid and the fixed layer near the membrane, is a suitable parameter for the qualitative characterisation of the apparent membrane surface charge. The zeta potential can be determined by using an electrokinetic measurement method like the determination of streaming potentials as function of the applied hydrostatic pressure.

Streaming potentials can be measured by flowing an electrolyte solution along a membrane surface under a hydrostatic pressure gradient. As a consequence of this, counter-ions at the membrane surface will accumulate downstream resulting in an electrical potential difference along the flow path, i.e. the streaming potential (ΔV_{str}). The relation between the zeta potential and the streaming potential is [7]:

$$\zeta = \frac{\eta \cdot \left(\Gamma_0 + \frac{2 \cdot \Gamma_S}{b} \right)}{\varepsilon} \cdot \frac{\Delta V_{str}}{\Delta P_{str}} \qquad (4.16)$$

The surface conductivity (Γ_S) is only important at concentrations below 10^{-3} M. At higher concentrations this term can be neglected and the equation becomes:

$$\zeta = \frac{\eta \cdot \Gamma_0}{\varepsilon} \cdot \frac{\Delta V_{str}}{\Delta P_{str}} \qquad (4.17)$$

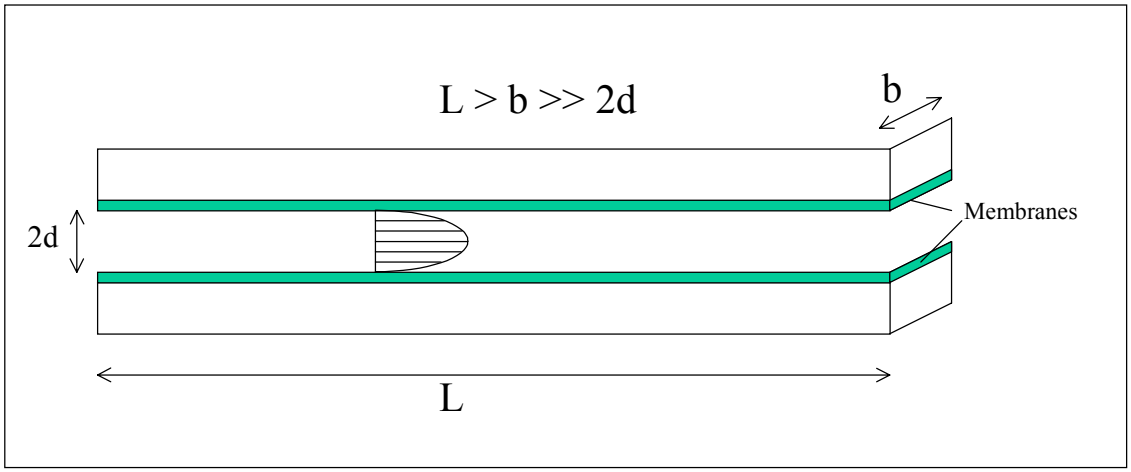

Figure 4.11 Schematic representation of the streaming potential cell.

4.7.3 Experimental set-up

An experimental set-up similar to [9] and [10] was used. The streaming potential cell was mounted between two reservoirs. The hydrostatic pressure drop over the measuring cell was applied by putting air pressure on one of the reservoirs by a system of valves. The driving pressure was monitored with a pressure difference meter (Endress and Hauser, Deltabar S) with an accuracy of 1 mbar. The electrical potential difference over the cell (streaming potential) was measured using black platinum electrodes connected to a high input impedance (> 10 GOhm) electric potential meter (Keithley 617), referred to as 'electrometer'. The slit height between the membranes was 200 μm.

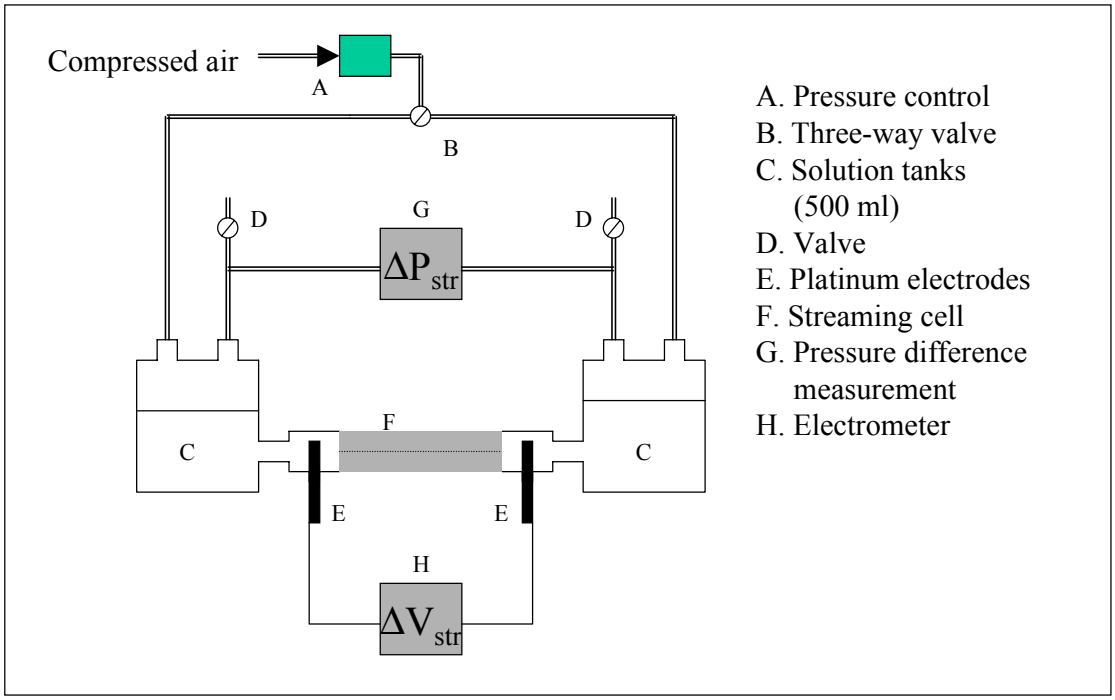

Figure 4.12 Experimental set-up streaming potential

Right-angled membrane slides (76mm x 26mm) were cut out of the membrane tubes. These slides were pressurised (~ 1500 Pa) for at least 24 hours in order to make them flat. The membranes were glued onto the glass slides by the use of a primer and glue system under pressurisation again (~ 1500 Pa). Vacuum grease was put between the teflon sheets and the

glass slides in order to prevent bypass streaming and between the cell halves in order to prevent leakage.

The reservoirs and cell were filled with 500 ml of a 0.01 M NaCl-solution. This solution was prepared in demineralised water with a conductivity less than 5 µS/cm. Air bubbles in the cell were removed before start up of an experiment. The cell with solution was stayed overnight in order to condition the membranes. Streaming potential measurements were done at pressures of 100, 200, 300, 400 and 500 mbar. After the measurement samples of 100 ml were taken out of the reservoirs for measuring the pH and conductivity. Two experimental runs were done at varying pH, one for the pH of 2, 3, 4, 5 and 7 and one for the pH 7, 8, 9, 10 and 11. Between these two experimental runs the system was flushed with demineralised water. The pH was adjusted by addition of HCl and NaOH.

4.7.4 Results

Zeta potentials at varying pH were calculated for the NF membrane and the RO membrane (figure 4.13). The NF membrane has its iso-electric point at pH ~ 3 and the RO membrane at pH ~ 7. According to the manufacturer the nanofiltration membranes contain negatively charged groups, which give the membrane its special ion rejecting properties. The membrane will reject the anionic polyvalent ions, according to the Donnan theory, over the pH range from 3-11. It was observed that the RO membrane at high alkalinity has approximately the same charge as the NF membrane. It is very likely for both membranes that fouling build-up and removal is dependent on the pH.

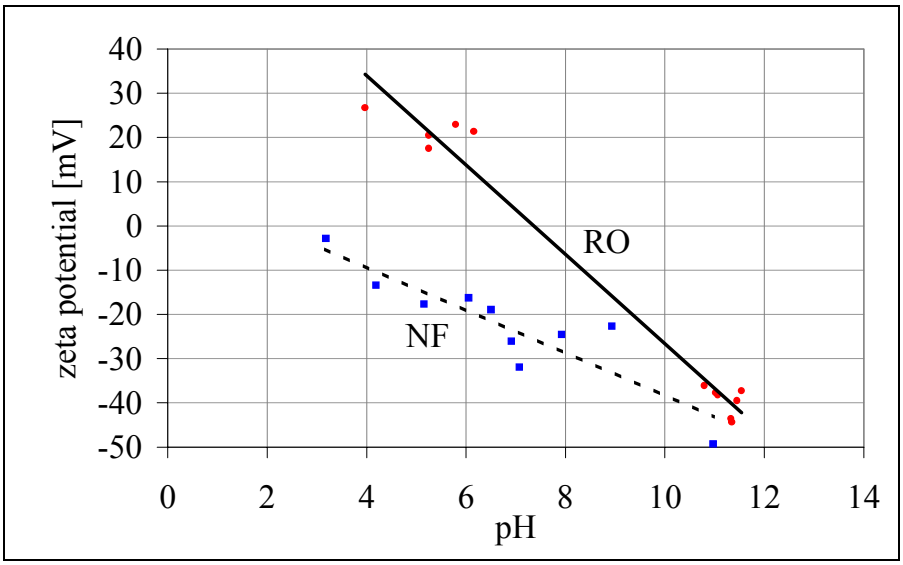

Figure 4.13 Zeta potential vs. pH; Nanofiltration membrane Stork WFN: conductivity = 1022 ± 127 µS/cm. Reverse osmosis membrane Stork WFC-X: conductivity = 1806 ± 310 µS/cm.

4.7.5 Conclusion

The zeta potential, an electrostatic phenomenon, of Storks' RO-WFCX and NF-WFN membranes has been measured at varying pH and at ~0.01 M NaCl solution. A streaming potential method, an electrokinetic characterisation method, where a laminar flow is established along the surface has been used for this purpose. The NF membrane has a negative zeta potential over the pH range from 3-11, as was expected. The RO membrane has an iso-electric point near pH 7. The results of this characterisation method will be used to explain experiments with synthetic wastewater.

4.8 Electrodynamic properties of the RO and NF membrane

4.8.1 Introduction

From a thermodynamic standpoint, adsorption of components onto a membrane surface will occur if the total free energy of a system (membrane + solvent + solute) is decreased. From a mechanistic standpoint of view, electrodynamic forces, representing the mutual influences of components on their electron distributions, will next to electrostatic forces described in chapter 4.7, determine the complex scheme of mutual attraction and repulsion between components involved. Electrodynamic properties are in membrane technology often simplified to hydrophilic (water-attractant) or hydrophobic (water-repellent) membrane surfaces and solutes. According to this simple theory membrane fouling will be more severe when dealing with more hydrophobic membranes and more hydrophobic solutes.

The simple theory of hydrophilic – hydrophobic often fails for an adequate description of membrane fouling tendencies. The theory of Van Oss, Chaudhurry and Good (VCG theory) [11] describing the electrodynamic part of the interfacial forces as a summation of apolar and polar interactions will be used here.

In this paragraph the electrodynamic properties of both the RO and the NF membrane will be determined according to the VCG theory and interaction energies between the surfactant sodium dodecylsulphate and the membranes will be examined in order to explain why and how these surfactants adsorb onto the membrane.

The description, as given in [12] for adsorption of SDS on nylon, cellulose acetate and 'dirt' surfaces, has been applied here for the RO and the NF membrane.

4.8.2 Theoretical background

The VCG theory considers the total interaction energy between a solute and an other solute or surface in a liquid medium to be the summation of apolar (Lifschitz -Van der Waals, LW), polar (Lewis Acid-Base, AB) and electrostatic (EL) forces. The surface tension γ, expressed in $N \cdot m^{-1}$ is defined as half the free energy change necessary to create a unit surface area of a material in vacuum. The total surface tension can, in analogy to the energy, be divided into LW, AB and EL contributions.

$$\gamma_1 = \sum_i \gamma_1^i = \gamma_1^{LW} + \gamma^{AB}{}_1 + \gamma_1^{EL} \qquad (4.18)$$

The AB component is subdivided into an electron acceptor (γ^+) and an electron donor part (γ^-). It is this separation of the AB component that allows the AB interaction to be either repulsive or attractive.

$$\gamma_1^{AB} = 2 \cdot \sqrt{\gamma_1^+ \cdot \gamma_1^-} \qquad (4.19)$$

The interaction between the membrane surfaces (1) and a solute (2) immersed in a liquid 3 can be described by the Dupré-equation, which gives the work necessary for adsorption [11]

$$\Delta G_{132} = (\gamma_{12} - \gamma_{13} - \gamma_{23}) \qquad (4.20)$$

If only the electrodynamic contribution (LW and AB) is taken into account the Dupré equation will yield:

$$\Delta G_{132} = 2 \cdot (\sqrt{\gamma_1^{LW} \cdot \gamma_3^{LW}} + \sqrt{\gamma_2^{LW} \cdot \gamma_3^{LW}} - \sqrt{\gamma_1^{LW} \cdot \gamma_3^{LW}} - \gamma_3^{LW} + \sqrt{\gamma_3^+} \cdot (\sqrt{\gamma_1^-} + \sqrt{\gamma_2^-} - \sqrt{\gamma_3^-}) + \sqrt{\gamma_3^-} \cdot (\sqrt{\gamma_1^+} + \sqrt{\gamma_2^+} - \sqrt{\gamma_3^+}) - \sqrt{\gamma_1^+ \cdot \gamma_2^-} - \sqrt{\gamma_1^- \cdot \gamma_2^+}) \quad (4.21)$$

This equation will be used here to describe the adsorption of a sodium dodecylsulphate onto the membranes using the method proposed by [12]. The electrodynamic contribution to the adsorption of respectively the tail and the head of the surfactant will be treated separately.

Table 4.18. Surface tension parameters of contact angle liquids at 20°C [11]

	γ^{LW} [10^{-3} N/m]	γ^+ [10^{-3} N/m]	γ^- [10^{-3} N/m]
α-Bromonaphthalene	44.4	0	0
Water	21.8	25.5	25.5
Glycerol	34	3.92	57.4
Ethylene Glycol	29	4.18	41.78

In order to determine the one LW and two AB parameters of a membrane surface, contact angle measurements with three liquids with known LW and AB parameters should be done. Parameters of frequent used liquids are summarised in table 4.18 [11]. The relation between the measured contact angle (θ) and the surface tension parameters is (subscript S = solid, subscript L = liquid).

$$(1 + \cos(\theta)) \cdot \gamma_L = 2 \cdot (\sqrt{\gamma_S^{LW} \gamma_L^{LW}} + \sqrt{\gamma_S^+ \gamma_L^-} + \sqrt{\gamma_S^- \gamma_L^+}) \quad (4.22)$$

4.8.3 Experimental part

The sessile drop method was used with the liquids glycerol, glycol and water. The frequent used apolar liquid α-bromonaphtalene could not be used as the membrane material dissolves in this liquid. Membrane slides of .5 mm wide were cut out of the tubular shape RO and NF membranes. The contact angle measurements were performed on a GI-goniometer (Krüss GmbH). For every liquid several (8-14) drops of 0.05 ml were put on the membrane surface and the contact angle was determined automatically by image recognition of the droplet. This means that from the shape of the droplet on the surface the contact angle was determined.

4.8.4 Results

Table 4.19. Contact angles, values in brackets are the standard deviations

	Water	Ethylene glycol	Glycerol
RO membrane	71.7° (1.5°)	21.8° (0.8°)	55.9° (4.0°)
NF membrane	76.9° (3.5°)	47.6° (4.4°)	71.9° (1.8°)

The averaged experimental determined contact angles are shown table 4.19 and the calculated surface tension parameters are shown in table 4.20. From these data the LW and AB interaction of both membranes with a SDS molecule are calculated and compared to the values calculated for nylon [13].

Table 4.20 Electrodynamic parameters of components and materials considered in this study.

	RO membrane	NF membrane	Nylon 6,6 [13]	SDS-tail part [12]	SDS-head part [12]
γ^{LW}	46.5	38.3	36.4	23.8	34.6
γ^{+}	0.5	0	0.02	0	0
γ^{-}	6.1	9.8	21.6	0	46

The free energies of adhesion between the two SDS parts on one hand and the membrane material and the SDS parts on the other hand, all immersed in water can now be calculated:

Table 4.21 Free energy of adhesion i.e. ΔG_{132} (in mJ/m^2).

	RO mem	NF mem	Nylon 6,6	SDS tail part	SDS head part
SDS tail part	-70.8	-71.0	-54.2	-34	-1.06
SDS head part	-16.2	-5.6	9.63	-1.06	1.16

The electrodynamic measurements and calculations show that adsorption of SDS on an uncharged RO membrane (at pH 7), the uncharged NF membrane (~ pH = 1) or uncharged nylon will occur preferably by a tail attachment to the membrane surface. This tail attachment (hemimicelle formation) is thermodynamically favoured over the micelle formation in solution. Furthermore in alkaline conditions the tail attachment will be favoured even more as the head of the SDS molecule will be confronted with an electrical repulsion by the similar membrane surface charge (determined in chapter 4.7).

4.8.5 Conclusion

The adsorption of SDS onto the RO and NF membrane surface has been analysed with the theory of electrodynamic interactions according to Van Oss [11]. The electrodynamic parameters of the RO and NF membrane have been determined by measuring contact angles with three liquids (glycerol, glycol and water). Using the analysis presented by Van Oss and Constanzo [12], it could be proven that, in absence of electrostatic interactions between surfactant and membrane, the surfactant tail to membrane surface adsorption is favoured over the micelle formation and the surfactant head to membrane surface adsorption. The results of these electrodynamic measurements in combination with the electrostatic measurements of chapter 4.7 will be used for explaining the adsorption of SDS onto the membranes and membrane fouling.

Acknowledgement

F. Spenkelink and M. van Stratum are acknowledged for the filtration measurements of the inorganic salt solutions. B. Quirke is acknowledged for the zeta-potential measurements.
S. Rekveld is acknowledged for the discussion and supply of articles about the VCG-theory.

Symbols

	description	unity
β	equation parameter = $J_v/v^{0.8}$	$[m/s]^{0.2}$
Γ	conductivity	[S/m]
Γ_0	bulk conductivity	[S m^{-1}]
Γ_s	surface conductivity	[S]
γ	(total) surface tension	[N/m]

γ^+	electron acceptor parameter to surface tension	[N/m]
γ^-	electron donor contribution to surface tension	[N/m]
γ^{AB}	Acid-Base contribution to surface tension	[N/m]
γ^{EL}	electrostatic contribution to surface tension	[N/m]
γ^{LW}	Lifschitz -Van der Waals contribution to surface tension	[N/m]
$\Delta\Pi_{i.p}$	osmotic pressure difference across membrane	[Pa]
ΔG_{132}	free energy of interaction between material 1 and 2 in medium 3	[N/m]
Δm	mass difference	[kg]
ΔP	transmembrane pressure (TMP)	[Pa]
ΔP_{str}	pressure drop streaming potential cell	[Pa]
Δt	time interval	[s]
ΔV_{str}	streaming potential	[V]
ε	dielectric constant	[F m^{-1}]
ζ	zeta potential	[V]
η	dynamic viscosity	[Pa sec]
θ	contact angle	[-]
ν	kinematic viscosity	[m^2/s
ρ	density	[kg/m^3]
A	hydrodynamic membrane permeability	[m/(s·Pa)]
a	equation parameter	[m/s]$^{0.2}$
b	slit depth	[m]
B_0	real solute transport parameter across membrane	[m/s]
B_m	observed solute transport parameter across membrane	[m/s]
C_b	concentration in bulk	[mole/m^3]
C_i	concentration at membrane interface	[mole/m^3]
C_p	concentration in permeate	[mole/m^3]
C_R	concentration in retentate	[mole/m^3]
d	slit height cell	[m]
D	diffusion coefficient	[m^2/s]
d_i	internal membrane tube diameter	[m]
J_v	permeate flux	[m/s]
k	solute transport parameter in boundary layer	[m/s]
L	slit length	[m]
N_s	solute flux across membrane	[mole/(m^2·s)]
R	gas constant	[J $mole^{-1}$ K^{-1}]
Re	Reynolds number	[-]
Ret	intrinsic retention	[-]
Ret_m	observed retention	[-]
S	membrane surface	[m^2]
Sc	Schmidt number	[-]
Sh	Sherwood number	[-]
T	temperature	[K]
v	cross-flow velocity (CF)	[m/s]

Literature

[1] Hunter, R.J., Zeta potential in colloid science, principles and applications. 3rd ed. (1988).
[2] Rekveld, S. Ellipsometric studies of protein adsorption onto hard surfaces in a flow cell. Doctoral thesis University of Twente (1997).
[3] Weast, R.C., CRC handbook of chemistry and physics. 1st student edition ed. (1988).
[4] Murthy, Z. V. P. and S. K. Gupta, Simple graphical method to estimate membrane transport parameters and mass transfer coefficient in a membrane cell. Separation science and technology 31(1): 77-96 (1996).
[5] Mulder, M., Basic principles of membrane technology, (1991).
[6] Rard, J. A. and D. G. Miller, The mutual diffusion coefficients of NaCl-water and CaCl2-water at 25 °C from Rayleigh interferometry. Journal of solution chemistry 8(10): 701-716 (1979).
[7] Davies, J.T. and E.K. Rideal, Interfacial Phenomena. 2nd ed. (1963).
[8] Lyklema, J., Fundamentals of interface and colloid science, vol II. solid-liquid interfaces. (1996).
[9] Peeters, J.M.M., Characterization of nanofiltration membranes, Doctoral thesis University of Twente, (1997).
[10] Wagenen, v. R. A. and J. D. Andrade. Flat plate streaming potential investigations: hydrodynamics and electrokinetic equivalency. Journal of Colloid and Interface Science 76(2): 305-314 (1980).
[11] Oss, C.J. v., Interfacial forces in aqueous media. New York, M. Dekker (1994).
[12] Oss, v.C.J. and P.M. Costanzo, Adhesion of anionic surfactants to polymer surfaces and low-energy materials. J. Adhesion Sci. Technol., 6 (4): p. 477-487 (1992).
[13] Oss, C.J. v., R.J. Good, and H.J. Busscher, Estimation of the polar surface tension parameters of glycerol and formamide for use in contact angle measurement on polar solids. J. Dispersion Science and Technology, 11(1): p. 75-81 (1990).

Appendix 4A. Concentration build up in a recycle membrane filtration system

Two operation modes for a feed/bleed membrane filtration set-up will be discussed here (figure 3.10).

1. Both retentate and permeate are not flowed back to the feed tank
2. Both retentate and permeate are flowed back to the feed tank

It is obvious that if the retentate is flowed to the feed tank and the permeate not, the concentration in the recirculation loop will change in time. So when a constant mean concentration in the recirculation loop is desired one of the proposed operation modes is preferred. However in these two systems also a considerable concentration increase can occur. A dynamical model will be presented here to calculate this concentration build-up in time and measures to manage this unwanted concentration build-up will be given here.

Before start up the recirculation loop is filled with the feed under no ‘significant’ transmembrane pressure. The permeate flux is thus zero and the mean concentration in the recirculation loop is the same as in the feed. At start up the transmembrane pressure is increased within a few seconds causing the permeate flow to rise and the retentate flow to drop. This will increase the mean concentration in the recycle loop as the membrane rejects the solutes. This increase will last until the massflow of solute discharged by the retentate stream is the same as the massflow of solute brought into the recycle loop by the feed stream as is shown in equation 1.

$$\Phi_R \cdot C_R = \Phi_F \cdot C_F \qquad \text{(A4.1)}$$

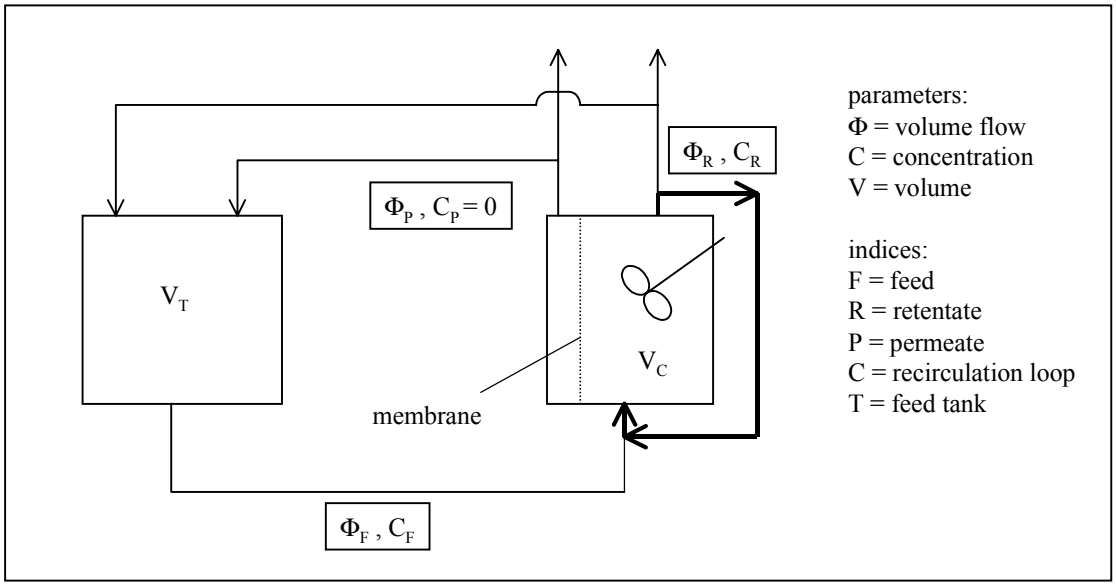

Figure A4.1. Schematic representation of a feed/bleed set-up of a membrane filtration system

Model descriptions

1. Membrane set-up without flow back of retentate and permeate stream to the feed tank

The dynamical model can be written as:

$$V_C \cdot \frac{dC_R}{dt} = \Phi_F \cdot C_F - \Phi_R \cdot C_R \qquad \text{(A4.2)}$$

Solving this differential equation the concentration of the retentate as function of time is:

$$C_R = C_F \cdot \left[VRF - (VRF - 1) \cdot \exp\left[\frac{-t}{VRF \cdot \tau_{CF}} \right] \right] \qquad \text{(A4.3)}$$

Here C_F is constant en $C_R(t=0) = C_F$. VRF is the volume reduction factor ($1<VRF<\infty$).

$$VRF = \frac{\Phi_F}{\Phi_R} \qquad \text{(A4.4)}$$

And τ_{CF} the residence time in the circulation system referring to the feed stream.

$$\tau_{CF} = \frac{V_C}{\Phi_F} \qquad \text{(A4.5)}$$

2. Membrane set-up with flow back of retentate and permeate stream to the feed tank

In this system the ratio volume feedtank / volume circulation loop is an important parameter. Dynamic mass balances for both the feed tank and circulation loop must be solved
For the feed tank this is

$$V_T \cdot \frac{dC_F}{dt} = \Phi_R \cdot C_R - \Phi_F \cdot C_F \qquad \text{(A4.6)}$$

and for the recycle loop

$$V_C \cdot \frac{dC_R}{dt} = \Phi_F \cdot C_F - \Phi_R \cdot C_R \qquad \text{(A4.7)}$$

Both equations are divided by Φ_F to give:

$$\tau_{TF} \cdot \frac{dC_F}{dt} = \frac{C_R}{FR} - C_F \qquad \text{(A4.8)}$$

$$\tau_{CF} \cdot \frac{dC_R}{dt} = C_F - \frac{C_R}{FR} \qquad \text{(A4.9)}$$

The combination of these two equations leads to the trivial relationship:

$$\tau_{CF} \cdot \frac{dC_R}{dt} = -\tau_{TF} \cdot \frac{dC_F}{dt} \qquad \text{(A4.10)}$$

Differentiating eq (A4.9) to t gives:

$$\tau_{CF} \cdot \frac{d^2C_R}{dt^2} = \frac{dC_F}{dt} - \frac{1}{FR}\frac{dC_R}{dt} \qquad \text{(A4.11)}$$

Substituting the trivial relationship eq (A4.10) in eq (A4.11) gives:

$$\tau_{CF} \cdot \frac{d^2C_R}{dt^2} = -\left[\frac{1}{FR} + \frac{\tau_{CF}}{\tau_{TF}}\right]\frac{dC_R}{dt} = -\alpha \cdot \frac{dC_R}{dt} \qquad \text{(A4.12)}$$

This equation is solved with the boundary conditions:

t = 0: $C_R = C_F$ or: $C_R = C_0$

t = ∞ $C_R = C_F \cdot FR$

As both concentrations C_R and C_F change in time, a solute mass balance over time should be calculated to determine the concentrations at infinite time as function of the process parameters:

$$(V_T + V_C) \cdot C_0 = V_T \cdot C_F + V_C \cdot C_R \qquad \text{(A4.13)}$$

The last boundary condition becomes thus:

$$C_R = \left[\frac{V_T + V_C}{\frac{V_T}{FR} + V_C} \right] \cdot C_0 = \beta \cdot C_0 \qquad \text{(A4.14)}$$

Solving the equation with the given boundary conditions results in:

$$C_R = C_0 \cdot \left[\beta - (\beta - 1) \cdot \exp\left[\frac{-\alpha \cdot t}{\tau_{CF}} \right] \right] \qquad \text{(A4.15)}$$

Criterion for steady state

The criterion for steady state should be defined as the time (t*) at which the concentration is 'close' to the concentration at t = ∞. In mathematical form:

$$Q = \frac{C_R(t^*)}{C_R(t = \infty)} \approx 1 \qquad \text{(A4.16)}$$

A reasonable value for Q is 0.98, which is comparable with the situation where a ideal stirred tank should be rinsed during 4 times the residence time in order to reach steady state (Q = 0.982). For the membrane set-up 1 this time is:

$$t^* = \tau \cdot FR \cdot \ln\left[\frac{FR - 1}{FR \cdot (1 - Q)} \right] \qquad \text{(A4.17)}$$

For membrane set-up 2 this time is:

$$t^* = \frac{\tau_{CF}}{\alpha} \cdot \ln\left[\frac{\beta - 1}{\beta \cdot (1 - Q)} \right] \qquad \text{(A4.18)}$$

Two membrane filtration recycle systems, the former typical for NF the latter typical for RO, have been calculated. The concentration build-up problem is more severe for NF as its permeate flow is much higher than the permeate flow of the RO.

Table A4.1 Characteristic concentration build-up (maximum values) of RO and NF experiments performed in this research.

	I (NF)	II (RO)
1. Without back-flow of permeate and retentate		
Feed flow, Φ_F	60 lt/hr	50 lt/hr
Retentate flow, Φ_R	50 lt/hr	48 lt/hr
FR	1.2	1.042
t* [min]	25.4	8.7
2. With back-flow of permeate and retentate		
Volume tank, V_T	50 litre	50 litre
Volume circulation loop, V_C	10 litre	10 litre
α	1.033	1.16
β	1.161	1.034
t* [min]	18.8	5.3

The concentration build-up of the NF cases is presented in figure (A4.2).

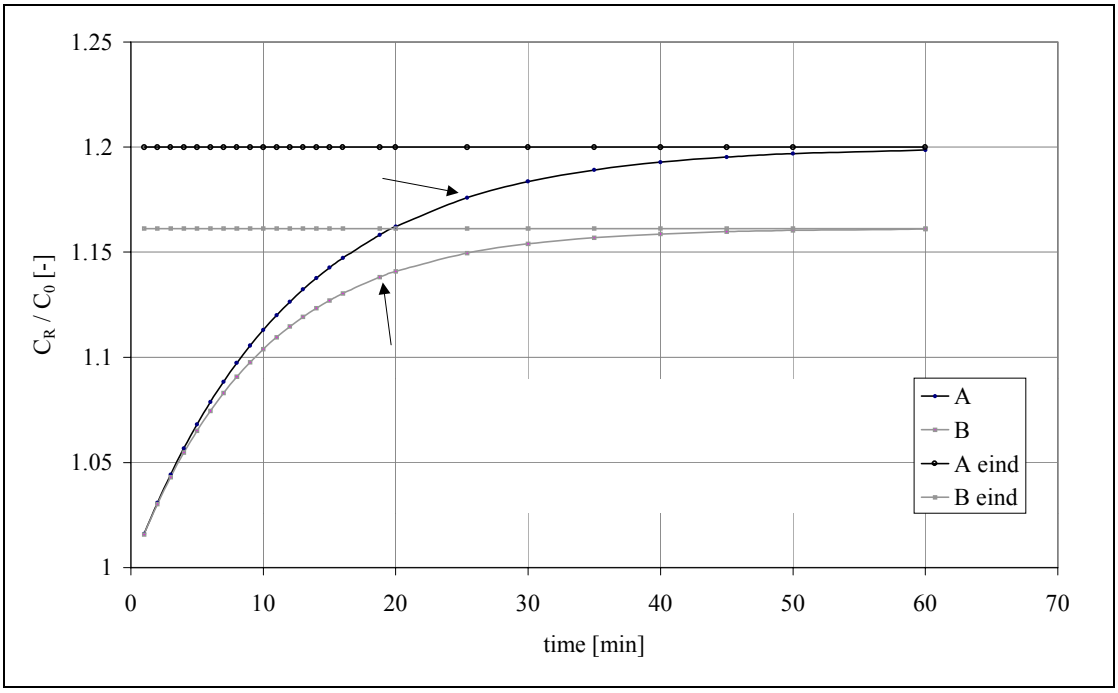

Fig. A4.2 Concentration build-up in time for case I (nanofiltration); A: without flow back of permeate and retentate (eq. A4.3) ; B: with flow back of permeate and retentate (eq. A4.15); arrows indicate the criterion for steady state.

It is shown in this graph that the maximum concentration overshoot above the feed concentration is less than 20 % and this fact is considered not to be a major issue influencing membrane fouling. Measures to decrease the influence of the concentration build-up are:

1. Keep volume reduction factor low.
This actually has been done in the reverse osmosis experiments. However when the permeate flow is relatively high (e.g. NF) the feed and retentate streams must be raised. The system will become a more one-pass system.

2. Fill the total system and decrease the concentration in the feed tank by dilution with water. There are different ways to do this:

2a. Fill the system, stop the pump, and decrease the concentration in the feed concentration at once to the end concentration expected.

2b. Fill the system, do not stop the pump but add that much water to the feed tank in order to decrease the feedconcentration and to keep the retentate concentration constant.

However the volume reduction factor will not be constant during a fouling/flux decline experiment. A good control system will then be necessary.

3. Use a little feed tank. ($V_T << V_C$)

The feed tank is then 'part' of the circulation system. However the total wastewater volume and availability of fouling components used for the experiment will be decreased drastically.

If these measures can't be taken a good dynamical process description will be necessary, based on the model presented here combined with descriptions of the fouling process.

Symbols of Appendix 4A

α	assistant parameter	[-]
β	assistant parameter	[-]
τ_{CF}	residence time in recirculation loop referring to the feed stream	[s]
τ_{TF}	residence time in feed tank referring to the feed stream	[s]
Φ_I	volumetric flow stream I	[m^3/s]
C_I	concentration in stream I	[mole/m^3]
Q	criterion parameter steady state	[-]
t	time	[s]
t*	steady state time	[s]
V_J	volume of system J	[m^3]
VRF	volume reduction factor membrane process	[m^3/m^3]

Indices

F	Feed
R	Retentate
P	Permeate
C	Recirculation loop
T	Feed tank

Chapter 5

Membrane filtration of actual wastewater from a reactive dyeing process leading to selection of components in synthetic wastewater

Summary

Wastewater streams from two textile reactive dyeing plants have been treated by reverse osmosis and nanofiltration. The purpose was to identify wastewater components, which contribute to membrane fouling. Based on these experiments, other research [1] and data about textile auxiliaries [2] components were selected for the make-up of synthetic wastewater in order to investigate membrane fouling systematically. The reverse osmosis and nanofiltration experiments described in chapters 6 and 7 were executed with this synthetic wastewater.

5.1 Introduction

A systematic and scientific study of membrane fouling requires filtration experiments with wastewater of which the compositions are known and can be varied according to specification. Since industrial wastewater does not satisfy these requirements, synthetic wastewater, containing components which are representative for components in the textile wastewater, has to be designed.

In this chapter reverse osmosis and nanofiltration experiments of industrial wastewater from two reactive dyeing plants will be described. The main purpose of these experiments is to identify the components in the wastewater, which contribute to membrane fouling. The results of these investigations together with results from other research [1] and data about textile components will provide the components for the synthetic wastewater.

5.2 Experiments on textile wastewater from reactive dyeing processes

5.2.1 Experimental set-up

Experiments have been performed with wastewater from two different textile reactive dyeing processes.

Table 5.1 Origin of the textile wastewater.

Company	Abbreviation	Process
Ten Cate Protect Nijverdal	TCP	Pad-steam
KTV Eibergen	KTV	Pad-batch

The feed for the membrane experiments was made in conformity with the dye content of the wastewater from the washing processes by diluting the samples to 1 g/l dye content. The pH of all feed streams was set to neutral conditions (pH 6-8) by addition of hydrochloric acid. All the wastewater from KTV (pad-batch) had a very high pH, so adjusting the pH was necessary in order to stay within the operation limits of the membranes. Doing so it turned out that waterglass, present in the KTV-samples, forms a gel, so prefiltering with a microfilter to remove this silica gel was necessary. In table 5.2 the components present in the samples, according to the data given by textile companies, and their concentration, after dilution to 1 g/l total dye content and prefiltration, are listed. No extra inorganic salt and textile auxiliaries were added.

NF experiments were carried out with all the waste streams. The RO experiments only with: TCP A; TCP B; KTV-1. The installation was rinsed with demineralised water between the different dye batches. In some cases the membrane was replaced by a new one. Experiments were performed at varying transmembrane pressures and cross-flow velocities. During an experiment, which lasted at least two hours, the permeate flux was measured and at the end of the experiment samples of both retentate and permeate were collected and analysed for their dye content. The membrane equipment used was the recycle set-up with recirculation of the retentate and permeate stream to the feed tank (chapter 4).

Table 5.2 Estimated concentrations in the feed water of the preliminary study. The KTV wastewater is given before the prefiltration step! All concentrations are in g/l [1]except Zetex Jet (ml/l) and waterglass (as reactive silica in mg/l). [2]commercial name of dye components all Remazol dyes. [3]Colour Index number (R = Reactive). [4] commercial name of dye components all Levafix dyes.

Dye [2]	CI nr [3]	KTV-1	KTV-2	KTV-3	KTV-4	KTV-5
yellow GR	R. yellow 15		0.28			
brill. yellow GL	R. yellow 37			0.37		0.15
brill. orange 3R	R. orange 16				0.66	
brill. red F3B	R. red 180	0.04	0.66			
red BB	R. red 21				0.27	
turquoise blue PG	R. blue 21			0.61		0.49
blue HR	R. blue 158				0.07	
brill. blue R spec.	R. blue 19	0.96		0.02		0.36
black B	R. black 5		0.06			

Auxiliary component	KTV-1	KTV-2	KTV-3	KTV-4	KTV-5
Waterglass	1.3	2	1.6	2.9	2.5

Dye [4]	CI nr [3]	TCP-A	TCP-B
brown E2R	R. brown 19	0.57	0.03
brill. red E4BA	R. red 158	0.34	
black EB	R. black 5	0.09	
yellow E3RL	R. orange 30		0.12
brill. blue EB	R. blue 29		0.05

Auxiliary component	TCP-A	TCP-B
Zetex Jet [1]	0.05	0.72
Zetex MI	0.14	2.17
Zetex HP LFN	0.005	0.07
Leophen RA	0.01	0.18

The concentration of reactive silica is estimated under the condition that the filtrate of the prefiltration step contains at maximum the saturated concentration of reactive silica at pH =7 (i.e. 100 mg/l). If the prefiltration had not been executed, the concentration of silica would have been 1900 mg/l at maximum. The contents and function of the auxiliary components in the TCP wastewater are listed in table 5.3.

Table 5.3. Contents and function auxiliary components

auxiliary component	content	function
Zetex Jet	Emulsion based on polydimethyl siloxane	anti-foaming agent
Zetex MI	solution of a polymer based on acryl	flame retarding agent
Zetex HP LFN		wetting agent
Leophen RA	(solution of) sodium sulfo succinic acid ester	wetting agent

5.2.2 Results reverse osmosis

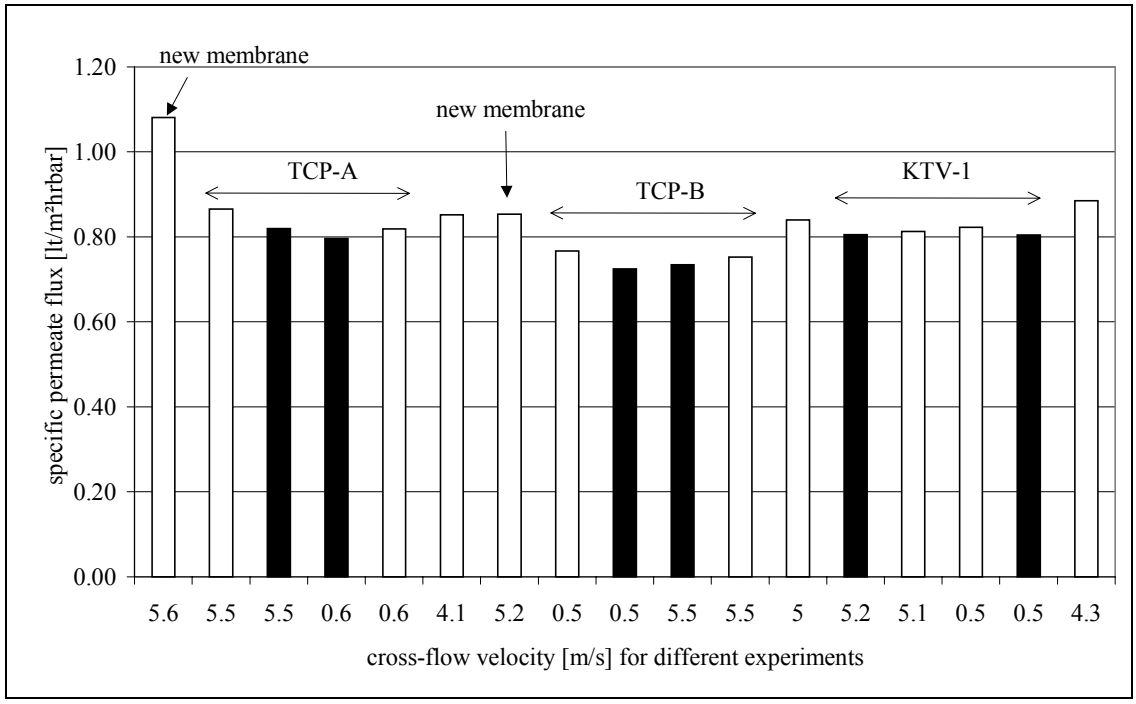

Figure 5.1 Results preliminary study reverse osmosis, experiments are chronologically ordered. open bars = clean water flux at 20 bar, shaded bars = wastewater flux at 20 bar, filled bars = wastewater flux at 30 bar.

The (RO) permeate fluxes did not severely decrease in time for any experiment. Figure 5.1. show the specific permeate end flux (permeate flux divided by transmembrane pressure) for the clean water fluxes and experiments with wastewater at varying transmembrane pressures and cross-flow velocities. The permeate fluxes in the wastewater experiments were just slightly lower than the clean water fluxes (within 75 %)!

Variation of the transmembrane pressure and cross-flow velocity only had a slight influence on the specific permeate flux. There was thus no severe influence of membrane compaction, concentration polarisation or membrane fouling detected.

All permeate streams of the reverse osmosis were colourless, i.e. no dyes could be detected by means of spectrophotometrical analysis.

5.2.3 Results nanofiltration

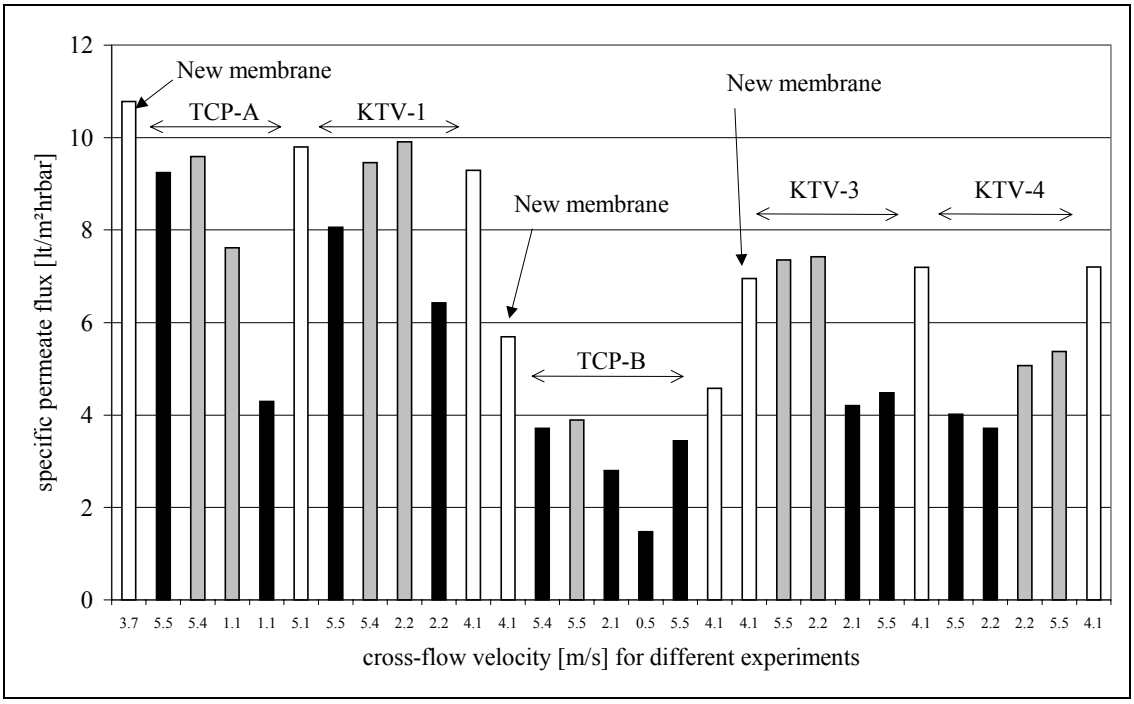

Figure 5.2 Specific permeate flux NF-preliminary study. experiments are chronologically ordered. white bars = clean water at 10 bar, grey bars = wastewater at 10 bar, black bars = wastewater at 20 bar.

Figure 5.2 shows the specific permeate fluxes, defined as the permeate flux at the end of the NF experiment divided by the transmembrane pressure, of the samples TCP-A and B and KTV- 1, 2 and 3 after at least two hours of filtration. It was generally observed that a higher transmembrane pressure and a lower cross-flow velocity cause a lower specific permeate flux. This points to an influence of concentration polarisation and membrane fouling on the permeate flux. From the experiments it is not clear directly which components are responsible for lower fluxes.

Cleaning the installation between the different dye batches by rinsing it with demineralised water turned out to be effective to restore the clean water flux. However there was a big difference in clean water flux among the membranes observed! It could be that there are big differences between new nanofiltration membranes. Furthermore rinsing and cleaning procedures, before installing a new membrane, were extended and improved in order to decrease the influence of impurities on the start-up of a new membrane (chapter 6 and 7).

In order to compare the experiments with the different membranes with each other relative specific permeate fluxes have been calculated (Appendix 4A). The relative specific permeate flux is defined as the specific permeate flux of a wastewater filtration divided by the specific permeate flux of the proceeding clean water filtration.

Remarkable flux decline during the experiment was in some cases observed with the KTV wastewater, but not with the TCP wastewater. In an experiment with KTV-1 wastewater at 30 bars running more than 4 hours this flux decline was recorded (figure 5.3.). The total dye concentration in this particular experiment was 5 g/l. Most part of the waterglass had been removed by the prefiltration leaving an estimated concentration after dilution of 6.5 mg/l reactive silica in this experiment.

The dynamic effect as mentioned in paragraph 4.5. does not play an important role in this experiment: the feed stream is fixed at 59.5 lt/hr and a decreasing permeate flow reduces the volume concentration factor from 1.19 to 1.03 during this experiment. The concentration build up at the start of the experiment last about 20 minutes (eq. A4.18) and the concentration in the recirculation loop at the end is only 3 percent higher than the concentration in the feed at the start of the experiment.

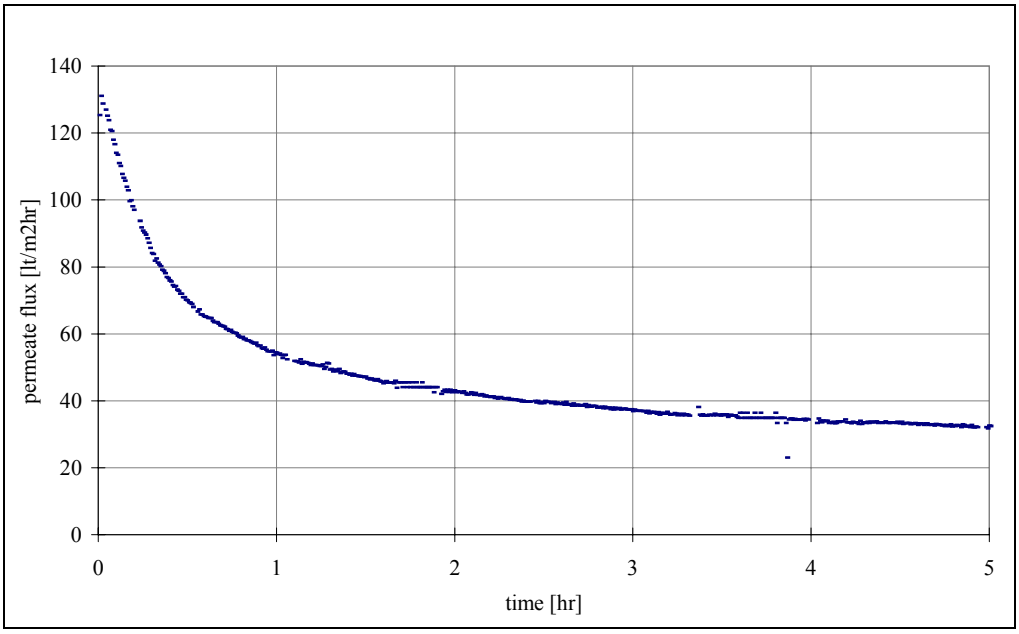

Figure 5.3 Flux decline in time NF filtration of KTV-1 at transmembrane pressure of 30 bar and cross-flow velocity of 2 m/s.

In NF experiments with pure waterglass-solutions remarkable flux decline was only observed above a concentration of ~ 300 mg/l reactive silica. Waterglass is thus a possible fouling component however it is questionable if it was responsible for the observed flux decline in time in experiments with KTV wastewater, as the concentration of reactive silica was estimated to be below its' solubility concentration. The prefiltration step might not reject all colloidal silica and thus the silica concentration in the feed may be underestimated.

The permeate streams during experiments with some KTV-batches had a reddish/yellowish colour. If so the permeate streams from the experiments at the highest transmembrane pressure (20 bar) and the lowest cross-flow velocity (~ 1-2 m/s) were analysed spectrophotometrically (table 5.2.4.). The corresponding retentate streams were also analysed (table 5.2.5) and the colour retention at the wavelength of maximum absorbance of the permeate was determined (table 5.2.6). In the permeate streams of the KTV-2 and KTV-3 experiments no absorption peaks with a spectral absorbance >3 m^{-1} were found. The permeate streams of the nanofiltration may not be discarded into the sewer system if the legislation requires a 'colourless' waste stream or the values set by the German legislation. However the influence of the cross-flow velocity on the dye retention has not been fully examined here.

Table 5.4 Spectrophotometrical analysis of the permeate streams.

Dye sample	wavelength of maximal absorbance [nm]	Spectral absorbance permeate [m^{-1}]	Most likely permeating dye component
KTV-1	480.8	11.7	Reactive red 180
KTV-4	512.8	4.6	Reactive red 21 / Reactive orange 16
KTV-5	483.3	6.6	Reactive yellow 37

Differences in membrane permeability between red-yellow and blue components might be attributed to the different chemical nature of mono-azo (yellow-red) and antraquinon (blue) dyes.
However the pinpointing of the permeating components (table 5.2.6) is questionable:

- The permeate sample of the KTV-5 experiment was detected to be yellow while the permeate sample of the KTV-3 experiment did not show any significant absorption peak, despite the fact that the feed stream of the KTV-3 contains more Reactive Yellow 37 than the feed stream of KTV-5.
- The most likely permeating component in the KTV-1 experiment should be Reactive Red 180 but in the permeate stream of the KTV-2 no significant absorption peak was detected, despite the fact that the concentration of this compound in the KTV-2 feed was 16 times higher than in the KTV-1 feed.

Table 5.5 Spectrophotometrical analysis of the retentate streams. * The spectrophotometrical analysis of these retentate samples showed two peaks.

Dye sample	wavelength of maximal absorbance [nm]	Spectral absorbance retentate [m^{-1}]
KTV-1 *	505.6	635
	590.0	534
KTV-4	507.2	1366
KTV-5 *	623.2	323
	660.8	288

Table 5.6 Colour retention at wavelength of maximal absorbance permeate.

Dye sample	wavelength of maximal absorbance permeate [nm]	Spectral absorbance retentate [m^{-1}]	Colour retention [%]
KTV-1	480.8	565	97.9
KTV-4	512.8	1350	99.7
KTV-5	483.3	57	88.4

Conclusion concerning the permeation and retention of specific dye components should be taken with great care :

- Dye manufacturers sometimes add other dye compounds (so-called) ‘shading colours’ in their dye formulation in order to adjust the colour.
- Although dye compounds are very insensitive to chemical and biological attack, conversion into other components can not be fully excluded. During the decolourisation of wastewater streams from reactive dyeing processes by an an-aerobic biological process [3], it was generally observed that the wavelength of maximal absorbance is shifted to lower values (towards the UV-region). A blue component will for example be converted to (smaller) red or yellow components before it is fully converted to colourless components.
- Spectrophotometrical analysis methods are more sensitive towards red components than blue components. Generally spoken, red dyes have a lower detection limit than blue dyes.

In order to detect if a specific dye component in a mixture of dye components permeates through the membrane the dye components should be separated from each other before spectrophotometrical analysis. High pressure liquid chromatography (HPLC) will be used for this purpose in the parametric study.

5.3 Component selection for the synthetic wastewater

In another membrane filtration study with textile wastewater from reactive dyeing processes [1] it was found that waterglass, surfactants and loose fibres are possible fouling compounds. A pre-filtration step like microfiltration, to remove loose fibres and colloidal matter, was recommended. However it was stated that this is not always adequate for waterglass and surfactants, as only the aggregates of these components are rejected by MF. Components, not fully rejected by the MF pre-filtration, will be concentrated in the RO or NF process and can still cause fouling.

This preliminary study, experiences from other studies and literature data about textile auxiliaries [2] give some indication which components present in the textile wastewater can cause flux decline. In order to determine the effect of these components and give measures how to avoid membrane fouling, experiments under well-defined conditions have to be done. This implied that the research switched from real textile wastewater to (own-made) synthetic textile wastewater. By performing experiments with different compositions subsequently (i.e. a parametric study), components and combination of components responsible for flux decline can be detected. The selected components include dyes, waterglass, NaCl , NaOH and pure surfactants (table 5.7).

Table 5.7 Components used in the parametric studies.

Component	Molecular formula (Molecular mass)	Description	Manufacturer
Dye components			
Reactive Blue 4 (hydrolysed)	$C_{23}N_6O_{10}S_2H_{16}$ (600 g/mole)	Antraquinon dye (industrial formulation)	Zeneca
Reactive Red 2 (hydrolysed)	$C_{19}N_6O_9S_2H_{14}$ (534 g/mole)	Mono-azo dye (industrial formulation)	Zeneca
Auxiliary components			
Waterglass	$Na_2O{\cdot}SiO_2$ solution	Colloidal stabilisator in dyeing process	Aldrich
Cetyl trimethyl ammonium bromide (CTAB)	$C_{19}H_{42}N^+ Br^-$ (364.5 g/mole)	Modelcompound cationic surfactants	Merck
Sodium dodecyl sulphate (SDS)	$C_{12}H_{25}0S0_3{}^- Na^+$ (288.4 g/mole)	Modelcompound anionic surfactants	Merck
Sodium chloride	NaCl	Enhancing the dye uptake by the fabric	Merck
Caustic soda	NaOH	Enhancing the dyeing process	Merck

Two dye components, reactive blue 4 and reactive red 2, were chosen as modelcompound. Samples with these compounds (trade names: Procion Blue MX-R and Procion Red MX-5B) were kindly provided by Zeneca, Manchester UK. The samples contained according to the manufacturer 50 wt% dyestuff, 25 wt% NaCl, 12.5 wt% of an anionic surfactant, 12.5 wt% buffer components like disodium hydrogen orthophosphate and sodium dihydrogen orthophosphate. The dyes were not used in the pure form as pure dyes were hard to get and the purification was judged to be too elaborated. Moreover the dye samples thus used are similar to the components present in the washing water except that the dye components are in the reactive form, which differs from their appearance in the washing process were the unfixed dyes are in the hydrolysed form. In order to meet the conditions in the washing process the reactive dyes were hydrolysed during a two hours reaction in a NaOH solution at 100°C. The hydrolysation reaction was done with an excess of NaOH; each dye molecule reacts with 2 OH^- ions to form the hydrolysed dyes (figure 5.4).

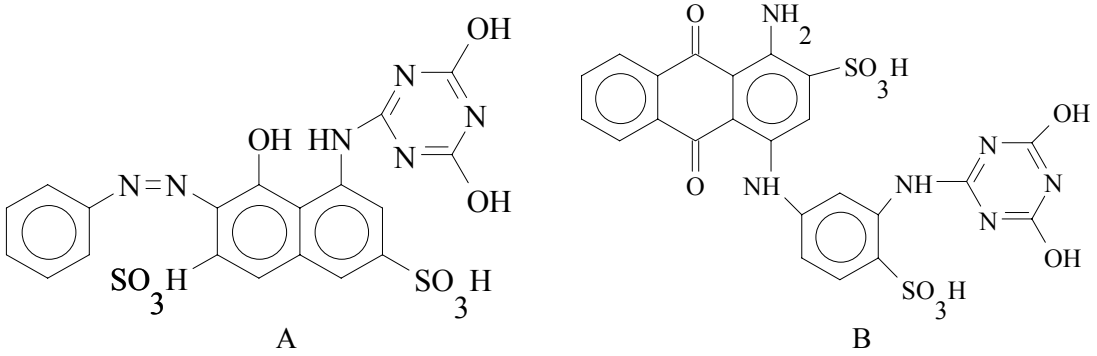

Figure 5.4 Hydrolysed Reactive Red 2 (A), molecular mass: 534 g/mole. Hydrolysed Reactive Blue 4 (B), molecular mass: 600 g/mole.

Next to waterglass two surfactants, CTAB (cationic) and SDS (anionic), were chosen as modelcompounds for textile auxiliaries. The background salt concentration and pH in order to research the influence of the colloidal stability of the solution (chapter 3) will be varied by adding NaCl and NaOH. All components (except the dye components) were used as received.

Three formulations of textile auxiliaries used in practice (table 5.3.2) were chosen in order to detect if the experiences with the pure surfactants are representative for real textile auxiliaries. Levapon is added in the washing process to enhance the washing process. Cibapon has the same effect, but differs from Levapon concerning the active contents. Tinofix was chosen as it is sometimes added in the last washing bath as a fixation agent.

Table 5.8 Textile auxiliaries used in the parametric studies

Textile auxiliary (manufacturer)	Contents	Function in washing process
Cibapon R (Ciba Geigy)	anionic compound based on modified polyacrylic acid	Washing agent in washing process
Levapon AN (Bayer)	anionic compound based on alkylsulphates and non-ionic based on alkylarylpolyglycolether	Washing agent in washing process
Tinofix ECO (Ciba Geigy)	cationic compound based on polyethylene /polyamine	Fixation agent in / after washing process

Parametric studies will be performed with synthetic wastewater containing the components of table 5.7 and table 5.8.

5.4 Conclusions

A preliminary study to the use of reverse osmosis and nanofiltration on textile wastewater from a reactive dyeing process has been performed. The main aim was to detect which components could cause flux decline and should be selected for further research. Besides that permeate flux as function of the hydrodynamic conditions and dye-separation characteristics for both membrane processes were collected.

Waterglass was detected to foul the NF membranes showing severe flux decline in time, which was confirmed in experiments with pure waterglass solutions. Other research data [1] and data about textile auxiliaries [2] led to the selection of components for further research in

the parametric studies (Chapter 6 and 7). Besides that NaCl and NaOH were selected with the aim to research the influence of the colloidal stability on the permeate flux.

The specific permeate fluxes for RO are within 80 percent of the clean water fluxes and are not sensitive to the hydrodynamic process conditions (transmembrane pressure and cross-flow velocity). The influence of concentration polarisation and membrane fouling was thus negligible.

The specific permeate fluxes for NF are very sensitive to the hydrodynamic process conditions. Concentration polarisation and membrane fouling did play an important role in this NF preliminary study. Also the influence of the hydrodynamic process conditions on the economical operation of NF on textile wastewater is thus very interesting and will be discussed further in chapter 8.

In all RO experiments no dyes were detected in the permeate streams and with respect to that RO seems thus very suitable for recycling of the process water in the textile washing range. The permeate streams of some NF experiments were coloured red or yellow. Conclusions about the difference in permeability of the NF-membrane for several dye components could not be made from these experiments as the compositions of the wastewater was too complex. Two reactive dyes originating from different dye classes are selected for the parametric studies of chapters 6 and 7.

Acknowledgement

W. Tieben and H. Ophoff are acknowledged for the experimental work in this chapter. Ten Cate Protect Nijverdal and KTV Eibergen are acknowledged for kindly supplying the actual textile wastewater and the information about the textile auxiliaries. Zeneca is acknowledged for kindly supplying the reactive dye samples. Ciba Geigy and Bayer are acknowledged for supplying the actual textile auxiliaries.

Literature

[1] Janisch I., Zum Problem der Membranverschmutzung bei der Umkehrosmose, PhD thesis, RWTH Aachen, (1987).
[2] Engbers B.J.J., Hulpmiddelen in de textielveredeling deel I en II. (1993).
[3] Schulze-Rettmer R.,Versuche der anaeroben Entfärbung von Farbstoffen und technischen Anwendung, Colloquium Produktionsintegrierter Umweltschutz 'Abwässer der Textilindustrie / Wollverarbeitung und Nahrungsmittelindustrie', Bremen (1997).

Appendix 5A Results NF preliminary study

Solution	Transmembrane pressure [bar]	Cross-flow velocity [m/s]	Permeate flux [lt/m^{2}hr]	Specific permeate flux [lt/m^{2}hr bar]	Relative specific permeate flux [-]
CWF	10	3.7	107.8	10.8	
TCP-A	20	5.5	184.9	9.2	0.86
TCP-A	10	5.4	95.9	9.6	0.89
TCP-A	10	1.1	76.2	7.6	0.71
TCP-A	20	1.1	85.9	4.3	0.40
CWF	10	5.1	98.0	9.8	
KTV-1	20	5.5	161.3	8.1	0.82
KTV-1	10	5.4	94.6	9.5	0.97
KTV-1	10	2.2	99.1	9.9	1.01
KTV-1	20	2.2	128.5	6.4	0.66
CWF	10	4.1	92.9	9.3	
CWF	10	4.1	56.9	5.7	
TCP-B	20	5.4	74.2	3.7	0.65
TCP-B	10	5.5	38.9	3.9	0.68
TCP-B	20	2.1	56.1	2.8	0.49
TCP-B	20	0.5	29.6	1.5	0.26
TCP-B	20	5.5	68.8	3.4	0.60
CWF	10	4.1	45.8	4.6	
CWF	10	4.1	69.5	6.9	
KTV-2	10	5.5	73.5	7.4	1.06
KTV-2	10	2.2	74.3	7.4	1.07
KTV-2	20	2.1	84.1	4.2	0.61
KTV-2	20	5.5	89.6	4.5	0.64
CWF	10	4.1	72.0	7.2	
KTV-3	20	5.5	80.4	4.0	0.56
KTV-3	20	2.2	74.3	3.7	0.52
KTV-3	10	2.2	50.7	5.1	0.70
KTV-3	10	5.5	53.7	5.4	0.75
CWF	10	4.1	72.0	7.2	

Chapter 6

Treatment of synthetic textile wastewater by reverse osmosis

Summary

A parametric study of the applicability of reverse osmosis for the treatment of textile wastewater from reactive dyeing and subsequent washing processes was executed. The parameters that were varied are components in laboratory-made synthetic wastewater, representative for components present in the actual textile wastewater. The aim of this study was to determine which components and especially the combination of which components affect the permeate flux and separation characteristics of the reverse osmosis membrane.

A tubular reverse osmosis membrane (Stork Friesland) with a thin-film composite active layer based on polyamide / polysulfone was used. All experiments were done at a transmembrane pressure of 35 bar and a cross-flow velocity of 2 m/s. The performance of the membrane is characterised by the (time dependent) permeate flux and the separation characteristic for conductivity and colour.

Filtration experiments (parametric study A) with two reactive dyes, two auxiliary components: sodium dodecyl sulphate (SDS) and water glass, NaCl and NaOH were performed to detect which (combination of) components are causing a flux decline. From these experiments it could be concluded that SDS causes a flux decline which is enhanced at higher salt concentrations and at lower pH.

Subsequently filtration experiments (parametric study B) were executed in order to determine the filtration behaviour of auxiliary components. This was done at varying concentrations of these components, varying NaCl-concentration ('background salt'- concentration) and varying pH. The components used were a 'model' anionic surfactant (SDS), a 'model' cationic surfactant cetyl trimethylammonium bromide (CTAB), water glass, and the industrial formulations: Cibapon, Levapon and Tinofix.

The cationic compounds (CTAB and Tinofix) are not causing (severe) flux decline, but in some cases even enhance the permeate flux. Water glass only fouls the membrane at concentrations far above the solubility concentration. SDS was again proved to cause a flux decline, as did Levapon that contains anionic surfactants based on alkylsulfates (i.e. like SDS). Cibapon a washing agent containing an anionic polyelectrolyte component did not cause any membrane fouling.

The retention for the coloured compounds was over 99.88 %. The retention for conductivity was compared to NaCl retention of experiments with NaCl-solutions by means of a graphical method to determine the salt transport parameter as presented in chapter 4.5.

6.1 Introduction

Reverse osmosis is a membrane technique that rejects almost all solutes like small organic components and inorganic salts. Although reverse osmosis is a technique known for many years now, its application to industrial wastewater is still limited due to the phenomena of flux decline and changing separation characteristics as a consequence of membrane fouling by components present in the wastewater.

The aim of this study is to determine which components or combination of components present in the textile wastewater from the washing processes subsequent to the reactive dyeing process are causing unwanted flux decline and failing separation characteristics in reverse osmosis.

6.2. Experimental part

Several components were selected (table 5.7 and 5.8) for this parametric study. Special attention was paid to the influence of NaCl and pH on the fouling behaviour of the dyes, surfactants, water glass and textile auxiliaries of the wastewater as it was presumed that these parameters have an influence on the adsorption behaviour of ionic compounds to ionic membrane surfaces i.e. surfaces with a net positive or negative charge.

In the experiments a1-a16 the components used were two hydrolysed reactive dyes (derived from Reactive Blue 4 and Reactive Red 2) and two components representative for auxiliary components (SDS and water glass). Four combinations with one dye and one auxiliary were examined at two levels of NaCl concentration (< 1 g/l and 15 g/l) and two levels of pH (7 and 10). The pH was adjusted by addition of HCl or NaOH. In the experiments b1-b24 six auxiliary components (SDS, CTAB, water glass, Cibapon, Tinofix, Levapon) were examined at two levels of concentration, pH and NaCl-concentration. The feed-bleed design set-up was used (figure 4.1). The membrane used was the RO-WFCX membrane of Stork Friesland (table 4.3). The transmembrane pressure in all experiments was set to 35 bar and the cross-flow velocity at 2 m/s.

The procedures for the experiments are given in table 6.1. Each experiment lasted 10 hours at minimum, except some experiments (a1, b17-b20 and b23) were it was judged that a constant permeate flux had already been reached. The permeate flux was continuously measured and samples of both retentate and permeate were taken at the end of each experiment.

Coloured samples were analysed for their colour content with a Philips PU 8700 spectrophotometer using cuvets with a pathlength of 1 cm. The dye content is expressed as the spectral absorbance (m^{-1}) at the wavelength of maximal absorbance in the visible region.

In case of the filtration experiments at high (15 g/l) NaCl concentration, the samples were analysed for conductivity with a Hanna conductivity meter HI9032.9047. The observed retention for conductivity can be interpreted as the retention for NaCl. The NaCl separation in this study will be compared to the NaCl-filtrations presented in chapter 4.6 using the graphical analysis of Method II.

Generally four experiments were executed with the same batch of wastewater with the same membrane. Between the experiments the membrane was tested with a standard filtration test (SFT) in order to check the consequences of irreversible membrane fouling. The SFT was a filtration with a 0.75 wt% NaCl solution (exp. a1 – a16) or a 0.5 wt% NaCl solution (exp. b1-b24). The observed retention for NaCl in the SFT was also determined by measuring the conductivity.

In order to perform a standard test between the experiments the wastewater was removed out of the installation. After the standard test and removal of its NaCl solution, the wastewater was poured back into the feed tank, a new component was added to the feed and the next experiment was executed.

If the flux decline during an experiment was considered to be large, the installation and the membrane were cleaned. The only cleaning action thus performed was a cleaning with a NaOH solution at pH 10 for at least 30 min. (base cleaning), as it was experienced that this cleaning was adequate in cases where the membrane was fouled by sodium dodecyl sulphate.

Table 6.1 Experimental procedures of the parametric studies

1.	Remove the old membrane and clean the installation before installing a new membrane according to the procedures in table 4.2.
2.	Install a new membrane.
3.	Execute the standard filtration test.
4.	Remove the salt solution out of the installation and rinse the installation with demineralised water during 15 min at no pressure, a cross-flow velocity of 2 m/s and a feed flow > 100 lt/hr.
5.	Remove the water out of the installation and feed the installation with the synthetic wastewater at no pressure, a cross-flow velocity of 2 m/s and a feedflow > 100 lt/hr for at least 15 minutes.
6.	Adjust the feed flow to 50 –75 lt /hr.
7.	Adjust the transmembrane pressure to 35 bar and the cross-flow velocity to 2 m/s.
8.	Start the flux measurement immediately after this adjustment.
9.	Run the filtration experiment at least for 10 hours.
10.	Take samples of both retentate and permeate at the end of the experiment and if relevant, analyse these samples.
11.	Remove the liquid out of the installation.
12.	Rinse and if necessary clean the installation.
13.	If a set of four experiments was performed then go (back) to item 1 else go back to item 3.

6.3 Results

6.3.1 Measurements of permeate flux and NaCl retention

In the sheets 6.1 to 6.10 main results and observations of the experiments are summarised. In the first table the composition of the waste streams is given. In the figure the permeate fluxes have been plotted as function of time. The black dots represent the permeate flux of the standard filtration tests. In the second table the permeate fluxes at the end of the experiment and the (observed) NaCl-retention are given. The permeate fluxes of the experiments are compared to the fluxes of standard filtration tests. Furthermore the fluxes of the standard filtration test before and after an experiment are compared to each other in order to determine the result of the cleaning and rinsing actions.

6.3.2 Separation of dyes in the experiments a1-a16

The dye content of retentate and permeate has been measured as spectral absorbance (m^{-1}) at wavelength of maximal absorption by a spectrophotometer. The wavelength was 595 nm for the experiments a1-a8 with hydrolysed reactive blue 4 solutions (table 6.2) and 530 nm for the experiments a9-a16 with the hydrolysed reactive red 2 (table 6.2). The mean spectral absorbance of the retentate samples of blue solutions was 1050 m^{-1}, and 2570 m^{-1} for the red samples.

Table 6.2 Dye separation in the experiments with the hydrolysed reactive blue 4 solutions.

Experiment	Spectral absorbance permeate at 595 nm [m^{-1}]	Dye retention [%]
a1	0.8	99.91
a2	1.2	99.89
a3	1.2	99.89
a4	1.2	99.88
a5	0.3	99.97
a6	0.1	99.99
a7	0.3	99.97
a8	0.4	99.96

Table 6.3 Dye separation in the experiments with the hydrolysed reactive red 2 solutions.

Experiment	Spectral absorbance permeate at 530 nm [m^{-1}]	Dye retention [%]
a9	0.4	99.98
a10	0.6	99.98
a11	0.7	99.97
a12	1	99.96
a13	0.4	99.98
a14	0.3	99.99
a15	0.4	99.98
a16	0.3	99.99

The colour of permeate samples could hardly be detected by eye and by the spectrophotometer as the detection limit of the apparatus was 0.1 m^{-1}. Considering the colour intensity and dye retention, the permeate quality is acceptable for discharge (table 4.4) or for reuse as textile wash water (chapter 2).

Sheet 6.1 Exp a1 – a4 Hydrolysed Reactive Blue 4 and SDS

Exp	Blue 4 [g/l]	SDS [g/l]	NaCl [g/l]	pH	extra cleaning afterwards
a1	1.5			6.5	
a2	1.5		15	7.4	
a3	1.5	0.3	15	7.4	base cleaning
a4	1.5	0.3	15	9.5	base cleaning

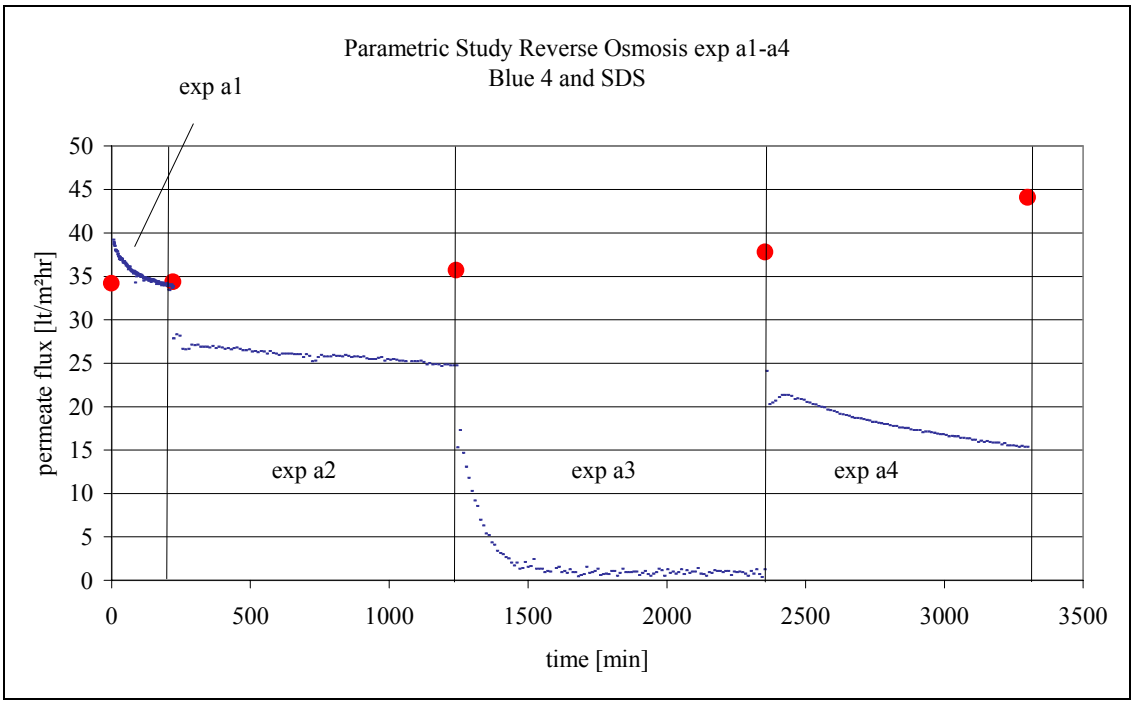

exp	permeate flux end of exp. [lt/m^{2}hr]	NaCl retention	permeate flux SFT [lt/m^{2}hr]	permeate flux exp / permeate flux SFT before	permeate flux SFT before / SFT after
ST			34.2		
a1	32.4		34.4	0.95	1.01
a2	23.6	94.8	35.7	0.69	1.04
a3	1	87.9	37.8	0.03	1.06
a4	15.4	87.4	44.1	0.41	1.17

Exp	Experimental observations
a1	A flux decline was observed filtering the reactive blue 4 solution, however the flux seems to reach a constant value.
a2	Addition of NaCl causes immediately a lower flux and a slight flux decline
a3	Addition of SDS causes a huge flux decline. The flux is almost reduced to zero.
a4	An increase of pH increases the flux compared to exp a3.

Sheet 6.2 Exp a5-a8 Hydrolysed Reactive Blue 4 and water glass

Exp	Blue 4 [g/l]	water glass [g/l] based on SiO_2	NaCl [g/l]	pH	extra cleaning afterwards
a5	1.5			7.7	base cleaning
a6	1.5	0.3		10.2	base cleaning
a7	1.5	0.3	15	9.9	
a8	1.5	0.3	15	6.8	

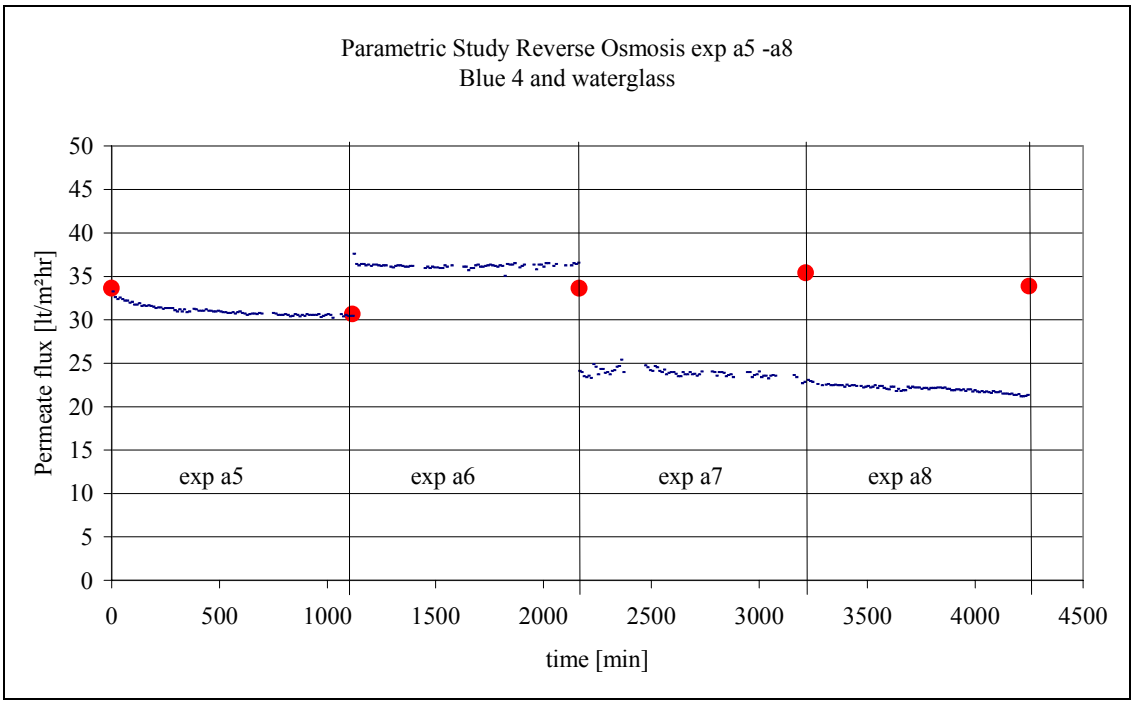

exp	permeate flux end of exp. [lt/m^2hr]	NaCl retention	permeate flux SFT [lt/m^2hr]	permeate flux exp / permeate flux SFT before	permeate flux SFT before / SFT after
ST			33.6		
a5	30.4		30.6	0.91	0.91
a6	36.5		33.6	1.19	1.00
a7	23.5	93.0	35.4	0.70	1.05
a8	21.3	96.6	33.8	0.60	0.96

exp	main observations / remarks
a5	The flux declines slightly and reaches a constant value at the end.
a6	Addition of water glass (0.3 g/l SiO_2) increases the flux. The permeate flux in the standard test increases also.
a7	Addition of NaCl leads immediately to a lower flux. The retention for NaCl is remarkably low
a8	A change of pH from basic to neutral conditions has almost no effect on the flux, the NaCl retention increases.

Sheet 6.3 Exp a9-a12 Hydrolysed Reactive Red 2 and SDS

Exp	Red 2 [g/l]	SDS [g/l]	NaCl [g/l]	pH	extra cleaning afterwards
a9	1.5			6.9	
a10	1.5	0.3		6.9	base cleaning
a11	1.5	0.3	15	6.5	base cleaning
a12	1.5	0.3	15	9.9	

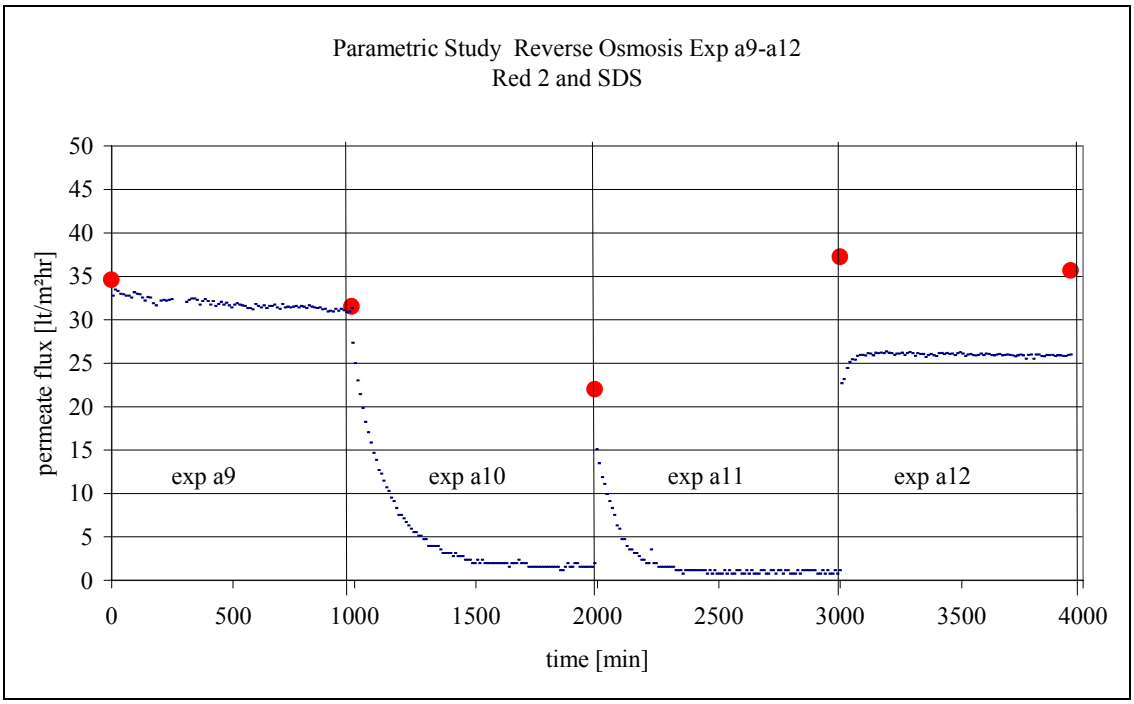

exp	permeate flux end of exp. [lt/m^{2}hr]	NaCl retention	permeate flux SFT [lt/m^{2}hr]	permeate flux exp / permeate flux SFT before	permeate flux SFT before / SFT after
ST			34.5		
a9	31.3		31.5	0.91	0.91
a10	1.6		22.0	0.05	0.70
a11	1.0	91.6	37.2	0.04	1.69
a12	25.9	91.1	35.6	0.70	0.96

exp	main observations / remarks
a9	A slight flux decline was observed during the filtration of the reactive red 2 solution.
a10	SDS causes a huge flux decline. Although a base cleaning was performed the flux in the standard test was remarkably low.
a11	NaCl increases the flux decline rate compared to exp a10. The NaCl-retention is low.
a12	Increasing the pH to 10 increases the permeate flux. The NaCl retention is hardly changed.

Sheet 6.4 exp a13-a16 Hydrolysed Reactive Red 2 and water glass

Exp	Red 2 [g/l]	water glass [g/l] based on SiO_2	NaCl [g/l]	pH	extra cleaning afterwards
a13	1.5			6.9	base cleaning
a14	1.5		15	6.5	base cleaning
a15	1.5	0.3	15	9.9	
a16	1.5	0.3	15	7.0	

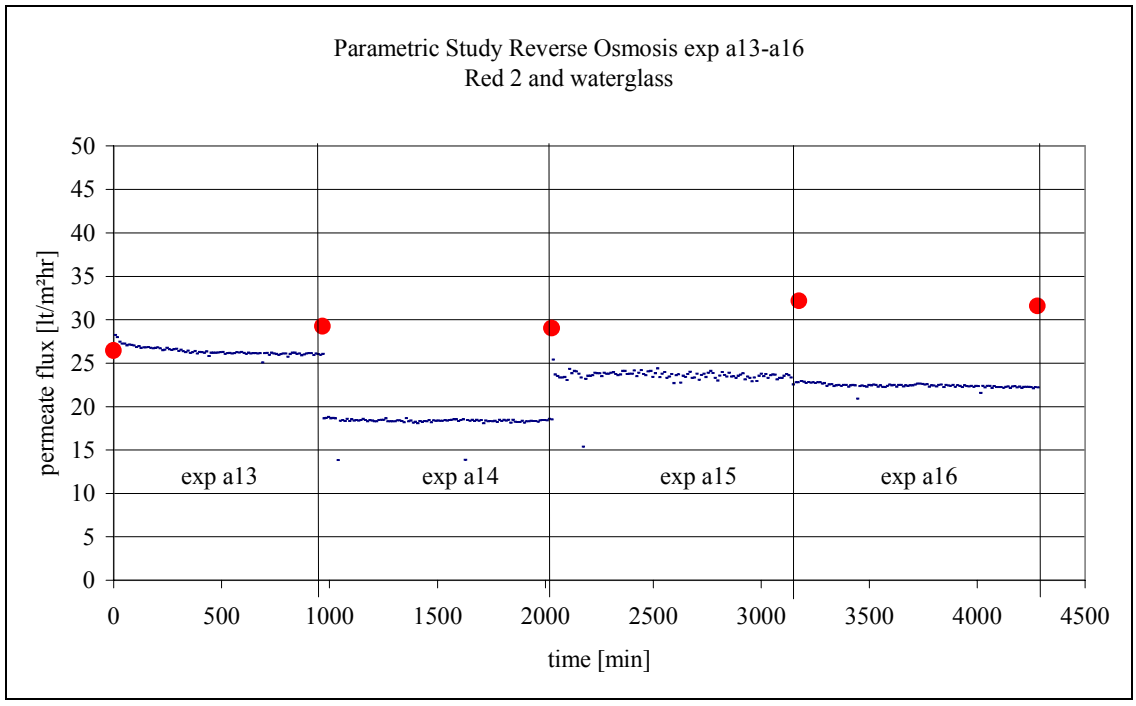

exp	permeate flux end of exp. [lt/m^2hr]	NaCl retention	permeate flux SFT [lt/m^2hr]	permeate flux exp / permeate flux SFT before	permeate flux SFT before / SFT after
ST			26.5		
a13	26.0		29.2	0.98	1.11
a14	18.5	97.0	29.0	0.63	0.99
a15	23.0	91.6	32.2	0.79	1.11
a16	22.2	96.0	31.6	0.69	0.98

exp	main observations / remarks
a13	A slight flux decline was observed during the filtration of the reactive red 2 solution.
a14	Adding 15 g/l NaCl results directly in a lower flux, however this flux remains constant
a15	Addition of water glass results in a higher permeate flux, the NaCl retention drops considerably
a16	Decreasing the pH to neutral conditions has almost no influence on permeate flux, but the NaCl retention is increased

Sheet 6.5 exp b1-b4 Sodium dodecyl sulphate

Exp	SDS [g/l]	NaCl[g/l]	pH	extra cleaning afterwards
b1	0.3		6.0	base cleaning
b2	0.3	15	6.3	base cleaning
b3	0.3	15	7.7*	base cleaning
b4	3.0	15	9.2*	base cleaning

* It turned out that SDS buffers the solution. In expb3 the pH was set at 9.6 but decreased during the experiment to 7.7. In exp.b4 the same phenomena was observed and the pH was increased to alkaline conditions at the end leading to a huge raise of permeate flux.

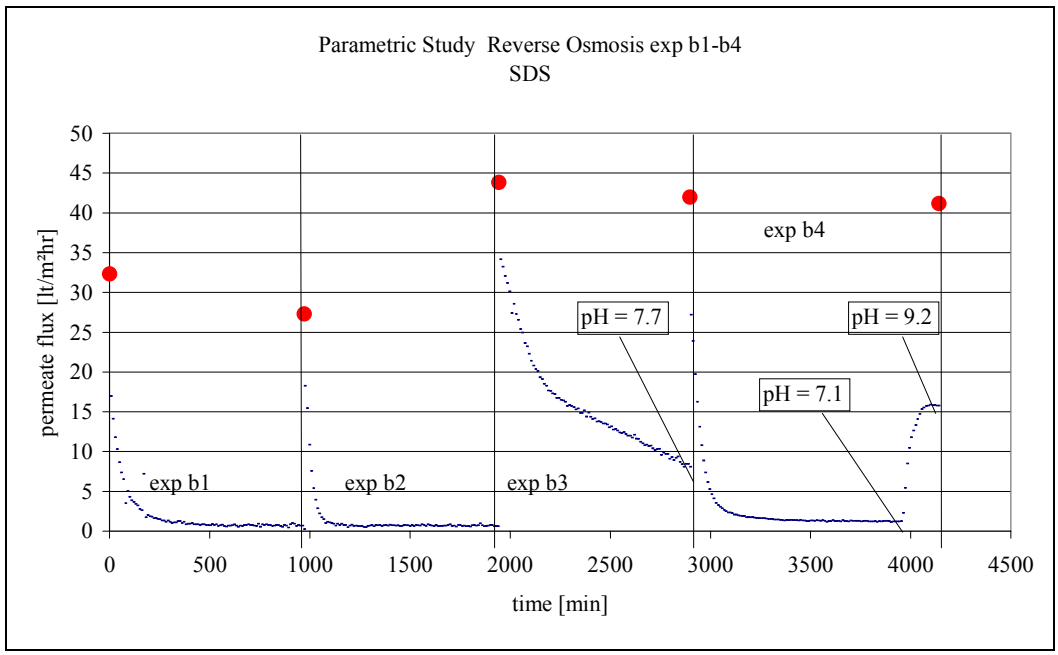

exp	permeate flux end of exp. [lt/m^{2}hr]	NaCl retention	permeate flux SFT [lt/m^{2}hr]	permeate flux exp / permeate flux SFT before	permeate flux SFT before / SFT after
ST			32.3		
b1	0.6		27.3	0.02	0.84
b2	0.7	94.2	43.9	0.03	1.61
b3	8.1	87.1	42.0	0.19	
b4	15.7	88.9	41.2	0.36	0.94

exp	main observations / remarks
b1	SDS causes a severe flux decline. The permeate flux in the SFT was not restored, despite of the alkaline cleaning.
b2	In combination with 15 g/l NaCl the flux decline rate was faster.
b3	At a higher pH the flux decline rate decreases considerably. A constant permeate flux at the end was not observed. However it turned out that the pH was also changed during the experiment.
b4	Raising the SDS concentration increases the flux decline rate. However the same problem of keeping the pH constant as in exp b3 occurred here. Changing the pH to alkaline conditions led to a fast increase of permeate flux to a constant value.

Sheet 6.6 exp b5-b8 Cetyl trimethyl ammonium bromide

Exp	CTAB [g/l]	NaCl [g/l]	pH	extra cleaning afterwards
b5	0.03		6.1	
b6	0.03	15	6.2	
b7	0.03	15	7.4	
b8	0.3	15	9.4	

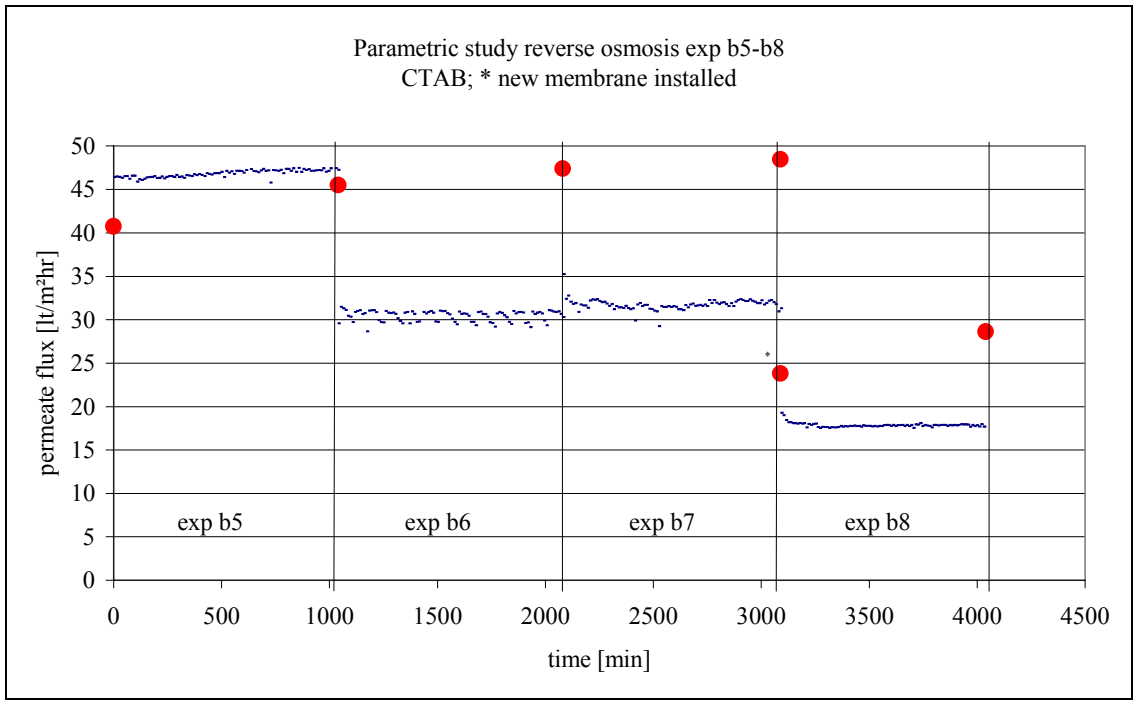

exp	permeate flux end of exp. [lt/m^{2}hr]	NaCl retention	permeate flux SFT [lt/m^{2}hr]	permeate flux exp / permeate flux SFT before	permeate flux SFT before / SFT after
ST			40.5		
b5	47.3		45.5	1.17	1.12
b6	30.4	96.0	47.3	0.67	1.04
b7	31.6	93.9	48.3	0.67	1.02
ST	23.7	98.6	23.7		
b8	17.9	96.1	28.7	0.75	1.21

exp	main observations / remarks
b5	The permeate flux was even higher then in the standard test.
b6	Increasing the concentration of NaCl to 15 g/l causes only an immediate permeate flux drop. No further flux decline observed.
b7	The pH was increased but remained below 8. A slight flux increase was observed and a lower NaCl retention.
b8	A new membrane was installed which had a lower permeate flux. However even an increase of the CTAB concentration and a higher pH have no influence: the permeate flux is constant.

Sheet 6.7 exp b9-b12 Water glass

Exp	water glass [g/l]	NaCl [g/l]	pH	extra cleaning afterwards
b9	0.3		4.6	
b10	0.3	15	6.7	base cleaning
b11	0.3	15	9.9	
b12	3	15	10.6	

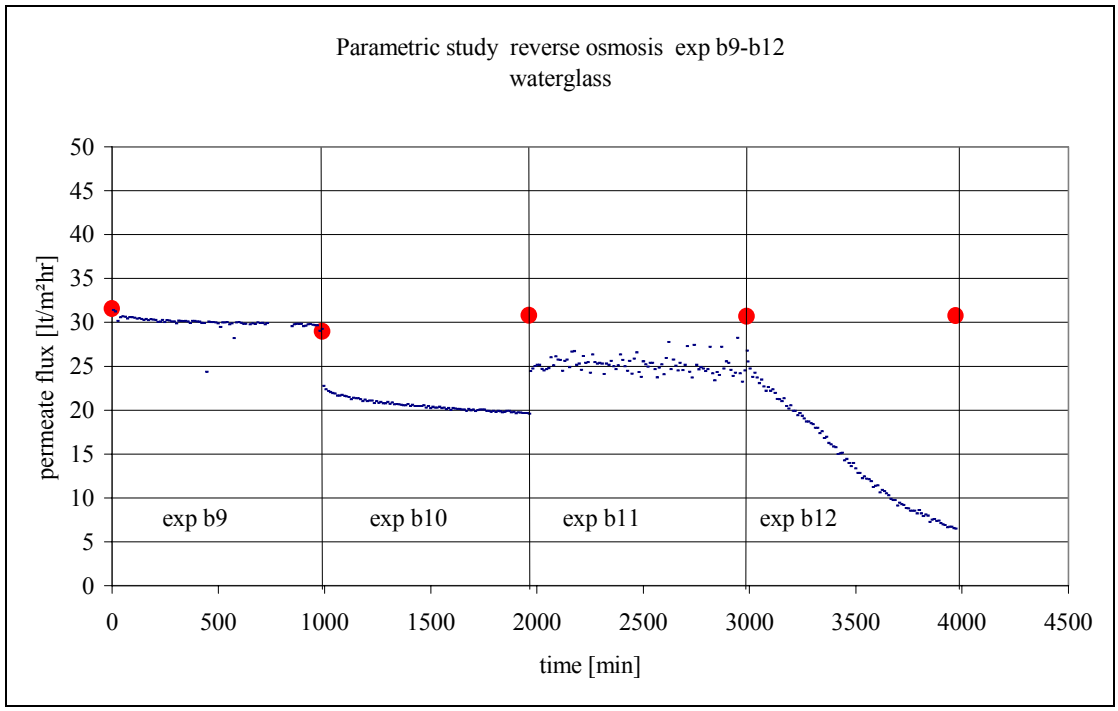

exp	permeate flux end of exp. [lt/m^{2}hr]	NaCl retention	permeate flux SFT [lt/m^{2}hr]	permeate flux exp / permeate flux SFT before	permeate flux SFT before / SFT after
ST			31.6		
b9	29.2		29.0	0.92	0.92
b10	19.7	96.3	30.8	0.68	1.06
b11	24.1	89.9	31.6	0.78	1.03
b12	6.6	90.4	30.9	0.21	0.98

exp	main observations / remarks
b9	water glass at 0.3 g/l does not decrease the permeate flux. The permeate flux is declining very slightly, but is still comparable with the permeate flux in the standard test.
b10	Raising the NaCl concentration to 15 g/l immediately causes a drop of the permeate flux. A slight flux decline was then observed during filtration.
b11	Changing the pH from neutral to basic conditions the flux was raised and the NaCl retention was lowered.
b12	An increase of the water glass concentration to 3 g/l causes a huge flux decline. The flux in the standard test was easily restored by rinsing with demineralised water only.

Sheet 6.8 exp b13-b16 Cibapon

Exp	Cibapon [g/l]	NaCl [g/l]	pH	extra cleaning afterwards
b13	0.3		7.4	
b14	0.3	15	6.5	
b15	0.3	15	9.4	
b16	3	15	7.4	

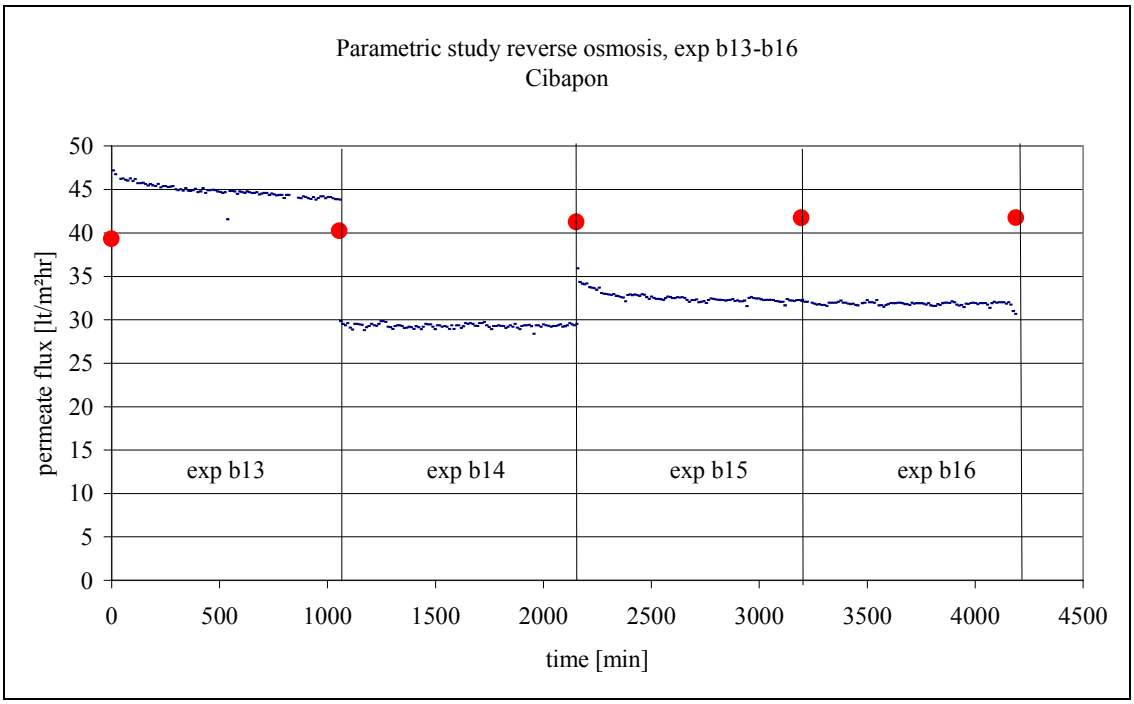

exp	permeate flux end of exp. [lt/m^{2}hr]	NaCl retention	permeate flux SFT [lt/m^{2}hr]	permeate flux exp / permeate flux SFT before	permeate flux SFT before / SFT after
ST			39.3		
b13	43.7		40.2	1.11	1.02
b14	29.4	97.1	41.3	0.73	1.03
b15	32.2	92.8	41.8	0.78	1.01
b16	31.0	96.8	42.3	0.74	1.01

exp	main observations / remarks
b13	The permeate flux was even higher then in the standard test. A slight flux decline was observed.
b14	An increase of the NaCl concentration to 15 g/l causes an immediate permeate flux drop.
b15	Raising the pH to basic conditions enhances the permeate flux but lowers the NaCl retention.
b16	Raising the Cibapon concentration to 3 g/l has no influence on the permeate flux.

Sheet 6.9 exp b17-b20 Tinofix ECO

note: The experiments were performed directly subsequent to each other; i.e. no standard tests between the experiments were executed.

Exp	Tinofix [g/l]	NaCl [g/l]	pH	extra cleaning afterwards
b17	0.03		6.6	
b18	0.03	15	6.4	
b19	0.03	15	9.8	
b20	0.3	15	8.1	

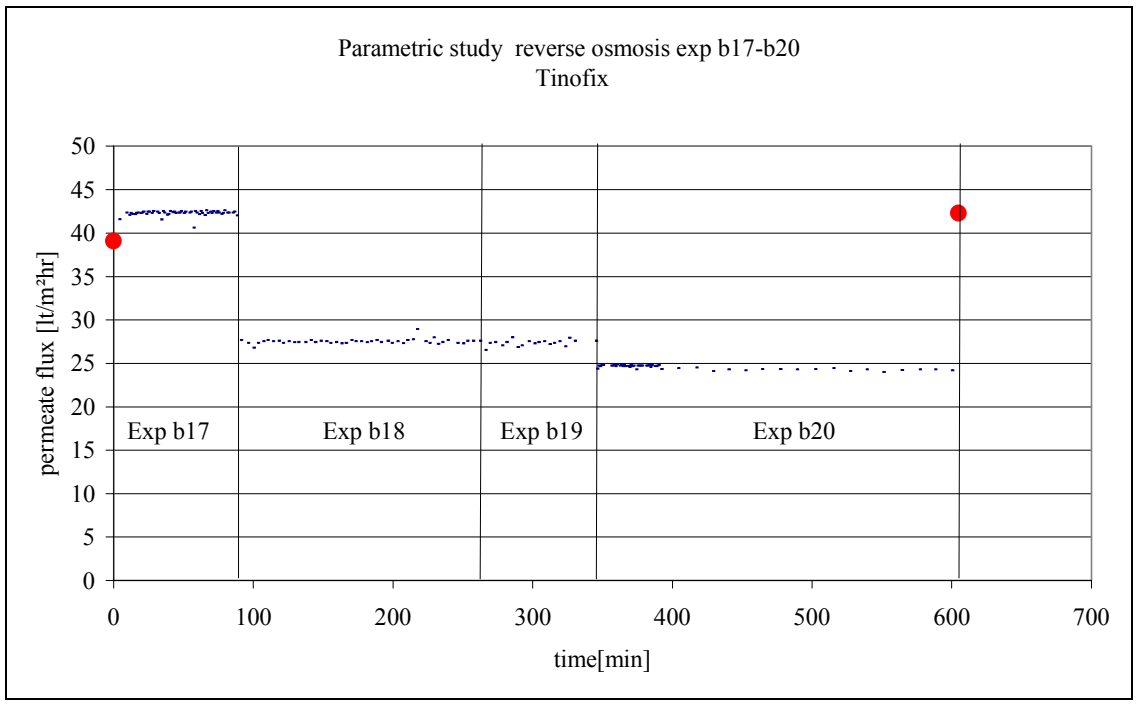

exp	permeate flux end of exp. [lt/m^{2}hr]	NaCl retention	permeate flux SFT [lt/m^{2}hr]
ST			37.4
b17	42.4		
b18	27.5	98.2	
b19	24.7	96.5	
b20	24.6	97.0	42.0

exp	main observations / remarks
all	The experiments are executed without performing standard tests between the experiments.
b17	Permeate flux higher then permeate flux in the standard test.
b18	Adding NaCl leads to a lower but constant permeate flux
b19	Surprisingly a higher pH leads to a lower permeate flux
b20	Raising the concentration of Tinofix to 0.3 g/l has no influence on the permeate flux.

Sheet 6.10 exp b21-b24 Levapon

note: The experiments were performed directly subsequent to each other; i.e. no standard tests between the experiments were executed.

Exp	Levapon [g/l]	NaCl [g/l]	pH	extra cleaning afterwards
b21	0.3		6.6	
b22	0.3	15	6.4	
b23	3	15	6.5	
b24	3	15	9.6	

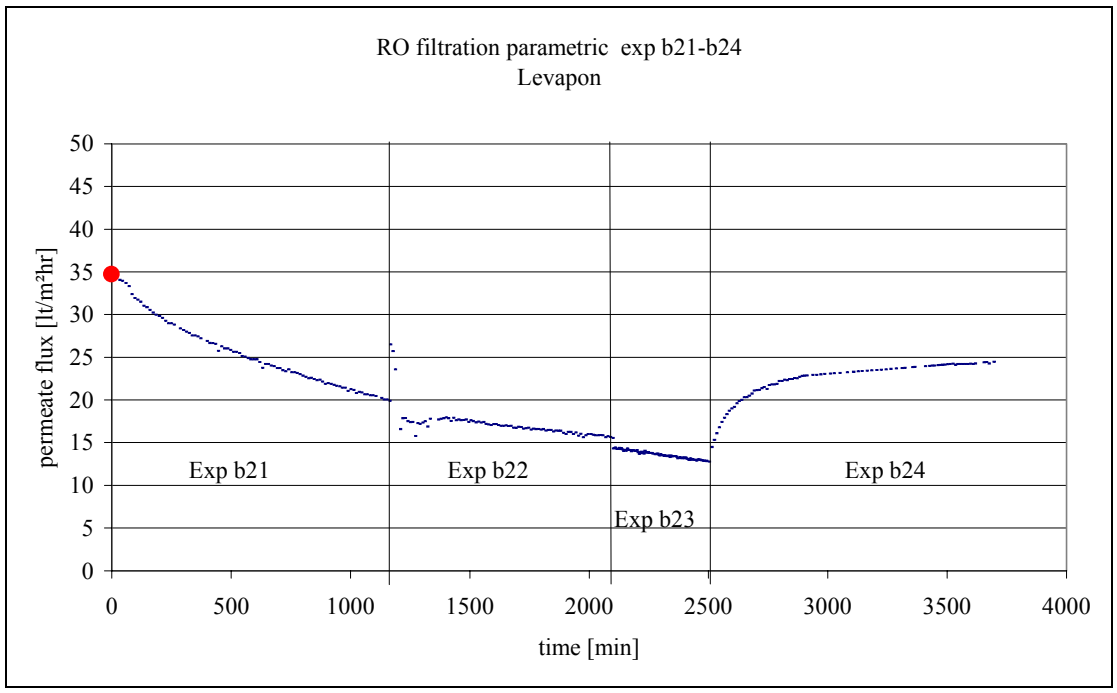

exp	permeate flux [lt/m^{2}hr]	NaCl retention	permeate flux SFT [lt/m^{2}hr]
ST			34.6
b21	20.9		
b22	15.9	0.982	
b23	12.9	0.973	
b24	24.3	0.970	

exp	main observations / remarks
all	The experiments are done subsequently without performing standard tests in between.
b21	A flux decline was observed.
b22	Increasing the NaCl concentration has no remarkable influence
b23	Increasing the Levapon concentration to 3 g/l has no remarkable influence
b24	Increasing the pH to basic conditions increases the permeate flux

6.3.3 Separation of NaCl

For all experiments where the salt concentration was about 15 g/l, the observed retention for NaCl and the salt transport parameter B_m were determined (tables 6.4 to 6.6). The B_m values are compared to the B_m values determined in the filtration with the pure NaCl solutions of NaClexp2 (3.2 g/l) and NaClexp4 (14.2 g/l) using the graphical analysis (Figures 6.1 to 6.3).

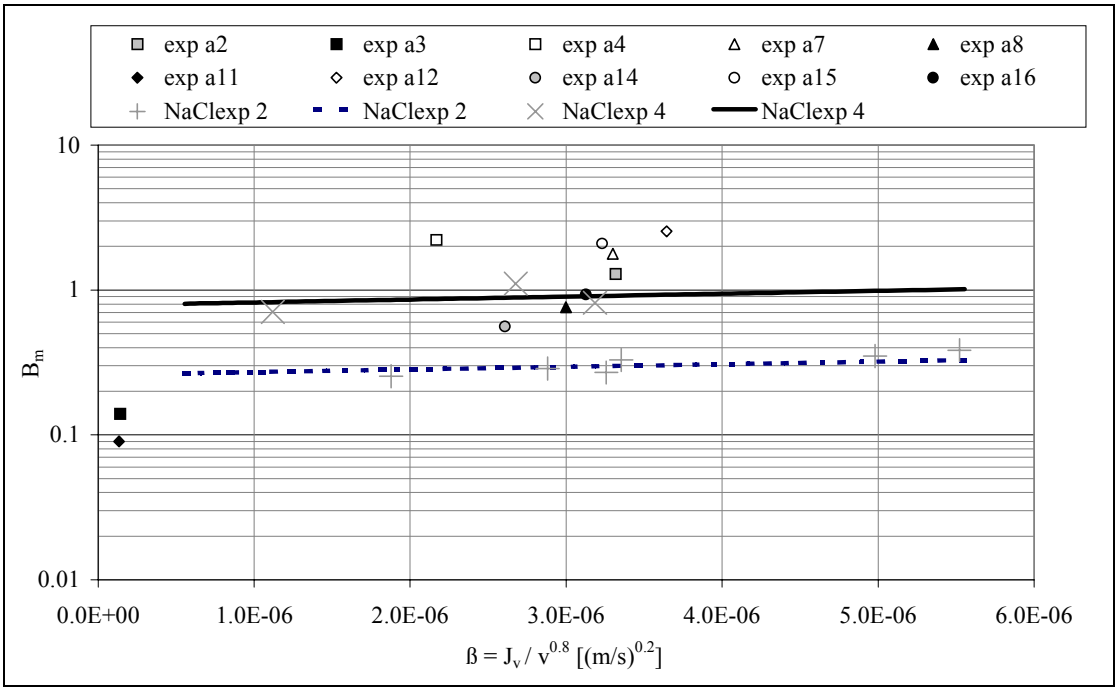

Figure 6.1 Comparison of NaCl transport parameter exp a1-a16 to experiments with pure NaCl solutions.

Table 6.4 Retention of NaCl exp a1-a16.

Exp	Components	pH	Permeate flux [lt/m²hr]	$\beta = Jv/v^{0.8}$ $[(m/s)^{0.2}]$	NaCl – retention	B_m [lt/m²hr]
a2	blue 4	7.4	23.6	11.9	94.8	1.29
a3	blue 4, SDS	7.4	1.0	0.5	87.9	0.14
a4	blue 4, SDS	9.5	15.4	7.8	87.4	2.22
a7	blue 4, water glass	9.9	23.5	11.9	93.0	1.78
a8	blue 4, water glass	6.8	21.3	10.8	96.6	0.76
a11	red 2, SDS	6.5	1.0	0.5	91.6	0.09
a12	red 2, SDS	9.9	25.9	13.1	91.1	2.54
a14	red 2,	6.5	18.5	9.4	97.0	0.56
a15	red 2, water glass	9.9	23.0	11.6	91.6	2.09
a16	red 2, water glass	7.0	22.2	11.3	96.0	0.93

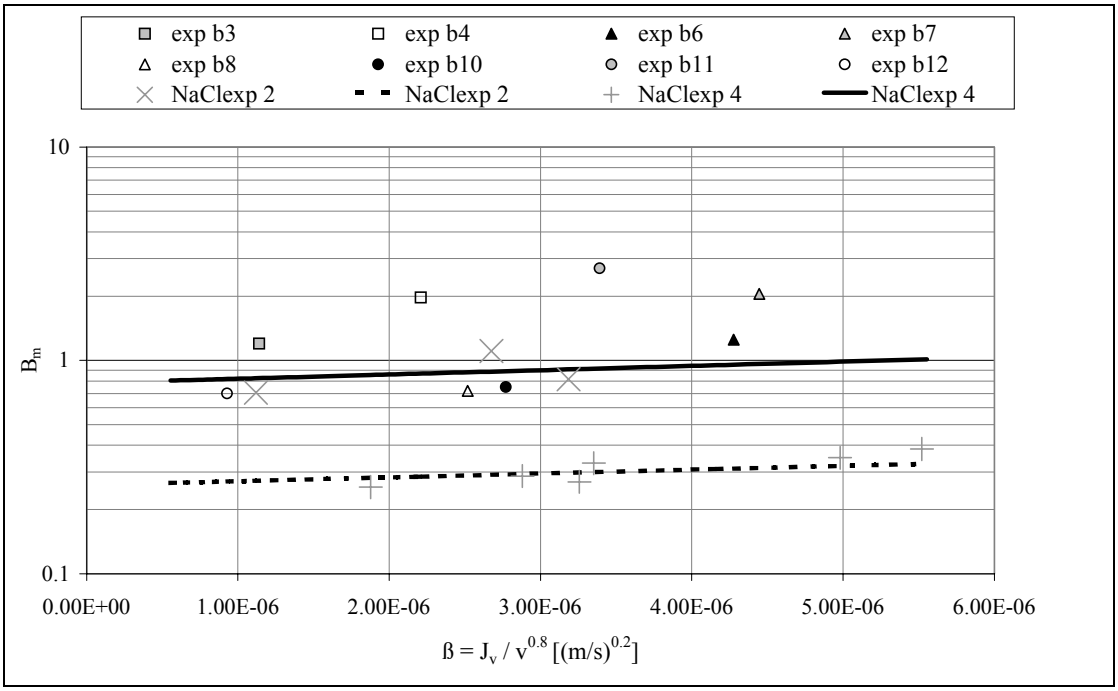

Figure 6.2 Comparison of NaCl transport parameter exp b1-b12 to experiments with pure NaCl solutions.

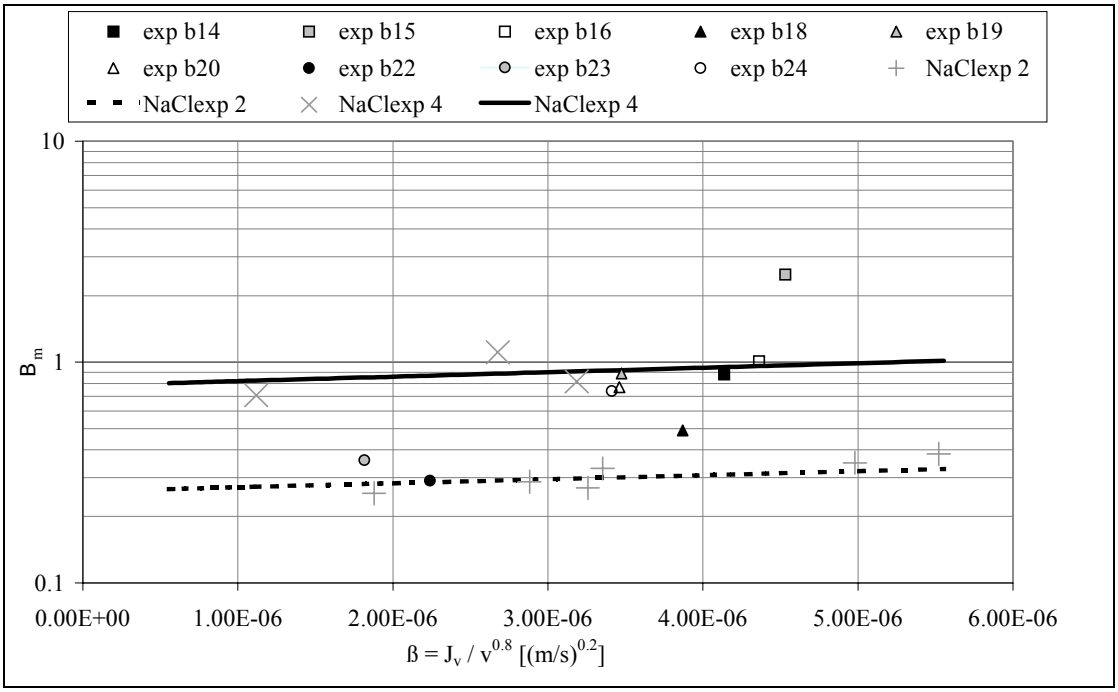

Figure 6.3 Comparison of NaCl transport parameter exp b13-b24 to experiments with pure NaCl solutions (NaClexp2 and NaClexp4 in chapter 4.6.)

Table 6.5 Retention of NaCl exp b2-b12.

exp.	components	pH	Permeate flux [lt/m^{2}hr]	$\beta = Jv/v^{0.8}$ [(m/s)$^{0.2}$]	NaCl – retention	B_m [lt/m^{2}hr]
b2	SDS	6.3	0.7	0.4	94.2	0.04
b3	SDS	7.7	8.1	4.1	87.1	1.20
b4	SDS	9.2	15.7	8.0	88.9	1.97
b6	CTAB	6.2	30.4	15.4	96.0	1.25
b7	CTAB	7.4	31.6	16.0	93.9	2.05
b8	CTAB	9.4	17.9	9.1	96.1	0.72
b10	water glass	6.7	19.7	10.0	96.3	0.75
b11	water glass	9.9	24.1	12.2	89.9	2.70
b12	water glass	10.6	6.6	3.3	90.4	0.70

Table 6.6 Retention of NaCl exp b14-b24.

exp.	components	pH	Permeate flux [lt/m^{2}hr]	$\beta = Jv/v^{0.8}$ [(m/s)$^{0.2}$]	NaCl – retention	B_m [lt/m^{2}hr]
b14	Cibapon	6.5	29.4	14.9	97.1	0.88
b15	Cibapon	9.4	32.2	16.3	92.8	2.49
b16	Cibapon	7.4	31.0	15.7	96.8	1.01
b18	Tinofix	6.4	27.5	13.9	98.2	0.49
b19	Tinofix	9.8	24.7	12.5	96.5	0.89
b20	Tinofix	8.1	24.6	12.5	97.0	0.77
b22	Levapon	6.4	15.9	8.1	98.2	0.22
b23	Levapon	6.5	12.9	6.5	97.3	0.29
b24	Levapon	9.6	24.3	12.3	97.0	0.36

The NaCl retentions in the experiments that were executed directly subsequent to each other (Tinofix and Levapon; b18 to b24) are higher than those in the other experiments. It seems thus that depressurising the filtration equipment, in order to be able to remove the waste solution and rinse the installation, has a negative influence on the salt rejection ability of the membrane. Due to this assumption, conclusions about the influence of the auxiliary components on the NaCl separation should be taken with care.

The NaCl retention and the permeate flux by the RO membrane were expected to increase with increasing pH, going from neutral to alkaline conditions. The origin for this is the increase of the number of negative charges, leading to more repulsion between the polymer segments and thus an increase of the free volume, in the membrane matrix. This can be proven by an increase of B_m with increasing pH, which was observed very strongly in the experiments with SDS (exp b3-b4), water glass (exp b10- b11), Tinofix (exp b18-b19), Cibapon (exp b14- b15) and Levapon (exp b23-b24).

In experiments where considerable membrane fouling occurs (permeate fluxes below 10 lt/m^{2}hr) the fouling layer decreases both the permeate solvent flux and the salt flux. This was observed for SDS (exp b2) and water glass (exp b11-b12).

6.3.4 Resistance of the fouling layer for water transport

Tables 6.8 and 6.9 show the resistance of the fouling layer for water transport (R_f) at the end of the experiments, using equation 3.6. For each filtration experiment, the solvent transport resistance of the virgin membrane (R_m) was determined from the standard filtration test, executed before this experiment. A typical value for **R_m is $36 \cdot 10^{13}$ m^{-1}** (corresponding to a solvent permeability of 1 lt/m^2hrbar).

Table 6.8 Determination of the solvent transport resistance of the fouling layer (R_f).

Exp	comp 1	comp 2	comp 3	pH	Rf [10^{13} m^{-1}]
a1	blue 4 (1.5g/l)			6.5	5.6
a2	``	NaCl (15 g/l)		7.4	-0.7
a3	``	NaCl (15 g/l)	SDS (0.3 g/l)	7.4	**826.2**
a4	``	NaCl (15 g/l)	SDS (0.3 g/l)	9.5	**27.0**
a5	blue 4 (1.5g/l)			7.7	7.5
a6	``		SiO_2 (0.3 g/l)	10.2	-3.0
a7	``	NaCl (15 g/l)	SiO_2 (0.3 g/l)	9.9	2.7
a8	``	NaCl (15 g/l)	SiO_2 (0.3 g/l)	6.8	8.2
a9	red 2 (1.5 g/l)			6.9	6.5
a10	``		SDS (0.3 g/l)	6.9	**723.8**
a11	``	NaCl (15 g/l)	SDS (0.3 g/l)	6.5	**867.0**
a12	``	NaCl (15 g/l)	SDS (0.3 g/l)	9.9	2.9
a13	red 2 (1.5 g/l)			6.9	3.9
a14	``	NaCl (15 g/l)		6.5	7.0
a15	``	NaCl (15 g/l)	SiO_2 (0.3 g/l)	9.9	-0.7
a16	``	NaCl (15 g/l)	SiO_2 (0.3 g/l)	7.0	4.3

The osmotic pressure difference between the retentate and permeate is determined using the relationship between the osmotic pressure and the conductivity derived in chapter 4.6. The experiments with a 'considerable' flux decline (arbitrarily set on $R_f > 10^{14}$ m^{-1}) are marked grey.

In some cases a negative R_f was observed, which points to a change towards a more open membrane structure or a more hydrophilic membrane. This is observed with water glass at 0.3 g SiO_2 / lt under alkaline pH conditions. Changing the pH to alkaline conditions may result in a more open membrane structure, as a consequence of an increased repulsion between the polymer segments in the membrane matrix as the number of charges in the membrane is increased at alkaline conditions.

Negative R_f values also argues for membrane damage, which is normally accompanied with a decreased NaCl retention. This is observed in some cases (CTAB, Tinofix and Cibapon). For Tinofix and Cibapon these effects are of minor importance as was proven by the fact that the differences between the permeabilities in the standard filtration test before and after an experiment with the same membrane is within 10 percent. In the case of CTAB the permeate flux in the standard filtration tests is increased more than 10 percent. Therefore this membrane was replaced.

Table 6.9 Determination of the solvent transport resistance of the fouling layer (R_f)

Exp	comp 1	comp 2	comp 3	pH	Rf [10^{10} m^{-1}]
b1	SDS (0.3 g/l)			6.0	**2111.2**
b2	SDS (0.3 g/l)	NaCl (15 g/l)		6.3	**1217.8**
b3	SDS (0.3 g/l)	NaCl (15 g/l)		7.7	**93.2**
b4	SDS (3 g/l)	NaCl (15 g/l)		9.2	**28.2**
b5	CTAB (0.03 g/l)			6.1	-2.6
b6	CTAB (0.03 g/l)	NaCl (15 g/l)		6.2	3.2
b7	CTAB (0.03 g/l)	NaCl (15 g/l)		7.4	2.7
b8	CTAB (0.3 g/l)	NaCl (15 g/l)		9.4	0.1
b9	SiO_2 (0.3 g/l)			4.6	5.2
b10	SiO_2 (0.3 g/l)	NaCl (15 g/l)		6.7	1.7
b11	SiO_2 (0.3 g/l)	NaCl (15 g/l)		9.9	-2.0
b12	SiO_2 (3 g/l)	NaCl (15 g/l)		10.6	**89.4**
b13	Cibapon (0.3 g/l)			7.4	-1.2
b14	Cibapon (0.3 g/l)	NaCl (15 g/l)		6.5	-0.5
b15	Cibapon (0.3 g/l)	NaCl (15 g/l)		9.4	-1.9
b16	Cibapon (3 g/l)	NaCl (15 g/l)		7.4	-0.1
b17	Tinofix (0.03 g/l)			6.6	-3.0
b18	Tinofix (0.03 g/l)	NaCl (15 g/l)		6.4	-5.0
b19	Tinofix (0.03 g/l)	NaCl (15 g/l)		9.8	-1.3
b20	Tinofix (0.3 g/l)	NaCl (15 g/l)		8.1	5.9
b21	Levapon (0.3 g/l)			6.6	**24.3**
b22	Levapon (0.3 g/l)	NaCl (15 g/l)		6.4	**15.4**
b23	Levapon (3 g/l)	NaCl (15 g/l)		6.5	**35.9**
b24	Levapon (3 g/l)	NaCl (15 g/l)		9.6	0.9

6.4 Discussion

6.4.1 Hydrolysed reactive dyes

The dye solutions (1 g/l) without additives always cause a slight flux decline. It is observed that the membranes were fouled by the dyestuff as they were coloured. This coloured fouling layer can easily be removed by wetting and rubbing it by hand, however not by rinsing at high cross-flow velocity. This means that in practice this fouling layer can not be removed easily as a mechanical cleaning action is dissuaded by the membrane manufacturer.

All permeate samples were visually inspected to be colourless or slightly coloured; the measured retention for the dyestuff (1.5 g/l) by the RO membrane is very high (> 99.85 % in all cases).

6.4.2 Sodium chloride

Three phenomena concerning the influence of sodium chloride on the permeate flux will be discussed here:

- Flux decline due to osmotic pressure difference
- Flux decline due to concentration polarisation
- Enhancement of the membrane fouling by other components

The phenomena of osmotic pressure and concentration polarisation result immediately in a lower permeate flux at the start of an experiment. This is observed in the experiments were 15 g/l is added to the dye solutions (exp a2 and exp a14) and to auxiliary components (exp b6, b10, b14 and b18). The influence of the osmotic pressure and the cross-flow velocity can be calculated by using the analysis of chapter 4.6.:

$$\exp\left[\frac{J_v}{k}\right] + \frac{J_v}{A \cdot \Delta\Pi_{b,p}} - \frac{\Delta P}{\Delta\Pi_{b,p}} = 0 \qquad (6.1)$$

In which the mass transport parameter can be calculated with:

$$k = 0.023 \cdot \frac{D^{0.67} \cdot \nu^{0.8}}{d^{0.2} \cdot \nu^{0.47}} \qquad (6.2)$$

Table 6.10 Input of equation 6.1

clean water permeability	A	1.14	lt /m²hrbar
transmembrane pressure	ΔP	35	bar
internal diameter membrane	d	13.75	mm
diffusion coefficient NaCl	D	$1.5 \cdot 10^{-9}$	m^2/s
kinematic viscosity	ν	10^{-6}	m^2/s

Table 6.11 Permeate fluxes of RO filtration of NaCl solutions calculated with the osmotic pressure model

NaCl concentration [g/l]	Corresponds to	Theoretical permeate flux at 35 bar and 2 m/s [lt/m²hr]
0.00	clean water flux (CWF)	40.0
1.87	SFT exp b1-b24	37.9
3.00	SFT exp a1- a16	36.8
15.00	experiments at high salt concentration	24.3

Calculations with four NaCl concentrations (table 6.11) show that at cross-flow velocities above 2 m/s concentration polarisation can be neglected and the flux decline can be explained by the osmotic pressure difference over the membrane (figure 6.4).

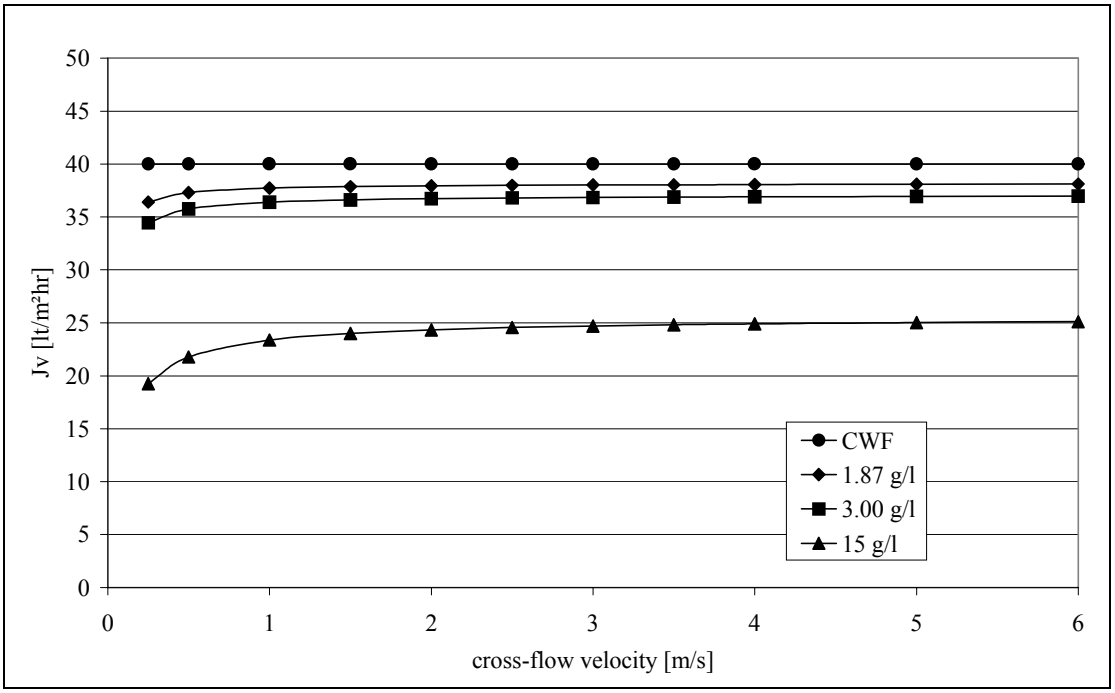

Figure 6.4 Theoretical calculated fluxes, using equations 6.1 and 6.2, for the filtration of NaCl solutions.

The influence of NaCl on the development of R_f in the experiments containing SDS will be discussed in 6.4.4.

The measured NaCl retention at the concentration of 15 g/l NaCl lies between 87 and 97 percent Generally it can be stated that, in absence of fouling components, a higher pH implies a higher permeate flux and a lower NaCl retention. (exp a6, a15, b11 and b15).

6.4.3 Water glass

In the experiments the reactive silica concentrations (i.e. 0.3 and 3 g/l) were always higher than the solubility concentration (i.e. ~ 0.1 g/l at pH 7 and ~ 0.3 g/l at pH 10). This means thus that the formation of colloidal silica was very likely to occur. Water glass, in the concentrations used in exp a6, a15 and b11 (0.3 g/l SiO_2) increases immediately the permeate flux as a consequence of the pH increase. Severe flux decline at this concentration was not observed. Increasing the concentration to 3 g/l SiO_2 leads to relative slow (compared to SDS) but substantial membrane fouling (exp b12).

6.4.4 Anionic surfactants

Filtration of SDS solutions at neutral pH shows a larger flux decline and a lower flux at the end than filtration at alkaline pH. This is in accordance with the fact that the electrostatic repulsion between surfactant and membrane will increase with increasing pH as the number of negative charges of both the membrane surface and the surfactants will increase.

In the experiments at neutral pH conditions, where SDS was present in the feed, a large decline in the permeate flux was observed. In order to determine the effect of NaCl and dyes on this flux decline the resistance of the fouling layer against water transport (R_f) as function of time is presented in figure 6.5.

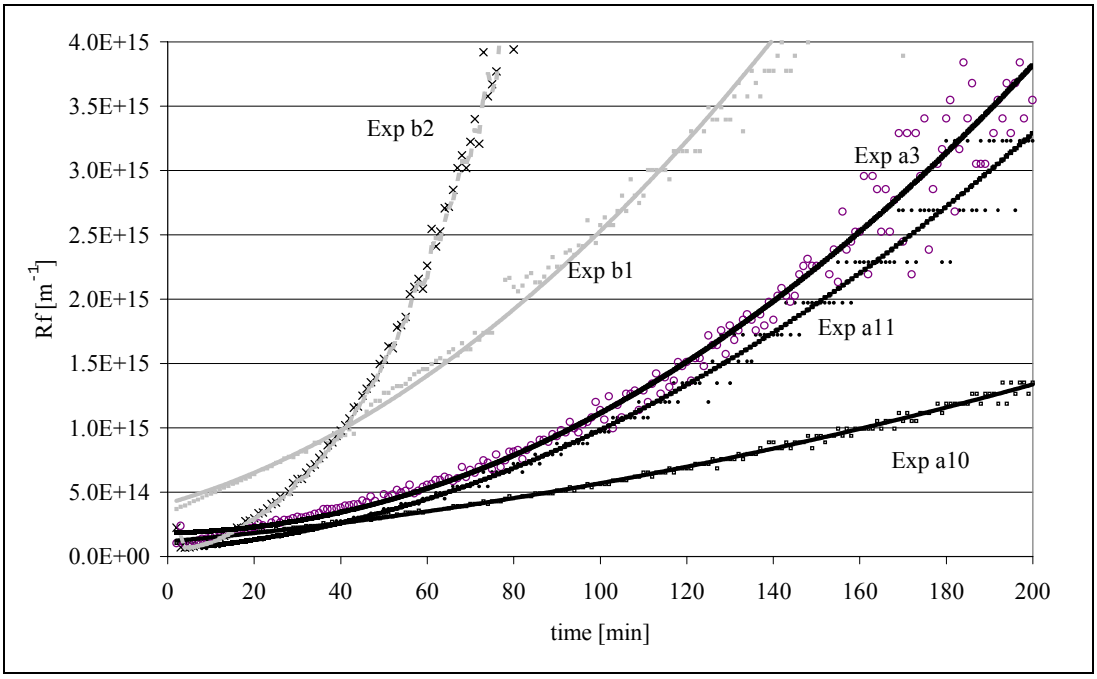

Figure 6.5 Influence of NaCl and dyes on (the development of) R_f due to adsorption of SDS.

It can be seen that NaCl enhances the flux decline rate (compare exp b2 to exp b1 and exp a11 to exp a10). The sodium ions lower the electrostatic repulsion, by shielding the negative charges, between the membrane and the surfactant, resulting in a stronger SDS adsorption on the membrane.

In the presence of a hydrolysed reactive dye (exp a3, a10 and a11) the flux decline rate by SDS is much slower than in the experiments b1 and b2. This is probably due to the competitive co-adsorption of dyes and SDS on the membrane, as the membranes were coloured after these experiments.

The washing formulation Levapon reduces the permeate flux. This is not surprising as Levapon consists of alkylsulphates, a group of surfactants like SDS. However, Cibapon, a washing agent containing anionic components based on polyacrylic-acid, did not show any flux decline effect at any circumstance. The reason for this may be that the electrostatic repulsion between the anionic Cibapon components and the membrane is stronger than between SDS and the membrane as the Cibapon consists of an anionic polyelectrolyte polymeric component.

6.4.5 Cationic surfactants

The concentration of the cationic components in the experiments was small (for CTAB far below the CMC) because of the facts that

- Cationic components are only applied in very small amounts in the textile washing process
- Cationic components are notorious for their fouling behaviour, and it was expected that even a small concentration would cause a considerable membrane fouling (i.e. flux decline).

However no considerable membrane fouling was observed in any of the experiments with the cationic components at varying NaCl concentration and pH. In chapter 9 membrane filtration

of CTAB solutions with higher concentration levels and solutions containing a mixture of cationic and anionic textile auxiliaries will be investigated.

6.4.6 Consequences for application of RO on textile wastewater from a reactive dyeing process

For the practical application of the RO process it is important to get permeate fluxes and retentions for key components (dyes and NaCl) without fast and severe flux decline phenomena.

As the main fouling components (silicates and alkylsulphates) have a colloidal character it is advisable to pretreat the feed by microfiltration. However surfactants and water glass, in the monomer form, will not be removed completely by these pretreatments [4]. If the concentration of water glass can be kept at or below 0.3 g/l SiO_2 the fouling will be absent or very slowly and cleaning operations don't have to be carried out too frequently.

The use of surfactants based on alkylsulphates should be minimised or the alkylsulphates should replaced by other surfactants, as they can lead to complete flux failure combined with NaCl retentions below 90 percent. However if this is not possible, the pH should be shifted to or kept between alkaline conditions before RO filtration.

The retention of the hydrolysed reactive dyes by the membrane was sufficient for recycling of the permeate in the washing baths with respect to contamination of coloured compounds. The retention of NaCl at 15 g/l is about 92-99 percent, provided that the permeate flux is above 20 lt/m^2hr. An increase of the pH, which might be necessary to minimise membrane fouling, decreases the NaCl retention.

Cationic components, examined here, do not cause a permeate flux decline. However the combination of these compounds with anionic surfactants or with textile auxiliaries, containing anionic surfactants was not examined.

6.5 Conclusions

Reverse osmosis experiments were performed with a synthetic wastewater containing components, which are present -or representative for components present- in textile wastewater from a reactive dyeing process and subsequent washing processes. The aim was to determine which (combinations of) components are responsible for changing permeate fluxes and separation characteristics. Severe flux decline was only observed with the anionic surfactant, sodium dodecyl sulphate (SDS), and water glass.

When filtrating a synthetic wastewater containing only an industrial formulation of (hydrolysed) reactive dyes (~ 1 – 1.5 g/l) a slight flux decline was observed. The permeate flux generally became stable at a value which was not less than 90 percent of the flux in the standard test and sometimes even higher. The retention of the dyes by the membrane was sufficient with respect to recycling of permeate in the textile washing range or draining to the environment.

Membrane fouling by water glass can be avoided if the SiO_2-concentration is kept below the solubility concentration (i.e. 0.1 –0.3 g/l depending on pH). Flux decline due to membrane fouling by SDS is a typical preferential adsorption phenomenon and will already occur at low concentrations (even below the critical micelle concentration). It was found that lowering the pH or increasing the salt concentration enhances the flux decline. The unwanted flux decline

by anionic surfactants, like SDS, can be avoided by operating the RO process at alkaline pH conditions or by choosing other, appropriate washing agents.

Contrary to the facts that the RO membrane has fixed negatively charged groups and adsorption of cationic compounds is likely to occur, no flux decline and only a little decrease of NaCl retention was observed when filtrating solutions of cationic compounds. The combination of anionic and cationic compounds was however not investigated in this parametric study.

Acknowledgement

F. Spenkelink and P. Nieland are acknowledged for the experimental work of this chapter.

Symbols

β	parameter graphical method [2]	$(m/s)^{0.2}$
$\Delta\Pi_{b.p}$	osmotic pressure difference (retentate-permeate)	bar
ΔP	transmembrane pressure	bar
ν	kinematic viscosity	m^2/s
A	clean water permeability	m/(s·bar)
B_m	observed solute (NaCl) transport parameter	m/s
d	internal diameter membrane	mm
D	diffusion coefficient NaCl	m^2/s
J_v	permeate flux	m/s
k	solute mass transport parameter in boundary layer	m/s
R_f	hydraulic permeability fouling layer	m^{-1}
R_m	hydraulic permeability membrane	m^{-1}
v	cross-flow velocity	m/s

Literature

[1] Mulder, M.H.V., Basic principles of membrane technology. Kluwer Academic Publishers Dordrecht, (1996).
[2] Murthy, Z. V. P. and S. K. Gupta. Simple graphical method to estimate membrane transport parameters and mass transfer coefficient in a membrane cell. Separation science and technology **31**(1): 77-96 (1996).
[3] Comb, L. F. Silica, silica chemistry and reverse osmosis. Ultrapure water 13(1): 41-43. (1996).
[4] Janisch, I., Zum Problem der Membranverschmutzung bei der Umkehrosmose, Doctoral Thesis, RWTH Aachen (1987).
[5] Myers, D. Surfaces, interfaces, and colloids. VCH New York (1990).

Chapter 7

Treatment of synthetic textile wastewater by nanofiltration

Summary

Nanofiltration of synthetic textile wastewater solutions with various compositions was executed. The composition was altered with two hydrolysed reactive dyes, an anionic surfactant, water glass, NaCl and NaOH. The retention of NaCl by the NF membrane is about 10 percent which means that osmotic pressure effects do indeed play a role. Like the nanofiltration experiments with actual wastewater, complete decolourization of the synthetic waste streams by nanofiltration was not always achieved. Comparing this NF parametric study to the RO parametric study (A), it can concluded that the membrane fouling by the anionic surfactant SDS is sever and shows the same tendencies. Membrane fouling by the hydrolysed reactive dyes and water glass was more severe in the NF than in the RO experiments at 0.3 g/l silicate concentration. Filtration experiments with a mixture of hydrolysed reactive dyes, NaCl, Cibapon (washing auxiliary) and Tinofix (after-fixation auxiliary) showed that the addition of the cationic component Tinofix to this combination caused severe membrane fouling.

7.1 Introduction

Nanofiltration can be used to concentrate a (textile) waste stream containing organic components (e.g. dyes and surfactants), as these components will be rejected by the membrane. If the waste stream contains a high NaCl concentration the reduction of waste volume can be larger compared to treatment by reverse osmosis, as the osmotic pressure difference will be considerably smaller cause NaCl will not be rejected by the membrane.

In the treatment of real wastewater by NF (chapter 5) it has been observed that some components (e.g. water glass) could cause a flux decline. Furthermore the NF membranes did not always reject the dye components to such an extent that the permeate streams were colourless.

The aim of this study with the synthetic wastewater is to determine which components or combination of components present in the textile wastewater are causing unwanted flux decline and failing separation characteristics. Furthermore two dyes originating from the two main dye classes (i.e. antraquinon dyes (blue colours) and mono-azo dyes (yellow, orange and red colours) have been selected in order to check the hypothesis that mono-azo dyes permeate the membrane more easily than the antraquinon dyes.

7.2 Experimental procedures and design

The one pass set-up, as shown in figure 4.2, equipped with one nanofiltration membrane (table 4.1) is used here. The temperature was controlled at 20 ± 0.5 °C by a heat exchanger, fed by tap water. All filtration experiments were done at a transmembrane pressure of 10 bar and a cross-flow velocity of 1 m/s.

Four sets of four experiments were performed. The first experiment of each set started with a synthetic waste solution of one hydrolysed reactive dye (reactive blue 4 or reactive red 2). Subsequently in every set the influences of one auxiliary component (i.e. water glass or sodium dodecyl sulphate (SDS)), the background salt concentration, by adding NaCl, and the pH, by adding NaOH or HCl, were investigated. These three experiments in a set were designed in order to detect the (combination of) fouling components.

The time for an experiment was at least 1000 min (i.e. one night), except for experiment 7.2. At the end of the filtration experiments samples were taken of both retentate and permeate. NaCl concentrations (> 10 g/l) were determined by measuring the conductivity on a Knick 703 conductivity apparatus equipped with a Schott-probe LF 1100. Dye concentrations were measured as spectral absorbances (m^{-1}) at wavelength of maximal absorption. From these data the retention for the key compounds NaCl (conductivity) and dyes (colour) were calculated.

The osmolalities of the samples were measured with Advanced Instruments` wide-range osmometer 3W2, in order to be able to correct the transmembrane pressure for the osmotic pressure difference between retentate and permeate. This osmometer uses the freezing point method to determine the osmolality.

Table 7.1 standard test and cleaning actions

Procedure	Description
SFT	standard filtration test with 0.5 wt% $MgSO_4$ at a transmembrane pressure of 10 bar and a cross-flow velocity of 1 m/s
Acid	rinsing the system with Ultrasil 70 (200 ml pro 20 litre) for 30 minutes
Base	rinsing the system with Ultrasil 10 (150 gr. pro 20 litre) for 30 minutes
NaOH	rinsing the system with NaOH solution at pH=10 for 30 minutes
Enz	rinsing the system with Ultrasil 53 (enzymatic cleaning agent)

After an experiment the solution was removed out of the filtration equipment and the membrane and equipment were rinsed with tapwater for some time at a transmembrane pressure of 10 bar. Subsequently some cleaning actions, summarised in table 7.1, were performed. Before continuing with the next experiment (of the same set) the membrane was tested with a standard filtration test (SFT), in order to check if the toplayer of the membrane hadn't been damaged and the membrane could be used for this next experiment.

During the first eight experiments the $MgSO_4$ retention in the SFT was not always determined properly and was therefore not reported.

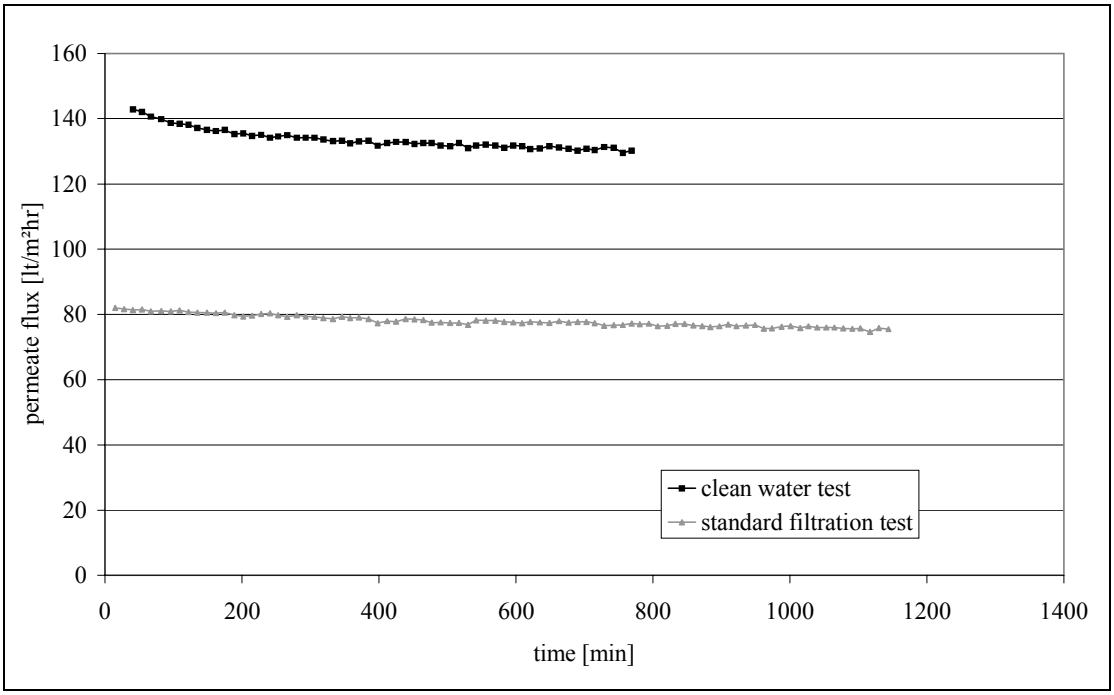

Figure 7.1 Measured permeate flux of a clean water test and a standard filtration test as function of time.

In order to detect if flux decline phenomena due to membrane compaction or membrane structure alterations already occurs when no membrane fouling is expected, a 'clean' water test (filtration at 10 bar with demineralised water) and a SFT on a new membrane have been examined over a longer timescale (figure 7.1). In both filtration tests a slight flux decline in time was observed Furthermore the permeate flux in the SFT was considerably lower than the flux of the clean water test, due to concentration polarisation and the osmotic pressure difference over the membrane in the SFT.

Table 7.2 Parameters for the osmotic pressure model for the SFT of the NF.

membrane permeability	$3.6 \cdot 10^{-6}$ m/(s·bar) (130 lt/m²hr at 10 bar)
transmembrane pressure	10 bar
cross-flow velocity	1 m/s
concentration	0.5 wt % ~ 0.04 mole/lt ~ 0.08 eq/lt
osmolality [2]	0.055 Os/kg
osmotic pressure difference at retention of 0.95	1.27 bar
Diffusion coefficient [1] of $MgSO_4$ in water 20°C	$6.2 \cdot 10^{-10}$ m^2/s

The osmotic pressure difference is estimated to be about 1.3 bar in case of 95 % retention of the 0.5 wt% $MgSO_4$ solution, resulting in an effective driving pressure of ~8.7 bar. The permeate flux at no concentration polarisation is then ~108 lt/m²hr.

The influence of the concentration polarisation effect has been calculated with the osmotic pressure model as presented in chapter 6 (eq. 6.1 and 6.2). The input for this model concerning the SFT of the NF is presented in table 7.2 and the permeate flux at varying cross-flow velocities are shown in figure 7.2. The osmotic pressure difference at 1 m/s is then about 3-4 bar. The permeate flux of the SFT is calculated to be 83 lt/m²hr which is close to the measured permeate flux.

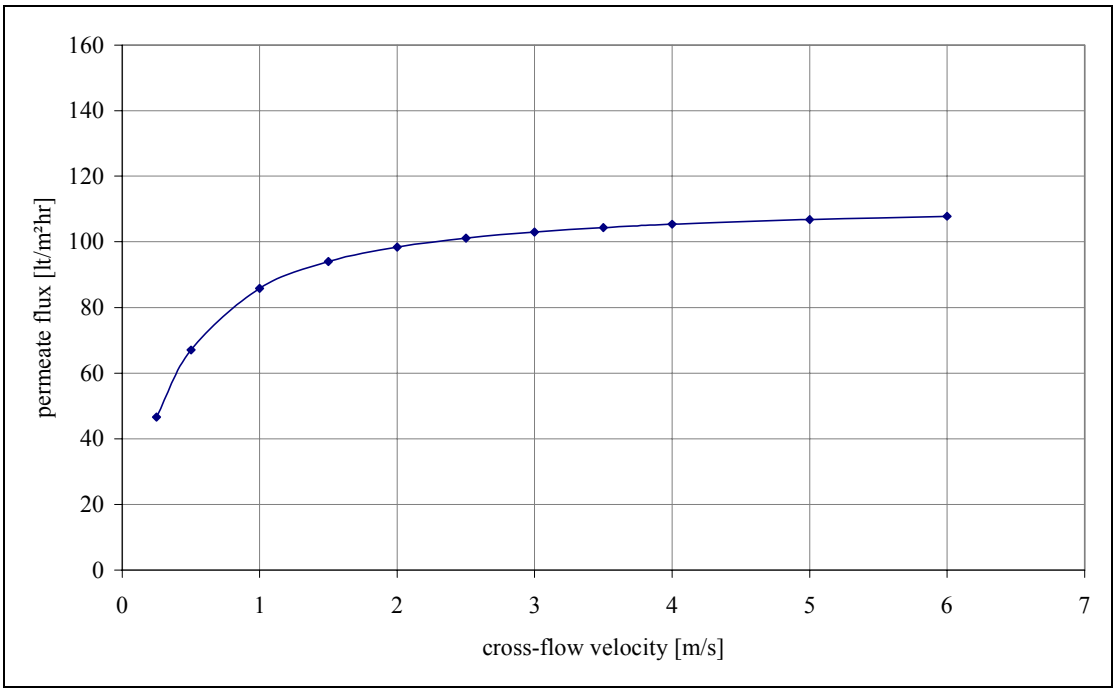

Figure 7.2 Calculated permeate fluxes as function of the cross-flow velocity for NF filtration of $MgSO_4$-solutions.

Sheet 7.1 Experiments 7.1-7.4 Hydrolysed reactive blue 4 and SDS

Exp	NaCl [g/l]	Blue 4 [g/l]	SDS [g/l]	pH	Cleaning actions
7.1	---	1.5	---	7.2	B(10),Acid,Base
7.2	30	1.5	---	6.9	Acid, B(10) + new membrane
7.3	30	1.5	0.3	7.0	Acid, B(10)
7.4	30	1.5	0.3	9.6 → 8.0*	

* pH shift occurred during experiment

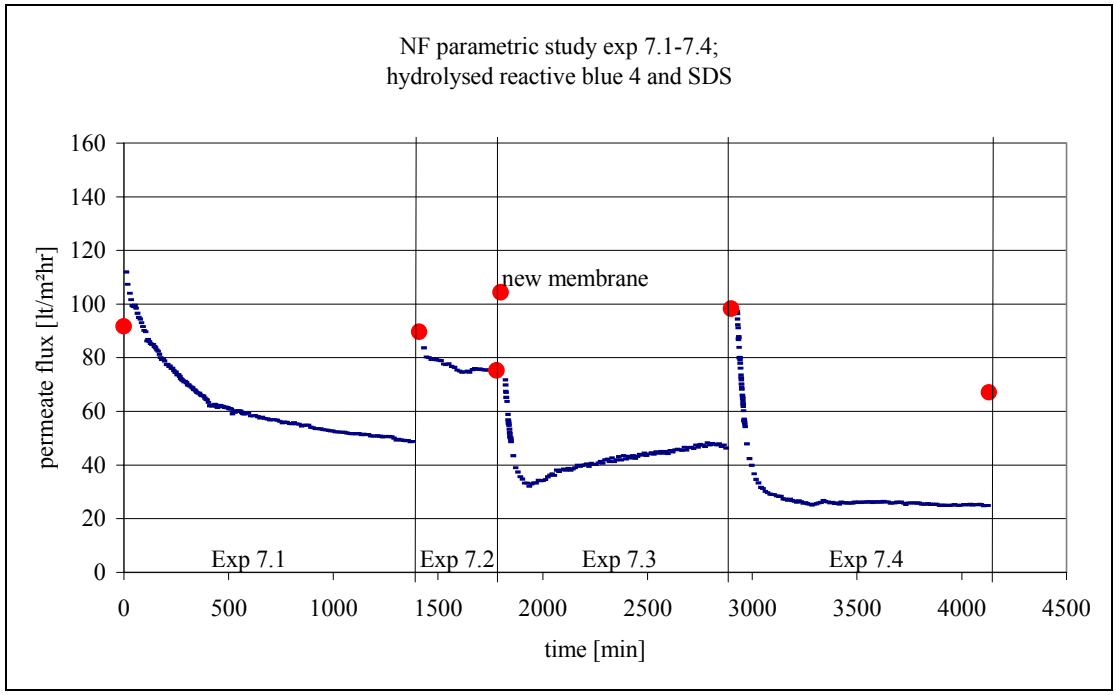

Exp	Permeate flux [lt/m²hr]	Permeate flux SFT [lt/m²hr]	Retention Mg SFT [%]
SFT 7.1		93	0.963
7.1	49.3	90.5	0.968
7.2	76.3	77.7	*
SFT 7.3		109.2	0.954
7.3	48.0	99.2	0.965
7.4	25.3	75.8	*

*: Retention measurements were unreliable

Main observations:

exp	
7.1	considerable permeate flux decline observed
7.2	slight permeate flux decline observed. permeate flux was judged to be constant and the experiment was run for only 300 minutes.
7.3	fast permeate flux decline observed, flux increased after 200 minutes.
7.4	severe flux decline observed but influence of pH not detectable as pH also drops during filtration

Sheet 7.2 Exp 7.5-7.8 Hydrolysed reactive blue 4 and water glass

Exp	NaCl [g/l]	Blue 4 [g/l]	water glass [g/l]	pH	Cleaning actions
7.5	---	1.5	---	7.2	B(10),Acid, Base
7.6		1.5	0.3	10.0	Acid,B(10)
7.7	30	1.5	0.3	9.7	Enz,Acid, B(10)
7.8	30	1.5	0.3	7.5	Enz,Acid, B(10)

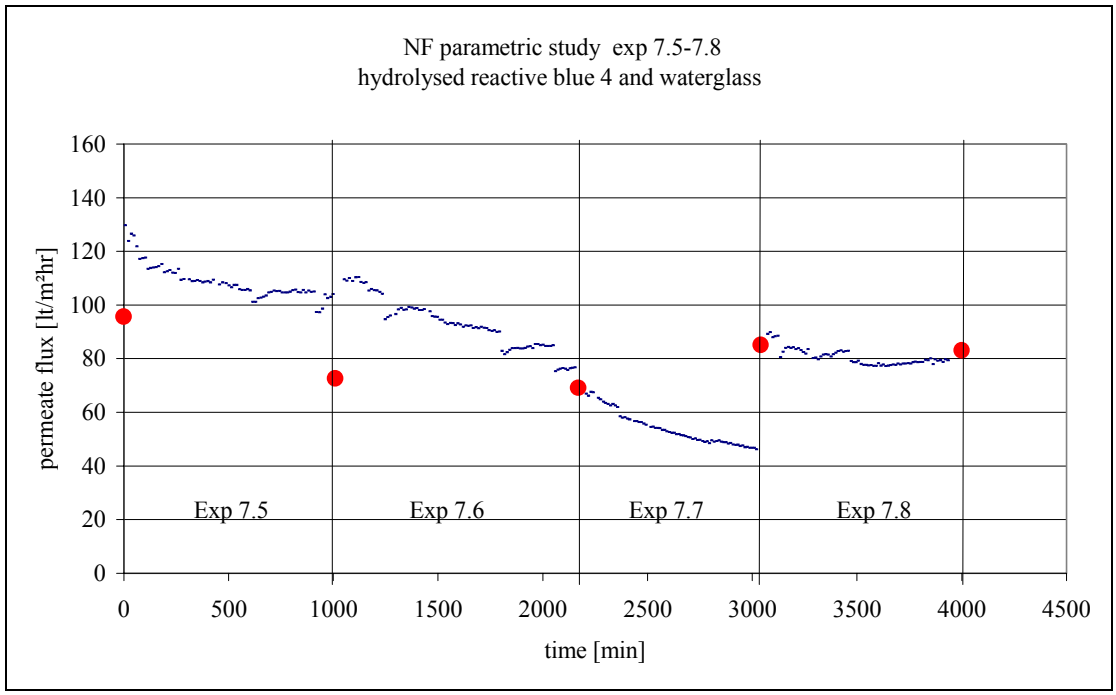

Exp	Permeate flux [lt/m²hr]	Permeate flux SFT [lt/m²hr]	Retention $MgSO_4$ SFT [%]
SFT 7.5		96.6	0.951
7.5	100.2	73.3	0.968
7.6	77.6	69.9	0.967
7.7	46.9	86.1	*
7.8	78.1	84.0	*

*: Retention measurements were unreliable

exp	
7.5	some permeate flux decline. permeate flux remains constant after ~ 400 minutes
7.6	permeate flux decline observed.
7.7	addition of salt leads to further permeate flux decline
7.8	Enzymatic cleaning increases the permeate flux in the standard test. No (considerable) permeate flux decline observed

Sheet 7.3 experiments 7.9-7.12. Hydrolysed reactive red 2 and SDS

Exp	NaCl [g/l]	Red 2 [g/l]	SDS [g/l]	pH	Cleaning actions
7.9	---	1.5	---	6.8	Enz,Acid, B(10)
7.10		1.5	0.3	6.8	Enz,Acid, B(10)
7.11	30	1.5	0.3	6.4	Enz,Acid, B(10)
7.12	30	1.5	0.3	9.3→8.6	none

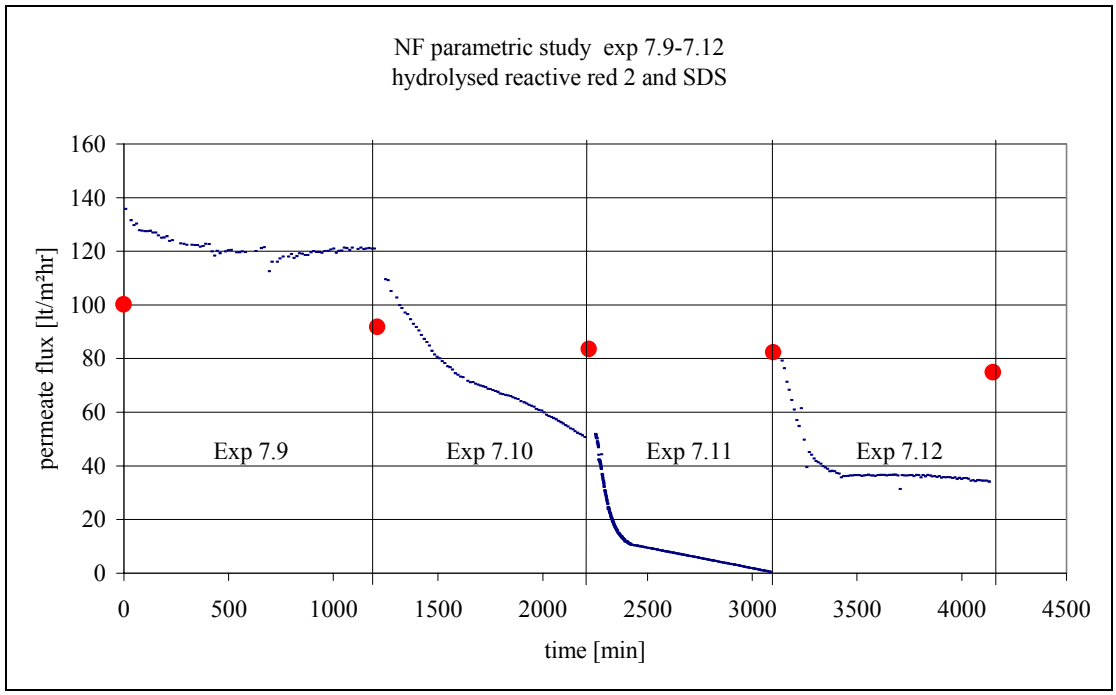

Exp	Permeate flux [lt/m²hr]	Permeate flux SFT [lt/m²hr]	Retention $MgSO_4$ SFT [%]
ST 9		101.2	0.943
7.9	121.6	92.8	0.938
7.10	51.9	84.4	0.937
7.11	1.0	81.8	0.940
7.12	34.7	75.6	0.934

exp	
7.9	slight permeate flux decline observed reaching constant value
7.10	addition of SDS increases the flux decline
7.11	flux decline is enhanced at higher salt concentration leading to almost no permeate flux
7.12	increasing the pH decreases the flux decline rate

Sheet 7.4 Experiments 7.13-7.16 Hydrolysed reactive red 2 and SDS

Exp	NaCl [g/l]	Red 2 [g/l]	water glass [g/l]	pH	Cleaning actions
7.13	---	1.5	---	6.7	Enz,Acid, B(10)
7.14	30	1.5	---	6.3	Enz,Acid, B(10)
7.15	30	1.5	0.3	9.8	Enz,Acid, B(10)
7.16	30	1.5	0.3	7.2	none

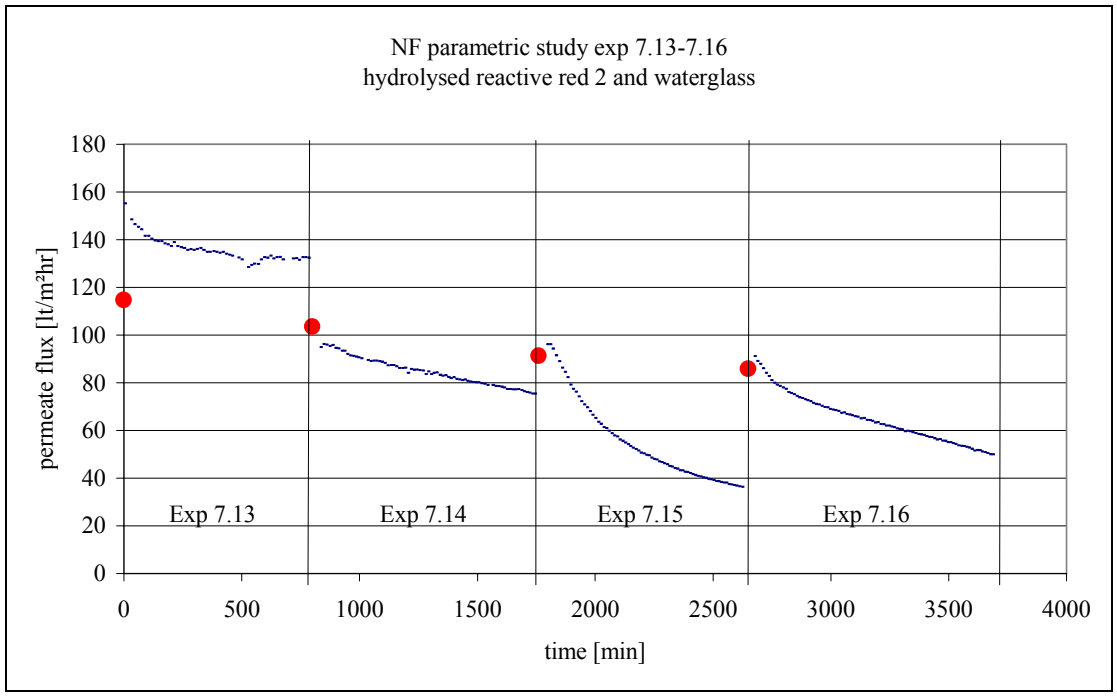

Exp	Permeate flux [lt/m²hr]	Permeate flux SFT [lt/m²hr]	Retention $MgSO_4$ SFT [%]
SFT 7.13		115.9	0.956
7.13	134.3	104.6	0.962
7.14	76.4	92.3	0.959
7.15	36.9	86.7	0.960
7.16	50.7		

exp	
7.13	slight permeate flux decline observed
7.14	addition of NaCl leads immediately to a lower flux, a slight flux decline is observed
7.15	addition of water glass does immediately raise the permeate flux. a considerable flux decline was observed.
7.16	the flux decline at pH 7 is lower than the flux decline at pH 10

7.3 Results and discussions

7.3.1 Permeate flux

In the sheets 7.1 to 7.4 experimental actions, cleaning actions and main observations have been summarised. In the figures the permeate fluxes as function of time have been plotted. The black circles between the experiments represent the permeate flux of the SFT.

In the experiments with a dye solution without any other additives (exp 7.1, 7.5, 7.9 and 7.13) the flux didn't decrease considerably comparing it to the flux decrease determined with the clean water test or SFT, except for experiment 7.1. An explanation for this could be that the installation was not totally clean before running experiment 7.1.

Similar to the reverse osmosis parametric study the resistance in series model is applied to these NF experiments. Results are summarised in table 7.3. The cleaning procedures did not always restore the initial permeate flux, which can be seen in the scattered data for R_m.

Table 7.3 Influence NaCl retention on the osmotic pressure difference across the membrane.

Exp.	R_m [10^{13} m^{-1}]	NaCl Retention	$\Delta\Pi_{b,p}$ [bar]	R_f [10^{13} m^{-1}]
7.1	2.5		0.5	4.3
7.2	2.6	0.138	2.1	0.5
7.3	1.9	0.129	1.7	3.8
7.4	2.3	0.118	1.4	9.7
7.5	2.4		0.2	1.1
7.6	3.5		0.3	0.9
7.7	3.8	0.128	1.9	1.9
7.8	2.8	0.147	1.9	0.4
7.9	2.2		0.2	0.6
7.10	2.5		0.4	4.0
7.11	2.9	0.086	1.2	324.2
7.12	3.1	0.097	1.0	6.0
7.13	1.7		0.2	0.9
7.14	2.1	0.144	1.9	1.2
7.15	2.6	0.123	1.4	5.4
7.16	2.8	0.123	1.4	2.9

When NaCl (30 g/l) had been added to a dye solution the flux became immediately remarkable lower (exp 7.2 and 7.14). In both experiments a slight flux decline in time was observed, which may be explained by an enhanced adsorption of anionic dye components at increased NaCl concentration, according to the theory presented in chapter 3.2.3.3. But the initial lower flux is mainly due to an osmotic pressure difference over the membrane, as can be derived from table 7.3 in which the measured osmotic pressure difference is tabulated as well. This osmotic pressure difference was also determined from the measured conductivity difference (i.e retention of NaCl), which gave similar results as determined with the measurements with the osmometer.

Considerable flux decline was observed if 0.3 g/l SDS had been added to the waste solution. The rate and the amount of membrane fouling was enhanced at higher NaCl concentrations (compare exp 7.10 and 7.11) according to the theory that the electric repulsion of similar charges decreases at higher NaCl concentration (Ch. 3.2.3.3.). In experiment 7.3 a slight increase of the permeate flux was observed. It may be that the surfactant molecules at the surface undergo a rearrangement leading to a more open structure of the fouling layer.

In all NF experiments, where SiO_2 was added (0.3 g/l as water glass) a considerable permeate flux decline was observed. Changing the NaCl concentration did not have an observable effect on the permeate flux decline. In the similar RO experiments (chapter 6) this flux decline at 0.3 g/l SiO_2 was not observed (but even a flux increase). This may be explained by the fact that the higher flux in the NF experiments resulted in an increased effect of the concentration polarisation or that the SiO_2 can enter the pores of the NF (internal membrane fouling).

Membrane fouling at neutral pH was not larger than membrane fouling at alkaline pH in both the SDS and silicate experiments, which is in disagreement with the theory (chapter 3). Possible reason for this discrepancy is that in the SDS experiments the pH, set at 10 at the begin of the experiment, shifted to less alkaline conditions. In the water glass experiments two opposite effects may have been occurred. The first effect is that an increase of the pH will increase the solubility of the silicate. The second effect is that an increase of the pH will increase the free volume in the membrane matrix. The first effect will decrease the membrane fouling as the second effect can increase the internal membrane fouling.

During a set of experiments the permeate flux of each subsequent SFT declines due to (irreversible) fouling of the membrane surface. The acid/base cleaning did not restore the flux of the SFT in the experiments 7.1 to 7.7. Therefore an enzymatic cleaning before the acid/base cleaning was introduced after experiment 7.7. The permeate flux in the SFT after experiment 7.8. was considerably enhanced and the enzymatic cleaning seemed to be very successful. However in the subsequent experiments the permeate fluxes of the SFTs were not restored completely.

The fouling layer, easily detected by the human eye when observing the membranes after usage, could easily be removed by wetting and rubbing it by hand. Therefore a mechanical rinsing was done by scrubbing fouled membranes after experiments 7.2 and 7.4 with a sponge. This mechanical rinsing however damaged the selective toplayer of the NF membrane, as the permeate flux of the SFT was indeed restored but the retention of $MgSO_4$ dropped tremendously to values below 20 percent.

7.3.2 Retention of the dye components

The spectral absorbances of the retentate and permeate samples are shown in table 7.4 (reactive blue 4) and table 7.5 (reactive red 2) and the retentions have been calculated. These spectral absorbances have been taken at the wavelength of maximal absorbance of the permeate samples. This wavelength was 535 nm for the permeates of exp 7.9-7.16, corresponding to the colour of the red dye, and 485 nm for the permeates of exp 7.1-7.8, not corresponding to the colour of the blue dye, which was 595 nm. So the conclusion is that a minor (orange coloured) component present in the synthetic wastewater, containing blue 4, permeates through the membrane.

The permeate and retentate samples of experiment 7.1 and two reactive blue 4 solutions respectively in the reactive form and the hydrolysed form have been extracted in their components by High Pressure Liquid Chromatography (HPLC) and analysed spectrofotometrically at 500 nm. All samples were filtered over a 0.45 μm filter before the HPLC in order to avoid clogging of the HPLC column. The HPLC extraction method was performed at 30 °C in a hypersil-BDS-C18 column with a length of 125 mm and a diameter of 3 μm. The extraction liquid was applied as a gradient from 5 to 80 % Acetonitryl in water at a velocity of 0.5 ml per minute.

The permeate stream analysed at 500 nm showed 2 peaks at 12.1 min and 16.5 min (the peak at 1.6 min. is the reference peak of water). At these timepoints no peaks at 600 nm were found (figure 7.5). Thus the peaks refer to red-orange coloured components in the retentate stream. These peaks were also found in the all other three samples (see arrows in the figures 7.3 and 7.4). So the

conclusion is that the orange component had already been present in the sample obtained from the dye manufacturer.

This origin of the orange compound in the dye sample is not clear. The most likely explanation, according to the dye manufacturer, is that a certain (orange coloured) component from which the reactive blue 4 is synthesised, was not completely converted in this synthetisation process. Two other explanations, i.e. the addition of so-called shading colours to the dye formulation and biological degradation during storage seem less likely. Shading colours are added to a dye formulation in very small concentrations in order to obtain the right hue, however the shading colour for reactive blue 4 is .. reactive red 2. Biological degradation occurs at anaerobic conditions (chapter 1) and this is unlikely to occur during storage.

Table 7.4 Spectrofotometrical analyses of the streams from exp 7.1 – 7.8 (hydrolysed reactive blue 4).

exp	permeate flux [lt/m²hr]	Spectral absorbance at 485 nm permeate [m^{-1}]	Retention for colour at 485 nm
7.1	49.3	7.9	0.975
7.2	76.3	8.7	0.948
7.3	48.0	8.6	0.949
7.4	25.3	7.5	0.952
7.5	100.2	4.5	0.976
7.6	77.6	3.1	0.982
7.7	46.9	7.3	0.955
7.8	78.1	5.9	0.961

Table 7.5 Spectrofotometrical analyses of the streams from exp 7.9 – 7.16 (hydrolysed reactive red 2).

exp	permeate flux [lt/m²hr]	Spectral absorbance at 535 nm permeate [m^{-1}]	Retention for colour at 535 nm
7.9	121.6	0.2	0.9999
7.10	51.9	1.1	0.9996
7.11	1.0	13.3	0.9953
7.12	34.7	1.8	0.9992
7.13	134.3	0.7	0.9998
7.14	76.4	1.2	0.9996
7.15	36.9	1.2	0.9995
7.16	50.7	1.2	0.9995

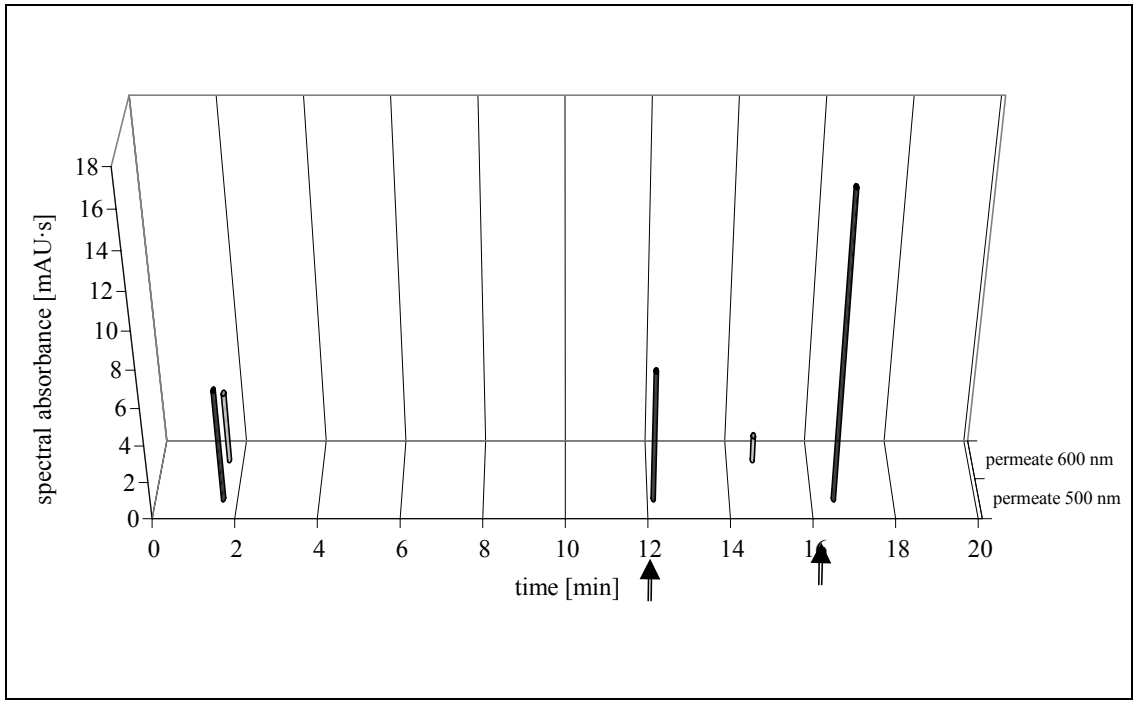

Figure 7.3 Spectral absorbance of permeate at 500 and 600 nm after HPLC extraction.

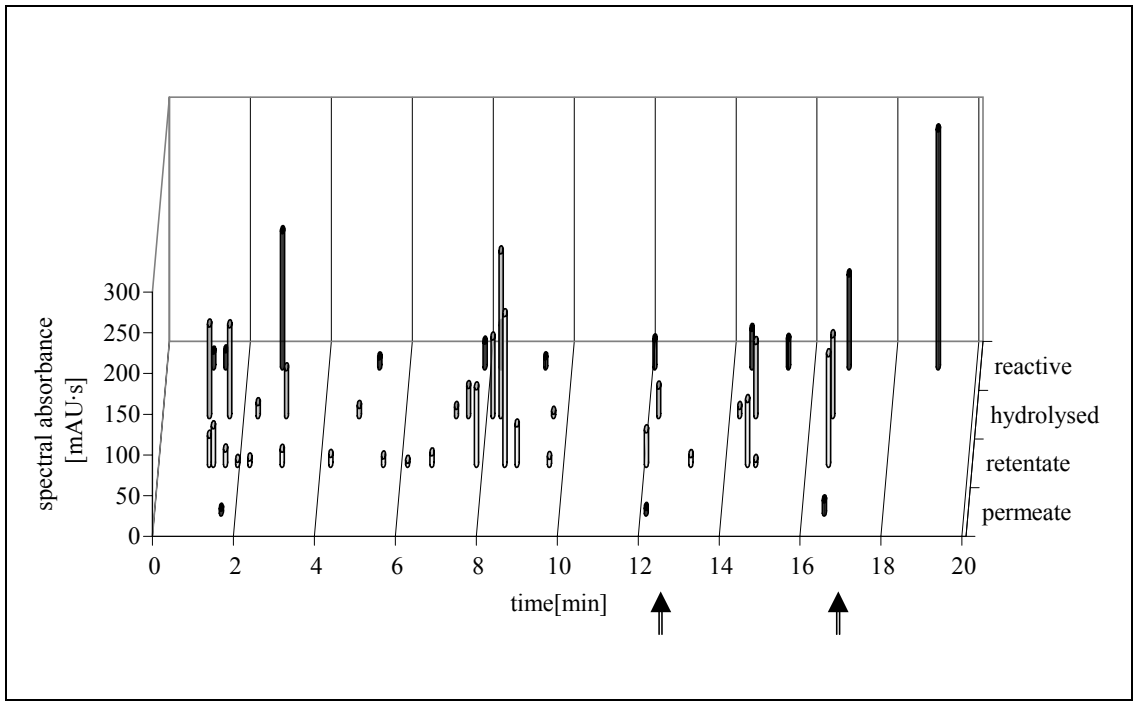

Figure 7.4 Spectral absorbance at 500 nm of all four samples after HPLC extraction. Arrows indicate the red coloured components in the permeate.

7.4 Influence of the combination of Cibapon and Tinofix on membrane fouling

7.4.1 Experimental set-up

Nanofiltration experiments with a mixture of a mono-azo dye (reactive red 2) and an antraquinon dye (reactive blue 4) have been performed on the experimental one-pass set-up installation (Figure 4.2). Subsequently the influence of NaCl, Cibapon, changing pH and Tinofix were investigated. The concentrations of Cibapon and Tinofix were chosen to be respectively 1 g/l and 0.1 g/l. In the RO parametric study it was found that neither of these components caused membrane fouling at these concentrations.

7.4.2 Results and discussion

The main experimental conditions and observations are summarised in table 7.6. The standard test before exp 7.4.A1 resulted in a permeate flux of 85 lt/m^2hr.

Table 7.6 NF parametric study with textile auxiliaries. * RR2 = hydrolysed reactive red 2; RB4 = hydrolysed reactive blue 4.

Exp.	RR2* [g/l]	RB4* [g/l]	NaCl [g/l]	Cibapon [g/l]	Tinofix [g/l]	pH	Permeate flux [lt/m²hr]
7.4.A1	0.75	0.75				6.6	101.1
7.4.A2	0.75	0.75	30			6.9	65.0
7.4.A3	0.75	0.75	30	1		7.0	66.9
7.4.A4	0.75	0.75	30	1		9.1	64.3
7.4.A5	0.75	0.75	30	1	0.1	9.9	16.6

In the experiments 7.4.A1 to 7.4A2 the measured permeate flux is in conformity with the observations in exp 7.1 to 7.16. The addition of NaCl reduces the flux but this can be explained by the increased osmotic pressure difference over the membrane, which is enhanced by the increased influence of the concentration polarisation. Till exp 7.4.A4 the permeate flux remains constant. Addition of a small amount of Tinofix however reduces the permeate flux drastically, within a few minutes. It seems thus that Tinofix, containing a cationic polyelectrolyte, does cause membrane fouling at 0.1 g/l if other anionic auxiliaries or dyes are present. This is strengthen by the fact that it is dissuaded by textile auxiliary manufacturers to contact the fabric with an cationic auxiliary and an anionic auxiliary at the same time as this will give ‘floccery precipitations’, i.e. an unwanted adsorption of colloidal material, on the fabric.

7.5 Conclusions

In this parametric study it was shown that silicates and dodecylsulphate are fouling components for the NF membrane. Fouling of the membrane by SDS is more severe at higher NaCl concentration and lower pH. This is due to a lower electrostatic repulsion between the surfactant molecules themselves leading to aggregation of the surfactant monomers into micelles. This phenomenon will increase the concentration polarisation effect as the diffusivity of the micelles is lower then the diffusivity of the monomers. Moreover the electrostatic repulsion between the surfactant and the membrane is decreased resulting in an enhanced adsorption of the surfactant onto the membrane.

A blue antraquinon dye and a red mono-azo dye have been chosen as modelcompounds as it was experienced in practice that NF membranes have ‘lower retentions for red then for blue colours’. Surprisingly the permeate of the filtration of the red dye solutions was practically colourless

(under the condition that the permeate flux was below 10 lt/m^2hr) while the permeate of the filtration of the blue dye solution was orange-coloured. The reason for this orange compound must be found in the dye manufacturing process as was proven by HPLC. An incomplete conversion of a low molecular mass (orange-coloured) starting component during production of reactive blue 4 seems the most likely explanation.

Membrane filtration of a mixture of hydrolysed reactive dyes and some textile auxiliaries showed that the combination of Cibapon, a washing auxiliary containing an anionic polyelectrolyte, and Tinofix, an after-fixation auxiliary containing a cationic polyelectrolyte give severe membrane fouling.

Acknowledgement

The author wishes to thank Prof. Dr.-ing. T. Melin and L. Eilers of the Institut für Verfahrenstechnik of the RWTH Aachen (Germany) for providing the filtration equipment and working place. T. Paesch is acknowledged for the filtration experiments in this chapter. G. Spalding is acknowledged for the HPLC measurements.

Symbols

$\Delta\Pi_{b.p}$	osmotic pressure difference (retentate-permeate)	bar
R_f	hydraulic permeability fouling layer	m^{-1}
R_m	hydraulic permeability membrane	m^{-1}

Literature

[1] Rard, J.A. and D.G. Miller, The mutual diffusion coefficients of Na_2SO_4-water and $MgSO_4$-water at 25 °C from Rayleigh interferometry. Journal of Solution Chemistry, 8(10): p. 755-766 (1979).

Chapter 8

Reverse osmosis and nanofiltration of anionic and cationic surfactant solutions

Summary

Membrane fouling and adsorption of an anionic (sodium dodecyl suphate, SDS) and a cationic (cetyl trimethylammoniumbromide, CTAB) surfactant was investigated. It was found that membrane fouling by SDS is strongly affected by the pH and the NaCl concentration, corresponding to the experiences in chapter 6 and 7. Increasing the cross-flow velocity will prevent the formation of the fouling layer by SDS to a certain extent but will not remove an already established fouling layer. Membrane fouling by the cationic surfactant CTAB was only observed at concentrations above the critical micelle concentration (cmc) and temperatures below the Krafft-temperature; i.e. when the conditions are such that crystallisation of CTAB will occur. Furthermore it was proven, by zeta potential measurements, that CTAB adsorbs on the nanofiltration membrane surface at concentrations below the cmc and thereby shifts the zeta potential from negative to positive.

8.1 Introduction

In the RO and NF parametric studies it was proven that the anionic surfactant sodium dodecylsulphate (SDS) contributes to membrane fouling considerably. This membrane fouling was strongly influenced by the pH and the NaCl ('background salt') concentration. In the first part of this chapter the following aspects concerning anionic surfactant filtration will be investigated:

- NF of SDS solutions at varying SDS concentration, at two levels of NaCl concentration and at two pH values (7 and 10).
- The influence of the cross-flow velocity on membrane fouling by SDS during NF and RO.

It was expected that cationic surfactants would contribute to membrane fouling as adsorption due to electrostatic attraction is very likely to occur if a membrane is negatively charged. Although both RO and NF membranes were negatively charged at alkaline conditions, no membrane fouling (i.e. flux decline) was observed when filtrating CTAB solutions. In the second part of this chapter the following aspects concerning CTAB will be investigated:

- NF of CTAB solutions at concentrations above the critical micelle concentration and crystallisation concentration at various temperatures.

Furthermore the influence of CTAB and SDS on the electric surface charge will be examined by determining their influence on the zeta potential.

8.2 Nanofiltration of SDS-solutions at various composition of the feed water

Both sets of experiments (i.e. 8.2A and 8.2B) were performed with the one-pass set-up (Figure 4.2). The cross-flow velocity was 1 m/s and the transmembrane pressure was 10 bar. The experimental set 8.2B was performed at high 'back ground-salt' concentration (30 g/l NaCl) and the experimental set 8.2A at low 'back ground-salt' concentration, except for experiments 8.2A-7. The concentration of SDS in the permeate and the retentate for the experiments 8.2A-1 to 8.2A-6 was measured according to the analytical method presented in [2].

8.2.1 Experimental part

The experiments were designed to check the influence of the SDS concentration (3 levels) pH (2 levels, pH adjustments done by addition of HCl and NaOH solutions) and NaCl concentration (2 levels). The initial conditions are summarized in table 8.1.

Table 8.1 Initial conditions SDS filtration experiments.

Experiment	SDS conc [mg/l]	NaCl conc [g/l]	pH
8.2.A-1	10		7
8.2.A-2	10		10
8.2.A-3	100		10
8.2.A-4	100		7
8.2.A-5	1000		7
8.2.A-6	1000		10
8.2.A-7	1000	30	10
8.2.B-0	0	30	7
8.2.B-1	10	30	7
8.2.B-2	10	30	10
8.2.B-3	100	30	10
8.2.B-4	100	30	7
8.2.B-5	1000	30	7
8.2.B-6	1000	30	10

8.2.2 Result and discussion

In all experiments the permeate flux was constant within 30 minutes, except for experiment 8.2A-7 where a flux increase was observed when the filtration was run for more than 16 hours. The reason for this flux increase, which was also observed in exp 7.3, may be explained by a rearrangement of the adsorbed surfactant molecules at the membrane surface. This fact is not fully understood and more research towards this phenomenon is needed.

Table 8.2 Results experiments 8.2A and 8.2 B. * The method to determine the SDS concentration could not be applied at higher NaCl concentrations. ** Not available.

Experiment	pH	Permeate Flux [lt / m^2 hr]	SDS Retentate [mg/l]	SDS Permeate [mg/l]
8.2A-1	6.9	121.2	0.6 (10)	<0.4
8.2A-2	9.7	129.3	1.3 (10)	<0.4
8.2A-3	9.7	119.5	56 (100)	0.5
8.2A-4	6.9	101.1	6.2 (100)	NA**
8.2A-5	7.1	74.9	868 (1000)	146
8.2A-6	9.7	111.0	856 (1000)	169
8.2A-7	9.3	11.7 → 32.5	*	*
8.2B-0	7.0	97.8	*	*
8.2B-1	7.0	103.2	*	*
8.2B-2	9.8	116.3	*	*
8.2B-3	9.6	103.4	*	*
8.2B-4	7.1	83.0	*	*
8.2B-5	7.1	24.3	*	*
8.2B-6	9.8	23.8	*	*

In both experimental sets 8.2A and 8.2 B it was observed that the permeate fluxes at pH 10 were higher than at pH 7, which is in accordance with the theory concerning membrane fouling by SDS presented in chapter 3.

Comparing the experimental set 8.2B to 8.2A, it can be seen that in general a higher NaCl concentration and a higher SDS concentration result in more membrane fouling. The permeate fluxes of all experiments at neutral pH are shown in figure 8.1 as function of the NaCl and the SDS concentration. The critical micelle concentration line [3] is plotted in the

same figure for comparison. It can be seen that the closer the SDS concentration is to the CMC line, the higher the membrane fouling.

The measured SDS concentrations in the retentate of the experimental set 8.2A were in all cases lower than what was solved in the original solutions. Apparently, the total amount of SDS at concentration at or below 100 mg/l was too small to cover the (whole) membrane.

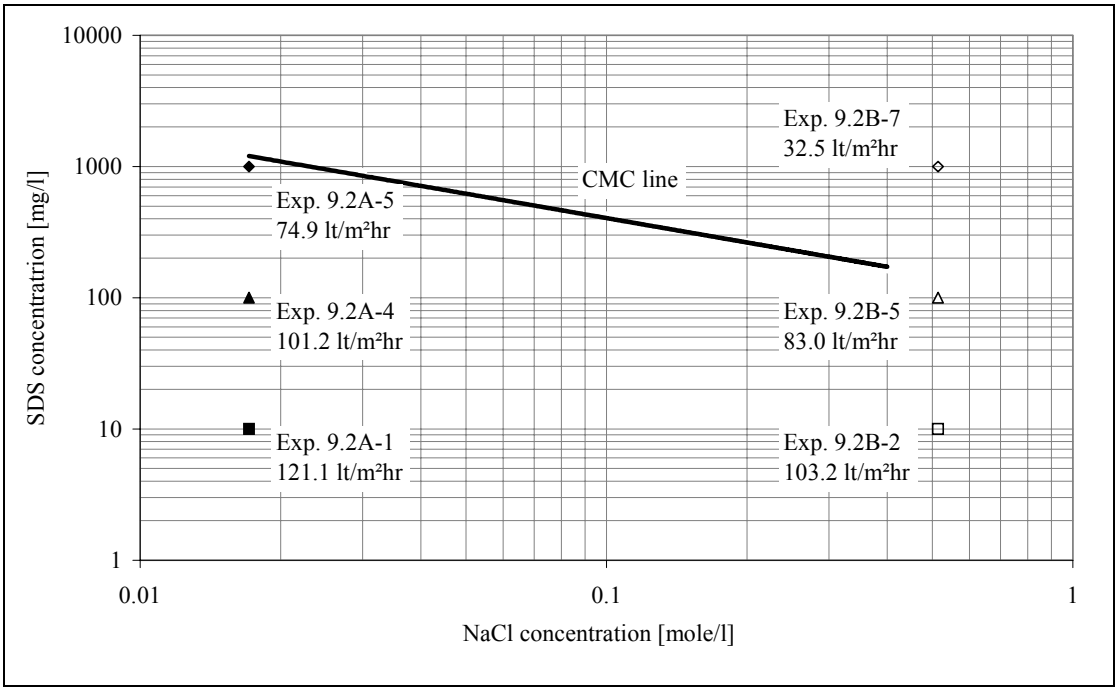

Figure 8.1 Comparison of the experimental results to the critical micelle concentration as function of the NaCl and SDS concentration.

Although a SDS molecule has a higher molecular mass as a SO_4^{2-}ion (283 g/mole to 96 g/mole) its retention by the NF membrane is surprisingly lower (80 % at 1 g/l SDS compared to 95 % for the sulphate ion). The reason for this can be the higher electrostatic repulsion by the negatively charged membrane of the more negative (two-charged) sulphate ion, which is completely deprotonated at pH > 6, compared to the (one charged) SDS-ion.

8.3 Influence of the cross-flow velocity on the membrane fouling by SDS

8.3.1 Experimental part

RO and NF filtration experiments have been executed with a 0.3 g/l SDS solution, i.e. the same as in the experiments of chapter 6 and 7, at varying cross-flow velocities. No other components were added! The main aim was to check if a membrane fouled by SDS could be cleaned with hydrodynamic methods. The feed-bleed set-up (figure 4.1) equipped with a RO and a NF membrane was used. The transmembrane pressure was set at 20 bar. The cross-flow velocity was altered from high (4 m/s) to low (0.5 m/s) and back to 4 m/s. Every experiment lasted at least 5 hours. At the end of each experiment the filtration installation was depressurised and stayed over one night without removing the SDS solution. Subsequently the next experiment was executed. An exception of this procedure was made between experiments 4 and 5 where the filtration installation had been stayed for 3 days in stead of one night (also without removing the SDS solution).

8.3.2 Results and discussion

The results of both membranes have been summarised in table 8.3. The pH was 5.5 and remained constant during the experiments.

Table 8.3 RO and NF filtration of a SDS solution at varying cross-flow velocities.

Exp.	C_{SDS} [g/l]	cross-flow velocity [m/s]	Permeate flux RO [lt/m^{2}hr]	Permeate flux NF [lt/m^{2}hr]
8.3.1	0.3	4	0.93	48.3
8.3.2	0.3	2	0.84	45.0
8.3.3	0.3	1	0.84	41.6
8.3.4	0.3	0.5	0.71	34.5
8.3.5	0.3	1	0.61	25.1
8.3.6	0.3	2	0.60	26.0
8.3.7	0.3	4	0.56	26.1

Figure 8.2 and 8.3 show the permeate flux as function of the cross-flow velocity. For both membranes the same pattern is observed. The permeate flux decreases when going from high to low cross-flow velocity. When going from low to high cross-flow velocity the permeate flux does not change. It can be concluded that the cross-flow velocity does prevent membrane fouling by SDS to a certain extent, but if the membrane is fouled by SDS, increasing the cross-flow velocity will not clean the membrane and will not restore the permeate flux.

The drop of the permeate flux between experiment 4 and 5 is larger than what would be expected. The reason for this is probably the fact that the filtration equipment was not running for three days in stead of 1 night.

It is also observed that the relative membrane fouling of the NF membrane is considerably lower than that of the RO membrane. The reason for this is that the RO membrane surface is positively charged at a pH of 5.5, as the NF membrane is still negatively charged (chapter 4.7). Thus adsorption of SDS on the RO membrane will be larger than on the NF membrane as explained in chapter 3.3.

The permeate flux of the NF experiment at 1 m/s is considerably lower than the permeate fluxes in experiment 8.2A5 and 8.2A6 of the preceding paragraph, although the SDS

concentration in the latter experiments was higher. The reason for this must be that exp 8.3.3 has been performed at lower pH (5.5 in stead of 7 and 10).

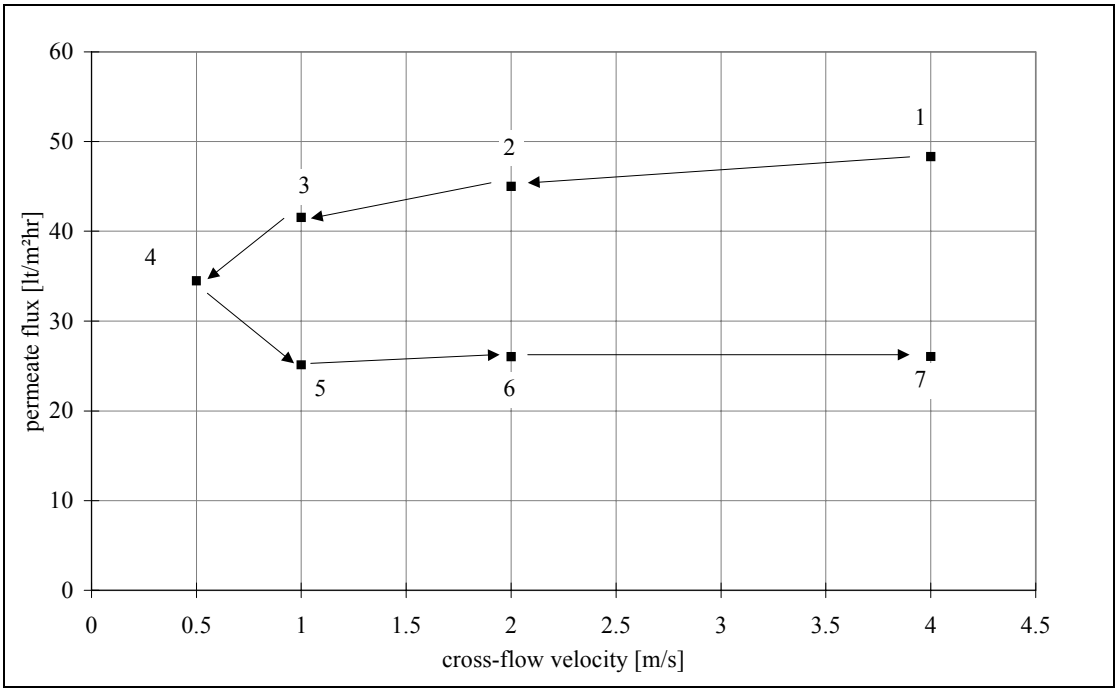

Figure 8.2 Nanofiltration with 0.3 g/l SDS solutions at 20 bar.

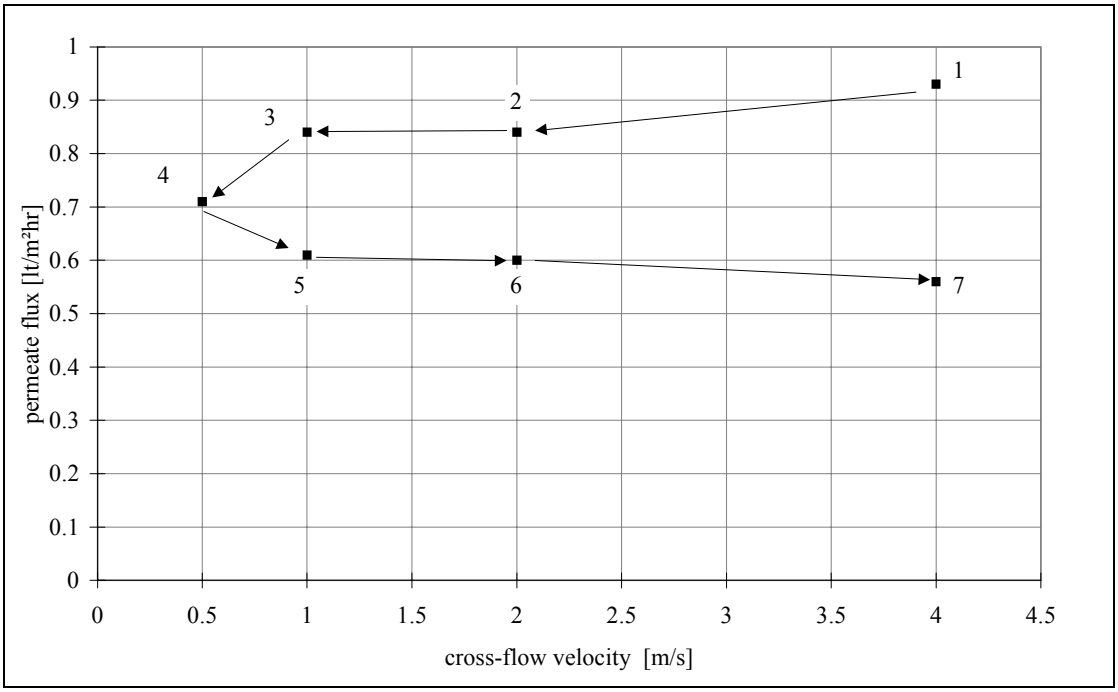

Figure 8.3 Reverse osmosis on 0.3 g/l SDS solution at 20 bar.

8.4 Nanofiltration of a CTAB solution above the cmc

8.4.1 Experimental design

Solutions of CTAB at a concentration of 1 g/l, which is higher than its critical micelle concentration (i.e. 0.34 g/l), were filtrated by NF in the experimental feed-bleed set-up (figure 4.1). The experiments were executed at varying temperatures between 20 – 30 °C. The transmembrane pressure was 20 bar and the cross-flow velocity 2 m/s. No extra additives were added.

8.4.2 Results and discussion

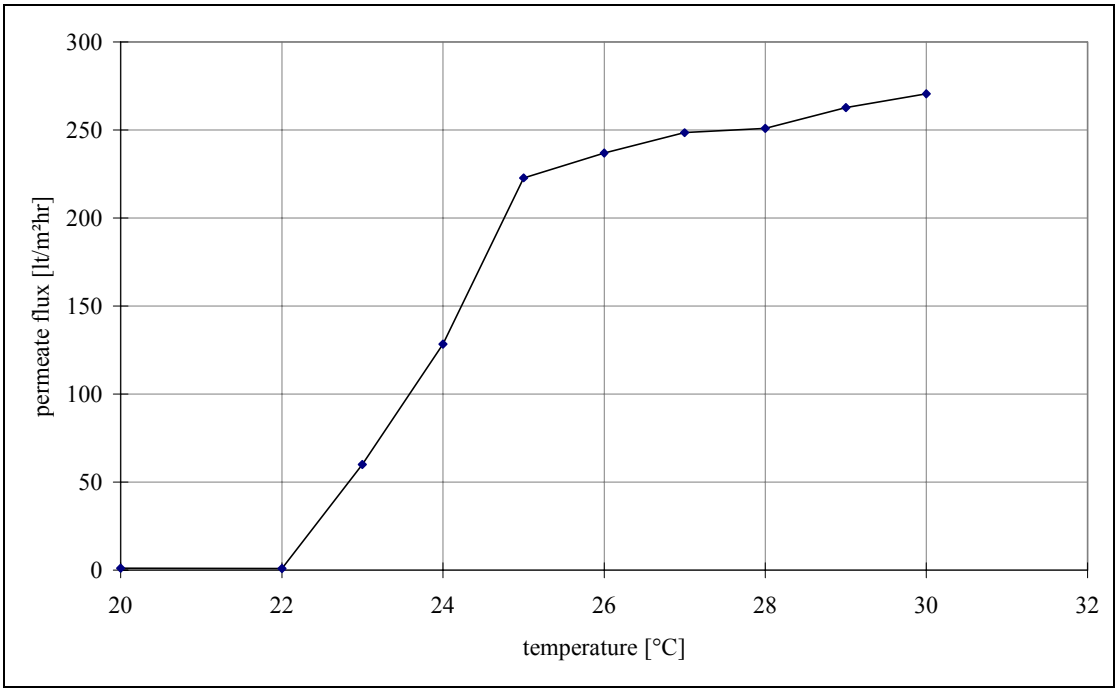

Figure 8.4 Nanofiltration of a 1 g/l CTAB-solution at varying temperatures.

Figure 8.4 shows the influence of the temperature on the permeate flux during the nanofiltration of the 1 g/l CTAB solution. The experiments, shown in the graph, were done from low to high temperature. Afterwards duplicate experiments were performed at 24 °C and 20°C yielding the same results as the first experiment. Below a temperature of 22 °C, the permeate flux is about 1 lt/m^{2}hr. Above this temperature the permeate flux is increased tremendously. The explanation for this phenomenon is that below 23 °C the insoluble CTAB monomers at 1 g/l do not form micelles in solution but do form (insoluble) crystal aggregates (figure 8.5) which will be deposited onto the membrane during filtration leading to a flux decline. This is very common for surfactant solutions containing ionic monomers and the 'solubility' temperature is often referred to as 'Krafft-temperature' [4, 5].

The permeate flux increase with temperature at temperatures above the Krafft-temperature can be explained by the decreasing solution viscosity with temperature (eq. 3.6).

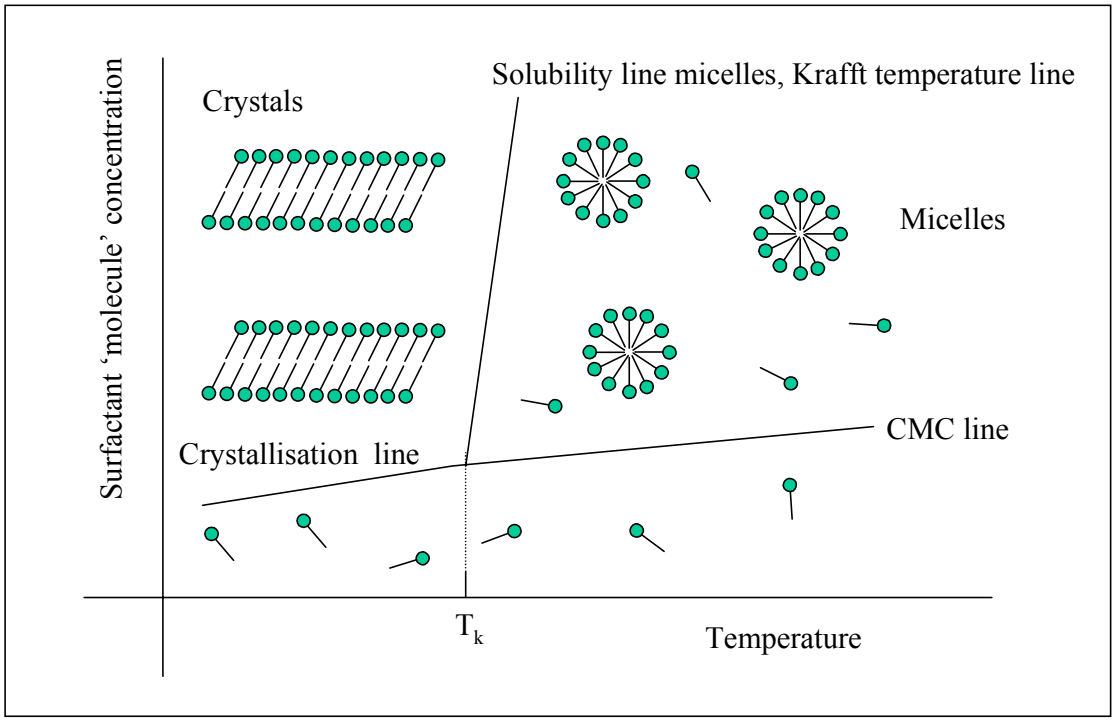

Figure 8.5 Phase diagram of a ionic surfactant solution (e.g. CTAB).

8.5 Zeta potential measurements with CTAB and SDS

8.5.1 Introduction and experimental set-up

In order to explain the influence of anionic and cationic auxiliaries and surfactants on membrane fouling the adsorption of the modelcomponents, SDS and CTAB, on a nanofiltration membrane was determined. This was done by determining the zeta potential, according to the streaming potential method presented in chapter 4.6. Two membrane slides (A and B) were used; slide A for SDS adsorption, slide B for CTAB adsorption. The zeta potential was first measured with a 10^{-3} M NaCl solution, in order to check if the membrane slides are comparable to the ones used in chapter 4.6. Subsequently three concentration levels of each surfactant in the NaCl solution were examined.

8.5.2 Results and discussion

In table 8.5 the measured zeta potentials for three SDS concentrations and three CTAB concentrations in a 10^{-3} M NaCl solution are shown.

Table 8.5 Determination of the zeta potential of a NF membrane with CTAB and SDS in NaCl-solutions.

mem. slide	NaCl [M]	SDS [g/l]	CTAB [g/l]	pH	conductivity [µS/cm]	zeta potential [mV]
A	10^{-3}	0.0		7.6	1249	-30.0
A	10^{-3}	0.3		8.0	1329	-37.7
A	10^{-3}	2.0		7.7	1587	-38.7
A	10^{-3}	5.0		6.3	1981	-42.5
B	10^{-3}		0.0	8.6	1269	-29.5
B	10^{-3}		0.1	6.4	1298	46.7
B	10^{-3}		0.3	6.1	1317	39.2
B	10^{-3}		3.0	6.1	1321	35.6

The zeta potential of the membranes determined with the NaCl solutions without addition of any surfactant are in good agreement with the ones measured in chapter 4.6. It was shown that both surfactants alter the zeta potential of the membrane by adsorption. The anionic surfactant SDS makes the membrane more negatively charged. The cationic surfactant, CTAB changes the membrane surface charge from negative to positive.

8.6 General discussion and conclusions

Membrane fouling by cationic and anionic textile auxiliaries and surfactants has been investigated with components present -or representative for components present- in the textile wastewater. The theory of the electrostatic and electrodynamic contributions to surfactant adsorption on the membrane, as presented in chapter 3, was confirmed by membrane filtration of SDS solutions at varying SDS concentration, varying NaCl concentration and varying pH. An increase of the SDS concentration, an increase of the NaCl concentration and a decrease of the pH from alkaline to neutral conditions does increase the (NF) membrane fouling by SDS, even at concentrations far below the critical micelle concentration. Furthermore adsorption of SDS on the membrane was confirmed by measuring a decrease of the (negative) zeta potential.

It was shown by a RO and NF filtration at the same conditions (e.g. neutral pH) that the relative flux decline of RO is larger than for NF, which is in accordance with the fact that at neutral pH the RO membrane has it‘s iso-electric point while the NF membrane is still negatively charged. If the membrane is fouled by SDS, it can easily be cleaned with an alkaline cleaning but not by increasing the cross-flow velocity. The cross-flow velocity only has an effect of preventing some membrane fouling by SDS, but already fouled membranes can not be cleaned by increasing the cross-flow velocity.

Membrane fouling by the cationic surfactant CTAB was only determined at concentrations above the crystallisation concentration and temperatures below the Krafft-temperature. This means that membrane fouling by CTAB occurs if the conditions are thus that crystallisation of CTAB in solution is likely to occur.

Adsorption of CTAB on the NF membrane occurs already at concentrations below the critical micelle concentration. Although this does not lead to substantial membrane fouling (i.e. flux decline) by CTAB itself, this adsorption can still ‘initialize’ membrane fouling by anionic polymers or surfactants as the membrane charge is altered from negative to positive. This may explain why the combination of Tinofix and Cibapon (chapter 7.4) causes membrane fouling. The cationic component alters the membrane surface charge and the anionic component will adsorb onto the membrane.

Acknowledgement

P. Nieland (8.3 and 8.4), T. Paesch (8.2) and B. Quirke (8.5) are acknowledged for their experimental work.

Literature

[1] Braun, G., Janitza, J., Kyburz, M. Abwasserreinigung und recycling in der Textilindustrie, Colloquium Produktionsintegrierter Umweltschutz „ Abwaesser der Textilindustrie / Wollverarbeitung und Nahrungsmittelindustrie, (pag. B13-B30), Bremen, 15-17 Sep. (1997).
[2] Deutsche Einheitsverfahren zur Wasser-, Abwasser-, und Schlamm-Untersuchung, 39. Lieferung, Wiley-VCH Beuth (1997).
[3] Williams, R.J., J.N. Phillips, and K.J. Mysels, The critical micelle concentration of sodium lauryl sulphate at 25 °C. Trans. Farad. Soc., 51: p. 728-737. (1955).
[4] Atkins, P.W., Physical Chemistry 4th edition, Oxford University Press p: 708 (1990).
[5] Brasser, P.J., Recycling of surfactants from wastewater of laundry washing plants. Thesis University of Delft (1998).

Chapter 9

Economic optimisation of a membrane filtration installation for the treatment of wastewater from reactive dyeing and subsequent washing processes

Summary

Nanofiltration on synthetic and actual textile wastewater with various compositions has been executed. Experimental data of permeate fluxes, at varying cross-flow velocities and varying transmembrane pressures make up the input of an economic model. With this model the optimal process operation conditions can be determined giving the lowest cost price per volume of produced fresh water. From the economic analysis of the NF filtration of synthetic wastewater it can be concluded that the operation time per year of the installation, the feed flow and the concentration have a tremendous influence on the permeate cost price. The influence of the cross-flow velocity is also apparent as the transmembrane pressure has only a minor effect. The cost price is very dependent on the achieved permeate flux. Filtration of actual textile wastewater showed that in practice the prices would be much higher, as a consequence of the relative low permeate fluxes.

9.1 Introduction

The objective of this study is to give a design and operation method for the nanofiltration installation in such a manner that the lowest price per m^3 permeate is reached. A higher cross-flow velocity (CF) or transmembrane pressure (TMP) will result in higher operation costs as more energy is needed but will result in lower investment costs as, due to a higher permeate flux at these conditions, less membrane area has to be installed.

The membrane system considered here is of a feed/bleed type with one recycle loop (figure 9.1). The feedstream is pressurised by the feedpump to achieve the necessary transmembrane pressure and directed into the circulation unit. The circulation pump maintains the cross-flow velocity.

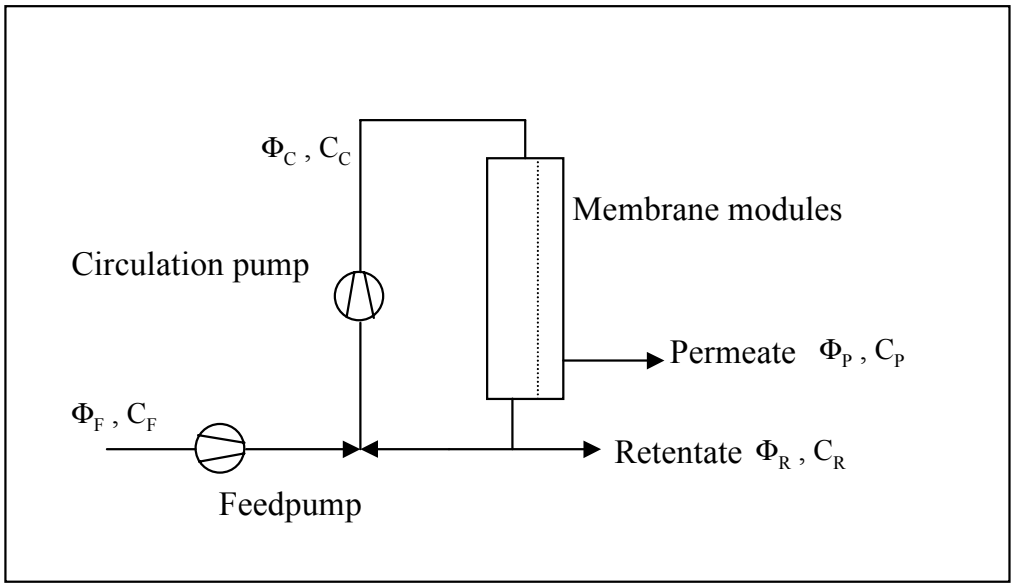

Figure 9.1 Membrane filtration system with one recycle loop.

Next to transmembrane pressure and cross-flow velocity, the following parameters, which influence the economics of the membrane process, will be considered in this study:

- the feed flow
- composition of feed
- the operation time per year

Two sizes of textile dyeing processes have been chosen producing respectively a total waste volume of 6000 and 30000 m^3/year. The dyeing and subsequent washing processes are batch processes. Only during 2000 hours per year this wastewater is produced. The nanofiltration process may then also be operated batch like for 2000 hours per year. However it can become more (economically) attractive to collect the feed for the membrane process in a storage tank and operate the membrane process continuously. Therefore two operation times have been chosen: 2000 and 8000 hours per year. So four cases are considered here (table 9.1). For all cases the volume concentration factor (the feed stream divided by the retentate stream) is set to 10.

Table 9.1 Schematic outline of the four cases.

Case	Waste volume [$10^3 m^3$/year]	Operation time [hours/year]	Feed stream [m^3/hr]	Permeate stream [m^3/hr]
1	6	2000	3.00	2.70
2	30	2000	15.00	13.50
3	6	8000	0.75	0.68
4	30	8000	3.75	3.38

Three concentration levels will be considered here (table 9.2). The concentration of NaCl in the retentate is the same as in the feed as NaCl is assumed not to be rejected by the NF-membrane.

Table 9.2 Compositions of the synthetic wastewater examined in this study.

Composition	Feed	Retentate Circulation system
CL1	Dye: 0.1 g/l no (extra addition of) NaCl	Dye: 1 g/l no (extra addition of) NaCl
CL2	Dye: 0.1 g/l NaCl: 30 g/l	Dye: 1 g/l NaCl: 30 g/l
CL3	Dye: 0.25 g/l NaCl: 30 g/l	Dye: 2.5 g/l NaCl: 30 g/l

Experiments at the concentration levels in the circulation system will be carried out to determine the flux and separation characteristics of the membrane at different transmembrane pressures and cross-flow velocities.

At the end the economic calculations will be applied to experiments with actual textile wastewater.

9.2 Economic optimisation method

In an economic optimisation method the total costs are distinguished in investment costs and operational costs. The mean price per cubic meter permeate during the total operation time is then determined by the (mean) costs per year divided by the (mean) volume of permeate per year (V_{tot}).

The investment and operation costs considered in this study are summarised in table 9.3 and table 9.4.

Table 9.3 Investment costs considered in this study

Investment costs (I)	included in this study as function of:
Pumps	power consumption
Electric engine for pumps	power consumption
Membranes	membrane area
Membrane modules	membrane area
Measuring and control devices	fixed amount
Construction material , installation, piping	investment for other hardware (Lang factor)
Extra storage tanks for feed and permeate	volume

Table 9.4 Operational costs considered in this study

Operational costs (O)	included in this study as function of:
Electric power consumption pumps	feed flow and required pressure increase
Personnel operation and maintenance	total investment costs
Membrane replacement costs	membrane area

The mean cost per year can be calculated with the method to calculate the total cost of ownership (TCO) per year. The yearly costs of the investments remain constant during the running time of the installation, by introduction of the annuity (α).

$$TCO = \alpha \cdot \sum I + \sum O \qquad (9.1)$$

α is the annuity factor that corrects for the time dependence of money. α is a function of the interest rate (i) and the depreciation time (ny).

$$\alpha = \frac{i \cdot (1+i)^{ny}}{(1+i)^{ny} - 1} \qquad (9.2)$$

In this case the interest rate is taken to be 10 % / y (i = 0.1) and the depreciation time 10 years, which results in α = 0.163 / y

The cost per cubic meter permeate (CP) is then calculated by:

$$CP = \frac{\alpha \cdot \sum I + \sum O}{V_{tot}} \qquad (9.3)$$

Equation 9.3 is the target function to be minimised. Data to fill in this target function will be extracted from literature and experiments described in this chapter. It turned out that, given a special case (i.e. operation time per year, feed flow, concentration level), the permeate cost

can be written down as a function of only the transmembrane pressure and cross-flow velocity. At a given value for the transmembrane pressure and the cross-flow velocity, the permeate flux, membrane area and power consumption can be calculated.

9.2.1 Investment costs

Both pumps (figure 9.1) are considered to be centrifugal pumps. The investment cost for a centrifugal pump can generally be related to its power consumption [1]. Figure 9.2 shows the pump investment costs as function of the power consumption on a log-log scale. The pumpmaterial is AISI 316. The following equation was derived with PC in Watt.

$$\log(I_{pump}). = 0.2781 \cdot \log(PC) + 3.1926 \qquad (9.4)$$

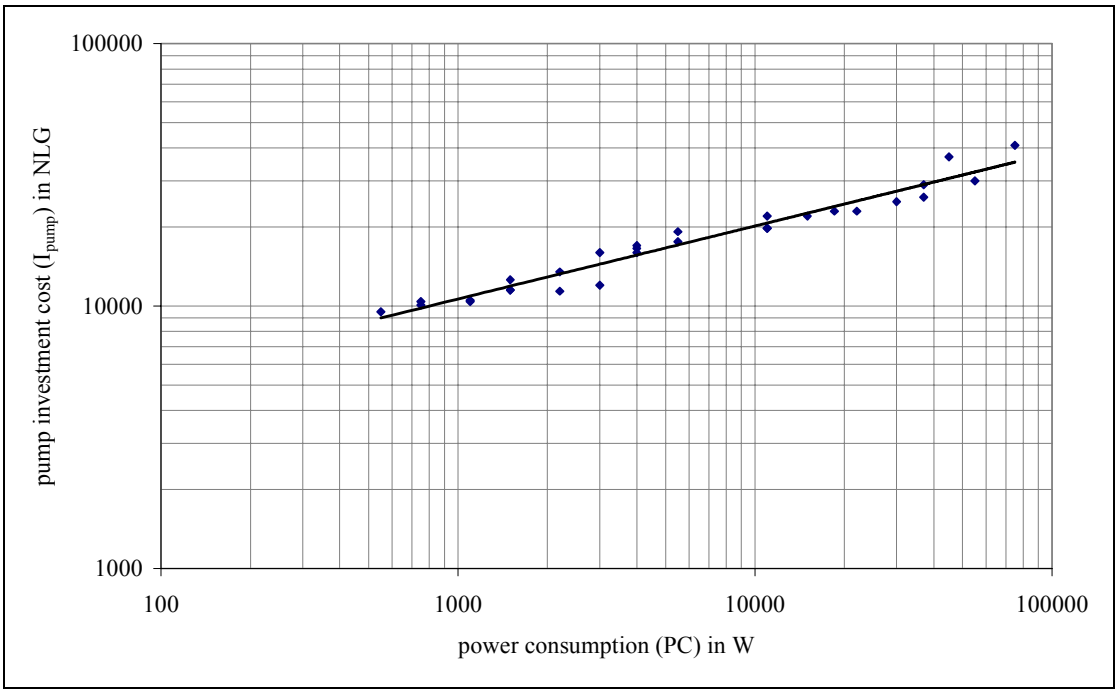

Figure 9.2 Centrifugal pump investment costs as function of its power consumption. Data from [1], 1997.

The data for the cost of the pumps does not include the costs for the electric engine. For the electric engine the following relationship as function of the power consumption is derived [1], with PC in Watt.

$$I_{electric\_engine} = 0.1395 \cdot PC + 299 \qquad (9.5)$$

The price for the membrane modules is 500 NLG/m^2 membrane and the price for the membranes is 500 NLG/m^2. For the modules (without membranes) the same depreciation time is taken as for the rest of the installation. The membranes however should be replaced every two years. These additional costs are included in the operational costs (section 9.2).

The cost for measuring and control equipment for this type of installation is set on 10.000 NLG.

When the installation is run continuously during the whole year (8000 hr/y) an extra storage tank is necessary to collect the feed stream before treatment. The investment cost for this storage tank (range 1-100 m^3) is a function of its volume [1]:

$$I_{ST} = 626.6 \cdot V_{ST} + 8876 \qquad (9.6)$$

The installation is included in this price. The total production of 6 hours of operation should be stored in the tank. For case 3 the volume of the tank is 18 m^3 and for case 4 90 m^3.

For the investment of other equipment and construction of the installation the sum of the (other) investment costs is multiplied by a factor of 1.3 for membrane installations.

9.2.2 Operational costs

The cost for operation of the membrane filtration equipment includes:

- Electrical energy costs of the pumps which is 0.22 NLG/kWh.
- Personnel operation and maintenance (cleaning of membranes) which is set on 5 percent of the total annual investment costs.
- Membrane replacement costs. The average membrane lifetime is set on 2 years.

9.2.3 Power consumption of pump

The power consumption of a pump is the product of the flow and the required head (i.e. pressure loss). If for a membrane separation process the feedflow and the operating pressure are given, the power consumption of the feed pump can be calculated.

$$PC = \Phi \cdot \Delta P \qquad (9.7)$$

For the circulation pump the required flow and head is determined whether the membrane modules are placed parallel or serial (figure 9.3) in the installation. A short-cut method can be applied to relate the power consumption to the installed membrane area. This short cut method is presented here for tubular membranes

$$\Delta P_c = 4 \cdot f \cdot \frac{L}{d_h} \cdot \frac{\rho \cdot v^2}{2} \qquad (9.8)$$

$$\Phi_c = n \cdot \frac{\pi}{4} \cdot d_h^2 \cdot v \qquad (9.9)$$

The equations are now arranged that the power consumption is only a function of the membrane area, de tube diameter and the cross-flow velocity by substitution of:

$$L = \frac{A_m}{n \cdot \pi \cdot d_h} \qquad (9.10)$$

$$PC = f \cdot A_m \cdot \frac{\rho \cdot v^3}{2} \qquad (9.11)$$

For turbulent flow the relation of Blasius [2] is used for the friction factor:

$$f = \frac{0.0792}{Re^{0.25}} = \frac{0.0792 \cdot \nu^{0.25}}{d_h^{0.25} \cdot v^{0.25}} \qquad (9.12)$$

For an aqueous system the power consumption is then:

$$PC = \frac{0.0792 \cdot \nu^{0.25}}{d_h^{0.25}} \cdot A_m \cdot \frac{\rho \cdot v^{2.75}}{2} \cong 1.252 \cdot \frac{A_m \cdot v^{2.75}}{d_h^{0.25}} \qquad (9.13)$$

The actual power consumption is not only determined by the pressure drop over the membrane modules but also by the pump efficiency (60 %) and by the pressure drop caused by the rest of the circulation unit (20% of the pressure drop over the membrane modules).

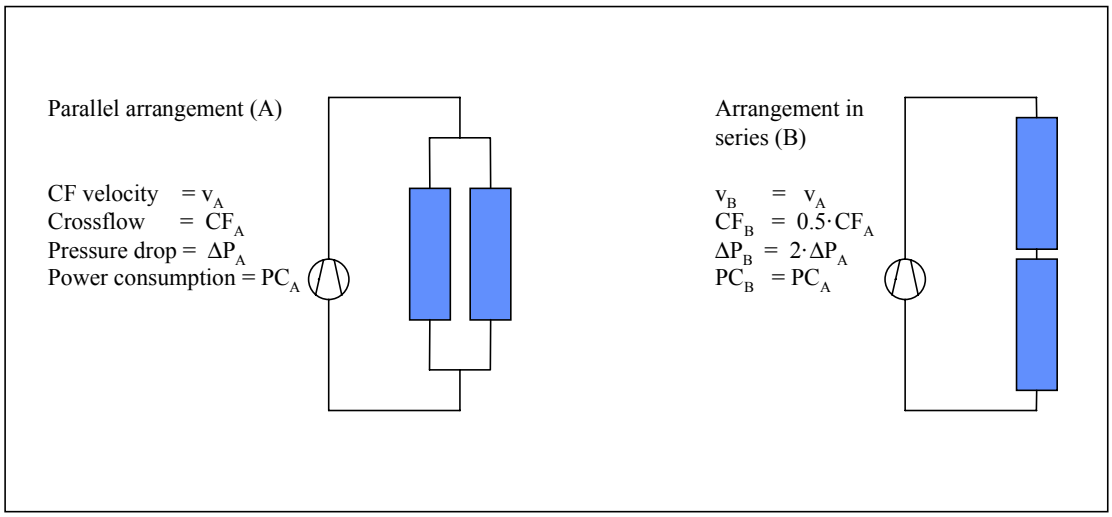

Figure 9.3 Arrangement of membrane(-module)s in the installation at the same cross flow velocity.

The power consumption is independent of the configuration of the membrane modules (parallel or serial), under the assumption that the decrease in transmembrane pressure and cross-flow velocity is not considerable. Therefore it seems that the parallel arrangement with modules which are kept 'as short as possible' is the best choice. However practical reasons are more decisive which design should be chosen.

1. The availability of a suitable circulation pump. A parallel arrangement of membrane modules means that the pump should have a big volume stream combined with a low pressure drop. In practice, a pump with a lower volume stream but a higher pressure drop might be preferable for technical and economic reasons leading to an arrangement of the modules in series.

2. The appearance of the membrane modules. In practice only standard modules are used with a given length and number of tubes, thus a fixed membrane area. In the final design more membrane area as calculated to be necessary will thus be installed.

So in every case the reasons mentioned above, together with limitations for a allowable drop in pressure drop or a drop in the cross-flow velocity, will result in a particular design for that case. It is beyond the scope of this study to go into this in detail as this study is only meant to give a estimation of the (optimal) permeate price as function of the process parameters using the short cut method presented in this chapter.

9.3 Membrane filtration performance

The membrane filtration performance is measured as
- (constant) permeate flux
- retention for dye component and 'colour' content permeate

These issues are measured as function of varying parameters:
- transmembrane pressure
- cross-flow velocity
- composition feed stream

The permeate flux is the main issue which is the input for the economic analysis. The colour measurements were done in order to decide if the permeate can be reused /discharged. The expected permeate flux as function of transmembrane pressure and cross-flow velocity is showed in figure 9.4.

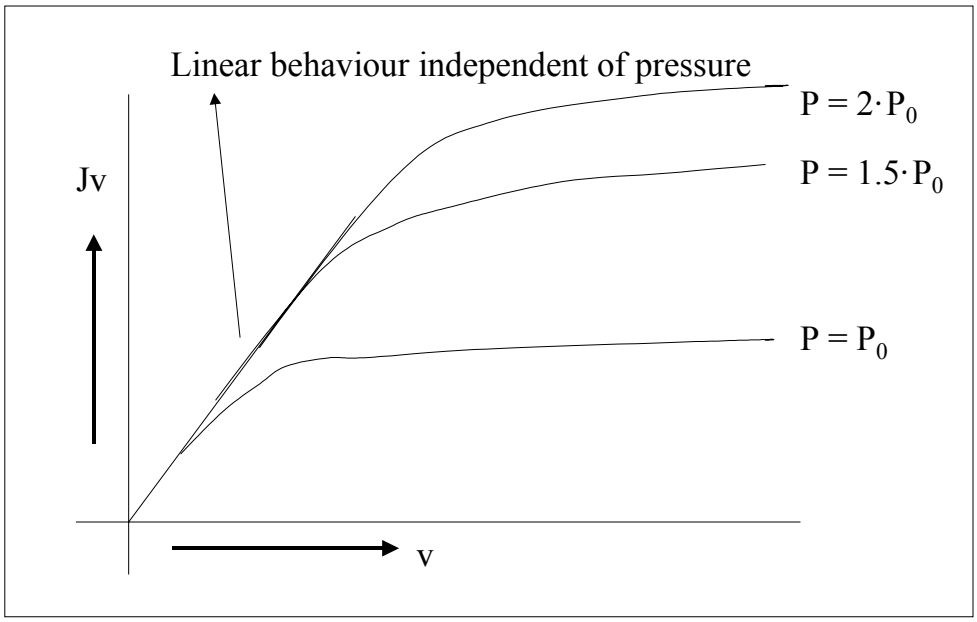

Figure 9.4 Expected permeate flux as function of cross-flow velocity (v) and transmembrane pressure (ΔP)

There are a few theoretical models available to describe the permeate flux as function of the transmembrane pressure and cross-flow velocity. The two most common are the osmotic pressure model and the gel layer model. The gellayer model (derived from the concentration polarisation model) describes the permeate flux in the region where it is independent of the transmembrane pressure:

$$Jv = k \cdot \ln \frac{C_g}{C_b} = a \cdot v^{0.8} \cdot \ln \frac{C_g}{C_b} \qquad (9.14)$$

This model is not used here because of:

- The gel concentration of the component system should be determined which needs a considerable amount of experiments at different concentration levels of all components, including thus varying salt concentration and pH.
- In situations were the flux is not independent of the transmembrane pressure at the concentrations used the gellayer is not applicable.

In the osmotic pressure model, the concentration polarisation model together with the hydrodynamic permeability description for the permeate flux is combined with a description of the osmotic pressure as function of the concentration.

$$Jv = A \cdot \Delta P - A \cdot f(\Delta C_{i,p}) = A \cdot \Delta P - A \cdot f(\Delta C_{b,p} \cdot \exp\left[\frac{Jv}{k}\right]) \qquad (9.15)$$

In which the function f describes the osmotic pressure difference as function of the concentration difference. Note that this is also described in chapter 3.2.2 where the Van 't Hoff law is substituted in the osmotic pressure function.

Although this description gives the permeate flux as function of all the parameters considered, it is not used in this study because of:

- The permeate flux is not a straightforward function. The solution of eq 9.15 can only be calculated by numerical iteration.
- It was observed that the OPM predicts the influence of the transmembrane pressure on the permeate flux inaccurately. i.e. at an increasing transmembrane pressure leading the permeate flux is often overestimated due to a formation of a (reversible) fouling layer combined with an increasing compaction of this fouling layer with increasing transmembrane pressure.

The best input for the economic analysis is thus fitting the measured permeate flux as function of the cross-flow velocity and transmembrane pressure. Equation 9.16 led to a satisfying description for the CL 1 and CL2 experiments.

$$Jv = a1 + \frac{a2}{TMP} + \frac{a3}{v^{a5}} + \frac{a4}{(TMP * v)} \qquad (9.16)$$

For the CL3 experiment no general fitfunction could be found and the measured permeate flux for a given transmembrane pressure was fitted only as function of the cross-flow velocity. The calculations for the fitting procedures and the economic analysis data were performed using computer program Maple V release 4.00A. Finally the total membrane area can be calculated.

$$A_m = \frac{\Phi_p}{Jv} \qquad (9.17)$$

9.4 Results and discussion permeate flux

For concentration level one (CL1) the experiments at varying transmembrane pressures and varying cross-flow velocities were randomly performed. Before these experiments a filtration with the wastewater at 30 bar and 0.25 m/s was executed to 'pre-foul' the membranes in order to avoid severe flux decline during the experiments. This approach worked very well and the results of this experimental set are shown in figure 9.5.

At concentration level two (CL2, 1 g/l reactive red 2 and 30 g/l NaCl) the permeate flux at TMP 30 bar and CF 0.25 m/s was very low (~ 5 lt./m²hr). Raising the pH above 8 turned out to be a good solution to obtain higher fluxes. The same procedure as in the experiments with CL1 was followed. Results are shown in figure 9.6.

For the case of concentration level three (CL3, 2.5 g/l reactive red 2 and 30 g/l NaCl) the constriction of no severe flux decline in time was not satisfied, despite the fact that the pH was raised above 8. As a consequence of the problems in experiments CL3, it was decided to perform the experiments not in random order but to go from high to low cross-flow velocity and from low to high pressure within the same cross-flow velocity. Thus to execute the experiments where the highest flux decline was expected at the end. It was decided to take the permeate fluxes after three hours, as the permeate fluxes did not reach a constant value within the time of an experiment. Results are shown in figure 9.7.

The results of experiments CL1 and CL2 have been fitted to equation 9.16. (table 9.5).

Table 9.5 Flux parameters components system CL1 and CL2

	CL 1	CL 2
a1	219.9	191.6
a2	-1315	-639.9
a3	-35.42	-80.50
a4	270.0	141.6
a5	1	0.5

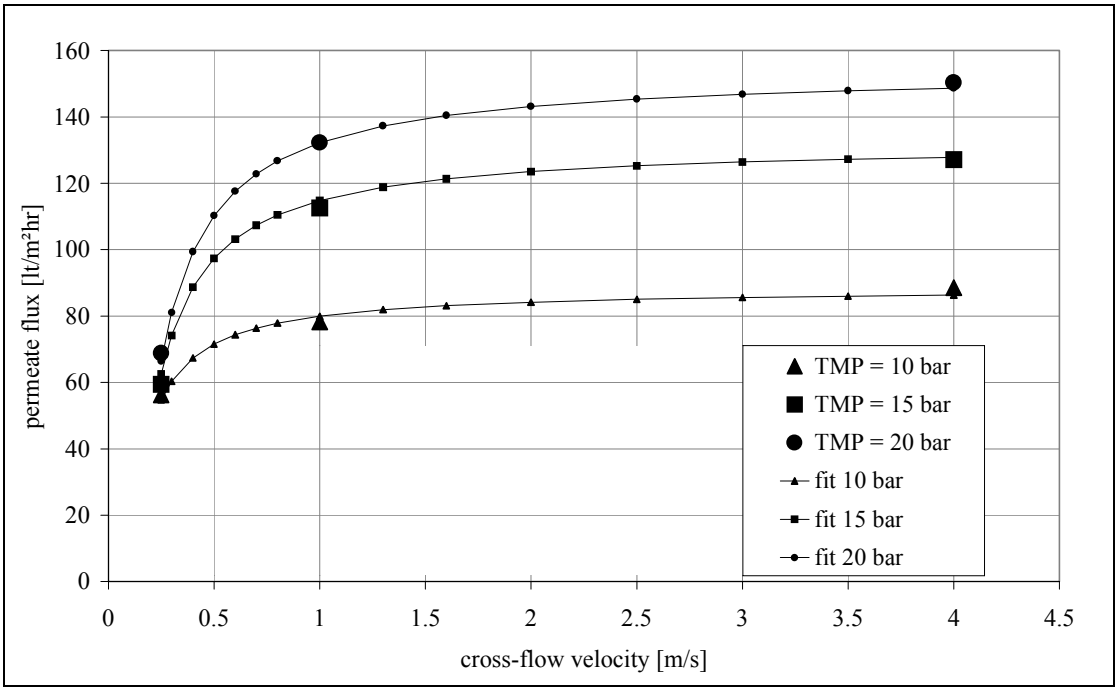

Figure 9.5 Experimental data with synthetic wastewater containing 1 g/l reactive red 2 (CL1) pH ~ 7.

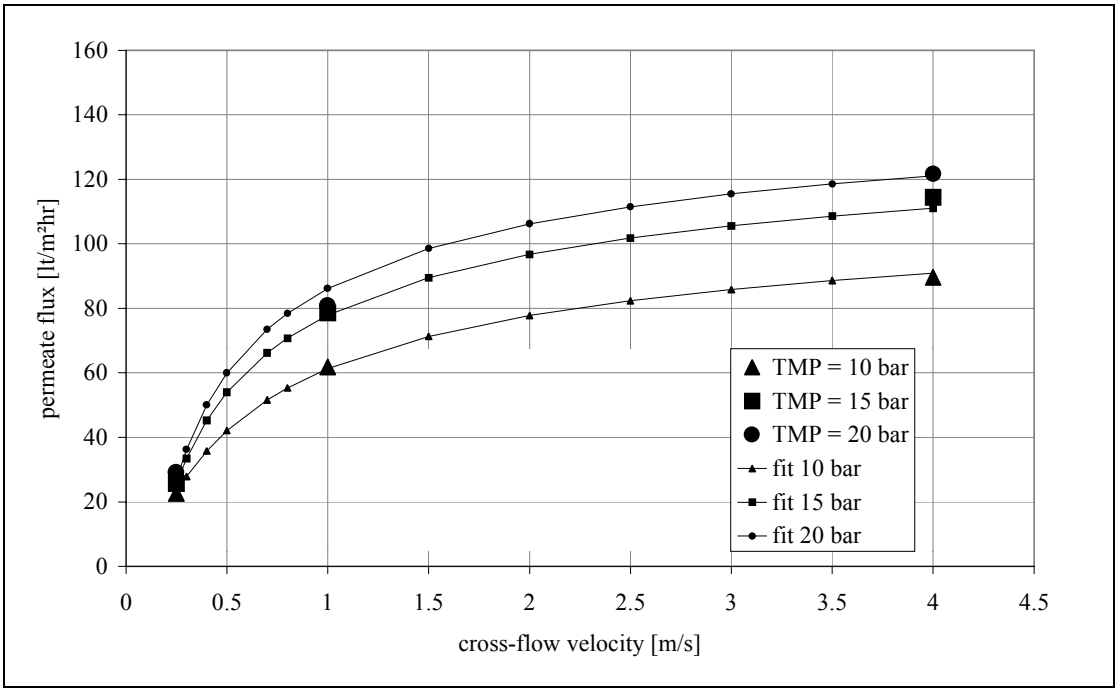

Figure 9.6 Experimental data with synthetic wastewater containing 1 g/l reactive red 2 and 30 g/l NaCl (CL2) pH ~8-9

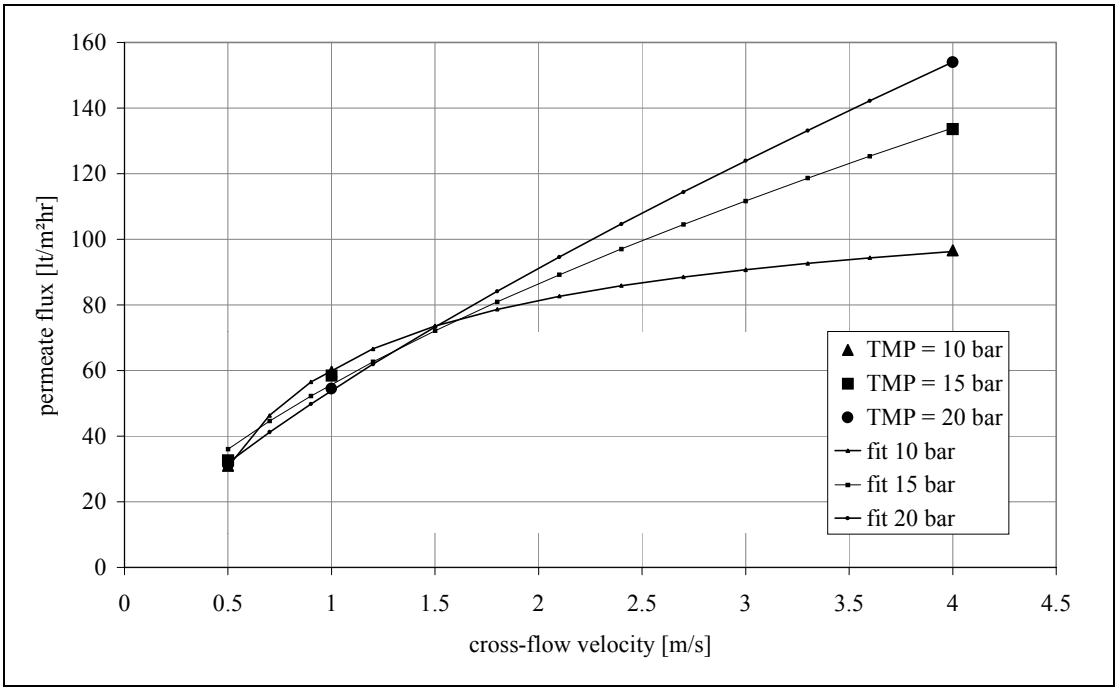

Figure 9.7 Experimental data with synthetic wastewater containing 2.5 g/l reactive red 2 and 30 g/l NaCl (CL3) experiments performed from low to high fouling potential. pH ~8-9

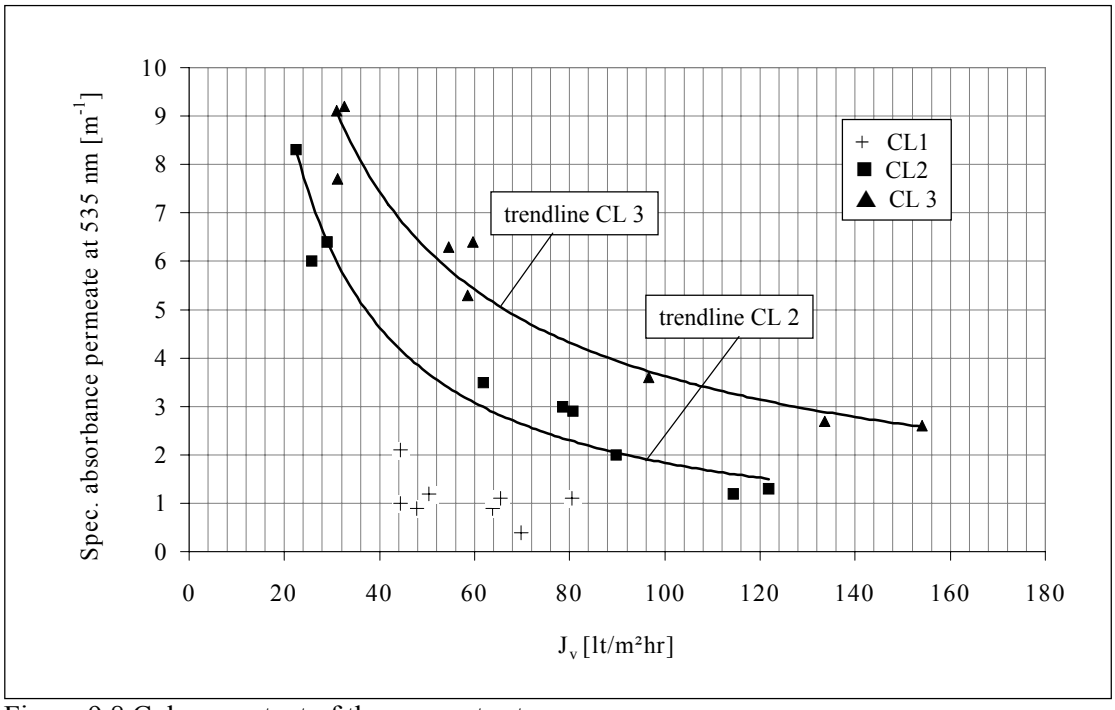

Figure 9.8 Colour content of the permeate streams.

9.5 Separation characteristics

In order to discharge or reuse the permeate water, its colour concentration in the permeate should not exceed a certain value. In this study the maximal tolerable spectral absorbance for discharge at 525 nm as set by the German legislation was taken (i.e. 5 m^{-1}). The samples were measured at a wavelength of 535 nm as this was the maximal absorption value for reactive red 2 solutions. It turned out that for the two different concentration levels the colour content of the permeate could be described as a function of the permeate flux. Above a critical flux (Figure 9.8) the constraint of a spectral absorbance below 5 m^{-1} was fulfilled. (i.e. 37.1 lt/m^2hr for CL2 and 63.9 lt/m²hr for CL3). The permeate streams of the CL1 experiment fulfilled the criterion in all cases.

The dye concentration in the permeate increases with higher dye concentration in the retentate and a lower permeate flux. Also an increase was observed between the experiments CL1 and CL2 were NaCl was added and the pH was raised from neutral to basic conditions. This latter fact can be explained by the circumstance that the membrane has a more open structure at high pH.

9.6 Economic calculations synthetic wastewater treatment

The calculated costs per cubic meter permeate and the design of the membrane processes for the four cases at the three concentration levels considered here are tabulated in tables 9.6 to 9.8.

Table 9.6 Results economic calculations **CL1**

Case	operation time [hr/y]	Flow (feed / permeate) [m^3/hr]	Optimal TMP [bar]	Optimal cross-flow [m/s]	J_v [lt/m²hr]	A_m [m^2]	Permeate price [NLG/m^3]
1	2000	3 / 2.70	20	1.09	134.3	20.1	3.72
2	2000	15 / 13.5	20	1.48	139.3	96.9	2.62
3	8000	0.75 / 0.68	16.5	0.71	113.3	6.0	2.88
4	8000	3.75 / 3.38	18	0.99	118.2	28.6	1.72

Table 9.7 Results economic calculations **CL2**

Case	operation time [hr/y]	Flow (feed / permeate) [m^3/hr]	Optimal TMP [bar]	Optimal cross-flow [m/s]	J_v [lt/m²hr]	A_m [m^2]	Permeate price [NLG/m^3]
1	2000	3 / 2.70	20	1.85	104.2	25.9	4.57
2	2000	15 / 13.5	20	2.24	108.9	124	3.32
3	8000	0.75 / 0.68	16	1.18	86.1	7.9	3.20
4	8000	3.75 / 3.38	18	1.48	95.5	35.4	1.96

Table 9.8 Results economic calculations **CL3**

Case	operation time [hr/y]	Flow (feed / permeate) [m^3/hr]	Optimal TMP [bar]	Optimal cross-flow [m/s]	J_v [lt/m²hr]	A_m [m^2]	Permeate price [NLG/m^3]
1	2000	3 / 2.70	20	3.67	144.4	18.7	4.53
2	2000	15 / 13.5	20	4.09	156.6	86.2	3.08
3	8000	0.75 / 0.68	10	1.44	73.1	9.3	3.30
4	8000	3.75 / 3.38	10	1.69	77.2	43.8	2.07

9.7 Discussion synthetic wastewater treatment

The operation time has a tremendous influence on the final cost. It is advisable to operate the process as continuously as possible, under the condition that the membrane is not applied to recover energy. So storage tanks have to be placed as a consequence of the batch-like operation of the textile dyeing and washing processes.

If the membrane is operated continuously the ideal cross-flow velocity is lower than for a batch like operation. This is due to the fact that the contribution of the operational cost to the total permeate cost will be increased if the membrane operation time is increased. Thus it becomes then more attractive to decrease these operational costs.

The optimal transmembrane pressure for NF, which can be determined from the experiments with the synthetic wastewater, is hard to determine as it turned out that the optimal pressures lay often beyond the experimental domain. However operating below 10 bar will often not be possible as the dye rejection by the membrane will be decreased. Operating above 25 bar might be an option, however it must be taken into mind that the investment costs of the installation will increase if higher pressures are required.

Furthermore it is dissuaded by the membrane manufacturer to operate the NF membrane process at higher transmembrane pressures than 20 bar, as severe fouling of the membranes is likely to occur at those conditions. This was also proven to be so with experiments performed at 35 bar as the fluxes were considerably lower than what would be expected from extrapolated data of experiments CL1.

In this economic analysis only the benefits of the recovery of water have been considered. Comparing the permeate cost per m^3 to the actual prices nowadays it must be concluded that membrane separation is economically seen not a viable option. However as discussed in chapter 2 membrane separation processes can also recover energy if they are applied for direct recovery of fresh process water. This is economically more attractive and a lot of textile refining companies have already installed heat exchangers. If 80 % of the energy, to heat up the process water from 20°C to 80°C can be recovered the subsequent energy savings per m^3 permeate can be achieved:

$$\Delta q = \frac{\rho \cdot c_p \cdot \Delta T}{\eta} = \frac{1000 \cdot \left[\frac{kg}{m^3}\right] \cdot 4.18 \cdot \left[\frac{kJ}{kg \cdot K}\right] \cdot 60 \cdot [K]}{0.8} = 312.5 \cdot \left[\frac{MJ}{m^3}\right] \qquad (9.18)$$

The energy cost for heating up the fresh water is 0.04 NLG/kWh (i.e. 0.04 NLG/3.6MJ). This results in a possible cost saving of 3,50 NLG per m^3 permeate and membrane filtration seems thus economically profitable.

There are however limitations to this energy recovery as the membrane separation processes have to be carried out at higher temperatures. Firstly the membrane material and the membrane modules must withstand these temperatures. Secondly the separation characteristics should not alter such that a worse permeate quality will be obtained. These facts need more membrane filtration research at higher temperatures.

Furthermore it must be emphasised that energy recovery is only important if the membrane separation process is primarily used to recover fresh process water and not to minimise the wastewater volume. As presented in chapter 2, the recovery of fresh process water is mainly done by applying RO as NF is applied to minimise the wastewater volume. So energy recovery is more important in RO process than in the NF process. It may be interesting to

replace NaCl by Na_2SO_4 in the dyeing process so that NF can be used to recover fresh process water directly in the washing process.

9.8 NF and RO filtration of actual textile wastewater

9.8.1 Experimental methods and results

Actual textile wastewater from the first washing bath subsequent to a pad-steam process was filtrated by nanofiltration. The aims of this research were to check if the research on the synthetic wastewater is representative for the NF filtration of actual textile wastewater in terms of membrane fouling and economics. Furthermore the same textile wastewater was filtrated by RO and these experiments were also economically analysed. A considerable amount of textile wastewater was used in one experiment in order to be close to the actual application.

The wastewater contained two (hydrolysed) reactive dye components, Cibacron rot C2G and Cibacron Orange CG. The accompanying colour index names are: Reactive Red 228 and Reactive Orange 116. The recipe of the dyeing solution, according to the textile refining manufacturer, is shown in table 9.9.

Table 9.9 Composition of the dyeing bath.

Component	Content	concentration dyeing bath
Cibacron Rot C2G		18 g/l
Cibacron Orange CG		13 g/l
Respumit SD	silicon oil	2 g/l
Primasol V	polyacrylate solution	6 g/l
Primasol CK	mixture of non-ionic surfactants and anti-foaming agent	0.2 g/l

The feed-bleed set-up (figure 4.1) was used, but the permeate stream and retentate stream were cast back to another storage tank in stead of the feed tank. The feed tank contained about 1 m^3 of textile wastewater. The composition and characteristics of the feed water, determined by the methods discussed in chapter 4, are summarised in table 9.10. The concentrations of the components in textile auxiliaries (Respumit and Primasol) are not known, but it can be assumed that these components are present in very small concentrations.

Table 9.10 Composition and characteristic data of the actual textile wastewater.

Component	
Hydrolysed Reactive Orange	0.08 g/l
Hydrolysed Reactive Red	0.11 g/l
pH	13, brought to 8 by HCl addition
conductivity	~ 18 mS/cm ~ 12.4 g/l NaCl
colour content retentate	320 m^{-1} at 550 nm

The applied transmembrane pressure was 20 bar in the NF experiments and 35 bar in the RO experiments. The membrane filtrations were performed at various cross-flow velocities between 0.5 and 4 m/s and lasted at least 200 minutes.

9.8.2 Results and discussion

The permeate flux as function of time is presented in the figures 9.9 and 9.10. These figures are only presented here to show the flux behaviour after an initial start-up period (whether they still decline due to membrane fouling or stay constant). The sharp flux decrease may be due to the initial concentration increase as described in appendix 4A. The maximal concentration increase was however in the NF experiments 14 percent and for the RO experiments 9 percent, thus other effects (e.g. membrane fouling) have an influence as well.

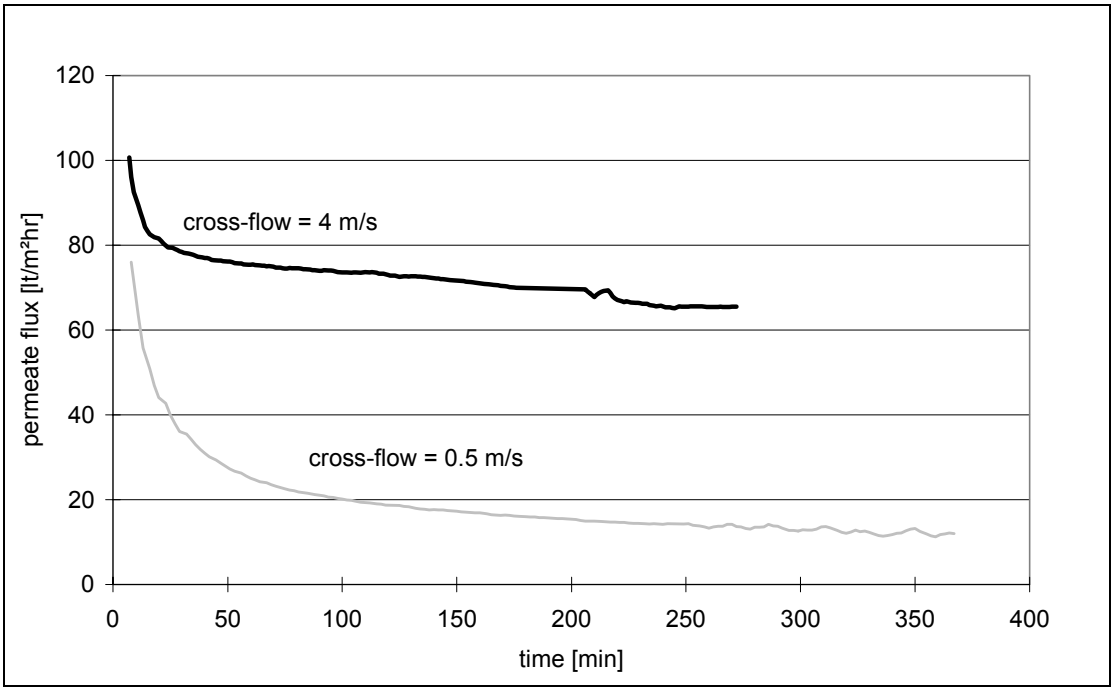

Figure 9.9 NF of actual textile wastewater.

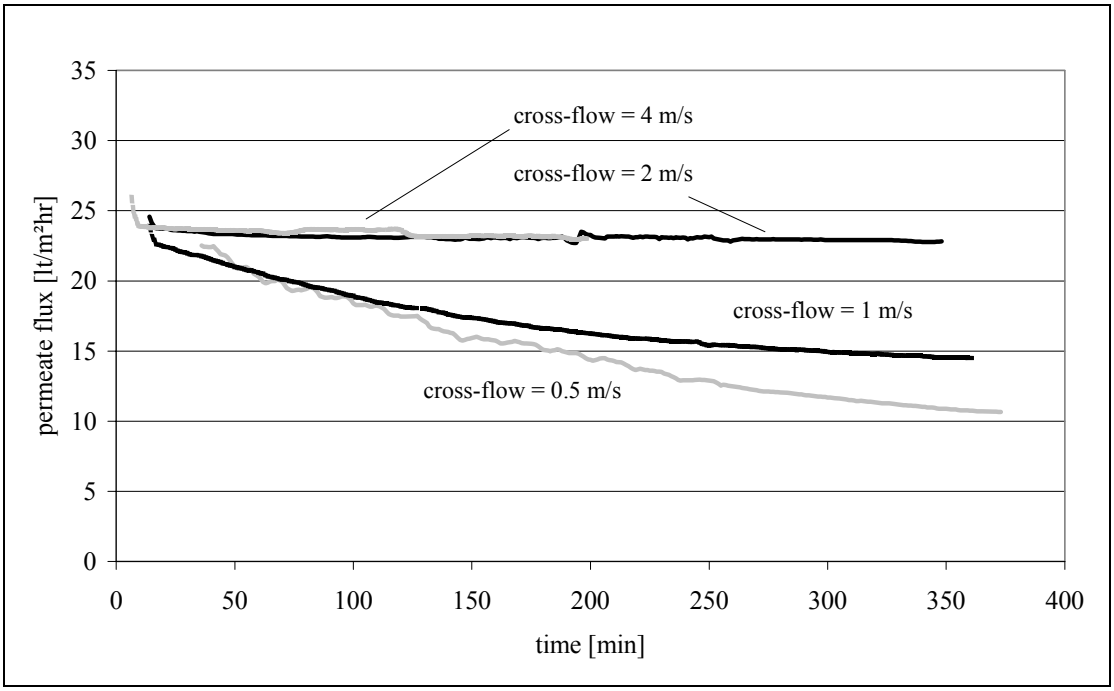

Figure 9.10 RO of actual textile wastewater

It can be seen that in the RO experiments at 4 m/s and 2 m/s the permeate flux reaches a constant value, whereas in all other experiments (RO at 1 and 0.5 m/s and NF at 4 and 0.5 m/s) a considerable flux decline in time can be observed. Therefore the economic analysis will be done substituting a permeate flux at a selected time point. This point is chosen at 200 minutes of filtration, corresponding to the maximal operation time of a washing process. The economic analysis will be done for an operation time of 2000 hours/year.

Table 9.11 Measured data of the NF and RO experiments.

Experiment	cross-flow [m/s]	permeate flux [lt/m²hr]	NaCl-retention [-]	colour retention [-]
NF9.1	4	65.4	0.124	0.999
NF9.2	0.5	15.3	0.110	1.000
RO9.1	4	23.0	0.963	0.998
RO9.2	2	24.3	0.953	0.997
RO9.3	1	16.2	0.935	1.000
RO9.4	0.5	14.7	0.914	0.999

The observed NaCl retentions are in the same range as measured in the parametric studies. It is thus not possible with these membranes to obtain higher salt rejections than 98 percent when filtrating the selected textile wastewater. The NaCl retention of the NF is also in the same range as measured before (chapter 4.6). The spectral absorbances at 550 nm of the permeate samples were always below 1 m^{-1} for both membranes and thus very high retentions were achieved. The highest spectral absorbances were measured in some RO permeate samples. This was confirmed by the fact that the RO membrane had ‘red spots’ at the outside of the backing layer of the membrane, whereas this layer of the NF membrane was visibly clear.

Table 9.12 Economic analysis of NF and RO of actual textile wastewater for an operation time of 2000 hr/yr.

Exp	cross-flow [m/s]	Feed flow [m^3/hr]	Membrane area [m^2]	Permeate price [NLG/ m^3]
NF9.1	4	3	41.3	7.84
NF9.1	4	15	206	6.21
NF9.2	0.5	3	176	18.98
NF9.2	0.5	15	882	17.90
RO9.1	4	3	117	18.72
RO9.1	4	15	587	16.30
RO9.2	2	3	111	13.93
RO9.2	2	15	556	12.40
RO9.3	1	3	167	18.66
RO9.3	1	15	833	17.34
RO9.4	0.5	3	184	20.00
RO9.4	0.5	15	918	18.83

The nanofiltration process shows lower permeate prices than RO, simply because of the fact that higher permeate fluxes compared to RO will be achieved. However the permeate fluxes determined with the actual textile wastewater are much lower than with the synthetic wastewater, despite the fact of the lower concentration of dye stuff (0.2 g/l) in the actual textile wastewater. It could be that in the actual textile wastewater the very low concentrations of textile auxiliaries (especially the silicon oil and the anti-foaming agents) are responsible for the severe flux decline. Alternative dyeing processes, without using these substances, may prevent the membrane fouling and the filtration of real textile wastewater becomes more similar to the filtration of the synthetic wastewater.

The economic analysis shows that the cost for the water intake must be very high before reverse osmosis will be introduced as proposed in chapter 2. Even if no severe flux decline was observed (at a cross-flow of 2 m/s) too much membrane area will be required as the permeate fluxes are relatively low.

Possibilities to make the RO process more attractive:

- Lower membrane prices. A calculation is done for the case of RO filtration at a cross-flow of 2 m/s, a membrane price of 50.-- NLG/m^2 and a feed flow of 3 m^3/hr. This leads to a permeate price of 8.81 NLG/m^3 (compared to 13.93 NLG/m^3 in the old case)
- Use spiral wound membranes with a prefiltration step. The same fluxes will be reached at a lower power input of the circulation pump as spacers in the modules will increase the mass transfer rate near the membrane surface.
- Use tubular membranes with a smaller diameter. The membrane process will then occupy less volume. The permeate cost will then decreased as the mass transfer rate in the boundary layer adjacent to the membrane surface will be increased. This increase will be 22 percent going from a tube diameter of 13.75 mm to 5 mm. However going to even smaller diameters ($d < 0.003$ m) will not help as the cross-flow will shift from turbulent to laminar conditions leading to smaller mass transfer rates.
- Operating at higher pressures to obtain higher permeate fluxes, however hydrostatic pressures above 60 bar require increasing investments in the other devices of the membrane filtration installation.

Despite these possibilities it must be concluded that the operation scale (< 15 m^3/hr) is such that the permeate prices for the RO installation will not be lower than 8.-- NLG / m^3.

9.9 Conclusions

An economic model is developed to estimate the permeate cost per m^3 for a given membrane filtration process (nanofiltration or reverse osmosis). NF experiments with synthetic wastewater at various composition and varying transmembrane pressures and cross-flow velocities are used as input in this economic model. Doing so the influences of the process parameters and other process conditions (like occupation time per year and feed flow) were determined. It turned out that a continuous operation is preferable to a batch–like operation despite the fact that extra storage tanks will be necessary.

Nanofiltration and reverse osmosis with actual textile wastewater were performed to check if the results of the synthetic wastewater are representative for actual applications. The permeate costs of the RO filtration are much higher due to the simple fact that the permeate fluxes are relatively low. The operation scale in the textile industry is such small that the permeate prices will be higher than 8.-- NLG/ m^3. The permeate fluxes of the NF with the actual textile wastewater were considerably lower than those with the synthetic wastewater, despite the fact of the lower concentration of the dye components. It could be that textile auxiliaries in the real textile wastewater in very small concentrations contribute considerably to membrane fouling. More research towards this membrane fouling is necessary.

Membrane processes will be economically more attractive if next to water recovery, energy recovery is considered (chapter 9.7). It must emphasised that energy recovery is only worthwhile if the membrane is used to recycle fresh process water directly to the washing process. This is the case for the application of RO as presented in chapter 2. For NF the energy recovery is less important as NF is mainly used to concentrate the wastewater volume. However it may be interesting to replace NaCl by Na_2SO_4 in the dyeing process and apply NF for the recovery of fresh process water. This latter fact needs more research.

Acknowledgement

Ten Cate Protect Nijverdal is acknowledged for supplying the textile wastewater. P. Nieland is acknowledged for the experimental work. H. Oude Velthuis is acknowledged for keeping the membrane filtration installation 'runnable'.

Symbols

symbol	description	unity
Δq	required heat energy per volume	$[J/m^3]$
ΔT	temperature difference	[K]
η	dynamic viscosity	[Pa·s]
ν	kinematic viscosity	$[m^2/s]$
ρ	(fluid) density	$[kg/m^3]$
Φ	volume stream	$[m^3/s]$
a	parameter gel layer model	$[(m/s)^{0.2}]$
a1..a5	parameters fit function	
A_m	membrane area	$[m^2]$
C_b	bulk concentration	$[mole/m^3]$
C_g	gel concentration	$[mole/m^3]$
d_h	(hydraulic) diameter	[m]
f	Fanning friction factor	[-]
J_v	permeate flux	[m/s]
L	length membrane tube	[m]
n	number of membrane tubes	[-]
PC	power consumption	[W]
Re	Reynolds number	[-]
TMP	transmembrane pressure	[bar]
v	cross-flow velocity	[m/s]

Financial symbols

symbol	description	unity
CP	cost per cubic meter permeate	$[NLG/m^3]$
TCO	Total cost of ownership	[NLG]
I	investment cost	[NLG]
O	operational cost	[NLG]
V_{tot}	volume permeate per year	$[m^3/y]$
α	factor	[1/y]
i	interest rate	[%/y]
ny	depreciation time	[y]

Subscripts	
c	circulation (unit)
F	feed
p	permeate

Literature

1 Dutch Association of Cost Engineers, DACE-prijzenboekje, 19th ed., May 1997
2 Bird, Stewart and Lightfoot, Transport phenomena, John Wiley New York, 1960.

Summary

In the textile refining industry a lot of chemicals are used in order to meet the product specifications. After processing, a considerable part of these chemicals has to be removed, which is done by rinsing with water partly at elevated temperatures. The large consumption of water, energy and chemicals leads to a considerable contribution to environmental problems, like the lowering of the groundwater-level, the salting of the soil, colourisation of surface water and contamination by components in the environment. Because of these issues, the textile refining industry is nowadays confronted with more stringent legislation and raising costs concerning fresh water intake and wastewater discharge.

In this thesis the application of membrane processes for the treatment of textile wastewater has been investigated. The research was part of the IOP-prevention program 'Recycling of process-streams in the textile industry' of Senter, an office of the Ministry of Economic Affairs stimulating applied research. The program was done in co-operation with TNO-centre of textile research, which performed research on the textile washing processes, and TNO-Institute of environmental sciences, energy research and process innovation (TNO-MEP), which performed the research on waste treatment techniques.

The application of reverse osmosis (RO) and nanofiltration (NF) for the recycling of process-water and the reduction of wastewater volume from washing processes subsequent to reactive dyeing processes was chosen as topic of study. The research focuses on the occurrence, understanding and prevention of membrane fouling by this wastewater.

The wastewater from the washing processes subsequent to reactive dyeing processes contributes considerably to the environmental problems. About 30 % of the applied reactive dyes do not fixate to the fabric but reacts with water to an unreactive form that has to be washed out. The wastewater contains further salt (NaCl or Na_2SO_4), NaOH and textile auxiliary components. The RO process can be applied in order to recycle process water and thermal energy directly to the washing process as it rejects almost all components, including NaCl. The reduction of the waste volume by RO will be limited by the increased osmotic pressure difference over the membrane. NF can than be used to concentrate the waste stream further as it separates the NaCl from the organic components (e.g. dyes and textile auxiliaries). If NaCl is replaced by Na_2SO_4, NF can be used for recycling in stead of RO.

In chapter 2 alternative washing processes are presented by applying membrane technology. Using a simplified process model, it was calculated that a seventy percent reduction of the fresh water consumption and a ninety percent reduction of waste volume could be technologically achieved. This will be economically profitable if reasonable membrane performance (i.e. solvent permeate fluxes and solute retentions) will be achieved at reasonable mechanical energy input. This implies that the influence of concentration polarisation and membrane fouling should be minimised.

In chapter 3 transport of solvent (i.e. water) and solute through reverse osmosis and nanofiltration membranes is reviewed. The separation performance of a membrane is a combination of solubility of components in the membrane and the transport of these components through the membrane and boundary layer. The permeate flux of the solvent and solutes is influenced by concentration polarisation and especially by membrane fouling. The origin of membrane fouling is discussed in terms of electrostatic and electrodynamic properties of the solutes and the membrane surface.

In chapter 4 the experimental filtration methods and membrane characteristics of the selected RO and NF membranes are presented. The membranes are of a tubular shape in order to have well defined flow conditions. The filtration performance of the RO membrane was characterised by filtration of NaCl solutions at different concentrations in order to compare these results with NaCl separation during the filtration of actual and synthetic textile wastewater.

The filtration performance of the NF membrane has been characterised by filtration of pure solutions of NaCl, Na_2SO_4 and $MgSO_4$. The NaCl retention is very dependent on the NaCl concentration, which can be explained by electrical charge (i.e. Donnan) exclusion. The separation of the Na_2SO_4 and $MgSO_4$ is mainly determined by the size exclusion and diffusion in the membrane and not by the Donnan exclusion.

The zeta potential, an electrostatic property, of both membranes was measured at varying pH in order to determine the membrane surface charge. It was found that the NF membrane surface is negatively charged over the pH range between 2 to 10. The RO membrane has an iso-electric point at pH 7, this means that the membrane surface is positively charged in acid conditions and negatively charged at alkaline conditions.

Preliminary RO and NF filtration experiments were carried out with (diluted) actual textile wastewater from two reactive dyeing processes. It turned out that water glass (i.e. an alkaline solution of sodium silicate) used as a dyeing auxiliary, contributes to membrane fouling. The results of these experiments, together with literature review, led to the formulation of synthetic wastewater to examine which components, or combination of components, are contributing to membrane fouling. The concentrations of the components were chosen similar to the concentrations in the actual textile wastewater. Next to water glass, the synthetic wastewater solutions contained the anionic surfactant sodiumdodecylsulphate (SDS), as representative for the washing and dyeing auxiliaries, and the cationic surfactant cetyltrimethylammonium bromide (CTAB) as representative for afterfixation auxiliaries. Furthermore the NaCl concentration and the pH were varied in order to investigate the (mutual) influence of the colloidal stability of the solution and the membrane surface charge on the membrane performance.

From the RO and NF filtration of synthetic wastewater, it could be concluded that the contribution of hydrolysed reactive dyes to the membrane fouling is only of minor importance. NaCl did cause lower permeate fluxes which can be explained by a combination of the osmotic pressure difference over the membrane enhanced by concentration polarisation in the boundary layer near the membrane.

Membrane fouling by silicates at 0.3 g/l SiO_2 was more severe in the NF experiments than in the RO experiments. This could be due to the fact that the higher NF permeate fluxes will result in more relative membrane fouling as the transport of solutes towards the membrane is higher. Moreover it could be that the NF membrane would suffer from more internal membrane fouling as the NF membrane has a more open structure than the RO membrane.

Severe membrane fouling was observed for both RO and NF, if the synthetic wastewater contained SDS. This membrane fouling was more severe at higher NaCl concentration and at lower pH. This can be explained by considering two electrochemical interactions (i.e. electrodynamic and electrostatic, of which the latter one is strongly influenced by the NaCl concentration and pH) between the SDS and the membrane surface leading to two opposing forces. The electrodynamic interaction is responsible for the hydrophobic attraction between the tail of SDS surfactant and the membrane material and the electrostatic interaction is responsible for the repulsion between the negatively charged head of SDS and the negatively charged membrane. The electrostatic repulsion will decrease with increasing NaCl concentration by shielding of the electric charges and with decreasing pH by protonation of the negatively charged groups at the membrane surface leading to a membrane with a lower membrane surface charge.

RO filtration experiments with textile washing auxiliaries showed that a washing component, based on alkylsulphates like SDS, does contribute to membrane fouling. In contrast to that a washing component, based on polyacrylate (a polyelectrolyte component) did not cause membrane fouling. The possible explanation for this is that due to the relatively high electrostatic charge density, the polyacrylate component shows a relative high electrostatic repulsion combined with a low hydrophobic attraction towards the negatively charged membrane.

Pure solutions of a (cationic) industrial afterfixation agent, Tinofix ECO, and pure solutions of the cationic surfactant, CTAB did not cause any permeate flux decline at the low concentrations in which they will appear in the wash water. Increasing the CTAB concentration above the crystallisation concentration and below the Krafft-temperature (i.e. crystallisation temperature) leads to severe membrane fouling.

It was proven, by zeta potential measurement, that SDS and CTAB adsorb onto the membrane. The fact that SDS causes a permeate flux decline and CTAB does not at concentrations below the critical micelle concentration may be explained by the different configuration of the surfactant layers on the membrane surface. More research towards this phenomena is needed.

Although pure solutions of the cationic components, examined in this study at the relatively low concentrations, do not cause membrane fouling, they may initiate membrane fouling by changing the membrane surface charge. The combination of the afterfixation agent and the polyacrylate washing component, at concentrations in which both auxiliaries do not cause membrane fouling separately, did result in severe membrane fouling in nanofiltration.

From the experiments with synthetic wastewater some practical remarks can be made. If the wastewater contains silicates a prefiltration step to remove colloidal silica is recommended. Washing auxiliaries containing alkylsulphates can cause severe membrane fouling. It is recommended to replace these washing auxiliaries with other types of washing auxiliaries or operate the membrane process at alkaline conditions. This latter measure however will decrease the NaCl retention ability of the RO membrane, as the membrane has a more open structure at alkaline pH. Concerning auxiliary components containing surfactants and polyelectrolyte components it is dissuaded to mix cationic and anionic components before filtration. This means that in practice the after fixation agent should be applied after the washing process in a separate unit operation and not in the washing process itself.

An economic model is presented in chapter 9 to calculate the optimal cross-flow velocity and transmembrane pressure in a tubular membrane module leading to the lowest cost price of the permeate for a NF process. It turned out that a continuous operation is preferable to a batch-like operation despite the fact that extra storage tanks will be needed. Typical permeate prices between 1,50 and 5 NLG/m^3 permeate were obtained. Applying the economical model to NF experiments with actual textile wastewater it appeared that the permeate cost price is higher than that determined with the synthetic wastewater, as the permeate fluxes were considerably lower. This may be attributed to the appearance of auxiliary components like anti-foaming and silicon oil in the actual wastewater.

The permeate cost price calculated for an RO filtration of actual wastewater appeared to be higher than 10 NLG/m^3 permeate. Main reasons for these high prices are the small-scale operation, the high required transmembrane pressures and the relatively high investment costs for the membranes.

The membrane filtration processes can become more profitable if the thermal energy recovery is included as well. A typical price of 3,50 NLG/m^3 permeate was calculated for the energy demand in the textile washing processes considered in this study. This thermal energy recovery is only an issue in the RO application, as NF is not applied for recycling of (hot) process water in the first place. Furthermore membrane modules should be designed such that they can operate at temperatures up to 80°C.

Possible further research to make membrane processes more attractive for the textile industry include:

- Methods to determine the physico-chemical phenomena at the membrane surface, as function of the applied components in order to understand and manage membrane fouling.
- Development of membranes and membrane modules for application at higher temperatures and higher pH values.
- Development of new membrane modules or the application of other existing membrane modules that require less energy input by optimising the flow management in the module.

Samenvatting

In de textielveredelingsindustrie worden veel chemicaliën gebruikt om de gewenste produkten en produkt-eigenschappen te verkrijgen. Na toepassing wordt een aanzienlijk gedeelte van deze chemicaliën, deels met heet water, uitgewassen. De grote consumptie van water, energie en chemicaliën draagt aanzienlijk bij aan milieuproblemen zoals de verlaging van de grondwaterstand, de verzilting van de bodem en de verkleuring van oppervlakte water. Vanwege deze problemen wordt de textielveredelingsindustrie geconfronteerd met meer stringente wetgeving en stijgende kosten voor het innemen van vers water (grondwater) en het afvoeren van afvalwater.

In dit proefschrift wordt een onderzoek beschreven naar de toepassing van membraanprocessen voor de behandeling van textiel afvalwater. Het onderzoek maakte deel uit van het IOP-preventie programma getiteld 'Recycling van processtromen in de textielindustrie' van Senter, een organisatie, onderdeel van het ministerie van economische zaken, die toegepast onderzoek stimuleert. Het IOP-programma werd uitgevoerd in samenwerking met TNO-centrum voor textielonderzoek, waar het onderzoek naar (verbetering van) de wasprocessen werd uitgevoerd, en TNO-centrum voor milieu, energie en procesinnovatie (TNO-MEP), waar het onderzoek naar (de combinatie van) afvalwater behandelingstechnieken werd uitgevoerd.

De toepassing van omgekeerde osmose (RO) en nanofiltratie (NF) voor het direct recyclen van proces water en de reductie van het afvalwater volume afkomstig van textiele wasprocessen volgend op reactieve verfprocessen is gekozen als onderwerp van studie. Met name het optreden, karakteriseren en voorkomen (of bestrijden) van membraan vervuiling door dit afvalwater werden onder de loep genomen.

Het afvalwater afkomstig van reactieve verfprocessen draagt aanzienlijk bij aan de milieu problemen, aangezien slechts 70 procent van de toegepaste verfstof aan het doek gefixeerd wordt. De overige 30 procent reageert met water tot de (niet reactieve) gehydrolyseerde vorm en dient na het verven uitgewassen te worden. Naast de kleurstoffen bevat het afvalwater aanzienlijke hoeveelheden zout (NaCl of Na_2SO_4), natronloog en textiele hulp stoffen. RO kan worden toegepast om (gezuiverd) proces water en thermische energie direct in het wasproces terug te voeren omdat praktisch alle opgeloste componenten (NaCl incluis) worden tegengehouden door RO-membranen. De reductie van het afvalwatervolume door RO wordt gelimiteerd door een relatief hoog osmotisch drukverschil over het membraan. In dat geval kan NF worden ingezet om de afvalstroom, met daarin de organische componenten, verder te verkleinen aangezien NF-membranen NaCl doorlaten. Indien in het verfproces Na_2SO_4 i.p.v. NaCl wordt toegepast, wordt het interessant om NF te gebruiken voor het recyclen van proceswater en thermische energie.

In hoofdstuk 2 worden alternatieve wasprocessen waarin membraantechnologie een rol speelt besproken. Met behulp van een procesmodel is berekend dat, met toepassing van membraantechnologie, een reductie van 70 procent van de vers water consumptie en een reductie van 90 procent van het afval water volume bereikt kon worden. Dit zal echter alleen economisch rendabel zijn indien hoge permeaatfluxen en toereikende scheidingskarakteristieken behaald worden bij lage (mechanische) energie input. Dit houdt in dat de invloed van concentratie polarisatie en membraanvervuiling geoptimaliseerd dient te worden.

In hoofdstuk drie wordt het transport van het oplosmiddel (i.e. water) en de opgeloste componenten door omgekeerde osmose membranen nader beschouwd. De scheidingsscherpte van het membraan wordt bepaald door de combinatie van de oplosbaarheid van de

componenten in het membraan en hun transportsnelheid in membraan en grenslaag. De permeaat fluxen van de opgeloste componenten en het oplosmiddel worden dus beïnvloed door concentratie polarisatie en membraanvervuiling. De oorzaak van membraanvervuiling wordt nader besproken in termen van de elektrostatische en elektrodynamische eigenschappen van de opgeloste componenten en het membraan oppervlak.

In hoofdstuk 4 worden de experimentele methoden zoals gebruikt in dit proefschrift besproken. De gebruikte RO en NF membranen zijn tubulair vormig zodat de stroming in de module goed gedefinieerd is. De filtratie eigenschappen van het RO membraan zijn gekarakteriseerd met NaCl als modelstof. De resultaten kunnen worden gebruikt als vergelijkingsmateriaal voor de scheiding van NaCl tijdens de filtratie van synthetisch en werkelijk afvalwater.

Het NF membraan is gekarakteriseerd middels de filtratie van zuivere oplossingen van de zouten NaCl, Na_2SO_4 en $MgSO_4$. The NaCl retentie is sterk afhankelijk van de NaCl concentratie, wat verklaard kan worden door de Donnan exclusie theorie (elektrische lading exclusie). De scheiding van de sulfaatzouten wordt, in tegenstelling tot NaCl, voornamelijk gedomineerd door de sterische exclusie (grootte van de ionen) en de diffusie van de ionen in het membraan.

De zeta potentiaal, een elektrostatische eigenschap, van beide membranen werd gemeten bij variërende pH om daarmee de lading van het membraanoppervlak te bepalen. Het NF membraan bleek over het gehele pH gebied van 2 tot 10 negatief geladen te zijn. Het RO membraan heeft een iso-electrisch punt bij pH 7, wat betekent dat het NF membraanoppervlak in zure condities positief en in alkalische condities negatief geladen is.

Filtratie experimenten zijn uitgevoerd met werkelijk textiel afvalwater afkomstig van twee reactieve verfprocessen. Uit deze eerste bevindingen kwam naar voren dat waterglas (een alkalische oplossing van natriumsilicaat), wat gebruikt wordt als hulpstof in de ververij, ernstige membraanvervuiling kan veroorzaken. Gecombineerd met data uit de literatuur, leidden deze experimenten tot de formulering van synthetisch afvalwater. De concentraties van de componenten in dit synthetisch afvalwater werden overeenkomstig met de concentraties in het werkelijke afvalwater gekozen. Het uiteindelijke doel daarbij was om te bekijken welke componenten of welke combinatie van componenten leiden tot membraanvervuiling. Naast waterglas werd gekozen voor de anionische surfactant natrium dodecyl sulfaat (SDS), die representatief is voor veel gebruikte was- en verfhulpstoffen, en de kationische surfactant, cetyl trimethyl ammonium bromide, die representatief is voor hulpmiddelen voor de nafixatie van gehydrolyseerde kleurstoffen. Verder werden daarbij de NaCl concentratie en de pH gevarieerd om de invloed van de colloïdale stabiliteit en de lading van het membraanoppervlak op de membraan prestaties te kunnen onderzoeken.

De gehydrolyseerde verfstoffen leiden op zich niet of nauwelijks tot membraanvervuiling in zowel de RO als de NF processen. Het toevoegen van NaCl aan deze oplossingen had een direct lagere permeaatflux tot gevolg, wat kon worden toegeschreven aan het verhoogde osmotische drukverschil over het membraan al dan niet versterkt door concentratie polarisatie.

De membraanvervuiling door silicaten (bij een concentratie van 0.3 g/l SiO_2) was sterker in de NF experimenten dan in de RO experimenten. De oorzaak hiervoor kan zijn dat de hogere permeaatfluxen bij NF (vergeleken met RO) tot meer membraanvervuiling leiden vanwege een grotere transportsnelheid van vervuilende componenten naar het membraan. Bovendien is het aannemelijk dat tevens de interne vervuiling bij de NF membraan sterker is dan bij het RO membraan, aangezien het NF membraan een meer open structuur heeft.

Sterke membraanvervuiling, voor zowel RO als NF, werd waargenomen indien het synthetische afvalwater de anionische surfactant SDS bevatte. Deze membraanvervuiling werd versterkt bij een hogere NaCl concentratie en een lagere pH, wat verklaard kan worden door de twee electrochemische interacties (i.e. elektrostatisch en elektrodynamisch) tussen surfactant en membraanoppervlak in ogenschouw te nemen. Vanwege elektrodynamische interacties is er een netto 'hydrofobe attractie' tussen de staart van de surfactant en het membraanoppervlak. De elektrostatische interactie is attractief indien de elektrostatische ladingen van de kop van de surfactant en het membraan ongelijk van teken zijn en repulsief indien gelijk van teken. Deze elektrostatische interactie is sterk afhankelijk van de NaCl concentratie en de pH. Bij verhoging van de NaCl concentratie worden de elektrostatische ladingen sterker afgeschermd, waardoor de invloed van de elektrostatische interactie minder wordt. Bij verlaging van pH zal door protonering van elektrostatisch geladen groepen de hoeveelheid elektrostatische ladingen veranderen.

In het RO onderzoek waarin de membraanfiltratie van verschillende textiele hulpmiddelen voor het uitwassen van kleurstoffen is onderzocht, bleek dat een wasmiddel met daarin een alkylsulfaat tot een sterke membraanvervuiling leidde. Dit in tegenstelling tot een wasmiddel met een wascomponent gebaseerd op een polyacrylaat (een polyelectrolyt). Een mogelijke verklaring voor dit feit is dat vanwege de hoge elektrostatische ladingdichtheid de polyacrylaat een relatief hoge elektrostatische repulsie en een relatief lage hydrofobe attractie vertoont met het negatief geladen membraanoppervlak.

Zuivere oplossingen van kationische componenten (nl. een oplossing met het nafixatie-middel, Tinofix ECO en een oplossing met de kationische surfactant, CTAB) leidden niet tot membraanvervuiling in de (relatief lage) concentraties zoals aanwezig in het afvalwater. Sterke membraanvervuiling werd bij CTAB alleen geconstateerd indien de omstandigheden dusdanig waren dat kristallisatie plaatsvindt (nl. bij een concentratie boven de kristallisatie concentratie en een temperatuur onder de 'Krafft'-temperatuur).

Door middel van zeta potentiaal metingen werd vastgesteld dat zowel de surfactant SDS als CTAB op het membraan adsorberen. Dat SDS daarbij wel tot membraanvervuiling leidt en CTAB niet moet verklaard worden d.m.v. verschil in configuratie van de surfactant lagen op het membraan. Meer onderzoek naar deze fenomenen is wenselijk.

Hoewel zuivere oplossingen van de kationische hulpmiddelen, onderzocht in deze studie, bij lage concentraties niet tot membraanvervuiling leiden, is wel aangetoond dat deze hulpmiddelen membraanvervuiling kunnen initiëren, mogelijk door het veranderen van de elektrostatische lading van het membraanoppervlak. De combinatie van Tinofix ECO en Cibapon (polyacrylate), bij concentraties waarbij beide niet tot membraanvervuiling leiden, leidde tot sterke membraanvervuiling in een NF experiment.

Uit het onderzoek met het synthetisch afvalwater kunnen enkele aanbevelingen voor de praktijk gegeven worden. Indien het afvalwater waterglas bevat dan is het zeer wenselijk het colloïdale silica middels een voorfiltratie stap te verwijderen. Het gebruik van wasmiddelen met daarin surfactants gebaseerd op alkylsulfaten, kan tot ernstige membraanvervuiling leiden. Het is daarom aanbevolen om deze middelen te vervangen door andere of het membraanproces onder alkalische condities te bedrijven. Deze laatste maatregel echter zal tevens de NaCl retentie van de RO membranen verlagen, aangezien het membraan een meer open structuur heeft bij hogere pH. Wat de textiele hulpmiddelen betreft, is het aan te raden om kationische middelen en anionische middelen van elkaar gescheiden te houden. In de praktijk betekent dit dat het nafixatie middel niet tijdens maar pas na het wasproces toegediend dient te worden.

In hoofdstuk 9 is een economisch model opgesteld om een optimale cross-flow snelheid en transmembraandruk voor een NF membraanproces met tubulaire membranen te bepalen zodat de laagste kostprijs per m^3 permeaat wordt verkregen. Het continu bedrijven van het membraanproces bleek goedkoper te zijn dan het batch-gewijs bedrijven, ondanks het feit dat, vanwege het batch-gewijze karakter van de verfprocessen, extra voorraadtanks bij de continu bedreven membraanproces geplaatst dienen te worden. Karakteristieke prijzen lagen tussen de 1,50 en 5,00 NLG per m^3 permeaat. Bij de kostprijs berekeningen voor NF op werkelijk afvalwater bleek dat deze laatste kosten hoger uitvielen vanwege het feit dat de permeaatfluxen aanzienlijk lager lagen dan bij NF van synthetisch afvalwater. Waarschijnlijk zijn hulpstoffen zoals b.v. siliconen olie, aanwezig in dit specifieke afvalwater, hier debet aan.

Voor enkele RO filtraties van werkelijk afvalwater werden kostprijzen berekend die hoger lagen dan 10,00 NLG/m^3. Belangrijke oorzaken voor deze hoge prijzen zijn de relatief lage RO permeaat fluxen, de kleine schaal van deze membraanprocessen, de hoge benodigde transmembraandrukken en de hoge investeringskosten voor de membranen.

Membraanfiltratie processen worden economisch aantrekkelijker indien de thermische energie teruggewonnen wordt. Een besparing van ongeveer 3,50 NLG/m^3 permeaat werd hiervoor berekend. Echter deze thermische energie terugwinning speelt alleen een rol in RO applicaties aangezien NF in eerste instantie niet gebruikt wordt voor de recycling van (heet) proces water. Daarnaast dienen de membraanmodulen zo ontworpen te worden dat ze toegepast kunnen worden bij temperaturen van 80 °C.

Mogelijk verder onderzoek om de membraanprocessen toepasbaar te maken voor recycling van proces water in de textielveredelingsindustrie omvat:

- Verder ontwikkelen van methoden om de fysisch-chemische eigenschappen van het membraan oppervlak te bepalen als functie van de aanwezige componenten ten einde membraanvervuiling beter te kunnen beheersen.
- Ontwikkeling van membranen en membraanmodulen voor de toepassing bij hogere temperaturen en hogere pH waarden.
- Ontwikkeling van nieuwe membraanmodulen of de toepassing van andere reeds bestaande membraanmodulen die vanwege een optimalisatie van de vloeistofstroming in de module een lager energieverbruik vertonen.

Curriculum vitae

Jacco van ‘t Hul werd op 25 december 1969 geboren te Coevorden. Aldaar doorliep hij de basisschool en het voortgezet onderwijs. In 1988 werd het Atheneum diploma aan de Rijksscholengemeenschap te Coevorden behaald. Aansluitend begon hij met de studie Chemische Technologie aan de Universiteit Twente. Tijdens deze studie voerde hij een stage-opdracht uit aan de Eidgenössische Technische Hochschule te Zürich (CH) op het gebied van de (de)stabilisatie van colloïdale water in olie emulsies. De afstudeeropdracht werd uitgevoerd bij de vakgroep Proceskunde waarbij een model voor stoftransport door ionselectieve membranen werd opgesteld. In februari 1994 werd het doctoraalexamen met succes behaald. Daarna was hij van 1994 tot 1999 werkzaam als onderzoeker bij de leerstoel ‘Scheidingstechnologie’ op het promotie onderzoek ‘Recycling van processtromen in de textielindustrie met behulp van membranen’. Resultaten van dit onderzoek, uitgevoerd onder de supervisie van Prof.dr.ir. Reith en Dr.ir. Rácz, staan beschreven in dit proefschrift. Een deel van het promotie onderzoek werd van oktober tot en met december 1997 uitgevoerd aan het Institut für Verfahrenstechnik van Prof.dr.-ing. T. Melin te Aachen. Sinds 1 mei 1999 is hij werkzaam bij TNO-Industrie te Delft.